On the Aggregation of Cereal β-Glucan and its Association with other Biomolecules

A Study using Asymmetric Flow Field-Flow Fractionation (AF4)

Zielke, Claudia

On the Aggregation of Cereal β-Glucan and its Association with other Biomolecules

On the Aggregation of Cereal β-Glucan and its Association with other Biomolecules

A Study using Asymmetric Flow Field-Flow Fractionation (AF4)

Claudia Katharina Zielke

LUND
UNIVERSITY

DOCTORAL DISSERTATION
which, by due permission of the

Faculty of Engineering, Lund University, Sweden,

will be publicly defended on Friday, 15th of December 2017,
at 10:15 in Lecture Hall C, Kemicentrum, Naturvetarvägen 14, Lund.

Faculty opponent

Dr. Andre Striegel

NIST, National Institute of Standards and Technology,
Gaithersburg, Maryland USA

Organization
LUND UNIVERSITY

Department of Food Technology, Engineering and Nutrition
Faculty of Engineering
P.O.Box 124, SE-22100 Lund, Sweden

Author(s) Claudia Katharina Zielke

Document name DOCTORAL DISSERTATION

Date of issue 2017-12-15

Sponsoring organization Swedish Research Council (VR)

Title and subtitle: On the Aggregation of Cereal β-Glucan and its Association with other Biomolecules - A Study using Asymmetric Flow Field-Flow Fractionation (AF4)

Abstract:

During recent years, numerous studies have shown the ability of dietary fiber to protect the colon from disease and to improve intestinal health. Beneficial health effects, such as the lowering of blood cholesterol levels and a reduction in the risk of coronary heart disease, are often directly related to cereal β-glucan, one of the major components of dietary fiber found in oat and barley. No definitive theory on the mechanisms of β-glucan during human digestion has yet been established, although it has been suggested that its solution and aggregation behavior, as well as its ability to form viscous slurries in the gut, are important and have the biggest impact. The aim of the first part of this work was to develop an extraction method for mixed-linkage β-glucan from oat and barley, in which the effects of extraction on its structure were minimized, and to improve current knowledge concerning the solution and aggregation behavior of β-glucan found in food products. Relatively high purities were obtained with the extraction method developed. β-Glucan was characterized using asymmetric flow field-flow fractionation (AF4) in combination with UV, multiangle light scattering (MALS), differential refractive index (dRI) and fluorescence detectors to obtain information on molecular size, molar mass distribution and conformation. The β-glucan analyzed contained high molar masses and large sizes. Cryo-transmission electron microscopy (cryo-TEM) showed the presence of highly aggregated structures in a widely distributed and loose arrangement in both oat and barley β-glucan, whereas barley β-glucan also showed surprisingly well-defined and dense aggregates. No proteins were found to be covalently bound to the β-glucan. However, as potential proteinaceous moieties in the extracts might affect the solution behavior of β-glucan, a study was carried out to investigate the relation between β-glucan and proteins. Aggregation patterns were found suggesting that electrostatic interactions play an important role during aggregation. In further studies, a direct relationship between the two macromolecules was confirmed. β-Glucan and proteins seem to aid each other during passage through the digestive system, enhancing the other's beneficial health effects. In an *in vitro* gastric and gastrointestinal digestion study, the digestive enzymes were not found to have any effect on the conformation of oat β-glucan. However, bile acids showed a molecular interaction with oat β-glucan able to cause a reduction in blood cholesterol. The results presented in this thesis shed light on the aggregation behavior of β-glucan, and possible working mechanisms during digestion are suggested, which will help in gaining a better understanding of its beneficial health effects. The second part of this thesis deals with the utilization of AF4-MALS for molar mass and size determination of macromolecules, with special attention on interference resulting from co-elution. Co-elution of only low quantities of very large analytes during AF4 fractionation was shown to cause disturbances in the MALS data, which can lead to errors in the size determination. Pre-injection filtering of samples was investigated to improve the results. A phenomenon often observed when determining the molar mass of highly polydisperse samples with AF4-MALS is a downturn (reduction) in the molar mass with elution time. This is usually regarded as an artifact and not further considered. However, it was shown in this work that this phenomenon might be a correct result arising from the inherent properties of the analyte.

Key words: β-glucan, oat, barley, molar mass, conformation, aggregation, asymmetric flow field-flow fractionation

Classification system and/or index terms (if any)

Supplementary bibliographical information — Language: English

ISSN and key title — ISBN 978-91-7422-555-6

Recipient's notes — Number of pages 78 — Price

Security classification

Signature  Date 2017-11-06

On the Aggregation of Cereal β-Glucan and its Association with other Biomolecules

A Study using Asymmetric Flow Field-Flow Fractionation (AF4)

Claudia Katharina Zielke

LUND
UNIVERSITY

Cover image by Catalina Fuentes

Faculty of Engineering
Department of Food Technology, Engineering & Nutrition

ISBN 978-91-7422-555-6 (print)
ISBN 978-91-7422-556-3 (pdf)

Printed in Sweden by Media-Tryck, Lund University
Lund 2016

Na und, ich tanze. *Ben Becker*

Popular Scientific Summary

Oats and barley are very common cereals, and their consumption has been directly linked to various health benefits. One of their main components, the polysaccharide β-glucan, is believed to be responsible for these health-promoting effects. Daily consumption of only 3 g of β-glucan leads to an improvement in blood glucose level and an effective reduction of blood cholesterol levels, helping to prevent chronic diseases such as cardiovascular disease. β-Glucan is a type of dietary fiber, meaning that the human body cannot digest it. Therefore, the most important property of β-glucan seems to be its influence on physiological effects, for example, increasing the viscosity of the contents of the gastrointestinal tract. When consuming β-glucan together with a meal, the viscosity of the food will be increased during digestion. The high viscosity has been suggested to reduce the absorption rate of macronutrients, e.g. fat and carbohydrates, reducing the lipid and glucose levels after a meal. The aim of this work was to analyze β-glucan and its solution behavior on the molecular level to better understand the effects of β-glucan, for instance, during digestion in the gastrointestinal tract.

β-Glucan was extracted from oats and barley using a mild process in order to preserve its integrity, and was investigated in terms of mass, size distribution and conformational properties in solution utilizing asymmetric flow field-flow fractionation (AF4). AF4 is able to separate mixtures of molecules with different sizes and masses by their size. Separation is based on the time the particles spend in the AF4 system; smaller molecules spending short times in the system than larger molecules. The separation and analysis of polysaccharides can be very challenging and few analytical techniques are suitable for the task. The difficulties encountered are typically related to the broad size and molar mass distributions, as well as the tendency of the substances to form supramolecular aggregates. However, AF4 is a powerful separation technique that has been found to be especially suitable for the analysis of polysaccharides such as β-glucan.

β-Glucan molecules were shown to interact with each other in solution to form assemblies of large molecules called aggregates, which explained the increasing viscosity in the digestive tract after β-glucan consumption. No protein was found to be bound directly to the β-glucan. However, a relation was found between the aggregation behavior of the β-glucan and proteins in several of the present studies, e.g. in beer. Simulation of digestion in the lab provided further information on the

behavior of β-glucan during its passage through the gastrointestinal tract. In conclusion, the work presented in this thesis led to a better understanding of the behavior and properties of β-glucan on a molecular level. Hopefully, the knowledge obtained can be used to develop food products with increased beneficial health effects.

Abstract

During recent years, numerous studies have shown the ability of dietary fiber to protect the colon from disease and to improve intestinal health. Beneficial health effects, such as the lowering of blood cholesterol levels and a reduction in the risk of coronary heart disease, are often directly related to cereal β-glucan, one of the major components of dietary fiber found in oat and barley. No definitive theory on the mechanisms of β-glucan during human digestion has yet been established, although it has been suggested that its solution and aggregation behavior, as well as its ability to form viscous slurries in the gut, are important and have the biggest impact.

The aim of the first part of this work was to develop an extraction method for mixed-linkage β-glucan from oat and barley, in which the effects of extraction on its structure were minimized, and to improve current knowledge concerning the solution and aggregation behavior of β-glucan found in food products.

Relatively high purities were obtained with the extraction method developed. β-Glucan was characterized using asymmetric flow field-flow fractionation (AF4) in combination with UV, multiangle light scattering (MALS), differential refractive index (dRI) and fluorescence detectors to obtain information on molecular size, molar mass distribution and conformation. The β-glucan analyzed contained high molar masses and large sizes. Cryo-transmission electron microscopy (cryo-TEM) showed the presence of highly aggregated structures in a widely distributed and loose arrangement in both oat and barley β-glucan, whereas barley β-glucan also showed surprisingly well-defined and dense aggregates. No proteins were found to be covalently bound to the β-glucan. However, as potential proteinaceous moieties in the extracts might affect the solution behavior of β-glucan, a study was carried out to investigate the relation between β-glucan and proteins. Aggregation patterns were found suggesting that electrostatic interactions play an important role during aggregation. In further studies, a direct relationship between the two macromolecules was confirmed. β-Glucan and proteins seem to aid each other during passage through the digestive system, enhancing the other's beneficial health effects. In an *in vitro* gastric and gastrointestinal digestion study, the digestive enzymes were not found to have any effect on the conformation of oat β-glucan. However, bile acids showed a molecular interaction with oat β-glucan able to cause a reduction in blood cholesterol. The results presented in this thesis shed

light on the solution and aggregation behavior of β-glucan and its association with other biomolecules, which will help in gaining a better understanding of its beneficial health effects.

The second part of this thesis deals with the utilization of AF4-MALS for molar mass and size determination of macromolecules, with special attention on interference resulting from co-elution.

Co-elution of only low quantities of very large analytes during AF4 fractionation was shown to cause disturbances in the MALS data, which can lead to errors in the size determination. Pre-injection filtering of samples was investigated to improve the results. A phenomenon often observed when determining the molar mass of highly polydisperse samples with AF4-MALS is a downturn (reduction) in the molar mass with elution time. This is usually regarded as an artifact and not further considered. However, it was shown in this work that this phenomenon might be a correct result arising from the inherent properties of the analyte.

Zusammenfassung

In den vergangenen Jahren haben viele Studien aufgezeigt, dass Ballaststoffe den Darm vor Krankheiten schützen und die allgemeine Darmgesundheit fördern können. Diese positiven Effekte, wie zum Beispiel eine Reduktion von Blut-Cholesterin und der einhergehende Schutz vor Herzinfarkten, stehen oftmals in direkter Verbindung mit der Aufnahme von β-Glukanen aus Getreide. Bis zur heutigen Zeit gibt es allerdings keine genauen Kenntnisse zum Wirkungsmechanismus der β-Glukane im menschlichen Verdauungstrakt. Ein des Öfteren auftauchender Erklärungsversuch basiert auf der Fähigkeit der β-Glukane, viskosen Schleim im Darm zu produzieren und somit die Absorption von Giftstoffen zu verhindern.

Das Ziel des ersten Teils dieser Arbeit war es, eine Extraktionsmethode für β-Glukane aus Hafer und Gerste zu entwickeln, welche die molekulare Integrität und Struktur der β-Glukane erhält, um deren Lösungs- und Aggregatverhalten während der Verdauung zu untersuchen.

Mit dieser Methode wurden β-Glukane mit relativ hohen Reinheiten extrahiert und danach mit Hilfe von Asymmetrischer Strömungsfeldflussfraktionierung (AF4) in Kombination mit UV, Mehrwinkel-Lichtstreuung (MALS), differentiellem Brechungsindex (dRI) und Fluoreszenz-Detektoren hinsichtlich ihrer molaren Masse, Größe und Konformation analysiert. Die untersuchten β-Glukane besaßen hohe molare Massen und große Größen. Kryo-transmissionselektronen-microskopische (cryo-TEM) Aufnahmen zeigten, dass β-Glukane aus beiden Getreiden über ein weites, lose arrangiertes Aggregatnetzwerk verfügen, wobei β-Glukane aus Gerste zusätzlich sehr dichte, sphärische Aggregate aufweisen. Es wurden keine kovalent-gebundenen Proteine gefunden. Da potentielle Proteinreste in Lebensmittelmatrizen jedoch das Aggregationsverhalten der β-Glukane beeinflussen können, wurde eine Studie konzipiert, um die genaue Beziehung zwischen Proteinen und β-Glukanen zu untersuchen. Erste Ergebnisse wiesen darauf hin, dass Proteine und β-Glukane aufgrund elektrostatischer Bindungen aggregieren. Diese Vermutung konnte in zwei weiteren Studien verstärkt werden. Es scheint, als ob Proteine und β-Glukane sich gegenseitig auf ihrem Weg durch den Verdauungstrakt unterstützen. Eine *in vitro* Studie der simulierten Magen-Darm-Verdauung zeigte keinen Einfluss von Verdauungsenzymen auf die β-Glukane. Gallensäure wiederrum zeigte eine molekulare Bindung zu β-Glukanen

auf, ein Umstand der während der Verdauung zu einer effektiven Senkung des Blut-Cholesterinspiegels führen kann. Die Ergebnisse, die in dieser Doktorarbeit präsentiert werden, beschreiben das Aggregations- und Lösungsverhalten der extrahierten β-Glukane und deren Umgang mit anderen biologischen Molekülen und tragen damit zu einem besseren Verständnis ihrer positiven Wirkung auf den menschlichen Körper bei.

Bei der Verwendung von AF4-MALS zur Analyse von molaren Massen und Größen von Makromolekülen muss speziell auf Co-Eluierungseffekte geachtet werden. Damit beschäftigt sich der zweite Teil dieser Arbeit.

Co-Eluierung von sehr geringen Mengen sehr großer Analyte während einer AF4-Fraktionierung kann ausgeprägte Fehler bei der Größenbestimmung der Probe hervorrufen. Zur Vermeidung dieser wird empfohlen, die Proben vor der Integrierung in das Analysesystem zu filtrieren, um so die Qualität der erhaltenen Daten zu verbessern. Ein anderes Phänomen, das besonders oft bei der Analyse von molaren Massen von polydispersen Proben beobachtet wird, ist ein sogenannter Downturn im Bereich der hohen Eluierungszeiten. Meistens wird dieses Ergebnis als Artefakt abgewertet und nicht weiter beachtet. In dieser Arbeit konnten wir jedoch zeigen, dass dieser Downturn ein wahres Resultat sein kann, hervorgerufen durch die Eigenschaften des Analyten.

List of Publications

Part I

Paper I – Characterization of Cereal β-Glucan Extracts from Oat and Barley and Quantification of Proteinaceous Matter

Zielke, C., Kosik, O., Ainalem, M.-L., Lovegrove, A., Stradner, A. & Nilsson, L.

PLoS ONE (2017) 12(2), e0172034.

Paper II – Characterization of Cereal β-Glucan Extracts: Conformation and Structural Aspects

Zielke, C., Stradner, A. & Nilsson, L.

Accepted for publication in Food Hydrocolloids

Paper III – Interaction between Cereal β-Glucan and Proteins in Solution and at Interfaces

Zielke, C., Lu, Y., Poinsot, R. & Nilsson, L.

Submitted to Colloids and Surfaces B: Biointerfaces

Paper IV – Characterization of the Molar Mass Distribution of Macromolecules in Beer for Different Mashing Processes Using Asymmetric Flow Field-Flow Fractionation (AF4) Coupled with Multiple Detectors

Choi, J., Zielke, C., Nilsson, L. & Lee, S.

Analytical and Bioanalytical Chemistry (2017) 409, 4551-4558.

Paper V – Analysis of β-Glucan Molar Mass from Barley Malt and Brewer's Spent Grain with AF4 and their Association to Proteins and Colon Health

Zielke, C., Teixeira, C., Ding, H., Cui, S., Nyman, M. & Nilsson, L.

Carbohydrate Polymers (2017) 157, 541-549.

Paper VI – The Effect of *in vitro* Gastrointestinal Conditions on the Structure and Conformation of Oat β-Glucan

Korompokis, K., Nilsson, L. & Zielke, C.

Food Hydrocolloids (2017) https://doi.org/10.1016/j.foodhyd.2017.11.007

Part II

Paper VII – Co-Elution Effects Can Influence Molar Mass Determination of Large Macromolecules with Asymmetric Flow Field-Flow Fractionation Coupled to Multiangle Light Scattering

Perez-Rea, D., Zielke, C. & Nilsson, L.

Journal of Chromatography A (2017) 1506, 138-141.

Paper VIII – Co-Elution Phenomena in Polymer Mixtures Studied by Asymmetric Flow Field-Flow Fractionation (AF4)

Zielke, C., Fuentes, C., Piculell, L. & Nilsson, L.

Submitted to Journal of Chromatography A

The Author's Contributions

Paper I: The author was involved in the design of the study, performed the experiments and analyses (apart from PACE and HPSEC-PAD), evaluated the results, and was responsible for writing the manuscript.

Paper II: The author was involved in the design of the study, performed the experiments and analyses, evaluated the results, and was responsible for writing the manuscript.

Paper III: The author was involved in the design of the study, coordinated the experiments, performed and evaluated the AF4 analyses, and was responsible for writing the manuscript.

Paper IV: The author was involved in the AF4 measurements and data analysis and contributed to writing the manuscript.

Paper V: The author was involved in the design of the study, performed the AF4 experiments and evaluated the results, and contributed to writing the manuscript.

Paper VI: The author designed the study, coordinated the experiments and data analysis, and helped in writing the manuscript.

Paper VII: The author was involved in the writing of the manuscript.

Paper VIII: The author was involved in the design of the study, performed the experiments and analyzed the results, and was responsible for writing the manuscript.

Papers not included in this Thesis

The Effect of Baking and Enzymatic Treatment on the Structural Properties of Wheat Starch

Fuentes, C., Zielke, C., Prakash, M., Kumar, P., Peñarrieta, J. M., Eliasson, A.-C. & Nilsson, L.

Food Chemistry (2016) 213, 768-774.

Role of Polysaccharides in Food, Digestion and Health

Lovegrove, A., Edwards, C. H., De Noni, I., Patel, H., El, N. S., Grassby, T., Zielke, C., Ulmius, M., Nilsson, L., Butterworth, P. J., Ellis, P. R. & Shewry, P. R.

Critical Reviews in Food Science and Nutrition (2017) 22, 57(2), 237-253.

Fluorescence Labelling for Analysis of Protein in Starch Using Asymmetrical Flow Field-Flow Fractionation (AF4)

Yoo, Y., Choi, J., Zielke, C., Nilsson, L. & Lee, S.

Analytical Science & Technology (2017) 30, 1, 1-9.

Flow-FFF Applications in Food Science and Technology

Nilsson, L. & Zielke, C.

in "Field Flow Fractionation: Principles and Applications", ISBN 978-3-527-34068-2, Eds: Celine Gueguen, Mohammed Baalousha, Kim R. Williams; John Wiley & Sons, Inc. In press.

Abbreviations

AF4	asymmetric flow field-flow fractionation
β-glucan	Mixed-linkage (1→3),(1→4)-β-$_D$-glucans
D	Brownian diffusion coefficient
DP	degree of polymerization
dRI	differential refractive index
FFF	Field-Flow Fractionation
FL	fluorescence
M	molar mass
MALS	multiangle light scattering
PEO	poly(ethylene) oxide
r_{hyd}	hydrodynamic radius
r_{rms}	root-mean-square radius, radius of gyration
SCFA	short-chain fatty acids
t_r	retention time

Contents

Introduction

Mittler zwischen Hirn und Händen muss das Herz sein.

(Metropolis, 1927)

β-Glucan

Origin and Structure of β-Glucan

Mixed-linkage (1→3),(1→4)-β-D-glucans (referred to as β-glucan) is a dietary fiber mainly found in cereal grains. Dietary fiber is defined as carbohydrate polymers that are neither digested nor absorbed in the small intestine (Codex Alimentarius Commission (2009)). β-Glucan is a linear polysaccharide, and is a major structural component of the starchy endosperm cell walls of vegetables and grains such as oat and barley. It is further characterized as an unbranched homopolysaccharide that consists of consecutive β-D-glucopyranosyl units linked via β(1→3) and β(1→4) linkages, where blocks of trimers and tetramers of (1→4) linkages are separated by (1→3) linkages (Lazaridou & Biliaderis, 2007), as illustrated in Fig. 1. There is considerable diversity between β-glucan from different cereals regarding their molar mass (M) and structure, for instance the distribution of β(1→3) and β(1→4) linkages (Lazaridou & Biliaderis 2007; Agbenorhevi, Kontogiorgos *et al.*, 2011). In oat β-glucan, β(1→4) trimers (53-61%) and tetramers (34-41%) dominate, and the molar ratio of the degree of polymerization (DP) DP3:DP4 ranges between 1.5 and 2.3 (Lazaridou & Biliaderis, 2007). Another structural characteristic of β-glucan is the ratio between (1→4) and (1→3) β-glycosidic bonds, which has been reported to be between 2.3 and 2.8 for oat β-glucan. Due to these irregular linkages, the β-glucan molecule is considered to be partially water soluble.

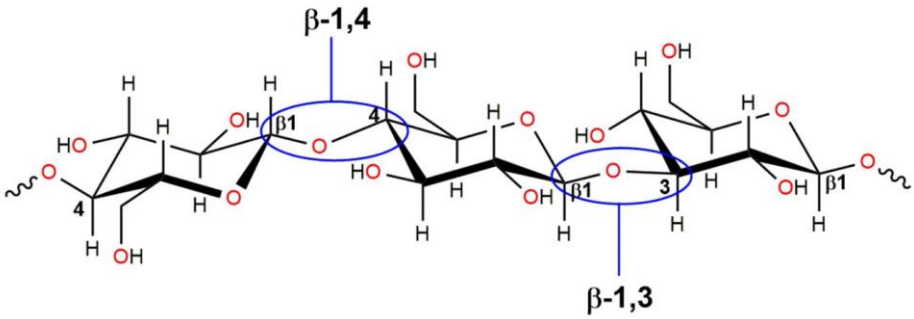

Figure 1 β-Glucan
Illustration of consecutive β-D-glucopyranosyl units linked via β(1→3) and β(1→4) linkages, forming the β-glucan molecule.

Health Benefits of β-Glucan and Colonic Health

Mixed-linkage β-glucan, acting as dietary fiber, has been associated with a number of health benefits for the consumer, which have been approved by both the U.S. Food and Drug Administration (FDA) (U.S. Food and Drug Administration, 1992, 2008) and the scientific panel of the EU (European Food Safety Authority, 2009, 2010). Health claims have been made regarding the cholesterol-lowering capacity of β-glucan and the regulation of blood glucose levels, as well as appetite-suppressing, antiproliferative, antihypertensive and immunomodulatory effects (Daou & Zhang, 2012; Lazaridou & Biliaderis, 2007; Rebello, O'Neil *et al.*, 2016; Thies, Masson *et al.*, 2014; Wang & Ellis, 2014). Therefore, β-glucan has been approved as a functional and bioactive food ingredient, and increased daily intake of which can reduce the risk of several chronic diseases. Although these claims have been accepted, we currently have no detailed understanding of the mechanisms of action of β-glucan, nor a potential way to utilize these benefits to improve food for health purposes.

Initially, it was assumed that dietary fiber only affected fecal bulk and prevented constipation. Nowadays, however, dietary fiber is known to affect human metabolism and physiological functions in the colon, leading to a reduction in colonic diseases such as colorectal cancer (Kumar, 2012; Mantovani, 2008). It has also been confirmed that the physicochemical and structural properties of β-glucan govern its nutritional functionality (Wood, 2004), and several possible mechanisms have been suggested.

In general, the action of dietary fiber during digestion can be divided into fermentative and non-fermentative mechanisms (Rose, Demeo *et al.*, 2007). Non-fermentative effects play a major role in increasing fecal bulk, reducing colonic transit time and binding toxic compounds and bile acids. Furthermore, some of the

functional properties of β-glucan are believed to have their origin in its solution behavior, particularly its ability to form viscous solutions (slurries) in the gut (Wolever, Tosh *et al.*, 2010). The beneficial health effects of β-glucan are often discussed in terms of the formation of gels and viscous slurries during digestion, which increase the viscosity of the digesta (e.g. Regand, Chowdhury *et al.* 2011), resulting in a reduction in the rate of macronutrient absorption (Wang & Ellis, 2014). Increased viscosity also results in an improved glycemic profile (i.e. a reduction in postprandial hyperglycemia (Ehrlein & Stockmann, 1998)), as well as a reduction in low-density lipoprotein cholesterol values (Wolever, Tosh *et al.* 2010). Another suggested mechanism is related to the ability of β-glucan to increase the formation of butyric acid in the colon (Hamer, Jonkers *et al.* 2008), and the increased abundance of butyric acid bacteria (Bränning & Nyman, 2011; Zhong & Nyman, 2014; Zhong, Nyman *et al.*, 2015), especially when the cereal is malted before consumption. It has been suggested that this increase can be attributed to a change in the M distribution, as well as an increase in the solubility of β-glucan after malting (Nilsson & Nyman, 2005). It has also been suggested that the relation between β-glucan and bile salts during human digestion mediates fecal excretion and hence stimulates the production of bile salts by the liver, utilizing blood cholesterol, resulting in a decrease in blood cholesterol (Andersson, Ellegard *et al.*, 2002; Kim & White, 2010; Lia, Hallmans *et al.*, 1995). In addition, it has been proposed that oat β-glucan can have positive effects on the absorption of dietary fats in the gastrointestinal lumen (Othman, Moghadasian *et al.*, 2011).

The fermentative effects of dietary fiber and β-glucan are based on the formation of short-chain fatty acids (SCFAs) originating from the fermentation of fiber in the colon by the microbiota (Rose, Demeo *et al.*, 2007). SCFAs help to maintain colonic function by locally supplying nutrients for the metabolic function of the colonocytes e.g. growth, mucosal proliferation, pH regulation, colonic mobility and the absorption of nutrients and electrolytes (Cummings, Englyst *et al.*, 1986; den Besten, van Eunen *et al.*, 2013), as well as glucose and cholesterol metabolism (Anderson & Bridges, 1984; Hara, Haga *et al.*, 1999). As a result, the health of colon mucosa improves and it can better perform as a barrier to prevent colonic conditions such as inflammations. One study on SCFAs focused especially on butyric acid, as it has been directly associated with anti-tumoric (angiogenesis inhibition), anti-inflammatory and anti-microbial effects (Tan, McKenzie *et al.*, 2014).

It is thus important to improve our understanding of the fermentation process, and the solution behavior of β-glucan in the digestive tract, by characterizing M and size distributions of β-glucan, as well as its interactions with other entities such as proteins and bile acids during digestion. Such knowledge can then be applied in the production and development of functional foods containing β-glucan, with beneficial health effects.

Aggregation Behavior of β-Glucan and its Impact

Self-association of β-glucan and the ability of high M species to form aggregates may play an important role in the beneficial health effects discussed above, mainly through the resulting increase in viscosity (Gomez, Navarro *et al.*, 1997; Wood, 2004; Cui & Wang, 2009; Håkansson, Ulmius *et al.*, 2012). This aggregation is known to be highly dependend on the M, the molar ratio of trimers and tetramers (DP3:DP4) in the individual β-glucan molecules, the hydrodynamic radius (r_{hyd}) and the chain conformation (Agbenorhevi, Kontogiorgos *et al.*, 2011; Håkansson, Ulmius *et al.*, 2012; Li, Cui *et al.*, 2010). In addition, intermolecular interactions of β-glucan as well as interactions with proteins can form physical cross-linkages between single molecules. These findings may provide the starting point for the understanding of the established health benefits of cereal β-glucan.

β-Glucan and Proteins

Nutrients such as proteins are essential for the human body. They have different functions within the organism, such as DNA replication, the catalysis of metabolic reactions, as building blocks for tissue, and in the transportation of molecules throughout the body. Furthermore, proteins store energy. The proteins in cereal grains support the structure of cell walls and act as a nitrogen source in the endosperm (Finnie & Svensson, 2014). Proteins consist of amino acid residues, forming one or several long polypeptides, and are considered macromolecules. They vary in conformation, protein folding and their specific amino acid sequence, actuating their respective activity. In terms of nutrition, proteins serve as a source of amino acids after being digested in the stomach, which is vital for the absorption of essential amino acids. Protein from barley endosperm, for instance, contains high amounts of hordeins, which are in turn rich in glutamine (Baik & Ulrich, 2008). Glutamine is generally considered a major energy source of epithelial cells of the mucosa and is involved in preservation and recovery of the intestinal mucosa (Kaya, Ceylan *et al.*, 2007). However, for the human body to be able to benefit from glutamine, it has to be transported by dietary fiber into the colon for subsequent fermentation, without being digested in the stomach or small intestine (Kanauchi & Agata, 1997). It therefore appears that there is a close relation between proteins and dietary fiber.

When discussing the solution behavior of β-glucan, the presence of proteins in β-glucan samples is another interesting aspect regarding the structural and nutritional properties of the β-glucan, as these protein-β-glucan links might influence molecular interactions, and thus the solubility and aggregation of the β-glucan. Several findings have been reported in the literature, suggesting a direct correlation between proteins and β-glucan. It has previously been suggested that β-glucan chains might be covalently bound to proteinaceous moieties (Forrest &

Wainwright, 1977; Webster & Woods, 2011). Vårum & Smidsrød found amino acid residues to be present in oat β-glucan preparations (Vårum & Smidsrød, 1988). Furthermore, it has been reported that the addition of proteases to viscous slurries of oat flour led to a decrease in viscosity, demonstrating a relationship between the protein content of the sample and its viscosity (Zhang, Doehlert *et al.*, 1997; Zhou, Robards *et al.*, 2000). Autio *et al.* came to the same conclusion after the addition of trypsin to oat β-glucan reduced the viscosity of the slurry (Autio, Myllymäki *et al.*, 1992). Other studies have found evidence for the binding of proteins to β-glucan, e.g. phosphate residues attached to oat β-glucan (Acker, Diemair *et al.*, 1955), and C-6 bound phosphate ester groups, revealed by NMR (Ghotra, Vasanthan *et al.*, 2007), as reversible phosphorylation of the amino acids serine, threonine and tyrosine in proteins is one of the most prominent types of modification (Hunter, 2012). Such protein-linked phosphate groups are able to form intra- and intermolecular hydrogen bonds and salt bridges, helping in the formation of stable aggregates by electrostatic interactions. Forrest *et al.* investigated β-glucan from barley endosperm cell walls and concluded that the β-glucan molecules might be firmly linked to one another through proteinaceous material resulting in high M aggregates of about 10^7 g/mol. These obtained aggregates were believed to associate further in solution by ionic or hydrogen bonds, resulting in the formation of more complex and even larger aggregated structures (Forrest & Wainwright, 1977).

The presence or absence of such proteinaceous moieties may thus explain the broad range of findings on β-glucan functionality, underlining the importance of gaining a better insight into the β-glucan-protein interaction in order to understand the effects of proteins on the solution and aggregation behavior of β-glucan (Forrest & Wainwright, 1977; Johansen, Wood *et al.*, 1993; Zhou, Robards *et al.*, 2000).

Extraction of β-Glucan

To evaluate the solution and aggregation behavior of β-glucan, it is necessary to isolate it from the (food) matrix. However, it should be borne in mind that the matrix might affect the behavior of the β-glucan. Furthermore, the extraction of β-glucan is still associated with major problems, such as low yields, low purities and polysaccharide de-polymerization, although high proportions of β-glucan from oats and barley are considered to be water-soluble. When using mild conditions, e.g. water extraction at low temperatures, it is not possible to extract all the β-glucan present in the sample, leading to low yields. As discussed in detail elsewhere, the pH, temperature and choice of solvent may affect the yield in β-glucan extraction (Webster & Wood, 2011). Higher yields have been obtained by using alkali solutions and higher temperatures (Dawkins & Nnanna, 1993; Wood, Paton *et al.*, 1977). However, harsh extraction methods, such as those used for the

commercial extraction of mixed-linkage β-glucan, can change the structure and nature of the polysaccharide, for example, the M and the ability to form aggregates (Ahmad, Anjum *et al.*, 2010). Such changes in the structure and properties may in turn affect the beneficial health effects of β-glucan. It is therefore of interest to develop an extraction method that minimizes the detrimental effects of extraction on β-glucan in order to preserve its native properties. No proteases and no harsh conditions were used during the extraction procedure developed in this work in order to maintain any possible proteinaceous moieties and the structural properties as present in foods.

Asymmetric Flow Field-Flow Fractionation

As mentioned above, cereal β-glucan is naturally polydisperse in size and M, and several studies have already demonstrated the use of asymmetric flow field-flow fractionation (AF4) in combination with a MALS detector to analyze cereal β-glucan (Håkansson, Ulmius *et al.*, 2012; Ulmius, Adapa *et al.*, 2012; Ulmius, Önning *et al.*, 2012). A UV-Vis detector or a differential refractive index (dRI) detector can be used in-line to determine the concentration of the separated sample as a function of time. Samples extracted from natural materials often contain mixtures of biomolecules, and it is necessary to specifically identify the β-glucan, e.g. through fluorescence labelling (Ulmius, Adapa *et al.*, 2012; Ulmius, Önning *et al.*, 2012). For a more detailed description of the set-up and the detectors utilized in each study, the reader is referred to the attached publications and manuscripts.

As the polymer size can influence the properties of a functional food ingredient, there is considerable interest in analytical methods that can provide detailed information on molecular size. The great variations in the size and complexity of β-glucan still pose a challenge in the analysis and characterization of this polymer. During recent decades, a number of analytical techniques have been used for size determination, such as static and dynamic light scattering, viscometry and ultracentrifugation. A drawback of these methods is, however, that they only provide an average size. If the polymer being investigated exhibits a broad size distribution, a separation method is required. It has been well established that AF4, a sub-technique of the field-flow fractionation (FFF) family, is very suitable as a separation method for the analysis of large polydisperse polysaccharides. (Giddings, 1993, Nilsson, 2013; Gomez, Navarro *et al.*, 1997; Tügel, Runyon *et al.*, 2015; Ulmius, Adapa *et al.*, 2012; Ulmius, Önning *et al.*, 2012). AF4 has the ability to analyze high M macromolecules ($M > 10^7$ g/mol), with a separation range from approximately 2 nm to >1 μm. Compared to other methods, such as size-exclusion chromatography (SEC), AF4 is considered a gentle separation method

due to the relatively low shear forces to which the sample is exposed in the separation channel.
A brief introduction to the AF4 technique is given below. For a more detailed description of the fundamental theory of AF4, the reader is referred to the literature (Litzén & Wahlund, 1989; Litzén & Wahlund, 1991a, 1991b; Litzén, 1993; Litzén, Walter *et al.*, 1993; Wahlund & Giddings, 1987; Wahlund & Litzén, 1989).

Short Introduction to AF4

AF4 is considered to be a chromatography-like technique without a stationary phase, where the retention time (t_r) is directly related to the diffusion coefficient D of the analyte, which is in turn directly related to the hydrodynamic radius (r_{hyd}) of the analyte through the Stokes-Einstein equation (Einstein, 1905; Giddings, 1981; Wahlund & Giddings, 1987). The main component in an AF4 instrument is a thin open channel without any packing material, where separation takes place. Compared to chromatographic techniques such as SEC, the absence of a stationary phase makes AF4 a gentle method that enables the separation of macromolecules under close to native conditions.

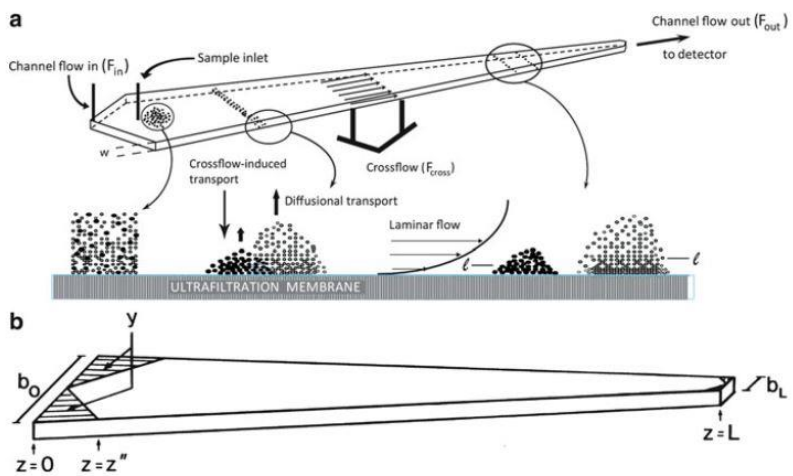

Figure 2 The illustration of the principle of trapezoidal AF4
a illustrates the separation of two analytes of different size. Filled symbols represent large analytes and open symbols represent small analytes. First, a homogeneous mixture was injected onto the channel through the sample inlet tube and was then relaxed and focused in the channel at a short distance in eluting direction from the sample inlet. Due to the parabolic flow, the two analyte populations will start to migrate with different velocities when the elution flow starts. By the end of the channel the two analyte zones are resolved. w represents the channel thickness and l is the center of gravity distances of the analyte populations from the accumulation wall. **b** illustrates the geometry of a trapezoidal channel. z is the distance along the length axis, z'' is the length of the trapezoidal cuts and L is the whole channel length. b_0 is the breadths of the channel's trapezoid at the inlet, whereas b_L is the breadths at the outlet ends. (Reproduced with permission from Litzén & Wahlund, 1991a, ©American Chemical Society)

In field-flow fractionation in general, an aqueous carrier is continuously pumped through the channel to establish a laminar flow. The sample is introduced onto the channel by injection, and transported down the channel by the carrier flow. During transport, the sample is subjected to a field and forced to accumulate close to the wall, the so called accumulation wall (Giddings, 1966; Giddings, 1973; Giddings, 2000). For AF4, the applied field is an additional flow perpendicular to the carrier flow, the so-called crossflow, and the accumulation wall is a semi-permeable membrane, which allows the carrier to pass through, while the sample accumulates close to the membrane (Wahlund & Giddings, 1987). An illustration of the principles of AF4 can be found in Fig. 2.

Two main elution modes are used with AF4, the Brownian or so-called normal mode and the steric/hyperlayer mode (Schimpf, Caldwell *et al.*, 2000).

In brief, the Brownian mode is referred to as "normal elution order", where smaller analytes elute earlier than larger analytes due to fast migration through the channel. It is the most commonly implemented operating mode of AF4 as it governs the migration of submicrometer particles and almost all macromolecules. The analytes are driven by the crossflow down towards the accumulation wall, creating a concentration gradient, which causes diffusion of the analytes away from the accumulation wall. Analytes with smaller hydrodynamic size have a higher diffusion coefficient, and thus a greater equilibrium distance from the accumulation wall than larger analytes. This is illustrated in the upper part of Fig. 3. Due to these opposing motions, a "cloud of analytes" with a steady state distribution (concentration profile during focusing/relaxation step) will be created, with higher concentration at the accumulation wall and exponentially decreasing concentration with increasing distance from the wall. Separation in an AF4 instrument thus takes place as analytes of different sizes have different distances to the wall, and the penetration of analytes with smaller sizes into faster streamlines of the parabolic flow increases, resulting in faster migration of the smaller analytes than the larger (more compressed) analytes (lower part of Fig. 3). Hence, in Brownian mode, smaller particles will elute earlier than larger analytes (Giddings, 1988; Giddings, 1991).

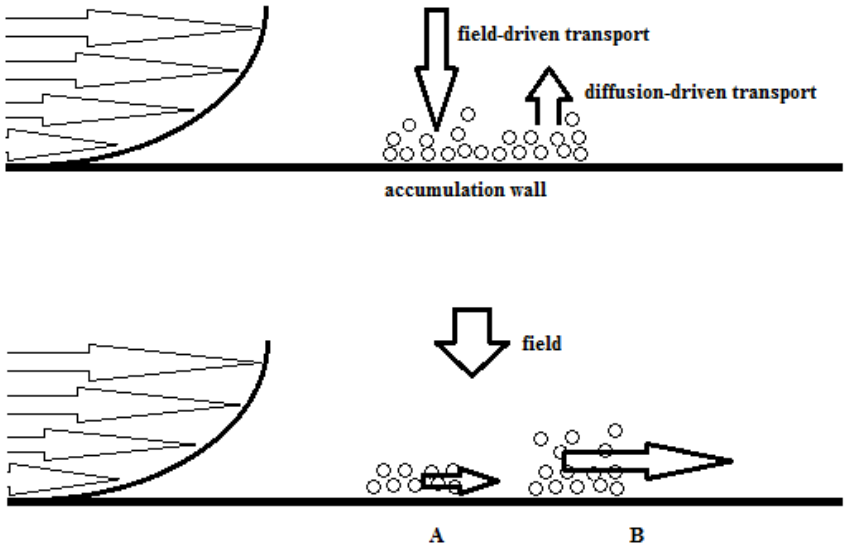

Figure 3 Schematic drawing of the Brownian (normal) mode in AF4
Upper panel: The balance between field-driven transport and diffusion-driven transport, causing an equilibrium distribution of particles. Lower panel: Separation of particles A and B occurs as the applied field (here: crossflow) exerts different forces on the particles, forming "clouds" of different thicknesses. The "clouds" are eluted with different velocities due to the parabolic flow profile. (Adapted from Schimpf, Caldwell & Giddings, 2000)

In Brownian mode, the aforementioned diffusion coefficient, D, of an eluting component can be calculated according to Eq. 1.

$$D = \left(\frac{t^0 Q_c w^2}{6\,V^0}\right) * \frac{1}{t_r} \qquad \text{(Eq. 1)},$$

where t^0 is the void time, Q_c is the crossflow rate, w is the channel thickness, V^0 is the geometric volume of the channel and t_r the retention time of the eluted component.

Using different detectors in-line with the AF4 instrument enables different kinds of results to be obtained, such as the concentration, M distribution, size distribution and the conformation of the analyzed polymer. When discussing size distributions, it is, however, necessary to take into account the polymer sizes being analyzed. One way of expressing the size of a polymer is the root-mean-square radius (r_{rms}), also known as the radius of gyration (r_g), which can be obtained experimentally using light scattering techniques (see: AF4-MALS for Molar Mass and Size Detection). r_{rms} is mathematically defined in Eq. 2.

$$\langle r_{rms}^2 \rangle = \frac{1}{2n^2} * \sum_i^n \sum_{j \neq i}^n \langle h_{ij}^2 \rangle \qquad \text{(Eq. 2)},$$

where n is a monomer unit, h_{ij} is the distance between the mass of i and the mass of j and $\langle h_{ij}^2 \rangle$ is the square of the averaged distance of all masses, and the sum over all segments results in r_{rms}.

Another way of expressing the size is the hydrodynamic radius (r_{hyd}), also known as the Stokes radius. As indicated above, r_{hyd} can be calculated from the diffusion coefficient D by means of the Stokes-Einstein equation (Eq. 3, Einstein, 1905),

$$r_{hyd} = \frac{kT}{6\pi\eta D} \qquad \text{(Eq. 3)},$$

where k is the Boltzmann constant, T is the temperature (in K) and η is the viscosity of the solvent. By combining Eqs. 1 and 3, it is possible to directly obtain the r_{hyd} distribution from the AF4 elution time (Eq. 4):

$$r_{hyd} = \frac{kTV^0}{\pi\eta t^0 Q_c w^2} * t_r \qquad \text{(Eq. 4)}.$$

The other elution mode in AF4 is the steric/hyperlayer mode (Caldwell, Nguyen *et al.*, 1979). This mode is commonly used when analyzing molecules and particles larger than 1 µm, as their diffusion away from the accumulation wall is negligible due to their large size. Here, the Brownian mode is no longer acting (Giddings, 1988; Giddings, 1991; Giddings & Myers, 1978). The analytes are forced down towards the accumulation wall by the crossflow and are only stopped when reaching the wall. Larger particles will hence, form a thicker layer, extending one radius above the accumulation wall. Due to their larger radius, the larger particles will be displaced more rapidly by the channel flow during elution, resulting in an inverted elution order. However, flow-induced hydrodynamic lift forces may act on large particles, driving them away from the accumulation wall and causing the particles to form layers at different levels in the channel (Caldwell, Nguyen *et al.*, 1979). When these layers are higher up in the channel than two radii of the analyte, this mode is called the lift-hyperlayer mode, also causing an inverted elution order. It is often not possible to distinguish between steric and lift-hyperlayer mode as both mechanisms occur in paralell, resulting in it being called the steric/hyperlayer mode (Schimpf, Caldwell *et al.*, 2000).

Hence, the AF4 technique suffers from limitations when analyzing samples with very broad size distributions, such as β-glucan. The challenge is to obtain adequate

separation of all the components over the whole size distribution, especially the separation of small analytes from the void volume, where a high crossflow is needed. However, a high crossflow will lead to long elution times with insufficient detectability of the large components, as they may be forced too close to the accumulation wall, or may even be virtually immobilized due to the high field strength. Therefore, a programmed field is recommended, starting with a high crossflow to resolve small sample components, and gradually reducing the crossflow with time to enable the elution of larger molecules under a weaker field in the same experimental run. The decrease in field (decay) can be linear, stepwise or exponential (Kirkland, Dilks Jr *et al.*, 1992; Leeman, Wahlund *et al.*, 2006; Wahlund, Winegarner *et al.*, 1986). For exponential decay, the half-life ($t_{1/2}$) of the decay should not be less than approximately 2.5 min to avoid extensive errors in the determination of r_{hyd} (Håkansson, Magnusson *et al.*, 2012). In general, shorter t_r and good separation and detectability will be obtained when the crossflow conditions are optimized.

AF4-MALS for Molar Mass and Size Detection

By connecting the AF4 instrument to a MALS detector, both the M and r_{rms} can be determined directly without the need for internal or external calibration with standards. In the work described in this thesis, MALS was utilized to obtain only M, r_{rms} and Kratky plots (see below), and the reader is referred to the literature for a detailed description of the technique (Wyatt, 1993; Zimm, 1948).

In brief, macromolecules and colloids in solution will scatter light. The scattering intensity depends, among other things, on the M of the species in solution, and is expressed as a function of the scattering angle θ (Eq. 5), where θ is the angle between the incident light and the scattered light ($\theta = 0\,°$ describes the direction of unscattered incident light):

$$\frac{R_\theta}{Kc} = M_w P(\theta) - 2A_2 {M_w}^2 P^2(\theta)c + \cdots \qquad \text{(Eq. 5)},$$

where R_θ is the Rayleigh ratio (given by Eq. 6), K is an optical constant given by Eq. 7, c is the concentration in weight of the analyte in solution, M_w is the weight-average M and A_2 is the second virial coefficient.

$$R_\theta = \frac{i_{u,\theta} * r^2}{I_0 * (1 + cos^2\theta)} \qquad \text{(Eq. 6)},$$

where $i_{u,\theta}$ describes the intensity of the scattered light passing through the detector at the angle θ, *r* is the distance between the molecule and the detector, and I_0 is the intensity of the incident beam.

$$K = \frac{2\pi^2 n_0^2}{\lambda_0^4 N_A} * \left(\frac{dn}{dc}\right)^2 \qquad \text{(Eq. 7)},$$

where n_0 is the refractive index of the solvent used, λ_0 is the wavelength of the incident light when in vacuum, N_A is Avogadro's number and $\frac{dn}{dc}$ describes the differential refractive index increment.

From Eq. 5 it can be concluded that the Rayleigh ratio, R_θ, is directly proportional to the weight-average M. Eq. 6 shows that R_θ is directly proportional to the intensity of the scattered light of the sample at an angle θ from the incident light beam. The particle scattering function $P(\theta)$ describes in detail the angular dependency of the scattered light intensity according to Debye (1915). After simplification, $P(\theta)$ can be approximated to Eq. 8 (Guinier, 1939):

$$P(\theta) = 1 - \frac{16\pi^2}{3\lambda^2} \langle r_{rms,z} \rangle^2 \, sin^2 \left(\frac{\theta}{2}\right) \qquad \text{(Eq. 8)},$$

where λ is denoting the wavelength of the incident light when in the medium.

Upon combining Eqs. 5 and 8, it can be seen that for $\theta = 0$, the expression will simplify to Eq. 9, as $P(\theta)$ will approach unity.

$$\frac{R_\theta}{Kc} = M - 2A_2 M^2 \mathrm{c} + \cdots \qquad \text{(Eq. 9)}.$$

If we now assume that either the concentration or the second virial coefficient A_2 is very low, and can be regarded as negligible, the M could, in theory, be obtained directly by analyzing the intensity of the scattered light at the angle 0° (Eq. 10) (Debye, 1944), as *K* and c are often known.

$$\frac{R_{\theta=0}}{Kc} = M \qquad \text{(Eq. 10)}.$$

However, this is not possible in practice as it is impossible to distinguish between unscattered light passing through the analyte solution and the light that is scattered

by the analyte. Therefore, a MALS detector is used, with which scattered light is detected at several angles greater than 0° and the intensity at $\theta = 0°$ is obtained by extrapolation. Different models (e.g. the Berry model) are used for this extrapolation, depending on the shape and conformation of the analyzed samples (Berry, 1966; Wyatt, 1993).

Conformation Studies

Additional information can be obtained in the conformation and shape of the analytes by utilizing the angular dependence of the scattered light of the analyte in a MALS detector. This is done by plotting the experimentally obtained data in so-called Kratky plots (Burchard, 1983; Kratky & Porod, 1949a, 1949b), where $u^2P(u)$ is plotted versus u, with:

$$u = r_{rms} * q \qquad \text{(Eq. 11)},$$

and the scattering vector, q, is given by:

$$q = \frac{4\pi n_0}{\lambda_0}\sin(\frac{\theta}{2}) \qquad \text{(Eq. 12)}.$$

The data obtained are then compared with model calculations for different polymer shapes, as shown in Fig. 4.

Another way of obtaining more information on the conformation of the analytes in the sample is by plotting the ratio of r_{rms} to r_{hyd} vs. M. A brief overview of the interpretation of these ratios is given in Table 1, where common values and their respective conformations are listed.

Table 1 r_{rms}/r_{hyd}
Overview of different ratios of r_{rms}/r_{hyd} and their corresponding conformation (+ theoretical values, ^ experimental results).

r_{rms}/r_{hyd}	Conformation	Reference
>2	Elongated, rod-like	Coviello, Kajiwara, Burchard, Dentini & Crescenzi, 1986^; Wittgren, Borgström, Piculell & Wahlund, 1998^
1.5-2	Random coil	Burchard, 1983+; Roger & Colonna, 1992^
1-1.5	Branched molecule	Burchard, 1999+
0.775	Homogenous, smooth sphere	
<0.7	Micro gel	Schmidt, Nerger & Burchard, 1979^

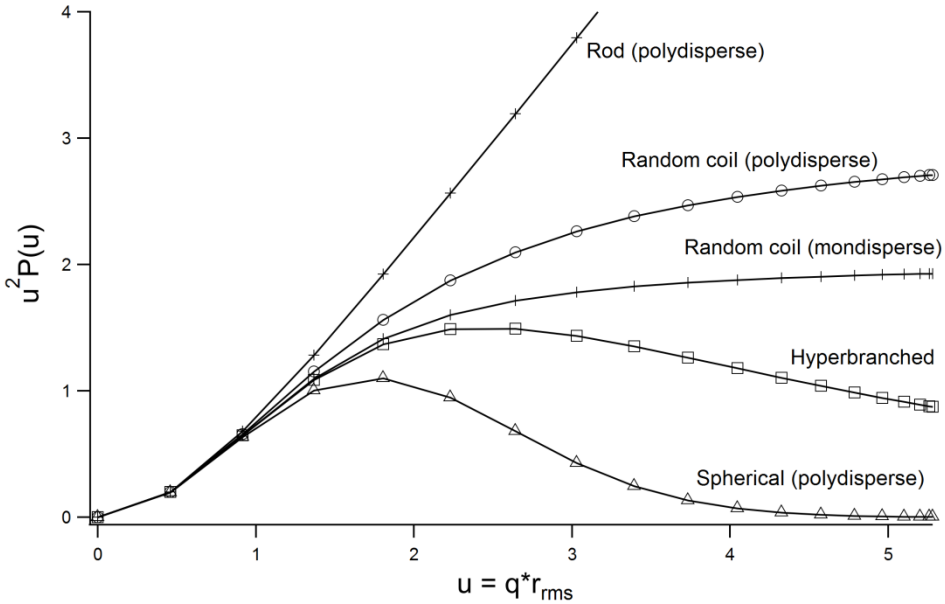

Figure 4 Kratky Plots
Kratky plots showing the result of model calculations for different polymer shapes.

Objectives

The main objectives of the presented study can be briefly summarized as follows:

- to develop an extraction procedure for analysis of β-glucan with relatively high and reproducible purities from oat and barley, while keeping their molecular integrity as present in food intact;
- to investigate conformational properties as well as the solution and aggregation behavior of the extracted cereal β-glucan from oat and barley;
- to obtain information in regard to more structural aspects such as persistence length of the macromolecular structures;
- to study the interplay of proteins on the β-glucan aggregation behavior in solution;
- to determine the structural and conformational features of oat β-glucan under simulated *in vitro* gastrointestinal conditions; and
- to further evaluate the applicability of AF4 for the efficient separation and characterization of molecules with wide M and size distributions.

Part I of the thesis (Papers I-VI) provides a more detailed insight into the extraction and characterization of β-glucan from oats and barley. The relationship between the solution and aggregation behavior of β-glucan is discussed in relation to the proteins present in the samples. Although a great deal of effort has been devoted to the development of AF4 in recent years, the analysis of natural macromolecules and polysaccharides with broad size distributions can still be challenging and care should be taken when evaluating the data. Part II of this thesis (Papers VII and VIII), deals with the phenomena observed when studying macromolecules with AF4 in combination with MALS.

Part I – Aggregation and Solution Behavior of β-Glucan and its Possible Beneficial Health Effects

5 years oat to be enough time, but I am barley done yet.

Extraction and Solution Behavior of β-Glucan

Paper I describes an extraction procedure for non-modified β-glucan from oat and barley, in which the high integrity of this polysaccharide as present in food matrices, is preserved. The extracts were of relatively high purity, considering the mild conditions applied in the method developed.

The main aim of developing a new extraction method was to preserve the native properties of the β-glucan polymer, e.g. M and/or protein-β-glucan linkages. Therefore, no proteases were added during the extraction procedure in the hope of maintaining any possible proteinaceous moieties or cross-links. Furthermore, harsh conditions, such as elevated pressure and alkaline treatments, were not used as these could affect the molecular integrity of the samples. The extraction procedure is described in detail in Paper I. The purity of the extracts obtained in this study varied between 65% (w/w) (Papers I and II) and 87% (w/w) (Paper VI) for oat β-glucan, and 53% (w/w) for barley β-glucan (Papers I and II). These purities can be described as good, bearing in mind the mild extraction conditions used and the method developed to maintain the native, natural structure of the polymers.

Purities of 57% (w/w) have been reported for oat β-glucan (Immerstrand, Bergenståhl *et al.*, 2009), and up to 90% (w/w) (Papageorgiou, Lakhdara *et al.*, 2005) for barley β-glucan extracted under acidic conditions (pH 4) when using more severe conditions, e.g. proteases or alkali treatment. The main impurities in

the extracts obtained in the present study were starch (11% (w/w) in both oat and barley extracts), various dextrins, probably originating from the degradation of starch during extraction, and very small quantities of other non-glucose monosaccharides (e.g. xylose, mannose, arabinose and galactose, see Paper I, Table 1). The main non-starch impurities were water-soluble sugar residues and polysaccharides originating from cereal polysaccharides, and/or hemicelluloses, such as arabinoxylans, glucomannans and starch dextrins (present in the endosperm or the cell walls of the grains).

AF4-MALS-dRI was used to obtain fundamental information on the structure, M distribution and r_{rms} distribution of the β-glucan. The plots in Fig. 5 show the fractionation patterns of the extracts (see also Figs. 3 and 4 in Paper I). The extracts consist of very polydisperse β-glucan with very high M fractions, and M distributions of 10^5-10^8 g/mol for both oat and barley β-glucan. The r_{rms} distributions were 20-120 nm for oat and 50-140 nm for barley β-glucan. However, the results from the differential M distributions of the extracts indicate that oat β-glucan is on average somewhat larger than barley β-glucan (Paper I, Fig. 5 and Paper II, Fig. 1C,D). These findings are in agreement with those in the literature (Beer, Wood *et al.*, 1997; Ahmad, Anjum *et al.*, 2012).

The results regarding the conformation and aggregation behavior of β-glucan are presented in Paper II. Information was obtained by plotting the ratio of r_{rms}/r_{hyd} (Paper II, Fig. 1C,D, black dots) versus M, and compared to theoretical and experimental values from the literature (as presented in the Introduction, Table 1 and Paper II, Table 2). Oat β-glucan showed a variety of conformational properties (Paper II, Fig. 1C, black dots), including a rod-like and stiff conformation (r_{rms}/r_{hyd} ~1.7–3.0) at low M, random coil conformation and branched molecular structures (1–1.5), down to a micro gel structure (<0.7) for high M above 2 x 10^6 g/mol, suggesting that the high M species are present as a micro gel (see Table 1). The plot of r_{rms}/r_{hyd} vs. M for the barley β-glucan (Paper II, Fig. 1D, black dots) showed lower maximum values for the low M species, starting at around 1.5, suggesting branched structures. As M increases, the value of r_{rms}/r_{hyd} decreases down to a value of 0.5, also indicating a micro gel for the high M β-glucan.

Additional information on the conformation was obtained from the in-line MALS data after separation in the AF4 channel by constructing Kratky plots (Fig. 6; see as well Paper II, Fig. 2). Data sets with two different values for t_r, chosen to represent low and high M species, were used for each sample. To aid the interpretation of the results, theoretical Kratky conformation values are plotted together with the experimental data. The data for the shorter t_r provided no conclusive information about possible conformations for oat and barley β-glucan for $u < 1$ (Paper II, Fig. 2A). This could be the result of too small analytes at this t_r compared to the wavelength of the MALS light source (λ = 658 nm) (Hupfeld, 2009).

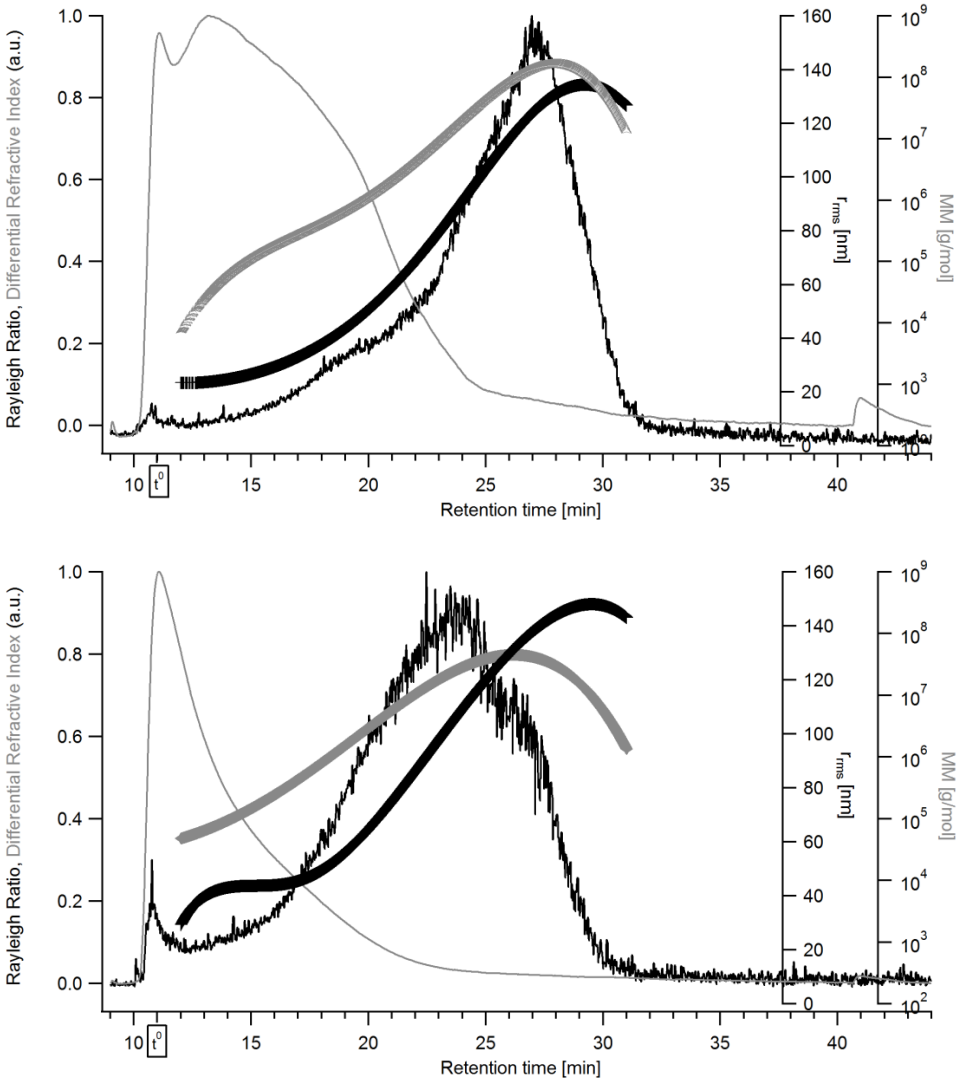

Figure 5 Typical AF4-MALS-dRI fractograms of β-glucan obtained in this study
Top: Oat β-glucan, bottom: barley β-glucan. The Rayleigh Ratio from MALS (solid black line) and dRI (solid gray line) are shown on the left y-axis and the r_{rms} (black crosses) and M distribution (here: MM, gray crosses) are shown on the right y-axis. t^0 is indicated on the x-axis.

For species with higher M and hence, longer t_r, the data obtained for oat β-glucan (red dots) approach values between those for a monodispersed random coil conformation (c) and hyperbranched structures (d) (Fig. 6 and Paper II, Fig. 2B; compare also Fig. 4). The analyzed fractions of β-glucan that elute from the AF4 channel have a narrow size distribution, although they are not monodisperse. Therefore, a monodispersed random coil conformation (c) seems less probable. In

conclusion, both oat and barley β-glucan seem to agree with the theoretical predictions for hyperbranched structures (d). However, it is well known that β-glucan molecules are linear, unbranched polysaccharides and are therefore expected to behave as chain-like molecules, being somewhat flexible due to β(1→3) linkages.

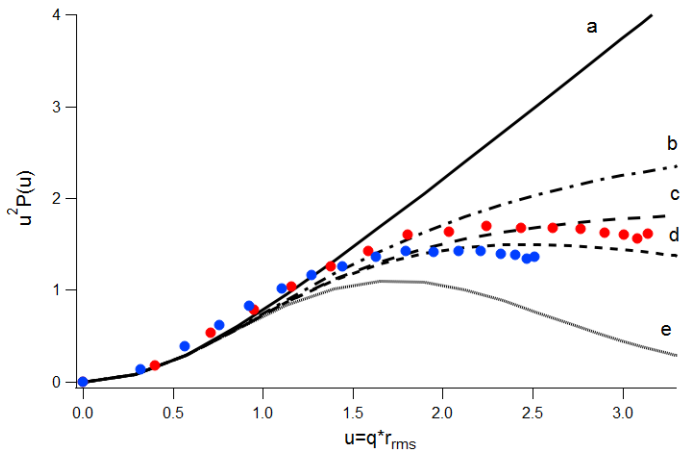

Figure 6 Kratky plots
Kratky plots for oat (red dots) and barley (blue dots) β-glucan obtained from MALS data at t_r = 27 min for oat and t_r = 23.5 min for barley (as shown in Paper II, Fig. 1A and 1C, respectively). The curves labelled a-e give the theoretical values for a = polydispersed rod, b = polydispersed random coil, c = monodispersed random coil, d = hyperbranched structure and e = polydispersed sphere (Andersson, M. *et al.* 2004).

Hence, only aggregated structures of a linear β-glucan molecule are likely to exhibit hyperbranched conformational properties. Håkansson, Ulmius *et al.*, (2012) have suggested and discussed such structures. They suggested that linear chains assemble along each other, forming a somewhat denser core with additional chains protruding into the surroundings, as illustrated in Fig. 7. Vårum, Smidsrød *et al.* (1992) also suggested that cereal β-glucan forms micellar-like aggregates, and Grimm, Krüger *et al.* (1995) described β-glucan as fringed micelle structures with a dense core resulting from the alignment of β-glucan chains.

Sitar, Aseyev *et al.* (2014) found evidence that linear poly(methacrylic acid) chains with random coil structures also followed the Kratky plot theory for hyperbranched structures, where the atactic species predominated. The function of hyperbranched structures (Fig. 4, Fig. 6 (d)) is often referred to as Debye-Bueche scattering function. This function describes hyperbranched but flexible chains and micro gels, originating from chemically cross-linked flexible chains (Savin & Burchard, 2004; Burchard 2004), which is in agreement with the presented results

showing that cereal β-glucan assembles and forms (hyperbranched-like structural) aggregates.

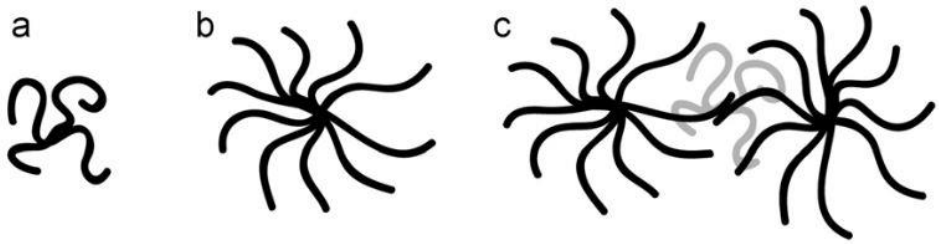

Figure 7 Schematic illustration of possible structures suggested for β-glucan
a and b resemble supramolecular aggregates where M(a) < M(b), while c resembles aggregated supramolecular aggregates. Illustration reproduced from Håkansson *et al.* (2012).

To further confirm the theory of aggregated structures, cryo-TEM micrographs were obtained (Fig. 8). In the case of oat β-glucan (Fig. 8A), loosely aggregated and highly polydisperse arrangements appearing as large hyperbranched structures or even complex networks were observed. Furthermore, the oat β-glucan aggregates appear in the micrographs like hyperbranched structures, confirming the results obtained with the Kratky plots.

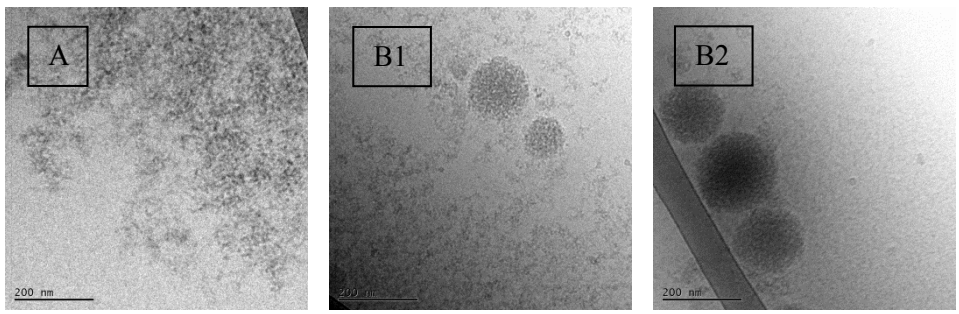

Figure 8 Cryo-TEM images
Cryo-TEM images of oat (A) and barley (B1,B2) β-glucan extracts.

Similar results have been reported previously by Buléon, Véronèse *et al.* (2007), who investigated polymeric aggregates of linear amylose molecules. They found that long linear chain molecules formed a wide spread aggregation network, which could induce the β-glucan to behave similarly to branched molecules with high M. This wide spread network supports the speculation of micro gel formation due to

aggregation, as suggested by the r_{rms}/r_{hyd} results (Paper II, Fig. 1C) (Burchard, 1999). Barley β-glucan displays a similarly complex network of highly aggregated, loosely arranged structures (Fig. 8B1,B2), and therefore, the same conclusions can be drawn as discussed above for oat β-glucan. However, in addition, relatively dense, very well-defined and spherical aggregates are visible with sizes between 50 and 170 nm. To the best of the author's knowledge, such distinct, relatively well-defined aggregates have not been reported previously. The cryo-TEM images support the assumption of highly aggregated β-glucan structures and as both oat and barley β-glucan have r_{rms}/r_{hyd} ratios < 0.5, the different aggregation pattern observed with cryo-TEM is surprising. It appears that the cereal origin of β-glucan plays an important role towards their physico-chemical properties and behavior, and thus, the cereal origin might influence their beneficial health effects. Denser structures, as seen for barley β-glucan, will form denser slurries (micro gels) in the gut, which may be able to prevent the human body from absorbing macronutrients, toxins or cholesterol better than loosely arranged micro gel structures, as seen for oat β-glucan.

As previously discussed by Lazaridou & Biliaderis (2007), a considerable variety in M and β(1→3) and β(1→4) linkage distributions in the β-glucan structure stands in direct correlation with their cereal origin, influencing their extractability (Immerstrand, Bergenståhl *et al.*, 2009). In agreement with that, Immerstrand, Bergenståhl *et al.* (2009) suggested that the variety, geographical origin and growing conditions of the cereals could influence their extraction behavior, yield and purity. It is therefore reasonable to expect the solution and aggregation behavior to differ between β-glucan from different origins.

To illustrate the possible impact of the applied extraction procedure, Fig. 9 shows a comparison of the β-glucan extracted from oat using the mild extraction method described in Paper I and a β-glucan commercially extracted from oats (OBC90, purity ≥90% (w/w)), as used in Paper III. The major difference in the applied extraction procedures is that for the extraction of OBC90, mild alkali conditions (pH 9-10) were used and a protein removal step was added. Both extracts are from oats grown in Sweden. As already discussed earlier, the use of alkali solutions will increase the yields during β-glucan extraction (Dawkins & Nnanna, 1993; Wood, Paton *et al.*, 1977). It is clear from Fig. 9 that the commercially extracted β-glucan with a higher purity has a narrower size distribution, with a maximum at higher M than the gently extracted β-glucan, but only r_{rms}/r_{hyd} ratio values of below 0.5, indicating a micro gel structure. The gently extracted β-glucan shows a variety of conformational properties, including a rod-like and stiff conformation at low M, random coil conformation and branched molecular structures, and a micro gel structure for high M, as discussed in detail above. The mild and gentle extraction method may explain the differences in the characteristics of the two types of β-glucan. However, the growing conditions of the oats may also have varied.

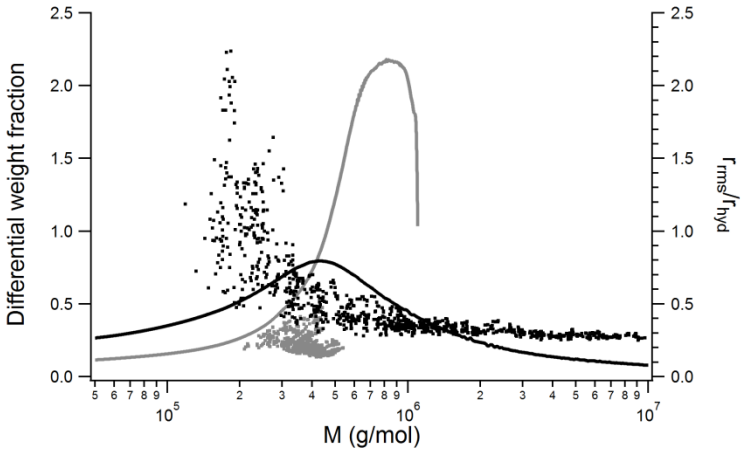

Figure 9 Differential weight fraction and r_{rms}/r_{hyd} ratio for β-glucan extracted with two different methods
Differential weight fraction (left axis, solid lines, a.u.) and r_{rms}/r_{hyd} (right axis, dots) for the extracted β-glucan from oat using the mild extraction method described in Paper I (black) and a commercially extracted β-glucan, also from oats (gray, OBC90, purity ≥90% (w/w)), both plotted vs. M.

AF4-MALS-dRI combined with fluorescence (FL) detection enabled the identification of specifically labelled β-glucan in the fractograms over most of the size distribution (Paper I, II, III, V and VI). However, the specific labelling of proteins to visualize possible polysaccharide-protein interactions or protein contamination of the extracts gave no results. Neither did the analysis of total protein content show the presence of proteinaceous matter. It was therefore concluded that no proteins are covalently bound to β-glucan. Nevertheless, since proteins in the complex β-glucan systems, although not covalently bound to the β-glucan, might play an important role in the formation of ultra-high M aggregates and may contribute significantly to the health benefits of β-glucan, a study was designed to help understand the potential of proteins promoting aggregate formation in β-glucan (Paper III).

β-Glucan and Proteinaceous Matter

The β-glucan extract was mixed with two different proteins, whey protein (WP) and gliadin, at different ratios and pH values and investigated utilizing batch UV transmission spectroscopy (Paper III).

Distinct aggregation was observed. The results for the WP-β-glucan mixture suggested that the degree of aggregation was more dependent on the β-glucan concentration than on the protein concentration (Paper III, Fig. 2A). Aggregates seem to form rapidly, as the transmission decreased immediately after mixing

(Paper III, Fig. 3A). No aggregates were detected at pH values above 4 for the WP-β-glucan mixture, or above pH 5 for the gliadin-β-glucan mixture. The transmission also varied for the same protein-β-glucan ratios. Therefore, the protein content in the aggregates was analyzed using the *Dumas Method* (Dumas, 1831). For WP, the results ranged between 10 and 50 %, whereas no significant difference was detected between the different protein-β-glucan ratios. Nevertheless, a tendency in the data suggested that higher levels of β-glucan in solution led to the formation of aggregates with a higher protein content. The percentage of protein in aggregates formed with the gliadin-β-glucan mixtures was low (below 3%) compared to their initial value, and no significant difference was found between the ratios. The formation of aggregates seems to depend not only on the pH, but also on the type of protein.

WP is a mixture of different proteins (serum albumins, α-lactoglobulins, β-lacto-globulins, and others) with isoelectric points (pI) in the pH range 4.8 to 5.3. Therefore, WP is closer to its pI at pH 4 than at pH 3 and hence, less soluble. The pI value of gliadin is 6.4. It seems that a lower pI value might be in direct correlation to the pH at which aggregates are formed between β-glucan and the respective protein.

During digestion in the human gastric tract, the pH value is below about pH 3, taking into account the substantial buffering effect of a consumed meal on the pH in the fasting state (~ pH 2; Minekus, Alminger *et al.* 2014). Therefore, the two proteins investigated in this study would facilitate aggregate formation of β-glucan in the gastric tract. The aggregation of β-glucan and the formation of viscous slurries in the gut are thought to be important factors in the beneficial health effects of β-glucan, as discussed in literature (e. g. by Regand, Chowdhury *et al.*, 2011). The proteins in cereal grains or other foodstuffs high in protein may thus enhance the ability of β-glucan to form aggregates and viscous slurries in the gut and to serve as a functional food with health benefits. β-Glucan also appears to capture proteins in aggregates, thus preventing them from being digested in the stomach or small intestines. Proteins can be transported with dietary fiber into the colon, where essential amino acids can be absorbed by the colon walls, preserving the intestinal mucosa. As gliadin is rich in glutamine, which is considered a major energy source for epithelial cells of the mucosa, and is involved in the recovery and preservation of intestinal mucosa, it is vital for the human body to transport glutamine into the colon for fermentation (Kanauchi & Agata, 1997; Kaya, Ceylan *et al.*, 2007). β-Glucan can promote this transport by aggregation with gliadin.

The results presented in Paper VI show that at pH 3 β-glucan is slightly net negatively charged, with a ζ-potential of -0.19 ± 0.07 mV, whereas both the proteins used in the study described before (Paper III) are below their pI, and thus positively charged. It is therefore reasonable to suggest that electrostatic interactions between β-glucan and the proteins lead to the formation of an insoluble complex. At pH ≥ 7, both the β-glucan (ζ-potential = -1.53 ± 0.08 mV,

Paper VI) and the proteins are net negatively charged and repel each other, explaining the lack of aggregate formation.

However, β-glucan is considered a neutral polysaccharide, which leads to the question of the origin of the detected net charges. Ghotra, Vasanthan *et al.* (2007) reported on the presence of C-6 carbon bound phosphomonoesters in purified oat β-glucan in addition to an unknown form of phosphorus, most likely phospholipids or phosphoproteins, probably causing β-glucan to appear to be net negatively charged. In agreement with the results in Paper VI, Vårum & Smidsød (1988) suggested a slight net negative charge on β-glucan aggregates. The presence and concentration of phosphate in the β-glucan extract was investigated using the *Murphy and Riley method* (Murphy & Riley, 1962; for details, see Paper III). A value of 0.136±0.002 mg P (as phosphate)/L was obtained for β-glucan in solution, which is equivalent to 0.027% phosphate (w/w, dry basis). Phosphate residues, although found only in small quantities, could give rise to the net negative charge observed on β-glucan explaining the suggested electrostatic interactions between the polysaccharide and proteins. However, it is difficult to believe that such low amounts of phosphate would be able to induce aggregate formation in high M species to the extent observed in the experiments described above. If the phosphate groups were irregularly distributed within the β-glucan molecule, they could form clusters in the β-glucan polymer chain, as has been shown previously for other polysaccharides, such as amylopectin (Blennow, Bay-Smidt *et al.*, 2000). In addition, phosphate substituents could be unevenly distributed over the whole M distribution. Unfortunately, no firm conclusions could be drawn from the results obtained in this study.

The addition of NaCl at a concentration of 340 mM creates an ionic strength in the system that is able to screen any electrostatic interactions. The transmission of the protein-β-glucan mixtures with added NaCl was significantly higher than without NaCl, confirming that electrostatic interactions play a major role in the interaction and aggregation of the macromolecules. This finding was also confirmed by ellipsometry (Paper III, Fig. 5). However, the detailed role of charged groups in the β-glucan molecule during the aggregation process still requires further investigation, in which other forces contributing to aggregation, e.g. apolar effects should be considered. In conclusion, different proteins show different behavior in aggregates with β-glucan, and the aggregation pattern seems to originate from electrostatic forces.

A direct connection between β-glucan and proteins was seen in Paper IV and Paper V as well.

Beer is one of the world's most popular beverages, and is consumed in large quantities, being ranked third after water and tea (Max, 2005). Beer is mainly composed of water, barley or another cereal grains, and is flavored using hops, together resulting in complex macromolecular structures containing

polysaccharides and proteins. The composition of macromolecules in beer is highly dependent on the brewing and mashing process during production. Moreover, the physicochemical properties of polysaccharides and proteinaceous molecules can greatly influence consumers' perception of beer, e.g. in terms of foam stability (Bamforth, 2004).

In Paper IV, the macromolecular composition of three different kinds of beers was investigated. The reference beer was a typical saccharification rest for American pale ale, and was compared to a protein rest beer with an additional heating step of 50 °C for 30 min before saccharification to maintain optimum activity of the proteases present; and a β-glucan rest beer with an additional heating step of 37 °C for 30 min before saccharification to maintain the optimum activity of the β-amylases present.

The beers were investigated using AF4-UV-MALS-dRI, and the results showed that the mashing conditions during brewing influenced the concentrations and range of M of the components in the beer significantly. Furthermore, it was found that the proteins affected the aggregation behavior of the macromolecules. Treatment with proteinase-K to degrade proteins affected the hydrodynamic size of the β-glucan molecules, and simultaneously reduced the amount of detectable β-glucan. In contrast, treatment with β-glucanase, to reduce the amount of β-glucan in the beers, resulted in no difference in the protein content. These results are not easy to explain. However, it is evident that there is a distinct relationship between the two macromolecules.

As the foam stability is directly correlated to the concentration of proteins and β-glucan in the beer (Asano, Shinagawa *et al.*, 1982; Bamforth & Kanauchi, 2003; Bamforth, 2004, 2012), the *Derek Rudin standard method* was used to investigate the foam stability of the different beers (Rudin, 1957; Bamforth, 2012). The results showed that the reference beer, with the highest amount of protein and β-glucan, had the highest foam stability. Lower amounts of protein (= protein rest beer) or β-glucan (= β-glucan rest beer), led to a beer with lower foam stability, compared to the reference beer.

More compelling evidence of a direct relation of protein and β-glucan was observed in a study utilizing brewer's spent grain, a by-product of beer production high in protein and fiber, thus supporting the theory that proteins promote the formation of β-glucan aggregates with ultra-high M (Paper V).

Analysis of the UV-active analytes of the extracts at short t_r suggested co-elution of low M β-glucan with proteins (Paper V, Fig. 5A,B). To eliminate proteins from the extracts, the extracts were enzymatically treated before being re-analyzed. Prior to enzymatic digestion, the enzymes used were tested for possible β-glucanase activity to avoid degradation of the β-glucan. No activity was found. A decrease in UV signal intensity was observed at t_r = 15 min after enzymatic treatment, indicating the presence of proteinaceous matter in this peak. The reason

for the UV peak not disappearing completely could be due to remaining proteins, remnants of the enzymes used, or insufficient digestion time. However, a distinct shift in t_r of the dRI signal (representing the concentration of the sample with time) was observed, from ~40–50 min to ~30–40 min (Paper V, Fig. 5C), implying a decrease in hydrodynamic size of large species to smaller hydrodynamic sizes. The same behavior was observed in the FL signal with specifically labelled β-glucan: the high M population of β-glucan shifted to shorter t_r after enzymatic digestion (Fig. 10; before (solid line) and after (dashed line) proteolytic enzymatic *in vitro* digestion).

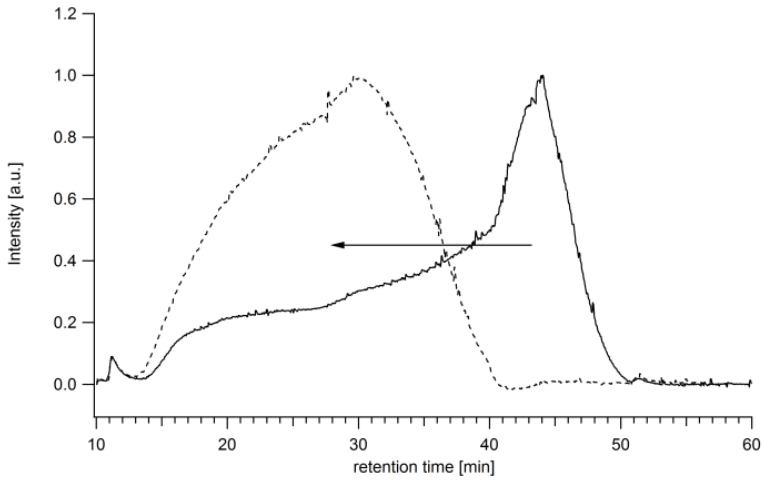

Figure 10 AF4-FL fractogram of β-glucan before and after enzymatic digestion
AF4-FL fractogram of selectively labelled β-glucan from Tipple malt, before (solid line) and after (dashed line) proteolytic enzymatic *in vitro* digestion (see also Paper V, Fig. 5).

It is clear from Fig. 10 that the proteolytic enzymatic treatment reduced the hydrodynamic size of the β-glucan, suggesting a direct relationship between β-glucan and proteins. As discussed above, it was possible to provoke the aggregation of β-glucan by the addition of proteins. The results presented in Paper V showed a change in the size and concentration of the ultra-high M species after enzymatic protein digestion, suggesting that proteins help β-glucan to form aggregates. The degradation of proteins will, in turn, cause the β-glucan to de-aggregate, decreasing the hydrodynamic size. Furthermore, it should be borne in mind that proteolytic enzymes are naturally present in the gastrointestinal tract, which could have implications on the size and M of β-glucan in the colon due to the digestion of proteins.

β-Glucan during *in vitro* Digestion

While proteolytic enzymes, which occur naturally in the gastrointestinal tract, can influence the β-glucan aggregation behavior (Paper V), the study described in Paper VI demonstrates the effect of *in vitro* gastric and gastrointestinal digestion on β-glucan conformation and aggregation, regardless of the presence of proteins.

The fractograms of the β-glucan investigated before simulated *in vitro* digestion showed broad size and M distributions (Paper VI, Fig. 1). After gastric digestion, a shift in M and r_{rms} to lower values was observed. This is surprising, as β-glucan is a dietary fiber and should not be digested in the human digestive tract. After simulated gastrointestinal digestion, M and r_{rms} values returned to higher values again. The conformational properties, in terms of the r_{rms}/r_{hyd} ratio for the β-glucan before and after gastric and gastrointestinal digestion, showed micro gel conformation for high M species, whereas the Kratky plots showed hyperbranched structures. These results are in good agreement with those presented in Paper II, and have been discussed above.

NMR spectroscopy measurements on the digested and undigested samples showed no increase in the reducing ends of the β-glucan (Paper VI). If β-glucan were enzymatically digested, more reducing ends of the polysaccharide chain would be created. The ratio of β(1→3) and β(1→4) glycosidic bonds in the extracts was calculated from the ^{1}H-NMR spectrum and found to be 1:2.5, which is in agreement with values in the literature (Mikkelsen, Jespersen *et al.*, 2010). NMR analysis of β-glucan after gastric digestion showed an identical spectrum as the undigested β-glucan (for details see Paper VI, Fig. 6). From these results it appears that no chemical degradation took place, as also reported by Johansson, Virkki *et al.* (2006), who found that no degradation of oat β-glucan occurred after 12 h incubation at pH 1 and 37 °C.

Another interesting finding reported on in Paper VI was the ability of the β-glucan to interact with bile acids. The association of β-glucan and bile salts during human digestion has been suggested to mediate fecal excretion of the bile salts and stimulate their production in the liver using blood cholesterol, resulting in a decrease in blood cholesterol levels (Andersson, Ellegard *et al.*, 2002; Kim & White, 2010). It was also found that β-glucan molecules can interact with bile acids as bile acids induced changes in the detected apparent density of aggregated oat β-glucan (Paper VI, Fig. 5B). As this could indicate a direct molecular interaction, further studies were performed using NMR to observe possible changes in the resonance of bile acid carbon atoms when in solution with β-glucan. The possibility of an interaction between β-glucan and bile salts has already been discussed in literature (Kim & White, 2010, 2011; Zacherl, Eisner *et al.*, 2011), and NMR has been demonstrated to be a powerful tool for the detection of complex binding mechanisms on the molecular level (Gunness, Flanagan *et al.*,

2010; Mikkelsen, Cornali *et al.*, 2014). However, no detailed investigations on β-glucan-bile salt interactions *in vitro* (simulated gastrointestinal conditions) or on the impact of bile acids on β-glucan conformation have been described previously.

Sodium cholate and sodium deoxycholate were chosen as model bile acids as they are the main components of bile (Ifeduba & Akoh, 2015). Possible interactions between bile acids and β-glucan were first investigated in terms of changes in apparent density in β-glucan extracts with and without bile acids (Paper VI, Fig. 5B). Their presence in the digesta increased the apparent density, whereas any synergistic effects resulting from digestive enzymes have been ruled out earlier in this study. To further investigate this finding, the chemical shifts of the bile acid in the ^{13}C-NMR spectrum were recorded, with and without the presence of β-glucan. Paper VI gives the relative chemical shifts, assigned according to Barnes & Geckle (1982). The addition of β-glucan led to many small changes in the chemical shifts of several of the carbon atoms of bile acids (upfield and downfield), suggesting a direct, dynamic molecular association between β-glucan and bile acids, most likely altering the formation of bile acid micelles and their working mechanism by reducing their mobility (Gunness, Flanagan *et al.*, 2010; Gunness Flanagan *et al.*, 2016). A reduction in the intensity of the resonance peaks of bile acids in the presence of β-glucan (spectrum not shown) provides evidence of their entrapment in the local environment of the aggregated β-glucan structures. However, bile acids had no effect on the chemical shifts of the β-glucan. This could be expected, as bile micelles are very small in size (~ 2–5 nm) compared to the β-glucan molecule, and the high abundance of non-interacting glucose units, in contrast to the bile acids, might further explain the lack of change in chemical shifts (Cheng, Oh *et al.*, 2014; Gunness, Flanagan *et al.*, 2016). Nevertheless, it could be concluded from these results that β-glucan can interact and entrap bile acids, leading to a reduction in blood cholesterol levels and thus improving the health of the consumer.

Conclusions

A mild extraction method was developed to isolate β-glucan from oat and barley showing good yields and purity, without influencing the original structure and molecular integrity of the β-glucan. AF4-MALS-dRI in combination with UV and FL detection was shown to be suitable for the investigation of complex β-glucan systems derived from grains. The extracted β-glucan had ultra-high M and a broad size distribution, and exhibited a range of conformational properties in terms of aggregation behavior. β-Glucan formed highly polydisperse polymers in aqueous solution, and highly aggregated structures with high M in a widely distributed network and micro gel formation. It was concluded that single, long-chain molecules assembled to form aggregates similar to hyperbranched structures, although β-glucan is a linear molecule. In addition, the cereal origin of β-glucan was discussed to have an impact on the specific health benefits, through different aggregation pattern.

No proteins were found to be covalently bound to the β-glucan. However, due to the in the literature suggested importance of proteinaceous moieties in the functionality of β-glucan and its beneficial health effects additional experiments have been performed and evidence was obtained leading into the direction of a close connection between β-glucan and proteins. Further aggregation studies showed the ability of β-glucan and two proteins to aggregate through electrostatic interactions at low pH. The net negative charge on β-glucan was suggested to originate from low amounts of phosphate found in the β-glucan solution. The exact aggregation process and resulting composition of the aggregates had not yet been fully elucidated, but appears to depend on the type of protein. A direct correlation was found between β-glucan and proteins, which constitutes a further step towards the understanding of the beneficial health effects of β-glucan.

β-Glucan may promote the transport of proteins into the distant colon where the resulting free essential amino acids can be absorbed, increasing mucosal health. Proteins appear to aid the aggregation and micro gel formation of β-glucan, which is believed to be the main reason for the health benefits of β-glucan. Furthermore, β-glucan was shown to be able to bind toxic compounds such as bile acids, what can lead to a reduction in the cholesterol levels in the blood.

Future Outlook

The work described in this section has shed light on the complex solution behavior of β-glucan and the often suggested direct relation between proteins and β-glucan. However, further investigations should be performed to gain a better understanding:

- The extraction method developed in this work could be improved to obtain better yields and reproducible purities, and to scale up the extraction process.
- The surprisingly dense and well-defined aggregates of barley β-glucan should be investigated more thoroughly, as their solution behavior may be different from that of the highly aggregated network structures observed for both oat and barley β-glucan.
- Further AF4 experiments should be performed for the size determination of the protein-β-glucan aggregates.
- *In vitro* models should be carried out simulating the digestion of β-glucan in the human body in the presence of proteins.
- *In vivo* models should be used to explore the effect of β-glucan on the digestive system in reducing or preventing inflammatory diseases.
- The importance of the conformation of β-glucan should be investigated in order to improve our understanding of the impact of colloidal differences on the beneficial health effects of β-glucan.

Part II – Co-Elution Effects when Analyzing Complex Samples with AF4-MALS

There are no problems – only challenges! (Lars Nilsson)

Co-Elution due to Steric/Hyperlayer Mode

If AF4 is to be used for the analysis of molecules with ultra-high M ($M>10^7$ g/mol), branched conformation or with high polydispersity, such as β-glucan or amylopectin, the method must be optimized to obtain accurate results. However, challenges may still arise, which must be addressed. A common phenomenon encountered in AF4 is the effect of co-elution of low amounts of very large species with smaller molecules, resulting in overestimation of the analyzed size. The transition between the two modes of elution, Brownian (normal) mode and steric/hyperlayer mode (as presented in the introduction), is dependent to some degree on the separation conditions, e.g. the crossflow velocity. Both modes may occur simultaneously, thus leading to co-elution. This was seen in the present work when analyzing amylopectin (Paper VII).

Amylopectin is the larger and more branched polymer found in starch, together with amylose. Starch is not only the most important source of energy in the human diet, it is also widely used in industry, e.g. in the food and pharmaceutical industries (Eliasson & Gudmundsson, 2006). Therefore, it is important to identify means of characterizing starch in terms of its M and size. Amylopectin is a polydisperse biopolymer with ultra-high M and with a high degree of branching; it consists of α(1→4) linked glucose units with α(1→6) branches (Pérez & Bertoft, 2010; Buléon, Colonna *et al.*, 1998). AF4 in combination with various detectors has already been shown to be a suitable method for the analysis of amylose and amylopectin (Perez-Rea, Bergenståhl *et al.*, 2015; Rolland-Sabaté, Colonna *et al.*,

2007; van Bruijnsvoort, Wahlund *et al.*, 2001; Wahlund, Leeman *et al.*, 2011; You, Stevenson *et al.*, 2002).

When analyzing waxy maize amylopectin with AF4-MALS, a substantial curvature was observed in the light scattering data, resulting in a poor fit in the size determination (Fig. 11; Paper VII, Figs. 2 and 4). If this curvature is taken into account and two linear fits are used – one for small scattering angles and one for large scattering angles – substantial deviations in the M are obtained, giving higher and lower values of r_{rms}, respectively. From these results, it is clear that the co-elution of larger analytes, despite being present at very small amounts, interferes with the MALS analysis.

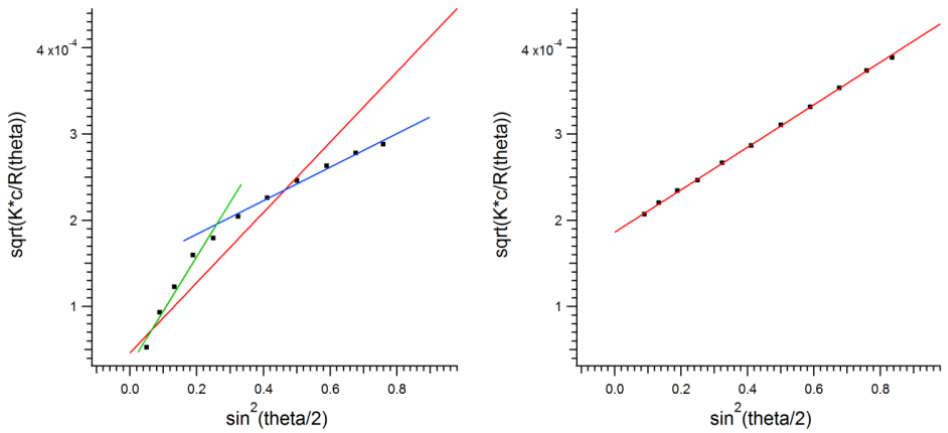

Figure 11 Berry plots of MALS data
Berry plots and corresponding 1st order fit (red) to MALS data for amylopectin, before (left) and after (right) filtering of the sample before injection. The left panel illustrates fitting taking the curvature into account, using two linear fits (green at small scattering angles; blue at large scattering angles).

As explained in the Introduction (Eq. 5), large particles scatter light more, resulting in a higher Rayleigh ratio. Therefore, large analytes will dominate the light scattering data at small angles, resulting in the overestimation of r_{rms}, which is also seen in the determination of r_{rms}/r_{hyd}. The r_{rms}/r_{hyd} ratio was determined (at t_r of 27 min), which for the hyperbranched polymer structure of amylopectin should result in a value of 1.0-1.3 (as obtained experimentally by Roger, Bello-Perez *et al.*, 1999). Using the larger scattering angles for r_{rms} determination (Fig. 11, blue) resulted in a value of r_{rms}/r_{hyd} of 1.0; while using the lower scattering angles for r_{rms} determination (Fig. 11, green) resulted in a value of r_{rms}/r_{hyd} of ~2.4. The latter value seems less likely as it represents a stiff, rod-like conformation (Hansen, 2004). It is thus clear that using the smaller scattering angles leads to an overestimation of r_{rms} due to the co-elution of larger species. After filtering the sample, the selectivity of the r_{rms} increased in comparison to the unfiltered sample, resulting in a ratio of r_{rms}/r_{hyd} of 1.2. After filtering the sample, a linear fit was

obtained over the whole range of scattering angles, as can be seen in the Berry plot in Fig. 11 (right).

Filtering the sample prior to injection improved the light scattering measurements, with only a small loss of sample (4% (w/v) for the amylopectin sample). Based on these results, possible changes in the quality of the data obtained when analyzing the β-glucan extracts was investigated. The sample was filtered through a 0.45 μm pore size syringe filter with a cellulose acetate membrane prior to injection onto the AF4 channel. In this case, filtering had no significant effect on the results (Paper I, Fig. 2), and the MALS and dRI signals, as well as the size distribution of the β-glucan were similar before and after filtering (the difference in mass recovery from the AF4 channel was only 3% (w/v)). However, a distinct improvement was seen in the signal-to-noise ratio of the r_{rms} size distribution after filtration, especially at sizes below 60 nm. The presence of only low amounts of large analytes, which could be aggregated or only partially dissolved structures, can cause significant disturbances in r_{rms} determination, when co-eluting in the steric/hyperlayer mode of AF4 (Caldwell, Nguyen *et al.*, 1979). As a consequence of these results, filtering was performed on all β-glucan samples prior to injection (Paper I, II, III, V, VI).

In conclusion, the presence of even very low amounts of large and ultra-large species in the sample can give rise to noisy MALS signals, resulting in erroneous size determination (Paper VII, Andersson, Wittgren *et al.*, 2001; Perez-Rea, Bergenståhl *et al.*, 2015). Care should therefore be taken when using AF4 in combination with MALS, and filtering of the sample is recommended prior to injection to improve the quality of data, despite the fact that small amounts of sample might be lost.

Co-Elution in Polymer Mixtures – The Downturn

Another often observed phenomenon when analyzing macromolecules is a downturn in the M distribution signal from MALS data at high t_r (Fuentes, Zielke *et al.*, 2016; Otte, Pasch *et al.*, 2011; Pitkänen & Striegel, 2014; Paper I, II, IV and V). This downturn is often explained as being an artifact of the fractionation analysis, and is attributed to various errors during detection and/or data processing. However, this downturn may represent a real effect, more precisely, smaller molecules eluting at longer t_r. Separation in the channel depends directly on differences in the r_{hyd} of the analytes, and hence, a downturn could occur if the sample contains populations of molecules for which the relation between r_{hyd} and M differ significantly. An example of this is analyte populations that differ in their conformation (mass and size).

To test this hypothesis, mixtures of heterogeneous macromolecular polysaccharides with different conformations and hydrodynamic sizes, but overlapping M distributions, were analyzed (Paper VIII). The molecules chosen were glycogen, pullulan and poly(ethylene) oxide (PEO). Pullulan and PEO are linear macromolecules, while glycogen is a highly branched polysaccharide. Branched molecules and linear molecules in random coil conformation with the same M are likely to have different hydrodynamic sizes, as illustrated in Fig. 12. Although the molecules have the same M, they should elute at different t_r.

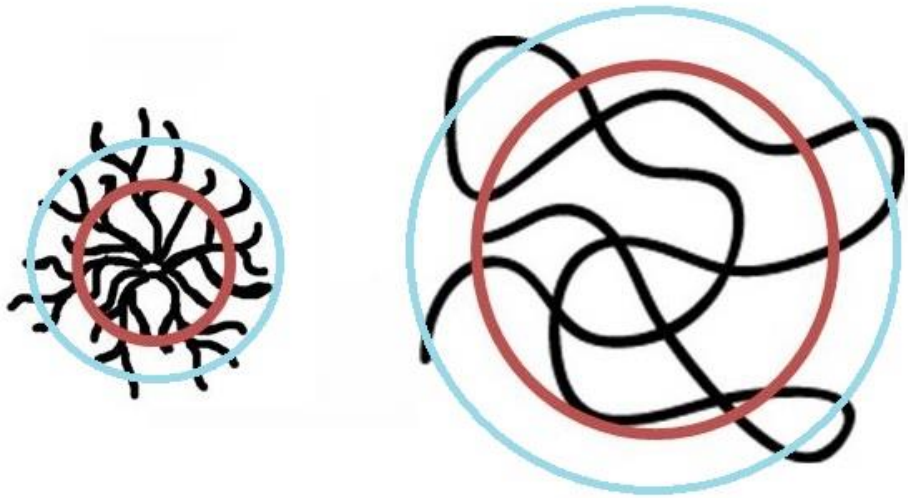

Figure 12 Glycogen and pullulan
Graphic illustration of r_{rms} (red) and r_{hyd} (blue) for hyperbranched glycogen (left) and the linear polysaccharides pullulan or PEO (right), with similar M, showing the differences in r_{rms} and r_{hyd}.

AF4-MALS-dRI results from the analysis of a mixture of pullulan and glycogen can be seen in Fig. 13. These two polysaccharides have a similar range of M with overlapping MALS signals, while glycogen elutes after a shorter t_r, as expected due to its more compact and branched structure. Striking differences can be seen in the M distributions of the individual polymers and the mixture.

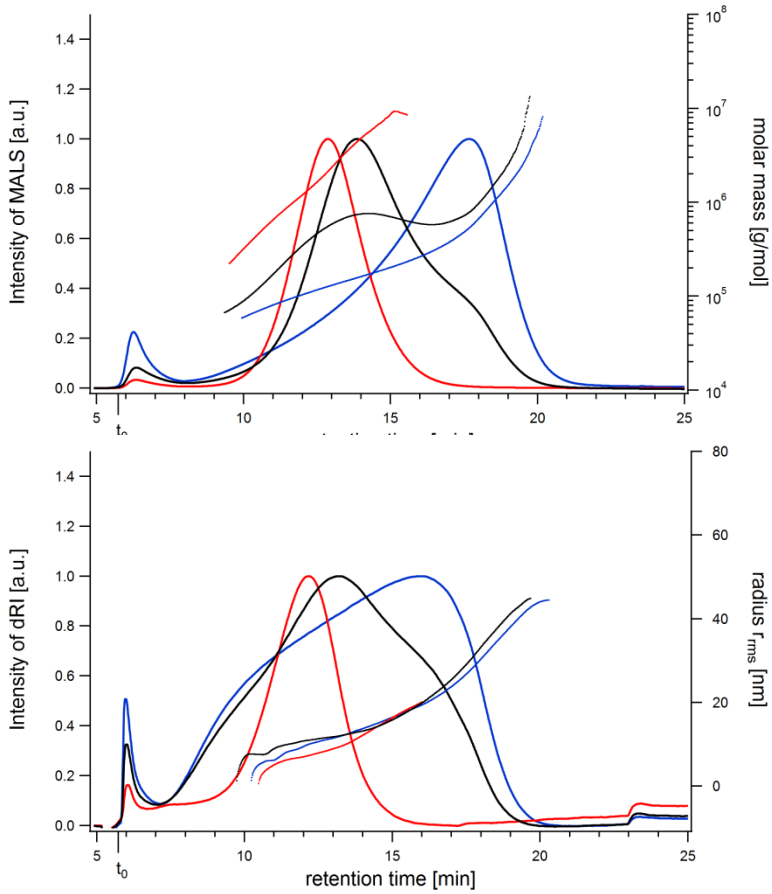

Figure 13 Fractograms of pullulan and glycogen
Fractograms of pullulan (blue), glycogen (red), and a mixture of both (1:1, black). The upper figure shows the Rayleigh ratio (from MALS) (solid lines, left y-axis) and M distribution (dots, right y-axis) plotted as a function of t_r. The lower figure shows the dRI signal (solid lines, left y-axis) and the calculated r_{rms} distribution (dots, right y-axis) as a function of t_r.

The more branched and compact glycogen has a higher M than the linear pullulan at any given t_r. In contrast, the M determined for the mixture at any t_r is an intensity-weighted average of both polymers. The M distribution of a mixture where comparable amounts of both glycogen and pullulan elute together lies in between those of the individual polysaccharides in the early t_r region. However, at t_r > ~15 min, the pullulan sample should be the dominating component of the mixture, as seen in the dRI fractogram for the individual polymers. A downturn in M of the mixture can be seen at ~14 min, followed by a subsequent upturn at ~16 min. It should be noted that in the high t_r region, where only pullulan should be eluting, the M curve for the mixture is also displaced towards lower t_r compared to the curve for the elution of pullulan alone. An indication that correct size

separation indeed occurred can be seen in the lower part of Fig. 13, where the r_{rms} distributions for glycogen (red), pullulan (blue) and a mixture of both (black) are shown as a function of t_r. It should be borne in mind that the separation mechanisms in AF4 are based on r_{hyd} (and not r_{rms}). The individual samples and the mixture show a steady monotonic increase in size (here: r_{rms}) over the complete fractogram and no downturn is observed, indicating that size separation does indeed occur. Moreover, only minor deviations are apparent when directly comparing the r_{rms} for pullulan, glycogen and their mixture. A slight shift of the mixture curve towards lower t_r is also visible for the r_{rms} distribution (as for the M data, Fig. 13, top) at long t_r, where pullulan should be dominant.

This study showed that the often observed downturn phenomenon could be the result of complex mixtures and insufficient resolution. To obtain better insight into what happens during the focusing or elution step in AF4 analysis of complex mixtures such as the pullulan/glycogen mixture, pullulan was mixed with the linear unbranched polymer, PEO, which at any given radius, has a lower M than pullulan. No downturn was observed in the M distribution of the mixture (Paper VIII, Fig. 2). As for the glycogen/pullulan mixture (Fig. 13), the M distribution of the pullulan/PEO mixture is also seen between the curves for the polymers analyzed individually at short t_r, where PEO and pullulan co-elute. When the contribution from PEO starts to decrease (t_r=14 min), a distinct upturn in the M curve for the mixture can be observed. At longer t_r, where only the pullulan contribution should be important, the curve for the mixture lies above that for pullulan alone, supporting the conclusion that the maximum of the pullulan peak is shifted towards shorter t_r in the mixture. Furthermore, analysis of the r_{rms} vs. t_r data indicates that size separation also took place for this mixture. Similar results were obtained for a mixture of two PEO polymers with distinctly different M (results not shown).

From these results it is clear that there can be a significant loss of M selectivity in mixtures of complex polymers with different size distributions, when the individual polymers have distinctly different relationships between r_{hyd} and M, leading to a downturn or upturn. When co-elution is taking place the observed M distribution of the polymers is the average of the results for each individual polymer, and a kink in the curve (down- or upturn) occurs at the t_r where the polymer with the largest size dominates.

It should be mentioned that variations in the relation between the M and r_{hyd}, such as those discussed here, can also occur for a sample consisting of a single type of polymer. This could be due, for instance, to different polymer structures distributed over the size range, or partial aggregation of polymers in solution leading to larger particles or aggregates with different (scaling) properties than the original individual molecules. Such particles are therefore expected to elute at longer t_r than the individual polymer, which could cause a leveling off, or a downturn, in the M distribution curve vs. t_r.

An example for that can already be seen in Fig. 13, where a downturn for the glycogen M at high t_r was observed. In this case, a fraction of high M (supramolecular) glycogen species, also called as glycogen α-particles, may be responsible for this downturn. Glycogen α-particles consist of several β-particles, which are primary glycogen molecules (Manners, 1991). Therefore, it is important to learn more about the elution and aggregation behavior of polymers to ensure that the results obtained for M distributions are interpreted in a consistent and reliable way, and that certain phenomena are not treated as artifacts.

The shifts in the peak maxima of MALS and dRI as a function of t_r (Fig. 13) consistently observed in the polymer mixtures, compared to the individual polymers, seem to be a more challenging matter. This effect might be due to interactions between the mixed polymers in solution. Possible interactions between molecules should be considered as particularly important in AF4 during the focusing/relaxation step of the analysis. A sample zone of higher concentration than the originally injected sample is generated during the focusing/relaxation step, and it is thus of interest to investigate the events taking place during this step in order to determine the influence this might have on separation in AF4. Unfortunately, it is not possible to draw any firm conclusions about the observed shifts in t_r at this point in the study. A lack of knowledge on how complex mixtures (inter)act during the focusing/relaxation step leads to difficulties in finding experimental approaches suitable for studying the observed results, and their explanation.

Conclusions

The use of AF4 with various detectors was shown to be a powerful and suitable method for the analysis of complex macromolecules and mixtures. However, care should be taken during sample preparation and data analysis. Filtering the sample prior to injection onto the AF4 channel was demonstrated to improve the data quality with only small sample losses. The often observed “downturn” phenomenon was shown to be a real result, which should not be regarded as an artifact and neglected. Peak shifts and peak broadening in complex polymer mixtures were observed, but it was not possible to determine the mechanism(s) responsible. Further experiments are needed to improve our understanding of the intricate mechanisms behind the separation of complex mixtures.

Future Outlook

The work described in this section shed light on method development and the effects of sample complexity during AF4 analysis. However, further experiments should be performed to gain better insight.

- Further knowledge should be obtained regarding the behavior of polymer mixtures during AF4 separation, for example, possible phase separation phenomena and interactions between the molecules in the mixture.
- The concentration profile should be determined precisely during the focusing/relaxation step in AF4, possibly using computer simulations.
- Experiments should be performed on different polymers to determine whether the conclusions presented in this work apply to a broader spectrum of substances.

References

Acker, L., Diemair, W. & Samhammer, E. (1955) Über das Lichenin der Hafers. Eigenschaften, Darstellung und Zusammensetzung des schleimbildenden Polysaccharides. (The lichenin of oats. 1. Properties, preparation and composition of the muciparous polysaccharides.) Zeitschrift für Lebensmittel-Untersuchung und – Forschung, 100, 180-188.

Adolphi, U. & Kulicke, W.-M. (1997) Coil dimensions and conformation of macromolecules in aqueous media from flow field-flow fractionation/multi-angle laser light scattering illustrated by studies on pullulan. Polymer, 38(7), 1513-1519.

Agbenorhevi, J. K., Kontogiorgos, V., Kirby, A. R., Morris, V. J. & Tosh, S. M. (2011). Rheological and microstructural investigation of oat β-glucan isolates varying in molecular weight. International Journal of Biological Macromolecules, 49(3), 369-377.

Ahmad, A., Anjum, F. M., Zahoor, T., Nawaz, H. & Ahmed, Z. (2010) Extraction and characterization of beta-D-glucan from oat for industrial utilization. International Journal of Biological Macromolecules, 46(3), 304-309.

Ahmad, A., Anjum, F. M., Zahoor, T., Nawaz, H. & Dilshad, S. M. R. (2012) Beta Glucan: A Valuable Functional Ingredient in Foods. Critical Reviews in Food Science, 52, 201-212.

Anderson, J. W. & Bridges, S. R. (1984) Short Chain Fatty Acid Fermentation Products of Plant Fiber Affect Glucose Metabolism of Isolated Rat Hepatocytes. Proceedings of the Society for Experimental Biology and Medicine, 177(2), 372-376.

Andersson, M., Ellegård, L. & Andersson, H. (2002) Oat bran stimulates bile acid synthesis within 8 h as measured by 7α-hydroxy-4-cholesten-3-one1'2'3'. The American Journal of Clinical Nutrition, 76(5), 1111-1116.

Andersson, M., Wittgren, B. & Wahlund, K. G. (2001) Ultrahigh molar mass component detected in ethylhydroxyethyl cellulose by asymmetrical flow field-flow fractionation coupled to multiangle light scattering. Analytical Chemistry, 73, 4852-4861.

Asano, K., Shinagawa, K. & Hashimoto, N. (1982) Characterization of hazeforming proteins of beer and their roles in chill haze formation. Journal of the American Society of Brewing Chemists, 40(4), 147-154.

Atkins, P. W. (2006) In Physical Chemistry (8th Ed.); Atkins, P. W., de Paula, J. (Eds.) Oxford University Press, Oxford New York, 200-240.

Autio, K., Myllymaki, O., Suortti, T., Saastamoinen, M. & Poutanen, K. (1992) Physical properties of (1→3),(1→4)-beta-D-glucan preparates isolated from Finnish oat varieties. Food Hydrocolloids, 5, 513-522.

Baik, B. K. & Ullrich, S. E. (2008) Barley for Food: Characteristics, Improvement, and Renewed Interest. Journal of Cereal Science, 48(2), 233-242.

Bamforth, C. W. (2004) The relative significance of physics and chemistry for beer foam excellence: theory and practice. Journal of the Institute of Brewing, 110(4), 259-266.

Bamforth, C. W. (2012) Foam: Practical Guides for Beer Quality (1st Ed.); American Society of Brewing Chemists.

Bamforth, C. W. & Kanauchi, M. (2003) Interactions between polypeptides derived from barley and other beer components in model foam systems. Journal of the Science of Food and Agriculture, 83(10), 1045-1050.

Barnes, S. & Geckle, J. M. (1982) High resolution nuclear magnetic resonance spectroscopy of bile salts: individual proton assignments for sodium cholate in aqueous solution at 400 MHz. Journal Lipid Research, 23(1), 161-170.

Beer, M.U., Wood, P. J. & Weisz, J. (1997) Molecular weight distribution and (1→3)(1→4)-β-D-glucan content of consecutive extracts of various oat and barley cultivars. Cereal Chemistry, 74, 476-480.

Berry, G. C. (1966) Thermodynamic and Conformational Properties of Polystyrene. I. Light-Scattering Studies on Dilute Solutions of Linear Polystyrenes. The Journal of Chemical Physics, 44(12), 4550-4564.

Blennow, A., Bay-Smidt, A. M., Olsen, C. E. & Møller, B. L. (2000) The distribution of covalently bound phosphate in the starch granule in relation to starch crystallinity. International Journal of Biological Macromolecules, 27(3), 211-218.

Bränning, C. E. & Nyman, M. E. (2011) Malt in Combination with Lactobacillus Rhamnosus Increases Concentrations of Butyric Acid in the Distal Colon and Serum in Rats Compared with Other Barley Products but Decreases Viable Counts of Cecal Bifidobacteria. The Journal of Nutrition, 141(1), 101-107.

Buléon, A.; Colonna, P., Planchot, V. & Ball, S. (1998) Starch granules: structure and biosynthesis, International Journal of Biological Macromolecules, 23, 85-112.

Buléon, A., Véronèse, G. & Putaux, J.-L. (2007) Self-Association and Crystallization of Amylose. Australian Journal of Chemistry, 60(10), 706-718.

Burchard, W. (1983) Static and dynamic light scattering from branched polymers and bio-polymers. Advances in Polymer Science, 48, 1-124.

Burchard, W. (1999) Solution Properties of Branched Macromolecules. In Roovers J. (Ed) Branched Polymers II. Advances in Polymer Science, Springer, Berlin Heidelberg, 143, 113-194.

Burchard, W. (2004) Light Scattering Techniques. In Ross-Murphy, A. S. (Ed.), Physical Techniques for the Study of Food Biopolymers. (1st ed) Dordrecht, The Netherlands: Springer Science+Business Media, 151-213.

Caldwell, K. D., Nguyen, T. T., Myers, M. N. & Giddings, J. C. (1979) Observations on anomalous retention in steric field flow fractionation. Separation Science Technology, 14(10), 935-946.

Cheng, C. Y., Oh, H., Wang, T. Y., Raghavan, S. R. & Tung, S. H. (2014) Mixtures of lecithin and bile salt can form highly viscous wormlike micellar solutions in water. Langmuir, 30(34), 10221-10230.

Codex Alimentarius Commission (2009) Report on the 30th Session of the Codex Committee on Nutrition and Food for Special Dietary Uses, Alinorm 09/32/26, Appendix Ii, In, Vol.

Coviello, T., Kajiwara, K., Burchard, W., Dentini, M. & Crescenzi, V. (1986) Solution properties of xanthan. 1. Dynamic and static light scattering from native and modified xanthans in dilute solutions. Macromolecules, 19(11), 2826-2831.

Cui, S. W. & Wang, Q. (2009) Cell wall polysaccharides in cereals: chemical structures and functional properties. Structural Chemistry, 20, 291-297.

Cummings, J. H., Englyst, H. N. & Wiggins, H. S. (1986) The Role of Carbohydrates in Lower Gut Function. Nutrition Reviews, 44(2), 50-54.

Daou, C. & Zhang, H. (2012). Oat Beta-Glucan: Its Role in Health Promotion and Prevention of Diseases. Comprehensive Reviews in Food Science and Food Safety, 11(4), 355-365.

Dawkins, N. L. & Nnanna, I. A. (1993) Oat gum and β-glucan extraction from oat bran and rolled oats: Temperature and pH effects. Journal of Food Science, 58, 562-566.

Debye, P. (1915) Zerstreuung von Röntgenstrahlen ("Scattering of X-rays"). Annalen der Physik, 4(46), 809-823.

Debye, P. (1944) Light Scattering in Solutions. Journal of Applied Physics, 15, 338-342.

den Besten, G., van Eunen, K., Groen, A. K., Venema, K., Reijngoud, D.-J. & Bakker, B. M. (2013) The Role of Short-Chain Fatty Acids in the Interplay between Diet, Gut Microbiota, and Host Energy Metabolism. Journal of Lipid Research, 54(9), 2325-2340.

Dumas, J. B. A (1831) Précédés de l'analyse organique. Annales de Chimie et de Physique, 247, 198-213.

Ehrlein, H. & Stockmann, A. (1998) Absorption of nutrients is only slightly reduced by supplementing enteral formulas with viscous fiber in miniature pigs. The Journal of Nutrition, 128(12), 2446-2455.

Einstein, A. (1905) Über die von der molekularkinetischen Theorie der Wärme geforderte Bewegung von in ruhenden Flüssigkeiten suspendierten Teilchen. Annalen der Physik, 322(8), 549-560.

Eliasson, A.-C. & Gudmundsson, M. (2006) Starch: physicochemical and functional aspects, in: A.-C. Eliasson (Ed.), Carbohydrates in Food, 2nd Ed., Taylor &Francis Group, Boca Ratón, Florida, USA, 391–470.

European Food Safety Authority. (2009) Scientific Opinion on the Substantiation of Health Claims related to Beta-Glucans and Maintenance of Normal Blood Cholesterol Concentrations (ID 754, 755, 757, 801, 1465, 2934) and Maintenance or Achievement of a Normal Body Weight (ID 820, 823) pursuant to Article 13(1) of Regulation (EC) No 1924/2006. EFSA Journal. 7.

European Food Safety Authority.(2010) Scientific Opinion on the Substantiation of a Health Claim related to Oat Beta-Glucan and Lowering Blood Cholesterol and Reduced Risk of (Coronary) Heart Disease pursuant to Article 14 of Regulation (EC) No 1924/2006. EFSA Journal. 8.

Finnie, C. & Svensson, B. (2014) Barley Grain Proteins. In Shewry, P. R. & Ullrich, S. E. (Eds.) Barley: Chemistry and Technology, 2nd Ed. AACC Int., USA, 123-168.

Forrest, I. S. & Wainwright, T. (1977) Mode of binding of beta-glucans and pentosans in barley endosperm cell walls. Journal of the Institute of Brewing, 83, 279-286.

Fuentes, C., Zielke, C., Prakash, M., Kumar, P., Penarrieta, J. M., Eliasson, A.- C. & Nilsson, L. (2016) The effect of baking and enzymatic treatment on the structural properties of wheat starch. Food Chemistry, 213, 768-774.

Ghotra, B. S., Vasanthan, T., Wettasinghe, M. & Temelli, F. (2007). 31P-nuclear magnetic resonance spectroscopic analysis of phosphorus in oat and barley β-glucans. Food Hydrocolloids, 21(7), 1056-1061.

Gibbs, J. W. (1906) In The Scientific Papers Vol 1 Thermodynamics; Longmans, Green and Co: London, New York and Bombay, 476.

Giddings, J. C. (1966) A New Separation Concept Based on a Coupling of Concentration and Flow Nonuniformities. Separation Science, 1(1), 123-125.

Giddings, J. C. (1973) The conceptual basis of field-flow fractionation. Journal of Chemical Education, 50(10), 667-669.

Giddings, J. C. (1981) Field flow fractionation. A versatile method for the characterization of macromolecular and particulate materials. Analytical Chemistry, 53(11), 1170A-1178A.

Giddings, J. C. (1988) Field-flow fractionation. Chemical & Engineering News, 66, 34-45.

Giddings, J. C. (1991) Unified Separation Science, Wiley & Sons, Inc., USA.

Giddings, J. C. (1993) Field-flow fractionation: Analysis of macromolecular, colloidal, and particulate materials. Science, 260, 1456-1465.

Giddings, J. C. (2000) The Field-Flow Fractionation Family: Underlying Principles. In Schimpf, M. E., Caldwell, K. D., Giddings, J. C. (Eds.), Field-flow Fractionation Handbook, Wiley & Sons, Inc., USA, 31-48.

Giddings, J. C. & Myers, M. N. (1978) Steric Field-Flow Fractionation: A New Method for Separating 1 to 100 μm Particles. Separation Science and Technology, 13, 637-645.

Gomez, C., Navarro, A., Gamier, C., Horta, A. & Carbonell, J. V. (1997) Physical and structural properties of barley (1→3),(1→4)-β-D-glucan Part III. Formation of aggregates analysed through its viscoelastic and flow behavior. Carbohydrate Polymers, 34(3), 141-148.

Grimm, A., Krüger, E. & Burchard, W. (1995). Solution properties of β-D-(1,3)(1,4)-glucan isolated from beer. Carbohydrate Polymers, 27(3), 205-214.

Guinier, A. (1939) La diffraction des rayons X aux très petits angles: application à l'étude de phénomènes ultramicroscopiques. Annales de Physique, 11(12), 161-237.

Gunness, P., Flanagan, B. M. & Gidley, M. J. (2010) Molecular interactions between cereal soluble dietary fibre polymers and a model bile salt deduced from 13C NMR titration. Journal of Cereal Science, 52(3), 444-449.

Gunness, P., Flanagan, B. M., Mata, J. P., Gilbert, E. P. & Gidley, M. J. (2016) Molecular interactions of a model bile salt and porcine bile with (1,3:1,4)-beta-glucans and

arabinoxylans probed by (13)C NMR and SAXS. Food Chemistry, 197(Pt A), 676-685.

Hamer, H. M., Jonkers, D., Venema, K., Vanhoutvin, S., Troost, F. J. & Brummer, R. J. (2008) Review Article: The Role of Butyrate on Colonic Function. Alimentary Pharmacology & Therapeutics, 27(2), 104-119.

Hansen, S. (2004) Translational friction coefficients for cylinders of arbitrary axial ratios estimated by Monte Carlo simulation. The Journal of Chemical Physics, 121, 9111–9115.

Hara, H., Haga, S., Aoyama, Y. & Kiriyama, S. (1999) Short-Chain Fatty Acids Suppress Cholesterol Synthesis in Rat Liver and Intestine. Journal of Nutrition, 129(5), 942-948.

Hunter, T. (2012) Why Nature chose phosphate to modify proteins. Philosophical Transactions of the Royal Society of London, Series B: Biological Science, 367, 2513-2516.

Hupfeld, S. (2009) Size Characterisation of Liposomes Using Asymmetrical Flow Field-Flow Fractionation: Factors Influencing Fractionation and Size Determination. PhD thesis, Department of Pharmacy, Faculty of Medicine. University of Tromsø, Norway. http://munin.uit.no/handle/10037/2134, accessed 2017-10-18.

Håkansson, A., Magnusson, M., Bergenståhl, B. & Nilsson, L. (2012) Hydrodynamic radius determination with asymmetric flow field-flow fractionation using decaying cross-flows. Part 1. A theoretical approach. Journal of Chromatography A, 1253, 120-126.

Håkansson, A., Ulmius, M. & Nilsson, L. (2012) Asymmetrical flow field-flow fractionation enables the characterization of molecular and supramolecular properties of cereal beta-glucan dispersions. Carbohydrate Polymers, 87, 518-523.

Ifeduba, E. A. & Akoh, C. C. (2015) Microencapsulation of stearidonic acid soybean oil in complex coacervates modified for enhanced stability. Food Hydrocolloids, 51, 136-145.

Immerstrand, T., Bergenståhl, B., Trägårdh, C., Nyman, M., Cui, S. & Öste, R. (2009) Extraction of β-Glucan from Oat Bran in Laboratory Scale. Cereal Chemistry, 86(6), 601-608.

Johansen, H. N., Wood, P. J. & Knudsen, K. E. B. (1993) Molecular weight changes in the (1→3),(1→4)-beta-D-glucan of oat incurred by the digestive processes in the upper gastrointestinal tract of pigs. Journal of Agriculture and Food Chemistry, 41, 2347-2352.

Johansson, L., Virkki, L., Anttila, H., Esselström, H., Tuomainen, P. & Sontag-Strohm, T. (2006) Hydrolysis of β-glucan. Food Chemistry, 97(1), 71-79.

Kanauchi, O. & Agata, K. (1997) Protein, Dietary Fiber-Rich New Foodstuff from Brewer's Spent Grain Increased Excretion of Feces and Jejunum Mucosal Protein Content in Rats. Bioscience Biotechnology Biochemistry, 61(1), 29-33.

Kaya, E., Ceylan, A., Kara, N., Guven, H. & Yildiz, L. (2007) The Effect of L-Glutamine on Mucosal Healing in Experimental Colitis Is Superior to Short-Chain Fatty Acids. Turkish Journal of Gastroenterology, 18(2), 89-94.

Kim, H. J. & White, P. J. (2010) In vitro bile-acid binding and fermentation of high, medium, and low molecular weight beta-glucan. Journal of Agricultural and Food Chemistry, 58(1), 628-634.

Kim, H. J. & White, P. J. (2011) Optimizing the molecular weight of oat beta-glucan for in vitro bile acid binding and fermentation. Journal of Agricultural and Food Chemistry, 59(18), 10322-10328.

Kirkland, J. J., Dilks Jr., C. H., Rementer, S. W. & Yau, W. W. (1992) Asymmetric-Channel Flow Field-Flow Fractionation with Exponential Force-Field Programming. Journal of Chromatography A, 593, 339-355.

Kratky, O. & Porod, G. (1949a) Diffuse small-angle scattering of X-rays in colloid systems. Journal of Colloid Science, 4(1), 35-70.

Kratky, O. & Porod, G. (1949b) Röntgenuntersuchung gelöster Fadenmoleküle. Recueil des Travaux Chimiques des Pays-Bas, 68(12), 1106-1122.

Kumar, V., Sinha, A. K., Makkar, H. P., de Boeck, G. & Becker, K. (2012). Dietary Roles of Non-Starch Polysaccharides in Human Nutrition: A Review. Critical Reviews in Food Science & Nutrition, 52(10), 899-935.

Lazaridou, A. & Biliaderis, C. G. (2007) Molecular aspects of cereal beta-glucan functionality: Physical properties, technological applications and physiological effects. Journal of Cereal Science, 46(2), 101-118.

Leeman, M., Wahlund, K. G. & Wittgren, B. (2006) Programmed cross flow asymmetrical flow field-flow fractionation for the size separation of pullulans and hydroxypropyl cellulose. Journal of Chromatography A, 1134(1-2), 236-245.

Li, W., Cui, S. W., Wang, Q. & Yada, R. Y. (2010). Studies of aggregation behaviours of cereal β-glucans in dilute aqueous solutions by light scattering: Part I. Structure effects. Food Hydrocolloids, 25(2), 189-195.

Lia, A., Hallmans, G., Sandberg, A.-S., Sundberg, B., Åman, P. & Andersson, H. (1995) Oat beta-glucan increases bile acid excretion and a barley rich fraction increases cholesterol excretion in ileostomy subjects. American Journal of Clinical Nutrition, 62(6), 1245-1251.

Litzén, A. & Wahlund, K. G. (1989) Improved separation speed and efficiency for proteins, nucleic acids and viruses in asymmetrical flow field flow fractionation. Journal of Chromatography, 476, 413-421.

Litzén, A. & Wahlund, K. G. (1991a) Zone broadening and dilution in rectangular and trapezoidal asymmetrical flow field-flow fractionation channels. Analytical Chemistry, 63(10), 1001-1007.

Litzén, A. & Wahlund, K. G. (1991b) Effects of Temperature, Carrier Composition and Sample Load in Asymmetrical Flow Field-flow Fractionation. Journal of Chromatography A, 548(1-2), 393-406.

Litzén, A. (1993) Separation speed, retention, and dispersion in asymmetrical flow field-flow fractionation as functions of channel dimensions and flow rates. Analytical Chemistry, 65(4), 461-470.

Litzén, A., Walter, J. K., Krischollek, H. & Wahlund, K. G. (1993) Separation and quantitation of monoclonal antibody aggregates by asymmetrical flow field-flow

fractionation and comparison to gel permeation chromatography. Analytical Biochemistry, 212, 469-480.

Manners, D. J. (1991) Recent developments in our understanding of glycogen structure. Carbohydrate Polymers, 16, 37-82.

Mantovani, M. S., Bellini, M. F., Angeli, J. P. F., Oliveira, R. J., Silva, A. F. & Ribeiro, L. R. (2008) Beta-Glucans in Promoting Health: Prevention against Mutation and Cancer. Mutation Research/Reviews in Mutation Research, 658(3), 154-161.

Max, N. (2005) The Barbarian's Beverage: A History of Beer in Ancient Europe. 1st Ed. Taylor & Francis.

Mikkelsen, M. S., Cornali, S. B., Jensen, M. G., Nilsson, M., Beeren, S. R. & Meier, S. (2014). Probing interactions between beta-glucan and bile salts at atomic detail by 1H-13C NMR assays. Journal of Agricultural and Food Chemistry, 62(47), 11472-11478.

Mikkelsen, M. S., Jespersen, B. M., Møller, B. L., Lærke, H. N., Larsen, F. H. & Engelsen, S. B. (2010) Comparative spectroscopic and rheological studies on crude and purified soluble barley and oat β-glucan preparations. Food Research International, 43(10), 2417-2424.

Minekus, M., Alminger, M., Alvito, P., Ballance, S., Bohn, T., Bourlieu, C., Carriere, F., Boutrou, R., Corredig, M., Dupont, D., Dufour, C., Egger, L., Golding, M., Karakaya, S., Kirkhus, B., Le Feunteun, S., Lesmes, U., Macierzanka, A., Mackie, A., Marze, S., McClements, D. J., Menard, O., Recio, I., Santos, C. N., Singh, R. P., Vegarud, G. E., Wickham, M. S. J., Weitschies, W. & Brodkorb, A. (2014) A standardised static in vitro digestion method suitable for food - an international consensus. Food & Function, 5(6), 1113-1124.

Murphy, J. & Riley, J. P. (1962) A modified single solution method for the determination of phosphate in natural waters. Analytica Chimica Acta, 27, 31-36.

Nilsson L. (2013) Separation and characterization of food macromolecules using field-flow fractionation: A review. Food Hydrocolloids, 30, 1-11.

Nilsson, U. & Nyman, M. (2005) Short-Chain Fatty Acid Formation in the Hindgut of Rats Fed Oligosaccharides Varying in Monomeric Composition, Degree of Polymerisation and Solubility. British Journal of Nutrition, 94(5), 705-713.

Othman, R. A., Moghadasian, M. H. & Jones, P. J. H. (2011) Cholesterol-Lowering Effects of oat β-glucan. Nutrition Reviews, 69(6), 299-309.

Otte, T., Pasch, H., Macko, T., Brull, R., Stadler, F. J., Kaschta, J., Becker, F. & Buback, M. (2011) Characterization of branched ultrahigh molar mass polymers by asymmetrical flow field-flow fractionation and size exclusion chromatography. Journal of Chromatography A, 1218(27), 4257-4267.

Papageorgiou, M., Lakhdara, N., Lazaridou, A., Biliaderis, C. G. & Izydorczyk, M. S. (2005) Water extractable (1→3,1→4)-β-D-glucans from barley and oats: An intervarietal study on their structural features and rheological behavior. Journal of Cereal Science, 42, 213-224.

Pérez, S. & Bertoft, E. (2010) The molecular structures of starch components and their contribution to the architecture of starch granules: A comprehensive review. Starch/Stärke, 62, 389–420.

Perez-Rea, D., Bergenståhl, B. & Nilsson, L. (2015) Development and evaluation of methods for starch dissolution using asymmetrical flow field-flow fractionation. Part I: dissolution of amylopectin. Analytical and Bioanalytical Chemistry, 407, 4315-4326.

Pitkänen, L. & Striegel, A. M. (2014) AF4/MALS/QELS/DRI characterization of regular star polymers and their "span analogs". Analyst, 139, 5843-5851.

Rebello, C. J., O'Neil, C. E., & Greenway, F. L. (2016). Dietary fiber and satiety: the effects of oats on satiety. Nutrition Reviews, 74(2), 131-147.

Regand, A., Chowdhury, Z., Tosh, S. M., Wolever, T. M. S. & Wood, P. (2011) The molecular weight, solubility and viscosity of oat beta-glucan affect human glycemic response by modifying starch digestibility. Food Chemistry, 129(2), 297-304.

Roger, P., Bello-Perez, L. A. & Colonna, P. (1999) Contribution of amylose and amylopectin to the light scattering behaviour of starches in aqueous solution. Polymer, 40, 6897-6909.

Roger, P. & Colonna, P. (1992) The influence of chain-length on the hydrodynamic behavior of amylose. Carbohydrate Research, 227, 73-83.

Rolland-Sabaté, A., Colonna, P., Mendez-Montealvo, M. G. & Planchot, V. (2007) Branching features of amylopectins and glycogen determined by asymmetrical flow field flow fractionation coupled with multiangle laser light scattering. Biomacromolecules 8, 2520–2532.

Rose, D. J., Demeo, M. T., Keshavarzian, A. & Hamaker, B. R. (2007) Influence of Dietary Fiber on Inflammatory Bowel Disease and Colon Cancer: Importance of Fermentation Pattern. Nutrition Reviews, 65(2), 51-62.

Rudin, A. D. (1957) Measurement of the foam stability of beers. Journal of the Institute of Brewing, 63(6), 506-509.

Savin, G. & Burchard, W. (2004) Uncommon Solution Behavior of Poly(N-vinylimidazole). Angular Dependence of Scattered Light from Aggregates in Ethanol. Macromolecules, 37, 3005–3017.

Schimpf, M. E., Caldwell, K. D. & Giddings, J. C. (2000) Field-Flow Fractionation Handbook. Wiley & Sons, Inc., USA.

Schmidt, M., Nerger, D. & Burchard, W. (1979) Quasi-elastic light scattering from branched polymers: 1. Polyvinylacetate and polyvinylacetate—microgels prepared by emulsion polymerization. Polymer, 20(5), 582-588.

Sitar, S., Aseyev, V. & Kogej, K. (2014) Microgel-like aggregates of isotactic and atactic poly(methacrylic acid) chains in aqueous alkali chloride solutions as evidenced by light scattering. Soft Matter, 10, 7712-7722.

Tan, J., McKenzie, C., Potamitis, M., Thorburn, A. N., Mackay, C. R. & Macia, L. (2014) The Role of Short-Chain Fatty Acids in Health and Disease. In Frederick, W. A. (Ed.), Advances in Immunology, Academic Press, Vol. 121, 91-119.

Tanford, C. (1961) Physical Chemistry of Macromolecules. Wiley & Sons, Inc., USA.

Thies, F., Masson, L. F., Boffetta, P. & Kris-Etherton, P. (2014). Oats and CVD risk markers: a systematic literature review. British Journal of Nutrition, 112 Suppl 2, 19-30.

Tügel, I., Runyon, J. R., Gomez Galindo, F. & Nilsson, L. (2015) Analysis of polysaccharide and proteinaceous macromolecules in beer using asymmetrical flow field-flow fractionation. Journal of the Institute of Brewing, 121, 44-48.

Ulmius, M., Adapa, S., Önning, G. & Nilsson, L. (2012) Gastrointestinal conditions influence the solution behaviour of cereal β-glucans in vitro. Food Chemistry, 130, 536-540.

Ulmius, M., Önning, G. & Nilsson, L. (2012) Solution behavior of cereal β-glucan as studied with asymmetrical flow field-flow fractionation. Food Hydrocolloids, 26, 175-180.

U.S. Food and Drug Administration. (1992) Food Labeling: Health Claims; Soluble Fiber from Whole Oats and Risk of Coronary Heart Disease. Federal Register. 62: 15343-15344.

U.S. Food and Drug Administration. (2008) Food Labeling: Health Claims; Soluble Fiber from Certain Foods and Risk of Coronary Heart Disease. Federal Register. 73: 47828-47829. PMID:18956498

van Bruijnsvoort, M., Wahlund, K. G., Nilsson, G. & Kok, W. T. (2001) Retention behavior of amylopectins in asymmetrical flow field-flow fractionation studied by multi-angle light scattering detection. Journal of Chromatography A, 925, 171–182.

Vårum, K. M. & Smidsrød, O. (1988) Partial chemical and physical characterisation of (1→3),(1→4)-β-D-glucans from oat (Avena sativa L.) aleurone. Carbohydrate Polymers, 9, 103-117.

Vårum, K. M., Smidsrød, O. & Brant, D. A. (1992) Light scattering reveals micelle-like aggregation in the (1-3)(1-4)-β-d-glucans from oat aleurone. Food Hydrocolloids, 5, 497–511.

Wahlund, K. G. & Giddings, J. C. (1987) Properties of an asymmetrical flow field-flow fractionation channel having one permeable wall. Analytical Chemistry, 59(9), 1332–1339.

Wahlund, K. G., Leeman, M. & Santacruz, S. (2011) Size separations of starch of different botanical origin studied by asymmetrical-flow field-flow fractionation and multiangle light scattering. Analytical and Bioanalytical Chemistry, 399, 1455–1465.

Wahlund, K. G. & Litzén, A. (1989) Application of an asymmetrical flow field-flow fractionation channel to the separation and characterization of proteins, plasmids, plasmid fragments, polysaccharides and unicellular algae. Journal of Chromatography, 461, 73-87.

Wahlund, K. G., Winegarner, H. S., Caldwell, C. D. & Giddings, J. C. (1986) Improved flow field-flow fractionation system applied to water-soluble polymers: programming, outlet stream splitting, and flow optimization. Analytical Chemistry, 58(3), 573-578.

Walsh, D. J., Graessley, W. W., Datta, S., Lohse, D. J. & Fetters, L. J. (1992) Equations of state and predictions of miscibility for hydrocarbon polymers. Macromolecules, 25, 5236-5240.

Wang, Q. & Ellis, P. R. (2014) Oat beta-glucan: physico-chemical characteristics in relation to its blood-glucose and cholesterol-lowering properties. British Journal of Nutrition, 112 Suppl 2, 4-13.

Webster, F. H. & Wood, P. J. (2011) Oats: Chemistry and Technology. 2nd ed. AACC International Inc., Minnesota, USA.

Wittgren, B., Borgström, J., Piculell, L. & Wahlund, K. G. (1998) Conformational change and aggregation of k-carrageenan studied by flow field–flow fractionation and multiangle light scattering. Biopolymers, 45, 85-96.

Wolever, T. M. S., Tosh, S. M., Gibbs, A. L., Brand-Miller, J. A., Duncan, M., Hart, V., Lamarche, B., Thomson, B. A., Duss, R. & Wood, P. J. (2010) Physicochemical properties of oat β-glucan influence its ability to reduce serum LDL cholesterol in humans: a randomized clinical trial. The American Journal of Clinical Nutrition, 92, 723-732.

Wood, P. J. (2002). Relationships between solution properties of cereal β-glucans and physiological effects - a review. Trends in Food Science & Technology, 13(6), 313-320.

Wood, P. J, Paton, D. & Siddiqui, I. R. (1977) Determination of β-glucan in oats and barley. Cereal Chemistry, 54(3), 524-533.

Wyatt, P. J. (1993) Review: Light Scattering and the absolute characterization of macromolecules. Analytica Chimica Acta, 272, 1-40.

You, S., Stevenson, S. G., Izydorczyk, M. S. & Preston, K. R. (2002) Separation and characterization of barley starch polymers by a flow field-flow fractionation technique in combination with multiangle light scattering and differential refractive index detection, Cereal Chemistry, 79(2002) 624–630.

Zacherl, C., Eisner, P. & Engel, K.-H. (2011) In vitro model to correlate viscosity and bile acid-binding capacity of digested water-soluble and insoluble dietary fibres. Food Chemistry, 126(2), 423-428.

Zhang, D., Doehlert, D. C. & Moore, W. R. (1997) Factors affecting viscosity of slurries of oat groat flours. Cereal Chemistry, 74(6), 722–726.

Zhong, Y. D. & Nyman, M. (2014) Prebiotic and synbiotic effects on rats fed malted barley with selected bacteria strains. Food & Nutrition Research, 58, 24848.

Zhong, Y. D., Nyman, M. & Fak, F. (2015) Modulation of gut microbiota in rats fed high-fat diets by processing whole-grain barley to barley malt. Molecular Nutrition & Food Research, 59(10), 2066–2076.

Zhou, M., Robards, K., Glennie-Holmes, M. & Helliwell, S. (2000) Effects of enzyme treatment and processing on pasting and thermal properties of oats. Journal of the Science of Food and Agriculture, 80, 1486-1494.

Zielke, C., Kosik, O., Ainalem, M.-L., Lovegrove, A., Stradner, A. & Nilsson, L. (2017) Characterization of cereal β-glucan extracts from oat and barley and quantification of proteinaceous matter. PLoS ONE, 12(2), e0172034. doi:10.1371/journal.pone.0172034

Zielke, C., Teixeira, C., Ding, H., Cui, S., Nyman, M. & Nilsson, L. (2017) Analysis of β-glucan molar mass from barley malt and brewer's spent grain with asymmetric flow field-flow fractionation (AF4) and their association to proteins. Carbohydrate Polymers, 157, 541–549.

Zimm, B. H. (1948) Apparatus and Methods for Measurement and Interpretation of the Angular Variation of Light Scattering; Preliminary Results on Polystyrene Solutions. The Journal of Chemical Physics, 16(12), 1099-1116.

Acknowledgements

"T-H-R-E-E pages of acknowledgement? Are there seriously so many people you want to thank?" I could see Mary's face showing up in front of me, although the only way we were connected was via a texting messenger. Her lips forming the words, her expression filled with surprise and doubt, I could hear her voice echoing in my head. "Yes", I said, "because five years ago, I would have never imagined that becoming a PhD student would be the greatest, craziest, most exhausting and definitely most exciting time. I learned a lot - about science and analytics, about life and people. I should thank everybody who was involved in this." I imagined her rolling her eyes and scratching her head, thinking about what to say. She gave in: "OK, so who do you want to thank?"

It took me some time to put my thoughts in order, and I started: "First of all, I want to express my sincere and honest gratitude to my supervisor – mein Doktorvater! – **Dr. Lars Nilsson** who actually became a good friend, and will hopefully remain one in the future. I want to thank him for giving me this position, for believing in me, for hilarious trips, for awesome supervisor meetings and, of course, for singing CCR's *Have you ever seen the rain* for me on my birthday at a random karaoke bar in South Korea. I would like to thank **Dr. Anna Stradner** and **Dr. Marie-Louise Ainalem**, for being my 2nd supervisors, for investing their time and their knowledge into my project. I would like to thank **Dr. Matilda Ulmius-Storm** and **Dr. Andreas Håkansson** for the help and input when we were, over and over again, struggling and fighting with the β-glucan or the AF4. I would like to thank **Dr. Björn Bergenståhl** who was always there to listen, to brainstorm and to share his knowledge and ideas when we got stuck in the project. I would like to thank **Dr. Seungho Lee**. During my four visits in his Separation Science Lab in Daejeon, South Korea, he made me feel welcome and supported, he was always open for discussions about work and about daily life, traveling or politics. I learnt a lot from him, about science and about Korea. 감사합니다."

"Well, I can definitely see where this is going…", Mary said. "I am going to the gym now, but please continue... I guess you will be busy for some time". I heard her laughter through the World Wide Web and went back, searching the wide fields of my thoughts for more people that should definitely be mentioned.

Catalina Fuentes pops up in my head. We were suffering and celebrating with the AF4 machines, we were traveling: USA, Bolivia, Germany, Korea, and I hope

many more countries will follow. I'm glad she decided to do a PhD and come to Sweden, and I am sure she will finish her work excellently. Muchos besos para ti, guapa. **Yi Lu**, **Daniel Osorio** and **Atma-Sol Bustos** for making our small FFF family in Lund, how it exists right now, complete. Thank you for all the support and good luck to you. I would like to thank **Dr. Daysi Perez** who made me familiar with AF4 and marked the tools so that I knew what is what (English-Spanish lab communication-confusion!). She gave me the best start into my AF4 life that I could have wished for! I would like to thank **Jaeyeong Choi**, for just everything. We had a blast and he became a great teacher and an awesome friend. I would like to thank **Dr. Ondrej Kosik** for a great time working together in Lund and for all the help and knowledge I received during my stay in Rothamsted, UK. (There can only be as much trouble as opportunities! Sincerely yours, Trouble!) I would like to thank **Dr. Cristina Teixeira**, my β-glucan-partner in crime. Whenever I was upset or angry with β-glucan, I knew I could go to her and she would understand me like no-one else. I'm glad I found her (in Poland!) and had the possibility to work with her. I would like to thank **Kostas Korompokis** who was the best Master student I could have wished for working on my project with me. He did great lab work, was so much fun to be with, became a friend and I am sure that he will be a much better PhD student than I have ever been. I would like to thank **Romane Poinsot** who wrote her project work under my supervision, and whose work and results contributed to this thesis. I would like to thank **Dr. Alejandra Castro** for being a great FFF support and a lovely friend. And **Dr. Ray Runyon**. Starting to work with the AF4 is not easy, and he might not have made it easier for me, but through him I learned a lot about the system, how to handle it and how to deal with its issues. And of course, I would like to thank **Dr. Lennart Piculell** who during the last few months became a really valuable member of the team when discussing AF4 theory.

"I am back!" The messenger's notification sound brings me back to reality, interrupting my thoughts. "How is it going? Are you still thanking people?" "I am, I am, it feels like a never-ending story right now. One and a half pages already. And honestly, there are a lot of people I didn't work with directly, but whom I only met due to my PhD studies, people that helped me along these five years, encouraged me or just distracted me when I really needed distraction, people in the department or people I met at conferences and trips. And people I don't want to miss in my life. So I should mention them as well, right?" No answer. "Mary?" No answer. I went to the kitchen to prepare some coffee in my lovely, red coffee machine I got from my colleagues for my birthday. While I am waiting and the kitchen starts to smell like freshly brewed coffee, I look outside my window facing Nobeltorget and its gray-ish sad appearance, enhanced by the typical colorless and cloudy Malmö pre-winter weather. I pour Oatly into my coffee and return to my computer. "Yes, yes, I am here.", is written on the screen. "Sure, you should thank

them if they had such a big impact on your work. And what is one page more or less, right?" She sends this big fat smiling emoji showing all its teeth. True, what is one page more or less?

"OK, let's continue! I would like to thank **Kataneh Aalaei**, min käraste. We started our PhD studies on the same day, she was always by my side, cheering me up, calming me down, sharing her thoughts and opinions with me, and supported me in every step or decision I made! **Edita Demir** who made us all so happy when she moved to Lund and we became even closer. Life is not always easy, but a lot easier with a girl like her by your side. I would like to thank the evil twins, **Yanita Yusof** and **Clau Lazarte**, for teaching us the levels of *meanosity*, for always being happy, positive and loving in all situations that life has to offer. I would like to thank **Cecy Curi** who just showed up in the department and stole my heart away. For being my friend and for being here, just like that. Without these girls, this time would have been only half as spectacular, half as successful and half as fun. **Federico Gomez**, who was never a Senior to me, but a very good and understanding friend. **Cuong Tran** who kept me from studying MALS, who had the time to go and see John and Britney at a memorable weekend in Las Vegas with me and who effectively kept me from writing my thesis. **Yannis**, for a great time in Rothamsted, in Korea and most of all – in Japan! The world is small and just amazing, remember that! And **Ab**, my Batman, for being there for me, even though we're far apart. And all my lovely Kemicentrum people, for working times, lunch times, lab times, fika times, laughing times, bar times, dinner times and whenever we didn't feel like working."

"Wow… and äähmm, what about your parents?" "Mary, I'm not there yet. Be patient! But if you want, here it comes. **Mutti**: Danke, dass du mich zum Chemie-Studium *überredet* hast. Obwohl ich doch des Öfteren Zweifel hatte und am liebsten alles hingeworfen hätte, habe ich letztendlich gefunden, was mir Spaß macht. **Papa**, danke für eure Unterstützung und dafür, dass ich weiß, ich werde immer ein Zuhause bei euch haben. Ich liebe euch. Liebste **Omi**, ich weiß, ich bin nicht sehr oft zu Hause und wir verbringen nicht so viel Zeit miteinander, wie wir beide gerne würden, aber es ist schön zu wissen, dass du da bist und mich bedingungslos unterstützt. **Carsten**. Danke, dass du mich ermutigt hast, nach Schweden zu gehen und meine Doktorarbeit zu schreiben. Wir hatten es nicht immer leicht, aber wenn es hart auf hart kam, warst du da für mich, und dafür werde ich dir ewig dankbar sein. In Liebe, ♥! In addition, I want to thank **Familie (Sn)Öresund – Kathi und Tilla –** you, **Mary**, **Nikki** and **Darina**, for endless support, always listening to my thoughts and complaints and trying to help, even from far away. What would I be without you in my life! I would like to thank **Uta**, meine Uti-Frutti, who gave me the best start in Sweden one could ever imagine. It was indeed nice to *meat* you! **Sebastian** and Genosse **David**, I'm so glad for the times we shared. And I would like to thank the *security chef*, for teaching us not to

interfere! Additionally, I would like to thank all the **blueberries** I ate for keeping up my vitamin levels, **Monki®** and **Buffalo®Boots** for the best fashion statements ever and **Stortorget Lund** for giving us a place to relax whenever we needed a break."

"C-L-A-U-D-I!!!! You are losing track right now. Focus!" Again, I can see this emoji popping up in the messenger. I guess Mary is right. I should finish this acknowledgement and bring my thesis to an end. I wonder: Is that it? Is it over now? What is next? My friend **André** occurs in my thoughts; he found the four-leaf clover for me! Maybe I should give him a call.

Paper I

Characterization of cereal β-glucan extracts from oat and barley and quantification of proteinaceous matter

Zielke, C., Kosik, O., Ainalem, M.-L., Lovegrove, A., Stradner, A. & Nilsson, L.

PLoS ONE (2017) 12(2), e0172034. doi:10.1371/journal.pone.0172034

PLOS ONE

RESEARCH ARTICLE

Characterization of cereal β-glucan extracts from oat and barley and quantification of proteinaceous matter

Claudia Zielke[1]*, Ondrej Kosik[2], Marie-Louise Ainalem[3], Alison Lovegrove[2], Anna Stradner[4], Lars Nilsson[1]

1 Department of Food Technology, Engineering and Nutrition, Lund University, Lund, Sweden, **2** Department of Plant Biology and Crop Science, Rothamsted Research, West Common, Harpenden, United Kingdom, **3** European Spallation Source ESS AB, Lund, Sweden, **4** Department of Physical Chemistry, Lund University, Lund, Sweden

* claudia.zielke@food.lth.se

OPEN ACCESS

Citation: Zielke C, Kosik O, Ainalem M-L, Lovegrove A, Stradner A, Nilsson L (2017) Characterization of cereal β-glucan extracts from oat and barley and quantification of proteinaceous matter. PLoS ONE 12(2): e0172034. doi:10.1371/journal.pone.0172034

Editor: Wei Wang, Henan Agricultural University, CHINA

Received: November 1, 2016

Accepted: January 30, 2017

Published: February 14, 2017

Data Availability Statement: All relevant data are within the paper.

Funding: Financial support was provided by the Swedish research council (VR), Stockholm, Sweden and from the Biotechnology and Biological Sciences Research Council of the United Kingdom. The sponsors had no influence on study design, collection, analysis and interpretation of data, nor in writing the manuscript and neither in the decision to submit the article for publication. European Spallation Source ESS AB, provided

Abstract

An extraction method for mixed-linkage β-glucan from oat and barley was developed in order to minimize the effect of extraction on the β-glucan structure. β-Glucan were characterized in terms of molecular size and molar mass distributions using asymmetric flow field-flow fractionation (AF4) coupled to multiangle light scattering (MALS), differential refractive index (dRI) and fluorescence (FL) detection. The carbohydrate composition of the extracts was analysed using polysaccharide analysis by carbohydrate gel electrophoresis (PACE) and high-performance anion-exchange chromatography (HPAEC). Whether there were any proteinaceous moieties linked to β-glucan was also examined. Purified extracts contained 65% and 53% β-glucan for oats and barley, respectively. The main impurities were degradation products of starch. The extracts contained high molecular weight β-glucan (10^5–10^8 g/mol) and large sizes (root-mean-square radii from 20 to 140 nm). No proteins covalently bound to β-glucan were detected; therefore, any suggested functionality of proteins regarding the health benefits of β-glucan can be discounted.

Introduction

The water soluble β-glucan from cereals, such as oat and barley, is a linear β-1,3 and β-1,4 linked polysaccharide formed solely of β-D-glucopyranosyl units. Several health effects of mixed-linkage β-glucan, acting as dietary fibre, have been approved by both, the U.S. Food and Drug Administration (FDA) [1,2] and the scientific panel of the EU (European Food Safety Authority (EFSA)) [3,4], including the reduction of serum cholesterol in the blood as well as reduced glycaemic and insulin responses [4]. Therefore, β-glucan is considered to be a functional and bioactive food ingredient which can reduce the risk of a number of chronic diseases with increased daily intake. Whilst these claims have been accepted, there is no understanding of the mechanism of action of β-glucan or potential ways to improve these health benefits in food for health purposes.

support in the form of salaries for author MLA], but did not have any additional role in the study design, data collection and analysis, decision to publish, or preparation of the manuscript.

Competing interests: Marie-Louise Ainalem is employed by the European Spallation Source ESS AB. There are no patents, products in development or marketed products to declare. This does not alter our adherence to all the PLOS ONE policies on sharing data and materials, as detailed online in the guide for authors.

Abbreviations: AF4, asymmetric flow field-flow fractionation; ANTS, 8-aminonaphtalene-1,3,6-trisulphonic acid; BSA, bovine serum albumin; DP, degree of polymerization; dRI, differential refractive index; EDAC, 1-ethyl-3-(3-dimethylaminopropyl) carbodiimide; HPAEC-PAD, high-performance anion-exchange chromatography equipped with pulse-amperometric detector; MALS, multiangle light scattering; M, molar mass; M_w, weight-average molar mass; N, nitrogen; PACE, polysaccharide analysis by carbohydrate gel electrophoresis; r_{rms}, root-mean-square radius; RT, room temperature, 20˚C; t^0, void time; TEMED, N, N,N′,N′—tetramethylethylenediamine; TFA, tetrafluoro amide; $(Xyl)_{1-6}$, xylo-oligosaccharides, DP 1–6.

Some of the functional properties are believed to have their origin in the dissolution behaviour, particularly their capability of forming viscous solutions in the gut [5]. Self-association and formation of aggregates may additionally increase viscosity [6–9]. Previous observations showed a considerable variety in molar mass (M) and distribution of β-1,3 and β-1,4 linkages in β-glucan structure originating from different cereal origin [10]. Indeed, the high M and polydispersity of cereal β-glucan, indicating a presence of aggregates of the polysaccharides, makes their characterization challenging.

An interesting aspect with regard to the structural properties of β-glucan is the possible presence of β-glucan chains covalently bound to proteinaceous moieties as suggested previously [11,12]. These protein/ β-glucan links may play an important role as the presence of such moieties could influence the molecular interactions, solubility and aggregation behavior of the β-glucan. It has been reported that the addition of proteases to viscous oat flour slurries cause a decrease in viscosity indicating a relationship between protein content and viscosity [13]. Furthermore, Vårum & Smidsrød [14] found amino acid residues to be present in oat β-glucan preparations. Acker, Diemair & Samhammer [15] suggested that the presence of phosphate residues attached to oat β-glucan implied the presence of covalently bound proteins to the polysaccharide molecule. Therefore, the presence or absence of such moieties may explain the diversity of data on β-glucan functionality [11,16,17]. Furthermore, this could also influence M and viscosity of β-glucan preparations and might in turn lower low density lipoprotein (LDL) cholesterol values by forming viscous slurries in the gut [5]. These authors also showed, that high M β-glucan decreases LDL cholesterol in the blood more drastically then lower M β-glucan.

Although high proportions of β-glucan present in oat and barley is considered to be water soluble, there are still major problems with the extraction of β-glucan. Low yield, low purity and polysaccharide de-polymerization are common challenges. Under moderate conditions, e.g. water extraction at low temperatures, not all the β-glucan present is extracted, resulting in low yields. As discussed in detail by Webster & Woods [12], temperature, pH and choice of solvent may increase the yield of the β-glucan extraction. Similarly, increased yields can be obtained by using alkali solutions and increased temperature [18,19]. On the other hand, harsh extraction methods used for production of commercial production of mixed-linkage β-glucan can influence the structure and nature of the polysaccharide, for example, the ability to form aggregates [20], and such alterations in structure and properties may influence their possible health benefits. Therefore, it is of great interest to develop a methodology that would minimize the detrimental effects of extraction conditions on the β-glucan structure.

The main characterization method used in this study was asymmetric flow field-flow fractionation (AF4), a separation method especially well-suited for large and polydisperse polysaccharides owing to its broad separation range and gentle conditions. AF4 has, in recent years, been proven to be a valuable method for separation and characterization of food-related macromolecules [21] and colloidal structures [22]. The suitability of this method for the study of e.g. β-glucan and polysaccharides in beer [23] and cereal β-glucan macromolecules and aggregates has been described previously [6,24,25]. However, the methodology used in the present study had previously only been used for the study of cereal β-glucan standards [24,25]. The method described is considered to be gentle due to the relatively low shear forces to which the sample is exposed in the separation channel [22]. Separation is achieved by a longitudinal transport flow and a perpendicular field (cross-flow), which transports the analytes towards an accumulation wall in the AF4 separation channel [26]. As smaller particles have a higher rate of diffusion than larger ones, those will, at steady state, have a longer average distance from the accumulation wall. After this so-called relaxation step, elution commences and a longitudinal flow (showing a laminar flow profile due to the narrow channel height and relatively low flow

rates) transports the analytes to the channel outlet. The smaller analytes with, on average, a longer distance from the accumulation wall will elute earlier due to the higher flow velocities experienced by analytes further from the accumulation wall. The larger analytes, being on average closer to the accumulation wall, will experience a lower flow velocity and will, thus, elute later. Hence, this results in size separation in what is referred to as Brownian mode separation.

The present study describes an extraction procedure for analysis of non-modified β-glucan from oat and barley. Mixed-linkage β-glucan was extracted from oat and barley flour of relatively high purity, considering the conditions of the method applied. The aim of the extraction method used, was to preserve the native properties of the β-glucan polymer such as possible aggregates or protein/ β-glucan links. No proteases were used during the extraction procedure in order to maintain any possible proteinaceous moieties. Polysaccharide analysis by carbohydrate gel electrophoresis (PACE) and high-performance anion-exchange chromatography (HPAEC) analysis of monosaccharide sugar composition were used to assess the purity of the β-glucan extracts. β-Glucan extracts were characterized using AF4 with multiangle light scattering (MALS) and differential refractive index (dRI) detection. Additional AF4 experiments were performed using in-line post-channel Calcofluor labelling for semi-quantitative fluorescence (FL) detection of β-glucan in the extracts. AF4-MALS-FL was also used for determination of the presence of proteinaceous moieties by pre-separation fluorescent labelling of peptide bonds.

Materials and methods

Substances and chemicals

Oat flour was from Oatwell CreaNutrition with a β-glucan content of 28% (w/w) (Swedish Oat Fiber AB, Väröbacka, Sweden). Barley flour was from Culinar ß-Fibre flour with a β-glucan content of 24% (w/w) (Culinar, Fjälkinge, Sweden). Both flours were rich in proteins and did not undergo any harsh treatment during production and therefore their structure was not substantially affected prior to these experiments. The acetone (technical grade) and ethanol (absolute grade) used during the extraction were purchased from VWR Chemicals, Fontenay sous Bois, France. The heat-stable α-amylase (from *Aspergillus oryzae*, ~30 U/ mg) was purchased from Sigma Aldrich, Darmstadt, Germany. For the preparation of the AF4 carrier liquid $NaNO_3$ (Merck, Darmstadt, Germany) and NaN_3 (BDH, Poole, UK) were used. Chemicals for fluorescence labelling were the following: Calcofluor fluorescent brightener 28 and EDAC (1-ethyl-3-(3-dimethylaminopropyl)carbodiimide) hydrochloride (Sigma Aldrich, Darmstadt, Germany), 7-methoxycoumarin-3-carboxylic acid (Invitrogen Molecular Probes, Thermo Fisher Scientific Inc., Waltham, Massachusetts, USA), tris(hydroxymethyl)-aminomethane (ICN Biomedicals Inc., Irvine, California, USA) and DMSO (Sigma Aldrich, Darmstadt, Germany). For enzymatic digestion prior to PACE, xylanase 11 or lichenase, were purchased from Prozomix Ltd., Haltwhistle, UK. The fluorophore ANTS (8-aminonaphtalene-1,3,6-trisulphonic acid) was purchased from Invitrogen Molecular Probes, Thermo Fisher Scientific Inc., Waltham, Massachusetts, USA. All other chemicals came from Sigma Aldrich, Darmstadt, Germany. Xylooligosaccharides $(Xyl)_{1-6}$ were from Megazyme International Ltd., Bray, Co. Wicklow, Ireland. All experiments were performed using Milli-Q water (18.2 MΩ) from a Milli-Q system (Millipore Corp., Billerica, Massachusetts, USA).

Extraction of β-glucan

In order to avoid proteases and harsh conditions, such as elevated pressure and alkaline treatments, the following procedure was used. The first extraction step involved defatting

2 g of flour with 75 mL acetone, stirring the suspension at RT for 2 h, followed by centrifugation for 20 min at 1,000 x *g*. The supernatant was discarded and the pellet dried overnight at RT. 1.5 g (~ 45 000 units) heat-stable α-amylase was re-suspended in 50 mL Milli-Q water and incubated at 100˚C for 30 min to terminate any non α-amylase related exogenous activities [27]. The pre-treated α-amylase was mixed with the defatted flour in 100 mL Milli-Q water. The suspension was boiled for 1 h and stirred until the slurry had cooled to RT. 100 mL ethanol was added to precipitate the water soluble β-glucan and the sample stirred at RT for 1 h. After centrifugation for 30 min (2,000 x *g*), the precipitation step was repeated using the supernatant from the previous step. The pellets from both precipitations were re-dissolved in 50 mL of Milli-Q water, combined and heated to 65˚C for 40 min. After cooling to RT, the viscous liquid was centrifuged for 1 h at 1,000 x *g* and the supernatant was oven-dried at 80˚C for 15 h. The final extract was re-purified by repeating the whole procedure, from α-amylase digestion, a further two times. The amounts of α-amylase and solvents used were adjusted accordingly.

The β-glucan content of the extracts was analysed using the Mixed-Linkage β-Glucan Assay Kit from Megazyme International Ltd., Bray, Co. Wicklow, Ireland, with some modification in order to analyse the high concentration of β-glucan in the preparations produced. The first incubation step at 100˚C was prolonged to 2 h. The amount of lichenase used in the next step was doubled, and the mixture incubated at 50˚C for 2 h. The reaction solution was mixed with 100 mL of sodium acetate buffer (100 mM with a pH of 4) and stirred for 15 min before being centrifuged. The rest of the procedure was unchanged from that described in the kit. The developed procedure was verified by processing and measuring various samples with known high content of β-glucan. The final extracts used in this study contain 65% (w/w) β-glucan in case of oat and 53% (w/w) β-glucan in case of barley flour extract. The starch content of the extracts was analysed using the Total Starch Assay Procedure Kit, available as well from Megazyme.

PACE (polysaccharide analysis by carbohydrate gel electrophoresis)

To check the quality of the extracted β-glucan and to identify possible impurities, PACE was performed as described elsewhere [28]. This method is used, among other applications, for elucidation of structure and characterization of carbohydrates. PACE relies on the migration of fluorophore-labelled mono- and oligosaccharides produced following digestion of a sample with specific glycosyl-hydrolases. The labelled sugars are separated based upon their size and structure. The fact that multiple samples can be run alongside each other on the polyacrylamide gels means that samples are exposed to exactly the same conditions during analysis.

Briefly, 250 μg aliquots of oat and barley extracts were prepared by drying stock solutions *in vacuo* (Savant Inc., Midland, Michigan, USA), they were then re-dissolved in water and digested with either xylanase 11 (4 μl ≈ 21.92 μg) or lichenase (1 μl ≈ 0.35 U) for 16 h at 40˚C. The same amount of material was digested with α-amylase (2 μL ≈ 35.9 U) for 30 minutes at 50˚C. The total reaction volume for all digestions was 500 μL. The digestion was terminated by boiling the sample for 30 min and samples dried *in vacuo*. Oat and barley fractions were labelled overnight with ANTS as described [28], as were xylo-oligosaccharides $(Xyl)_{1-6}$ and α-amylase digested soluble starch. Following labelling, the derivatized sugars were dried *in vacuo* and reconstituted in 200 μL of 3 M urea before running on PACE gels. Digested soluble starch samples were diluted fourfold prior to loading on gel. PACE gels were visualized under UV light using a GelDoc-It TS2 imager (UVP, Jena, Germany) equipped with a GFP emission filter (513–557 nm).

HPAEC-PAD analysis of monosaccharide sugar composition

HPAEC-PAD (high-performance anion-exchange chromatography equipped with pulse-amperometric detector) enables to study the monosaccharide composition of carbohydrates following acid hydrolysis. The monosaccharide analysis of β-glucan extracts was performed as described by Goubet et al. [29]. Briefly, 50 μg of either oat or barley β-glucan extract was incubated for 1 h at 121˚C in 400 μl of 2 M TFA. The hydrolysates were lyophilised, re-suspended in water and analysed using a Dionex ICS3000 HPLC equipped with CarboPac PA 20 column (Thermo Fisher Scientific Inc., Waltham, Massachusetts, USA).

AF4 analysis equipment and separation parameters

The AF4 instrument used was an Eclipse 3+ Separation System (Wyatt Technology Europe, Dernbach, Germany). The system was connected to a Dawn Heleos II multiangle light scattering (MALS) detector operating at 658 nm and an Optilab T-rEX differential refractive index (dRI) detector (both Wyatt Technology Europe) operating at the same wavelength. The carrier flow was delivered through an Agilent 1100 series isocratic pump with an in-line vacuum degasser and sample injection was via an Agilent 1100 series autosampler (Agilent Technologies, Waldbronn, Germany). To ensure that only particle free carrier liquid entered the system, a filter-holder with a 100 nm pore-size polyvinylidene fluoride (PVDF) membrane (Millipore Corp.) was placed between the pump and the channel inlet. The AF4 channel was a Wyatt long channel with a tip-to-tip length of 27.5 cm and a nominal thickness of 190 μm. The actual thickness was determined to be 156 μm by calibration with ferritin as described previously [30]. The ultra-filtration membrane forming the accumulation wall was made of hydrophilized polyethersulphone with a cut-off of 10 kDa (Microdyn-Nadir GmbH, Wiesbaden. Germany). 10 mM $NaNO_3$ and 0.02% (w/v) NaN_3 in Milli-Q water were used as carrier liquid. The samples were prepared at a concentration of 4 mg/ mL by dissolving the extracted β-glucan in the carrier liquid used for elution. The suspension was boiled for 30 min allowing the β-glucan to dissolve. The samples were cooled to RT and filtered through a 22 mm cellulose acetate membrane syringe filter with a 0.45 μm pore size (VWR International) prior to injection onto the channel. The sample was injected at 0.2 mL/ min for 4 minutes. The injected volume was 40 μl for oat and 80 μl for barley, corresponding to an injected mass of 160 μg and 320 μg, respectively. A focusing/ relaxation step of 5 min was performed prior to elution with a focusing flow rate of 0.5 mL/ min resulting in a void time (t^0) of 9 min. The initial cross-flow rate during elution was 1 mL/ min followed by an exponential decay with a half-life of 4.5 min in order to avoid excessive retention and elution times. After elution, the AF4 channel was flushed without any cross-flow for 5 min to ensure a clean channel before analysis of the next sample. During the whole measurement the detector flow rate was kept constant at 0.5 mL/ min.

Fluorescence measurements

The use of fluorescence detector enabled detection of both β-glucan and possible peptide residues through specific labelling of the purified β-glucan samples. A Jasco FP-1520 fluorescence detector (Jasco Inc., Easton, Maryland, USA) operating an Ushio Xenon Short Arc lamp (Ushio Inc., Tokyo, Japan) was used. Extracts were labelled in-line, post-channel with Calcofluor to detect β-glucan or pre-injection with EDAC to label peptide bonds, and analysed using the aforementioned AF4-MALS-FL set-up. For Calcofluor labelling of β-glucan, the method described by Ulmius, Önning, & Nilsson [25] was adopted, using a 25 mg/ L Calcofluor solution in 0.1 M tris(hydroxymethyl)-aminomethane buffer (pH 8), measuring the emission at λ_{em} = 445 nm (λ_{ex} = 415 nm). For labelling of possible proteinaceous matter in β-glucan extracts, the procedure described in [31] was adopted, with minor modification in that

the labelling agent was diluted 1 in 10. Thus, 1 mM solution of EDAC in Milli-Q water was mixed for 3 hours with 1 mM solution of 7-methoxycoumarin-3-carboxylic acid in two parts of Milli-Q water and one part of DMSO to enhance the solubility. After mixing, the labelling solution was added to an already dissolved β-glucan sample in 1:1 ratio (v/v), stirred for 1 h and immediately injected onto the AF4 channel. The wavelengths used for detection of possible proteinaceous matter were λ_{ex} = 336 nm and λ_{em} = 402 nm.

Elemental analysis

To measure the total protein content and other peptides that are possibly not associated with β-glucan, the extracts were analysed using Flash EA1112 elemental analyzer from Thermo Fisher Scientific, Delft, the Netherlands. The system uses the Flash Dynamic Combustion method, where complete combustion of the sample is reached through heating to 1000˚C, and subsequently followed by determination of the produced elemental gases, in this case nitrogen from proteinaceous matter. Aspartic acid at three different concentrations was used to calibrate the instrument. The percentage of protein per sample (w/w) was estimated by multiplying the nitrogen content by a 6.25 nitrogen-to-protein conversion factor. The elemental analyzer has sensitivity down to 100 PPM.

Data processing

Astra software in version 5.3.4.14 (Wyatt Technology Europe, Dernbach, Germany) was used to process the data obtained from the FL, MALS and dRI detectors following AF4 separation. M and root-mean-square radii (r_{rms}) were calculated using the Berry method [32,33] performing a 1st order fitting with the data obtained from the scattering detectors 9–14 (respective scattering angles: 69.3˚ - 121.2˚). Lower and higher scattering angles were excluded as they did not correspond to the plot. The RI increment (d*n*/d*c*) used was 0.146 mL/ g as defined for β-glucan in aqueous solutions [34] whereas the second virial coefficient A_2 was neglected.

Results and discussion

The β-glucan extracts were analysed for chemical composition using a commercial kit (enzymatic β-glucan determination), PACE and HPAEC-PAD. AF4-MALS-dRI was used to obtain fundamental information regarding β-glucan structure such as M and r_{rms} distributions. Additional AF4-MALS-FL experiments were performed on the extracts to identify β-glucan, any possible polysaccharide-protein interactions and protein contaminations in the β-glucan fractograms.

An oat β-glucan extract of 65% (w/w) purity and barley β-glucan extract of 53% (w/w) purity were prepared. These obtained purities should be recognized as good bearing in mind the mild extraction conditions and methodology designed to retain the natural structure of the extracted polymers. Extraction methods using more extreme conditions, for example protease and alkali treatments, resulted in 57% (w/w) purity for oats [35], and up to 90% (w/w) purity [36] for barley extracts using acidic conditions (pH 4). Immerstrand et al. [35] also mentioned a potential influence of the geographical origin and growing conditions of the starting material on the gained extraction purities and yields when using the same extraction method. Extraction yields for similar conditions as in the present paper could not be found in literature.

The amount of starting material was 2 g of oat or barley flour of which 28% and 24% is known to be β-glucan. The theoretical maximum yield would therefore be 560 mg and 480 mg, respectively. Our yields were around 200 mg for oat with purity of 65% which leads to 130 mg of β-glucan, and 180 mg for barley with purity of 53%, leading to 95 mg of β-glucan.

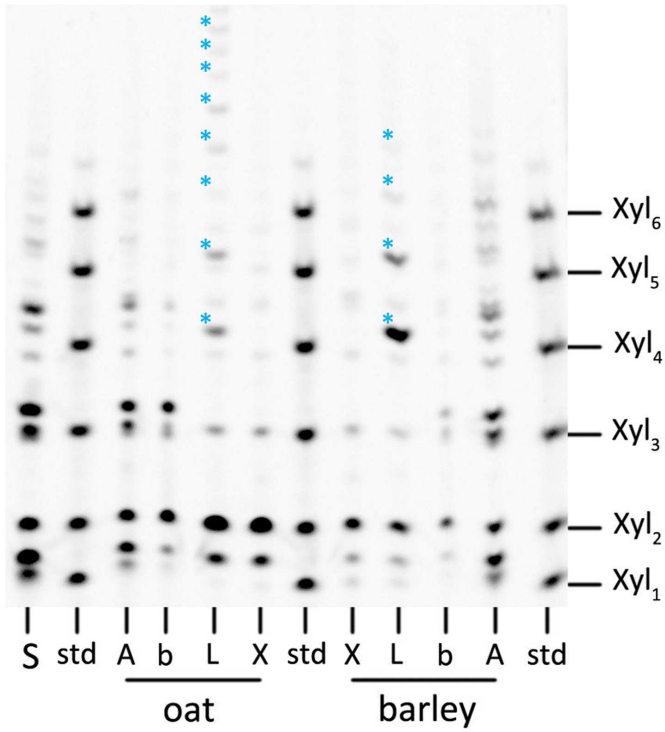

Fig 1. PACE gel. PACE gel showing extracted oat and barley mixed-linkage β-glucan, fingerprinted with specific glycosylhydrolases ('A'–with α-amylase to analyse starch related impurities; 'L'–with lichenase to analyse the presence and relative quantity of extracted β-glucan; 'X'–with xylanase 11 to analyse xylan related impurities and 'b'–background, non-digested sample) and their separation based on size and structure after derivatization with ANTS. 'S' shows starch sample digested with α-amylase and 'std' shows $(Xyl)_{1\text{-}6}$ standards used for oligosaccharides identification. Bands marked with blue asterisks are mixed-linkage β-glucan specific oligosaccharides DP $\geq$ 3. Xyl_1 –xylose, Xyl_2 –xylobiose, Xyl_3 –xylotriose, Xyl_4 –xylotetraose, Xyl_5—Xylopentaose, Xyl_6 –Xylohexaose. Shorter oligosaccharides migrate further in the polyacrylamide gel.

doi:10.1371/journal.pone.0172034.g001

Therefore, in this study, the extraction efficiency is around 23% of total available β-glucan for oat and 20% for barley.

The PACE gels of enzymatically digested oat and barley extracts with specific glycosyl-hydrolases are shown in Fig 1. Xylose to xylo-hexose standards $(Xyl)_{1\text{-}6}$ (labelled as 'std') and α-amylase digested soluble starch (labelled as 'S') were run alongside other digests to identify the main impurities present in oat and barley β-glucan extracts. 'b' are blanks; these samples were incubated with no addition of glycosyl-hydrolases. Even without digestion steps (lanes labelled 'b') small oligosaccharides are present, some of which co-incide with oligosaccharides released by amylase (A), indicating some remaining starch in the oat and barley preparations. 'X' indicates a sample digested with xylanase 11 showing (arabino)xylan-derived oligosaccharides and 'L' refers to samples digested with lichenase showing β-(1,3)(1,4)-glucan related

Table 1. Summary of characterization of the β-glucan extracts from oat and barley. The table includes purity and composition values, weight-average molar mass, average r_{rms} and mass recovery from the AF4 channel.

β-glucan source	β-glucan content [%(w/w)]	Starch content [%(w/w)]	content in extracts [%(w/w) of dry mass]						M_w [g/ mol][a]	r_{rms} [nm][b]	Mass recovery [%][c]
			glucose	xylose	arabinose	mannose	fucose	galactose			
oat	65	11	92.16	0.72	0.44	0.22	0.40	0.12	$5.6 \cdot 10^6$	96	72
barley	53	11	72.07	1.49	0.40	0.69	---	0.06	$2.4 \cdot 10^6$	82	98

[a] Weight-average molar mass

[b] z-average

[c] from the FFF channel, recovery of total injected mass, measured mass (integrated dRI-signal representing the concentration over the fractogram) / injected mass

doi:10.1371/journal.pone.0172034.t001

oligosaccharides. The position and the intensity of the labelled sugars/ bands are similar for both oat and barley extracts, although there is clearly more G3 oligosaccharide present in barley than in oats and there are higher DP glucan oligosaccharides present in the oat digest. Mixed-linkage glucan oligosaccharides are marked with blue asterisks in Fig 1. 'A' is the sample digested with α-amylase, showing starch related impurities in the oat and barley extracts.

To obtain additional information of the extracts' purity, HPAEC-PAD analysis of monosaccharide sugar composition was performed. The results are summarized in Table 1. On a dry weight basis, 92.16% (w/w) of the hydrolyzed oat extract is glucose while for the hydrolyzed barley extract the glucose content is 72.07% (w/w). In order to compare these values with the β-glucan content obtained using the commercially available β-glucan assay kit, from which values of 65% and 53% (w/w) for oat and barley, respectively, were obtained, the values need to be recalculated to correct for the difference in M (i.e. glucose: 180 g/ mol and glucose pyranosyl unit in a β-glucan chain: 162 g/ mol). Thus, a correction factor (162 [g/ mol]/180 [g/ mol]) needs to be multiplied with the glucose content in order to estimate how much of that glucose originates from β-glucan. The results show that approximately 17% (oat) and 12% (barley) of glucose does not come from β-glucan. The starch content of the samples was determined to be 11% (w/w) each in both extracts using a commercial starch assay kit (Megazyme).

The origin of the remaining glucose is most likely related to various dextrins originating from degradation of starch during the extraction. Hydrolysis of starch by α-amylase can result in various oligosaccharides and dextrins of which the composition depends on the substrate and the specific α-amylase utilized [37]. The solubility of these enzymatic products is relatively low in ethanol [38,39] and they may precipitate with the β-glucan during the extraction. The results from PACE analysis also indicate this. Other non-glucose monosaccharides were found in very small quantities in the hydrolyzed oat and barley extracts (e.g. xylose, arabinose, mannose and galactose). Rhamnose and galacturonic acid were not detected in any sample. Hence, the main impurities of the extracted samples, not being starch, are other water soluble polysaccharides or sugar residues, coming from other cereal polysaccharides and hemicelluloses e. g. glucomannans, arabinoxylans and starch dextrins in the endosperm or the cell walls of the oat and barley grains.

For further characterization of the β-glucan structure, AF4-MALS-dRI was utilized. Prior to the injection of the sample onto the AF4-channel, the prepared samples were filtered through a 0.45 μm pore size syringe filter with a cellulose acetate membrane. Sample filtering did not have any significant influence on the results but improved the signal-to-noise ratio as shown in Fig 2. These measurements were performed as pre-experiments and the flow conditions were different, resulting in different elution times compared to subsequent experiments reported in this study. The fractogram shows Rayleigh ratio signal (intensity of the scattered

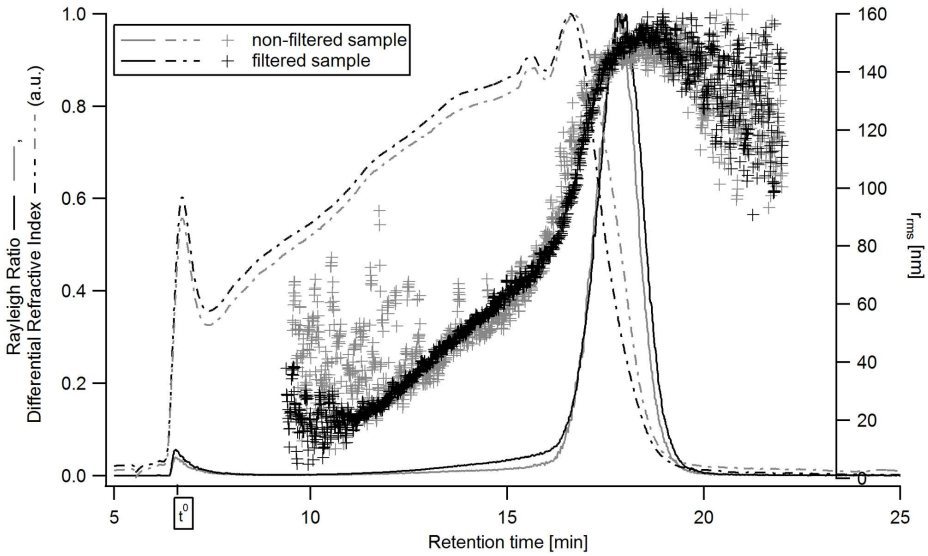

Fig 2. Fractogram of the β-glucan extract from oat, non-filtered and filtered sample. The signals are: grey solid line—Rayleigh ratio from MALS (a.u., 69.3˚ - 121.2˚) from non-filtered sample, black solid line—Rayleigh ratio from MALS (a.u., 69.3˚ - 121.2˚) from filtered sample, grey dashed line—dRI signal (a.u.) from non-filtered sample, black dashed line—dRI signal (a.u.) from filtered sample, grey crosses —r_{rms} of non-filtered sample, black crosses—r_{rms} of filtered sample. Channel and flow conditions as described in Materials and Methods, part e, except: initial cross-flow of 0.5 mL/ min with an exponential decay with half-life of 2 min, t^0 = 6.5 min.

doi:10.1371/journal.pone.0172034.g002

light) from the MALS detector and the dRI signal representing the concentration over the elution time as well as the calculated distribution for r_{rms}. The MALS and dRI signals were normalized against the peak maxima. The results (Fig 2) show that the signals and size distributions remain similar with a mass recovery from the AF4 channel of 99% for the non-filtered and 96% for the filtered sample.

It is also evident that the noise in the determined r_{rms} distribution is considerably lower in the filtered sample, especially for sizes below 60 nm. The higher noise in the non-filtered sample is most likely originating from very low amounts of very large analytes which co-elute in the steric/ hyperlayer mode of AF4 [40]. The presence of even very low amounts of large species may give rise to noisy MALS signals impairing the size determination [41,42].

The plots in Figs 3 and 4 display fractionation of the extracts as described for Fig 2, including the additional calculated distribution for the weight-average molar mass, M_w. It can be seen that the extracts are polydisperse samples with high M fractions. For oat (Fig 3), M_w ranges between 10^5–10^8 g/mol, the r_{rms} ranges between 50 and 120 nm. For barley (Fig 4) the values are in the same range for M_w but have a rather wider range of r_{rms} (20 to 140 nm). Mean values for M_w and r_{rms} for both extracts as well as their respective mass recoveries from the AF4 separation channel are summarized in Table 1. These results show that oat β-glucan is larger than the barley β-glucan which is in agreement with earlier findings i.e. by Beer, Wood, & Weisz [43] and Ahmad, Anjum, Zahoor, Nawaz, & Dilshad [44]. The differential M distribution of

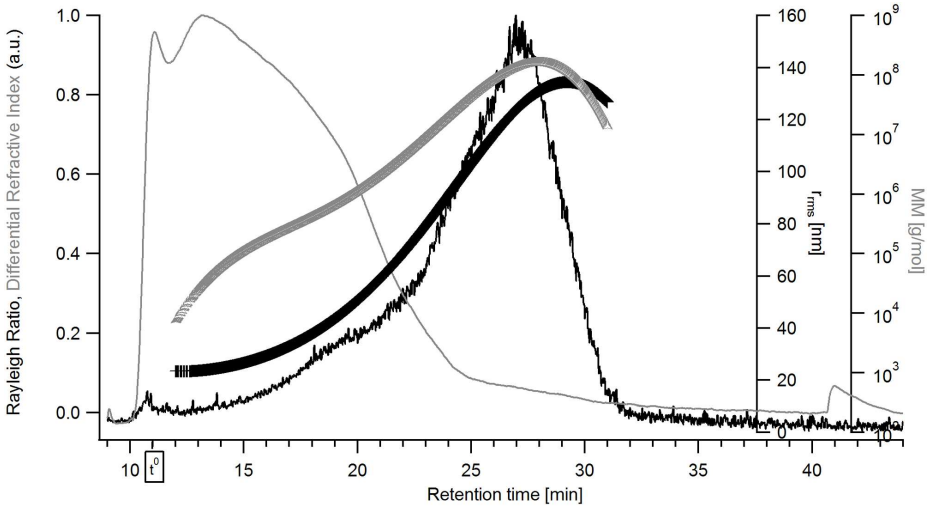

Fig 3. Fractogram of the β-glucan extract from oat. The signals are: black line—Rayleigh ratio from MALS (a.u., 69.3˚ - 121.2˚), grey line—dRI signal (a.u.), grey triangles—molar mass distribution [g/mol], black crosses—r_{rms} distribution [nm].

doi:10.1371/journal.pone.0172034.g003

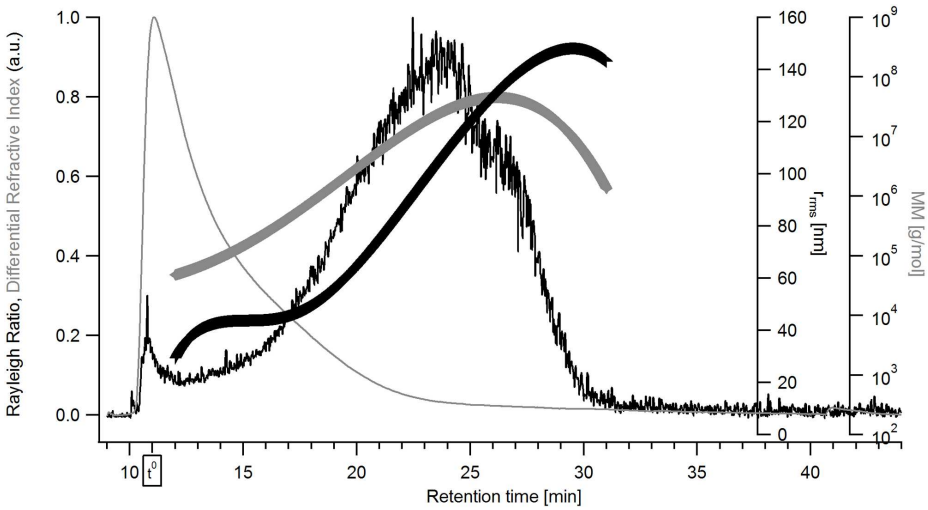

Fig 4. Fractogram of the β-glucan extract from barley. The signals are: black line—Rayleigh ratio from MALS (a.u., 69.3˚ - 121.2˚), grey line—dRI signal (a.u.), grey triangles—molar mass distribution [g/mol], black crosses—r_{rms} distribution [nm].

doi:10.1371/journal.pone.0172034.g004

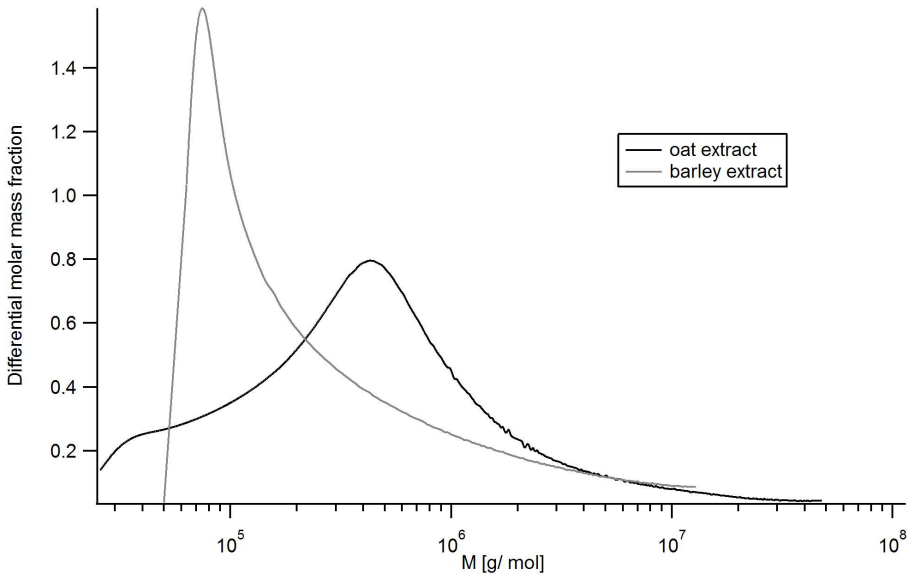

Fig 5. Differential molar mass fraction of the extracts. The colors denote: black—oat, grey—barley.

doi:10.1371/journal.pone.0172034.g005

the extracts, shown in Fig 5, also indicates barley β-glucan as smaller compared to oat β-glucan and that both extracts contain high M species.

Utilizing AF4 in combination with FL detection, β-glucan could be successfully labelled and made visible in the fractograms. The results of combining the AF4-MALS with selective FL labelling of the β-glucan can be seen in Fig 6 for oat and Fig 7 for barley. The signals were normalized against the peak maxima. A short delay in the elution times compared to the AF4-MALS-dRI was observed owing to different tubing configuration to allow the in-line labelling procedure. The β-glucan in the extracts have been selectively labelled with Calcofluor and detected at a wavelength of λ_{em} = 445 nm.

The results show the presence of β-glucan over the entire size distribution for oat β-glucan (Fig 6) while the late eluting analytes (retention time >25 min) in the barley β-glucan (Fig 7) sample appear to consist of low amounts of β-glucan or no β-glucan at all. The interpretation of Calcofluor labelled β-glucan data has some limitations as low M β-glucan (M_w approx. $4{\cdot}10^4$ g/ mol) tends to yield a lower signal intensity which for the low M analytes is also dependent on the ionic strength [45]. This might lead to underestimation of the content of low M β-glucan in the sample. For the late eluting analytes the low or non-existent FL-signal also coincides with a low dRI-signal (i.e. low concentration of analytes) in Figs 3 and 4 making it unclear whether the β-glucan content is lower or it is just a consequence of the very low analyte concentration. HPAEC-PAD showed xylose and arabinose, which are products of arabinoxylan hydrolysis, in small amounts (Table 1) when compared to data available in literature [46]. It is possible that the late eluting analytes (>25 min) in the barley extract are traces of very large size arabinoxylan species present at very low concentration and with no FL-signal but with

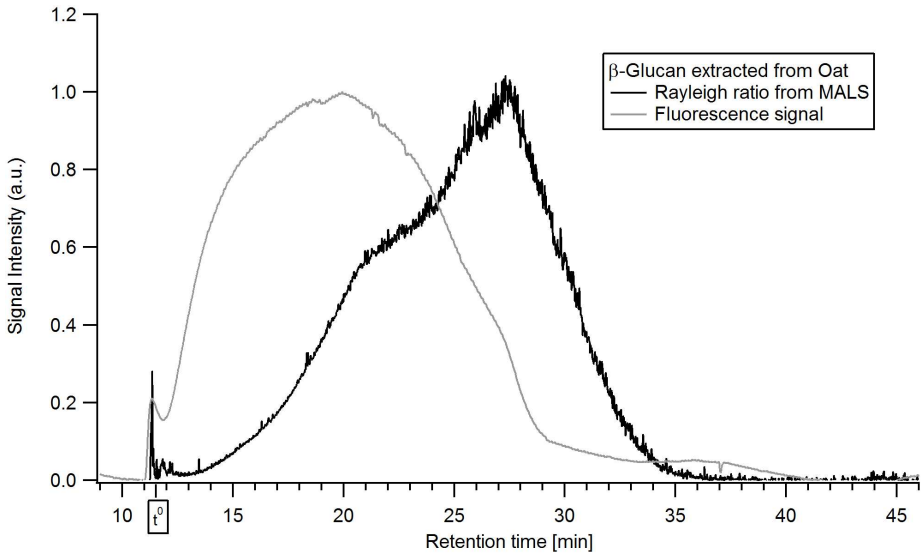

Fig 6. Fluorescence-fractogram of the β-glucan extract from oat. The colors denote: black—Rayleigh ratio from MALS (a.u.), grey—fluorescence signal of in-line Calcofluor-labelled β-glucan at λ_{em} = 445 nm (a.u.).

doi:10.1371/journal.pone.0172034.g006

distinct MALS-signal (Figs 3 and 7). These are also apparent in xylanase 11 digests of barley extract run on PACE gels (Fig 1). However, it is not possible to be conclusive that this is the case based on the results obtained.

Since a presence of protein in the β-glucan system would play an important role in formation of aggregates and could contribute to the claimed health benefits of β-glucan both extracts were analysed for protein content using two different approaches: AF4-MALS-FL (with pre-injection fluorescent labelling) and total N content determination through elemental analysis. AF4-MALS-FL did not show the presence of any proteinaceous moieties in either extracts (data not shown). Similarly, the elemental analysis showed no detectable amounts of nitrogen/protein (detection limit approx. 100 PPM). Although using an extraction procedure with mild conditions we found no evidence supporting the hypothesis of proteinaceous matter bound or creating a complex or aggregate with oat or barley β-glucan.

Conclusion

Mild extraction conditions were used to isolate β-glucan from oat and barley flour without modifying their original structure. The method gave β-glucan of good yield and purity. The main impurities are starch and possible starch degradation products and trace amounts of arabinose, xylose, mannose, galactose and fucose. The extracts contained β-glucan of high M_w (10^5–10^8 g/ mol) and large size (r_{rms} from 20 to 120 nm for oat, up to 140 nm for barley). Furthermore, the extracts were analysed for possible proteinaceous moieties in the β-glucan. There were no covalently bound proteins found in the β-glucan extracts produced by the method described and therefore this study does not strengthen the hypothesis of covalently

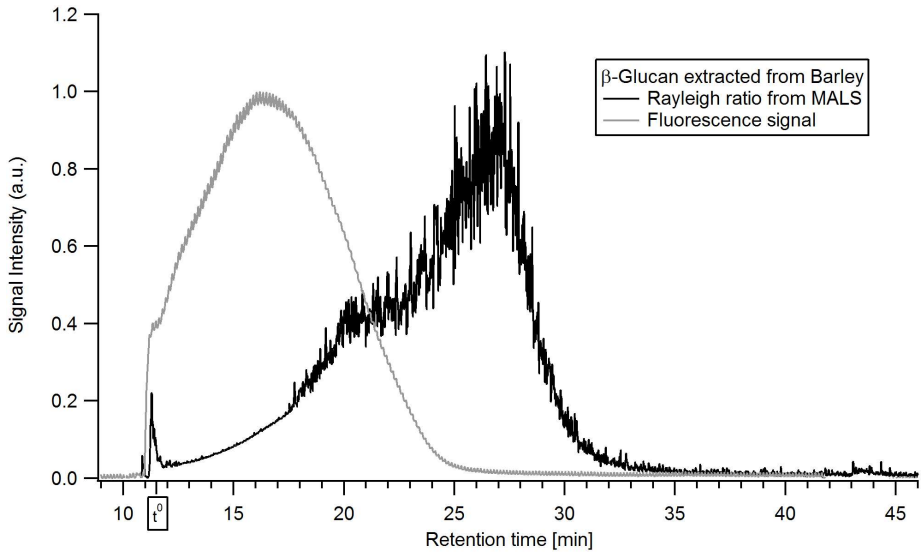

Fig 7. Fluorescence-fractogram of the β-glucan extract from barley. The colors denote: black—Rayleigh ratio from MALS (a.u.), grey —fluorescence signal of in-line Calcofluor-labelled β-glucan at λ_{em} = 445 nm (a.u.).

doi:10.1371/journal.pone.0172034.g007

bound proteins to β-glucan. Hence, the suggested importance of proteinaceous moieties for the functionality of β-glucan and their beneficial health effects cannot be supported.

Acknowledgments

Cristina Teixera, Centrum för preventiv livsmedelsforskning/Food for Health Science Centre at Lund University, Lund, Sweden, is acknowledged for the nitrogen determination with the elemental analyzer. Dr. Matilda Ulmius Storm, SOLVE Research & Consultancy AB, Lund, Sweden is acknowledged for fruitful discussions.

Author Contributions

Conceptualization: LN MLA AS.

Data curation: CZ OK.

Formal analysis: CZ OK.

Funding acquisition: LN MLA AS AL.

Investigation: CZ OK.

Methodology: CZ.

Project administration: CZ LN AL.

Resources: LN AL.

Supervision: LN AL.

Validation: CZ OK.

Visualization: CZ.

Writing – original draft: CZ.

Writing – review & editing: CZ OK MLA AL AS LN.

References

1. U.S. Food and Drug Administration. Food Labeling: Health Claims; Soluble Fiber from Whole Oats and Risk of Coronary Heart Disease. Federal Register. 1992; 62: 15343–15344.
2. U.S. Food and Drug Administration. Food Labeling: Health Claims; Soluble Fiber from Certain Foods and Risk of Coronary Heart Disease. Federal Register. 2008; 73: 47828–47829. PMID: 18956498
3. European Food Safety Authority. Scientific Opinion on the Substantiation of Health Claims related to Beta-Glucans and Maintenance of Normal Blood Cholesterol Concentrations (ID 754, 755, 757, 801, 1465, 2934) and Maintenance or Achievement of a Normal Body Weight (ID 820, 823) pursuant to Article 13(1) of Regulation (EC) No 1924/2006. EFSA Journal. 2009; 7.
4. European Food Safety Authority. Scientific Opinion on the Substantiation of a Health Claim related to Oat Beta-Glucan and Lowering Blood Cholesterol and Reduced Risk of (Coronary) Heart Disease pursuant to Article 14 of Regulation (EC) No 1924/2006. EFSA Journal. 2010; 8.
5. Wolever TMS, Tosh SM, Gibbs AL, Brand-Miller J, Duncan AM, Hart V, et al. Physicochemical properties of oat β-glucan influence its ability to reduce serum LDL cholesterol in humans: a randomized clinical trial. Am J Clin Nutr. 2010; 92: 723–732. doi: 10.3945/ajcn.2010.29174 PMID: 20660224
6. Gómez C, Navarro A, Gamier C, Horta A, Carbonell JV. Physical and structural properties of barley (1→3),(1→4)-β-D-glucan Part III. Formation of aggregates analysed through its viscoelastic and flow behavior. Carbohyd Polym. 1997; 34 (3): 141–148.
7. Wood PJ. Relationships between solution properties of cereal b-glucans and physiological effects—a review. Trends Food Sci Tech. 2004; 15: 313–320.
8. Cui SW, Wang Q. Cell wall polysaccharides in cereals: chemical structures and functional properties. Struct Chem. 2009; 20: 291–297.
9. Håkansson A, Ulmius M, Nilsson L. Asymmetrical flow field-flow fractionation enables the characterization of molecular and supramolecular properties of cereal beta-glucan dispersions. Carbohyd Polym. 2012; 87: 518–523.
10. Lazaridou A, Biliaderis CG. Molecular aspects of cereal beta-glucan functionality: Physical properties, technological applications and physiological effects. J Cereal Sci. 2007; 46 (2): 101–118.
11. Forrest IS, Wainwright T. Mode of binding of beta-glucans and pentosans in barley endosperm cell-walls. J I Brewing. 1977; 83: 279–286.
12. Webster FH, Woods PJ. Oats: Chemistry and Technology. 2nd ed. AACC International Inc., Minnesota, USA; 2011.
13. Autio K, Myllymaki O, Suortti T, Saastamoinen M, Poutanen K. Physical properties of (1→3),(1→4)-beta-D-glucan preparates isolated from finnish oat varieties. Food Hydrocolloid. 1992; 5: 513–522.
14. Vårum KM, Smidsrød O. Partial chemicial and physical characterisation of (1→3),(1→4)-β-D-glucans from oat (Avena sativa L.) aleurone. Carbohyd Polym. 1988; 9: 103–117.
15. Acker L, Diemair W, Samhammer E. The lichenin of oats. 1. Properties, preparation and composition of the muciparous polysaccharides. Z Lebensm Unters For. 1955; 100: 180–188.
16. Johansen HN, Wood PJ, Knudsen KEB. Molecular weight changes in the (1→3),(1→4)-beta-D-glucan of oat incurred by the digestive processes in the upper gastrointestinal tract of pigs. J Agr Food Chem. 1993; 41: 2347–2352.
17. Zhou M, Robards K, Glennie-Holmes M, Helliwell S. Effects of enzyme treatment and processing on pasting and thermal properties of oats. J Sci Food Agr. 2000; 80: 1486–1494.
18. Dawkins NL, Nnanna IA. Oat gum and β-glucan extraction from oat bran and rolled oats: Temperature and pH effects. J Food Sci. 1993; 58: 562–566.
19. Wood PJ, Paton D, Siddiqui IR. Determination of β-glucan in oats and barley. Cereal Chem. 1977; 54 (3): 524–533.

20. Ahmad A, Anjum FM, Zahoor T, Nawaz H, Ahmed Z. Extraction and characterization of beta-D-glucan from oat for industrial utilization. Int J Biol Macromol. 2010; 46 (3): 304–309. doi: 10.1016/j.ijbiomac.2010.01.002 PMID: 20083136

21. Nilsson L. Separation and characterization of food macromolecules using field-flow fractionation: A review. Food Hydrocolloid. 2013; 30: 1–11.

22. Giddings JC. Field-flow fractionation: Analysis of macromolecular, colloidal, and particulate materials. Science. 1993; 260: 1456–1465. PMID: 8502990

23. Tügel I, Runyon JR, Gomez Galindo F, Nilsson L. Analysis of polysaccharide and proteinaceous macromolecules in beer using asymmetrical flow field-flow fractionation. J I Brewing. 2015; 121: 44–48.

24. Ulmius M, Adapa S, Önning G, Nilsson L. Gastrointestinal conditions influence the solution behaviour of cereal β-glucans in vitro. Food Chem. 2012; 130: 536–540.

25. Ulmius M, Önning G, Nilsson L. Solution behavior of cereal β-glucan as studied with asymmetrical flow field-flow fractionation. Food Hydrocolloid. 2012; 26: 175–180.

26. Wahlund KG, Giddings JC. Properties of an asymmetrical flow field flow fractionation channel having one permeable wall. Anal Chem. 1987; 59 (9): 1332–1339. PMID: 3605623

27. Ajayi AO, Fagade OE. Heat activation and stability of amylases from Bacillus species. Afr J of Biotechnol. 2007; 6 (10): 1181–1184.

28. Kosik O, Bromley JR, Busse-Wicher M, Zhang Z, Dupree P. Studies of enzymatic cleavage of cellulose using polysaccharide analysis by carbohydrate gel electrophoresis (PACE). In: Gilbert HJ editor. Cellulases. Elsevier Academic Press Inc: San Diego, USA; 2012. pp. 51–67.

29. Goubet F, Barton CJ, Mortimer JC, Yu X, Zhang Z, Miles GP, et al. Cell wall glucomannan in Arabidopsis is synthesised by CSLA glycosyltransferases, and influences the progression of embryogenesis. Plant J. 2009; 60: 527–538. doi: 10.1111/j.1365-313X.2009.03977.x PMID: 19619156

30. Håkansson A, Magnusson E, Bergenståhl B, Nilsson L. Hydrodynamic radius determination with asymmetrical flow field-flow fractionation using decaying cross-flows. Part I. A theoretical approach. J Chromatogr A. 2012; 1253: 120–126. doi: 10.1016/j.chroma.2012.07.029 PMID: 22835686

31. Alftrén J, Peñarrieta JM, Bergenståhl B, Nilsson L. Comparison of molecular and emulsifying properties of gum arabic and mesquite gum using asymmetrical flow field-flow fractionation. Food Hydrocolloid. 2012; 26 (1): 54–62.

32. Berry GC. Thermodynamic and conformational properties of polystyrene. I. Light-Scattering studies on dilute solutions of linear polystyrenes. J Chem Phys. 1966; 44 (12): 4550–4564.

33. Andersson M, Wittgren B, Wahlund KG. Accuracy in multiangle light scattering measurements for molar mass and radius estimations. Model calculations and experiments. Anal Chem. 2003; 75 (16): 4279–4291. PMID: 14632147

34. Li W, Cui SW, Wang Q, Yada RY. Studies of aggregation behaviours of cereal b-glucans in dilute aqueous solutions by light scattering: Part I. Structure effects. Food Hydrocolloid. 2011; 25: 189–195.

35. Immerstrand T, Bergenståhl B, Trägårdh C, Nyman M, Cui S, Öste R. Extraction of β-Glucan from Oat Bran in Laboratory Scale. Cereal Chem. 2009; 86 (6): 601–608.

36. Papageorgiou M, Lakhdara N, Lazaridou A, Biliaderis CG, Izydorczyk MS. Water extractable (1→3,1→4)-β-D-glucans from barley and oats: An intervarietal study on their structural features and rheological behavior. J Cereal Sci. 2005; 42: 213–224.

37. Robyt JF. Enzymes and their action on starch. In: Bemiller JN, Whistler RL, editors. Starch: Chemistry and Technology. Academic Press: Elsevier, London, UK; 2009. pp. 238–292

38. Alves LA, Almeida e Silva JB, Giulietti M. Solubility of D-Glucose in Water and Ethanol/ Water Mixtures. J Chem Eng Data. 2007; 52: 2166–2170.

39. Gong X, Wang C, Zhang L, Qu H. Solubility of Xylose, Mannose, Maltose Monohydrate, and Trehalose Dihydrate in Ethanol-Water Solutions. J Chem Eng Data. 2012; 57: 3264–3269.

40. Caldwell KD, Nguyen TT, Myers MN, Giddings JC. Observations on anomalous retention in steric field-flow fractionation. Separ Sci Technol. 1979; 14 (10): 935–946.

41. Andersson M, Wittgren B, Wahlund KG. Ultrahigh molar mass component detected in ethylhydroxyethyl cellulose by asymmetrical flow field-flow fractionation coupled to multiangle light scattering. Anal Chem. 2001; 73: 4852–4861. PMID: 11681461

42. Perez-Rea D, Bergenståhl B, Nilsson L. Development and evaluation of methods for starch dissolution using asymmetrical flow field-flow fractionation. Part I: amylopectin. Anal Bioanal Chem. 2015; 407: 4315–4326. doi: 10.1007/s00216-015-8611-8 PMID: 25925852

43. Beer MU, Wood PJ, Weisz J. Molecular weight distribution and (1→3)(1→4)-β-D-glucan content of consecutive extracts of various oat and barley cultivars. Cereal Chem. 1997; 74: 476–480.

44. Ahmad A, Anjum FM, Zahoor T, Nawaz H, Dilshad SMR. Beta Glucan: A Valuable Functional Ingredient in Foods. Crit Rev Food Sci. 2012; 52: 201–212.

45. Kim S, Inglett GE. Molecular weight and ionic strength dependence of fluorescence intensity of the Calcofluor/ β-glucan complex in flow-injection analysis. J Food Compos Anal. 2006; 19: 466–472.

46. Izydorczyk MS, Dexter JE. Barley β-glucans and arabinoxylans: Molecular structure, physicochemical properties, and uses in food products—a Review. Food Res Int. 2008; 41: 850–868.

Paper II

Characterization of Cereal β-Glucan Extracts: Conformation and Structural Aspects

Zielke, C., Stradner, A. & Nilsson, L.

Accepted for publication in Food Hydrocolloids

Characterization of Cereal β-Glucan Extracts: Conformation and Structural Aspects

Claudia Zielke[1*], Anna Stradner[2], Lars Nilsson[1]

Accepted for publication in Food Hydrocolloids

[1] Department of Food Technology, Engineering and Nutrition, Lund University, Lund, Sweden
[2] Department of Physical Chemistry, Lund University P.O. Box 124, SE-221 00 Lund, Sweden

*Corresponding author, E-mail: claudia.zielke@food.lth.se

Abstract

Several health benefits have been established for cereal mixed-linkage β-glucan of high molar mass (*M*), and are said to be attributed to the ability of β-glucan to form viscous slurries in the gut. As no comprehensive understanding exists yet, the characterization of β-glucan solution behaviour is crucial. β-Glucan was characterized in terms of *M*, molecular size and conformation characteristics in aqueous solutions, utilizing asymmetric flow field-flow fractionation (AF4) coupled to multi-angle light scattering (MALS) and differential refractive index (dRI) detectors. Polymers and aggregates were investigated using conformational data from comparing hydrodynamic radii (r_{hyd}, from AF4) and root-mean-square radii (r_{rms}, from MALS), Kratky plots (from MALS) and persistence length determination (from small-angle x-ray scattering (SAXS)). Furthermore, the aggregated structures were also analysed with cryo-transmission electron microscopy (cryo-TEM). The results show the presence of highly aggregated structures in aqueous solution, in addition to dissolved, highly polydisperse polymers. The structural and conformational properties of the aggregates are different between oat and barley β-glucan. While oat β-glucan seems to be aggregated in a widely distributed, loose structure, barley β-glucan showed surprisingly dense and well-defined aggregates.

Keywords: hydrodynamic radius r_{hyd}, molar mass (*M*), asymmetric flow field-flow fractionation (AF4), small-angle X-ray scattering (SAXS)

Abbreviations: AF4 asymmetric flow field-flow fractionation; DP degree of polymerisation; dRI differential refractive index; FL fluorescence; l_p persistence length; *M* molar mass; MALS multi-angle light scattering; q scattering vector; r_{hyd} hydrodynamic radius; r_{rms} root-mean-square radius, radius of gyration; rt room temperature, defined as 20 °C; SAXS small-angle X-ray scattering

1. Introduction

The water soluble fiber β-glucan from oat and barley is a linear, β-1,3 and β-1,4 linked polysaccharide formed of β-D-glucopyranosyl units. Several health effects of mixed-linkage β-glucan have been established by the scientific panel of the EU (European Food Safety Authority, 2009, 2010.) and by the U.S. Food and Drug Administration (FDA) (U.S. Food and Drug Administration, 1992, 2008), claiming the reduction of serum cholesterol in the blood as well as reduced glycaemic and insulin responses of the consumer.

It has been suggested that the physicochemical and structural properties govern the nutritional

functionality of β-glucan (Wood, 2004; Cui & Wang, 2009; Gómez, Navarro, Gamier, Horta & Carbonell, 1997) and different possible working mechanisms have been suggested. One possibility is the ability of high molar mass (*M*) β-glucan to form aggregates, whereas this aggregation is highly dependent on the molar ratios of trimers and tetramers (DP3:DP4) in the individual molecules, the hydrodynamic radius (r_{hyd}) and the conformation (Agbenorhevi, Kontogiorgos, Kirby, Morris & Tosh, 2011; Håkansson, Ulmius & Nilsson, 2012; Li, Cui, Wang & Yada, 2011). Furthermore, intermolecular interactions can form physical cross-linkages between single molecules. In β-glucan from different cereal origins, a considerable diversity exists regarding *M* and structure, e. g. the distributions of β-1,3 and β-1,4 linkages (Agbenorhevi et al., 2011; Lazaridou & Biliaderis, 2007). In oat β-glucan, β-1,4 trimers (53 - 61%) and tetramers (34 - 41%) are the most dominant, whereas the DP3:DP4 ratios range between 1.5 and 2.3 (Lazaridou & Biliaderis, 2007). Another often discussed structural characteristic is the ratio between (1→4) and (1→3) β-glycosidic bonds and has been reported to be 2.3 - 2.8 for oat β-glucan.

Another suggested mechanism when discussing the health benefits is the ability of β-glucan to form viscous slurries in the gut (Papageorgiou, Lakhdara, Lazaridou, Biliaderis & Izydorczyk, 2005; Skendi, Biliaderis, Lazaridou & Izydorczyk, 2003), and hence, increase the viscosity of digesta in the alimentary tract. This could reduce the rate of macronutrient absorption (Wang & Ellis, 2014) and result in an enhanced glycaemic profile. This was discussed e. g. by Regand, Chowdhury, Tosh, Wolever & Wood (2011), suggesting the entrapment of starch in the β-glucan viscous gel. Furthermore, it was proposed, that β-glucan from oat might affect the absorption of dietary fats in the gastrointestinal lumen (Othman, Moghadasian, & Jones, 2011). Wolever et al. (2010) discussed an inverse linear correlation between viscosity, *M* and cholesterol-lowering capacity, as a clinical trial showed that an intake of only 3 g/day of oat β-glucan significantly lowered LDL cholesterol in blood. Therefore, investigating the structure of cereal β-glucan and the behavior in solution as well as rheological properties is crucial to understand the mechanisms and behavior in the digestion system.

However, the great size range and complexity of β-glucan and its possible aggregates are still a challenge for analysis and characterization. Established methods like batch light scattering or confocal scanning laser microscopy already suggested irregular aggregated structures (Li, Cui, Wang & Yada, 2010) or "fringed micelle" structures (Grimm, Krüger & Burchard, 1995). Another approach was made by Wu et al. (2006), utilizing atomic force microscopy in combination with confocal scanning laser microscopy to visualize aggregated β-glucan. They found an aggregation behavior similar to the "fringed micelle" structures previously suggested by Grimm et al.

Asymmetric flow field-flow fractionation (AF4) has been shown to be a separation method especially suited for large and polydisperse polysaccharides (Nilsson, 2013). Several studies investigating cereal β-glucan with the help of AF4 in combination with a multi-angle light scattering (MALS) and a differential refractive index (dRI) detector have been previously reported, e. g. the dissolution procedure for standard barley β-glucan at different pH (Håkansson et al., 2012) or at different temperatures as well as the effect of freezing of solutions on the β-glucan *M* by Ulmius, Önning & Nilsson (2012). Mäkelä, Sontag-Strohm & Maina (2015) utilized AF4 in combination with MALS and dRI to investigate the oxidative degradation of barley β-glucan through hydrogen peroxide or ascorbic acid. The separation range of AF4 is approx. 2 nm to >1 µm and it can readily handle macromolecules containing ultra-high *M* components (M $>10^7$ g/mol). AF4 is considered a chromatography-like technique, without stationary phase, where the retention time (t_r) is directly related to the r_{hyd} of the analyte (Giddings, 1981; Wahlund & Giddings, 1987). Briefly, the separation is based on the diffusion coefficient (i.e. hydrodynamic size) of the sample components. After sample injection onto the channel, the analytes are relaxed in a field (cross flow) perpendicular to the semi-permeable accumulation wall during a focusing step. The cross flow induced transport as well as the counteracting diffusional transport cause a steady-state concentration distribution, which is characterized by a concentration average distance (*l*) from the accumulation wall. At a given cross flow, larger molecules will accumulate closer to the accumulation wall,

resulting in a short *l*, compared to smaller molecules with a larger *l*, that are on average relaxed higher up in the channel and hence, further away from the accumulation wall. As a result of the parabolic flow profile during elution, smaller molecules will elute earlier than large species and will reach the online detectors first.

The aim of this study was to investigate the conformation and aggregation behavior of cereal β-glucan from oat and barley, as these characteristics are reported to play an important role in regard to their health benefits. The samples used for this study were extracted from flour in a way that minimizes detrimental effects of extraction on the β-glucan structure, as reported earlier (Zielke et al., 2017). A setup of AF4-MALS-dRI was utilized for obtaining information on *M* distributions in addition to conformational data from comparing r_{hyd} (from AF4 retention times) and root-mean-square radii (r_{rms}, from MALS). Furthermore, Kratky plots (from MALS data) were constructed and compared to theoretical values to get a deeper insight into the conformation and aggregate formation of β-glucan. Cryo-transmission electron microscopy (cryo-TEM) was utilized for comparison to the obtained data from AF4 about the aggregation behaviour of the β-glucan. Additional information in regard to more local aspects of the macromolecular structures like persistence length determination were obtained by utilizing small-angle x-ray scattering (SAXS) data.

2. Experimental section

Substances and chemicals

Mixed-linkage β-glucan was extracted from β-glucan rich oat and barley flour as described earlier (Zielke et al., 2017) to gain purities of 65 % for oat and 53 % for barley. For the preparation of the AF4 carrier liquid, NaN_3 (BDH, Poole, UK) and $NaNO_3$ (Merck, Darmstadt, Germany) were used. All described experiments were performed using pure water from a Milli-Q system (Millipore Corp., Billerica, MA, USA).

FFF analysis equipment, separation parameters and data processing

The AF4 instrument utilized was an Eclipse 3+ Separation System (Wyatt Technology, Dernbach, Germany). A Dawn Heleos II MALS detector and an Optilab T-rEX dRI detector (both Wyatt Technology), both operating at a wavelength of 658 nm, were connected to the system. An Agilent 1100 series isocratic pump with an in-line vacuum degasser delivered the carrier flow through the AF4 separation system and an Agilent 1100 series autosampler (Agilent Technologies, Waldbronn, Germany) handled sample injection. Between this pump and the channel inlet a filter-holder with a 100 nm pore-size polyvinylidene fluoride membrane (Millipore Corp.) was placed to ensure particle free carrier liquid. The carrier liquid used was a combination of 0.02 % (w/v) NaN_3 and 10 mM $NaNO_3$ dissolved in Milli-Q water. A long channel (Wyatt Technology) with a tip-to-tip length of 27.5 cm was used utilizing a spacer with a nominal thickness of 190 µm. Calibration with ferritin as described by Håkansson, Magnusson, Bergenståhl & Nilsson (2012) showed, that the actual thickness was 156 µm. The chosen ultra-filtration membrane forming the accumulation wall was made of PES (hydrophilized polyethersulphone) with a cut-off of 10 kDa (Microdyn-Nadir GmbH, Wiesbaden. Germany), based on previously published work (Ulmius et al., 2011).

Samples investigated with AF4 were prepared as 4 mg/mL by dissolving the extracts in carrier liquid via boiling the suspension with stirring for 30 min resulting in a clear sample. Samples were given time to cool down to rt (25 °C), filtered through a 22 mm syringe filter with a 0.45 µm pore size cellulose acetate membrane (VWR International) and subsequently injected onto the channel. The injection of the samples onto the AF4 channel was performed at a flow rate of 0.2 mL/min during 4 min. Injected volumes of the sample were 40 µl for oat and 80 µl for barley, resulting in a total injected mass of 160 µg and 320 µg, respectively. The injected amounts were carefully optimized by confirming that retention time for the individual samples was independent of injected amount to avoid potential overloading effects. A subsequent focusing/relaxation step was performed for 5 min prior to elution, utilizing a focusing flow rate of 0.5 mL/min whereas the detector flow rate was kept con-

stant at 0.5 mL/min during the whole measurement. The initial cross flow rate of 1 mL/min during elution was followed by an exponential decay ($t_{1/2}$ = 4.5 min) in order to avoid excessive retention and long analysis times. As a final step to ensure a clean channel before analysing the next sample, injection loop and AF4 channel were rinsed in elution mode without any cross flow for 5 min.

For M and r_{rms} estimations, processing of the obtained data from MALS and dRI detectors after AF4 separation was done by using the Astra software in version 5.3.4.14 (Wyatt Technology Europe, Dernbach, Germany). M and r_{rms} were calculated as described in literature (Berry, 1966; Andersson, Wittgren & Wahlund, 2003) performing a 1st order fit with the data obtained from the scattering angles 69.3 ° - 121.2 ° (angles 9-14 in the MALS-detector). Other available scattering angles were excluded as they did not correspond to the plot. The second virial coefficient A_2 was neglected whereas the RI increment (d*n*/d*c*) used was 0.146 mL/g as defined for β-glucan in aqueous solutions (Li, Cui, Wang & Yada, 2011).

The r_{hyd} of the extracted β-glucan was calculated from AF4 retention times using a numerical approach presented by Håkansson et al. (2012), accounting for an exponential decaying cross flow during the AF4 fractionation. With known channel geometry and flow conditions, the translational diffusion coefficient D_t of the analytes can be determined from the obtained retention time as described in Eq. (1), with L representing the channel length, z' the focusing point of the analyte and f the numerically solved function of the diffusion coefficient (Håkansson, Magnusson, Bergenståhl, & Nilsson, 2012).

$$(L - z') = \int_{t=0}^{t_r} f(D_t)dt \quad (1)$$

Subsequently, r_{hyd} can be calculated from the diffusion coefficient using the Stokes–Einstein equation (Eq. 2) (Einstein, 1905):

$$D_t = \frac{k_B T}{6\pi\eta r_{hyd}} \quad (2)$$

where k_B is the Boltzmann constant, T is the absolute temperature and η is the dynamic viscosity of the solvent.

Further information about the conformation is derived from the angular variation of the light scattering data from all available MALS angles (14.5 ° - 163.3 °; angles 3-18 in the MALS-detector) by generating Kratky plots (Kratky & Porod, 1949; Andersson, Wittgren, Schagerlof, Momcilovic & Wahlund, 2004) The angular variation is approximated by using the relationship of Rayleigh ratio (R_θ) and the concentration dependent optical constant of the analyte K_c (Eq. 3), with M as molar mass and $P(u)$ the scattering as a function of u, which is defined by Eq. 4.:

$$\frac{R_\theta}{K_c} = MP(u) \quad (3)$$

and

$$u = r_{rms} * q \quad (4)$$

where q is the scattering vector and can be calculated following Eq. 5:

$$q = \left(\frac{4\pi n_0}{\lambda_0}\right) \sin\left(\frac{\theta}{2}\right) \quad (5)$$

where n_0 is the refractive index of the solvent (1.33 for water), λ_0 is the wavelength of the incident light in vacuum (658 nm) and θ is the angle between the incident and the scattered light. Kratky plots are then constructed by plotting $P(u)u^2$ as a function of u. Theoretical values for $P(u)u^2$ and u can be found for different conformation and polymer structures (Burchard 1983, 2004, Kratky 1949) and are plotted along with the obtained data for comparison.

Cryo-TEM

Cryo-TEM allows imaging of samples without the use of a stain to increase contrast and was therefore suitable for our samples and was performed on β-glucan extracts at a concentration of 5 mg/mL. Samples were dissolved in AF4 carrier liquid in the same way as samples for AF4 were prepared. The samples were filtered through a 25 mm syringe filter with a 1.2 µm Versapor Membrane (Pall Life ScienceAnn Arbor, MI, USA). Here, a different pore size compared to the AF4 measurements was used, as a higher concentration is required for the cryo-TEM as for the AF4 analysis. The sample is highly viscous at a concentration of 5 mg/mL and therefore it is not possible to filter it with a smaller pore size. As shown in an earlier study, filtering of the sample extracts does not influence the β-glucan when analysed with AF4 (Zielke et al., 2017). A 5 µL drop was placed on a lacey carbon-coated copper grid and subsequently plunged into liquid ethane at -180 °C to allow rapid vitrification of the sample and thus, avoiding crystallisation of water. Until being transferred to the electron

microscope, the prepared grids were stored in liquid nitrogen. Transmission electron micrographs were recorded using a digital Philips CM120 Bio TWIN electron microscope. The microscope was operated at 120 kV and equipped with a Gatan MSC 791 cooled-CCD camera system (Gatan Inc, Pleasanton, CA, USA).

SAXS equipment and analysis

SAXS measurements were carried out with a pinhole camera Ganesha 300 XL Small-Angle X-ray Scattering System from SAXSLAB ApS, Lyngby, Denmark, covering a q-range of 0.013-0.75 $Å^{-1}$. The system was equipped with a high brilliance microfocus sealed tube and a Pilatus detector. All measurements were corrected for transmission, dark current and background radiation as well as for capillary thickness and carrier liquid. The SAXS measurements were performed to record the scattered intensity I(q) of the β-glucan as a function of the magnitude of the scattering vector q, which is defined in Eq. (6) as a simplified version of Eq. (5):

$$q = \frac{4\pi}{\lambda}\sin\frac{\theta}{2} \quad (6)$$

with λ being the wavelength of the radiation and θ being the scattering angle. Samples investigated with SAXS were prepared as 10 mg/mL by dissolving the extracts at 100 °C for 30 min in AF4 carrier liquid. The samples were filtered through a 1.2 µm pore size filter, as used for the cryo-TEM, prior to SAXS analysis. With the obtained SAXS data, log-log plots were constructed by plotting I(q) against q. In such a presentation, a q^{-1}-dependence of the scattered intensity is characteristic for rod-like structures whereas a potential q^{-2}- or $q^{-3/5}$-regime reflects the behaviour of a random coil in a theta solvent and a good solvent. The transition between such a q^{-1}-regime and a q^{-2}- or $q^{-3/5}$-regime, respectively, occurs at q^*, which can be roughly estimated by the intersection of the extrapolation of these two regimes. The persistence length l_p is directly related to this transition and can be calculated according to Eq. (7):

$$q^* * l_p \approx 1.9 \quad (7)$$

3. Results

Characterization of extracts

β-Glucan extracts from oat and barley flour were investigated with AF4-MALS-dRI in order to obtain fundamental information and parameters such as M and r_{rms} distributions. The extracts were specifically labeled post channel with Calcofluor and analysed with an online fluorescence detector to identify the β-glucan in the extracts. All experimental procedures and results can be found in detail elsewhere (Zielke et al., 2017), and AF4-MALS, fluorescence signal, M and r_{rms} distributions from both β-glucan are for a better understanding again displayed in Fig. 1A (oat) and 1B (barley). The fractograms show that the samples contain high M β-glucan (10^5 - 10^8 g/mol) and large sizes (r_{rms} from 20 to 140 nm). The results are briefly summarized in Tab. 1. As described previously (Zielke et al., 2017), main impurities of the extracts were identified as degradation products from starch, and no proteins were detected in the β-glucan sample.

Conformational studies and aggregation behavior obtained from AF4

The differential weight distribution of the oat β-glucan as seen in Fig. 1C (black solid line) shows a maximum at 5 x 10^5 g/mol. For oat β-glucan, the apparent density (Fig. 1C, grey dots) decreases at first with increasing M from 2 kg/m^3 to 0.1 kg/m^3. Reaching M values of above 2 x 10^6 g/mol, the apparent density shows an inflection point and thus, the values rise again slightly (~0.2 kg/m^3) with increasing M. Further conformational data was obtained by plotting the ratio of r_{rms}/r_h (black dots) versus M and can as well be seen in Fig.1C. An overview of how to interpret the ratios regarding the conformation can be found in Nilsson (2013). Tab. 2 lists some common values of r_{rms}/r_h and their corresponding conformation.

The oat sample shows a variety of different conformational properties over the M distribution, which settle to low and constant values of r_{rms}/r_{hyd} above M~2 x 10^6 g/mol. The ratios for oat β-glucan start above a value of 2, corresponding to a rod-like and stiff conformation (~1.7–3.0) (Coviello, Kajiwara,

Burchard, Dentini, & Crescenzi, 1986; Wittgren, Borgström, Piculell & Wahlund, 1998). With increasing *M*, the r_{rms}/r_{hyd} ratio decreases below 2, corresponding to a random coil conformation (1.5–2) as could be expected for molecularly dissolved β-glucan (Burchard, 1983), or 1-1.5, suggesting branched molecule structures (Burchard, 1999). At the maximum of the differential weight distribution (5×10^5 g/mol), the ratio values range between 0.5 and 1, what already corresponds to a micro gel structure (<0.7, Burchard 1999). The values drop further, until they even out at around 0.3 for high *M* species, and hence, the results suggest that high *M* β-glucan is present as a micro gel structure (Schmidt, Nerger, & Burchard, 1979). Looking at the differential *M* distribution of the β-glucan it can be seen that the barley β-glucan (Fig. 1D, black line) appears smaller compared to the β-glucan from oat (Fig, 1C, black line) whereas both extracts contain high *M* species. Barley has its maximum in the differential *M* distribution at 8×10^4 g/mol, followed by an exponential decrease with a lower limit at 1.5×10^7 g/mol. The value for the apparent density (Fig. 1D, grey dots) decreases as well with an increase in *M*, starting at 2 kg/m^3 for a *M* of 10^5 g/mol and decreasing to a value of 0.3 kg/m^3 for $M \sim 1 \times 10^6$ g/mol, whereas for higher *M* a slight increase is noticeable. Compared to the oat β-glucan (Fig. 1C, black dots), the plot of r_{rms}/r_h vs. *M* for barley (Fig.1D, black dots) shows lower maximum values for $M < 1 \times 10^5$ g/mol, starting at 1.5 and indicating branched structures. With increasing *M*, the value decreases sharply to a value of 0.5, indicating as well a micro-gelled structure for high *M* β-glucan.

Conformation analyses for the two β-glucan are shown in Fig. 2. Kratky plots for β-glucan from oat were obtained from MALS data for AF4 retention times of 20 min (Fig. 2A, red dots, corresponding to $M = 1 \times 10^6$ g/mol, r_{rms} =55 nm) and 27 min (Fig. 2B, red dots, $M = 1 \times 10^8$ g/mol, r_{rms} =125 nm) as marked in Fig. 1A, and Kratky plots for barley were obtained from MALS data for retention times of 20 min (Fig 2A, blue dots, corresponding to $M = 3 \times 10^6$ g/mol, r_{rms} =65 nm) and 23.5 min (Fig. 2B, red dots, $M = 5 \times 10^7$ g/mol, r_{rms} =100 nm) as marked in Fig. 1B. These retention times (20 and 27 min for oat, 20 and 23.5 min for barley) for constructing the Kratky plots were chosen, as former FL results (Fig. 1A,B, grey dashed lines) have shown that β-glucan is present at these retention times, with 20 min representing smaller *M* and the higher retention times representing high *M* species at the maximum of the respective light scattering signal. For data interpretation, theoretical Kratky conformation values are plotted besides the obtained data in Fig. 2A and B. For the results at shorter retention times (Fig. 2A), no distinct conclusion should be made from MALS data when compared with theoretical approaches, as $u^2P(u)$ for low u values is very similar in all theories. Nevertheless, it can be stated, that ß-glucan from oat (red dots) seems to follow the polydisperse rod-like conformation for lower *M* above u=1, whereas ß-glucan from barley (blue dots) seems to follow the theoretical values of a hyperbranched structure. For longer retention times (Fig. 2B), oat data (red dots) is overlapping with the theory of polydispersed random coil (b) for u values between 1.5 and 2, monodispersed random coil conformation (c) for values of u = 2.5, but approaching the shape of hyperbranched structures (d) for higher u values. The obtained data set for barley (blue dots), overlay the theoretical data for polydispersed random coil (b), monodispersed random coils (c) and hyperbranched structures (d) within u values of 1.5-2, but follow only the behavior of hyperbranched sturctures for higher u.

Cryo-TEM

Cryo-TEM micrographs can be seen in Fig. 3. Oat β-glucan show highly polydisperse and loosely aggregated structures which appear as large and hyperbranched networks and in a radius range of several 100 nm (Fig. 3A). β-Glucan from barley (Fig. 3B) show similar loosely aggregated structures, but in addition, relatively dense and sphere-like structures are visible. The relatively well-defined aggregates range in radius between 50 and 100 nm.

Persistence length determination

SAXS data from both oat and barley β-glucan in solution can be seen in Fig. 4A and B, respectively. For oat, a log-log plot of the data was obtained and a transition point q^*between the flexible chain asymptotic behavior (q^{-2}) and the rigid segment (q^{-1}) regimes was estimated to 0.008 nm^{-1} for oat. Through Eq. (7), a l_p of

2.4 nm was determined for oat β-glucan. For barley β-glucan (Fig. 4B), we see no indication of a cross-over from a flexible chain to rigid segment asymptotic behavior and therefore, no l_p could be obtained.

4. Discussion

β-Glucan from oat and barley were analysed and characterized in terms of conformation and aggregation behavior. The graphs displaying fractionation of the extracts (Fig. 1A and B) show that the samples are highly polydisperse regarding *M* and r_{rms}. A detailed discussion about the fractionation results can be found elsewhere (Zielke et al., 2017).

Additional conformational data supporting the presence of aggregated structures for high *M* species is obtained from the r_{rms}/r_{hyd} ratio, displayed vs. *M* in Fig. 1C for oat β-glucan and 1D for barley β-glucan. Expected for dissolved individual β-glucan chains would be values ranging from 1.5 to 2, representing a random coil conformation. This conformation is characteristic for molecules with a chain contour length that is substantially longer than l_p. Both samples show a variety of different conformational properties over the *M* distribution, from random coil conformation via hyperbranched stuctures (1 - 1.5), settling to low and constant values of r_{rms}/r_{hyd} below 0.5 for $M > 2 \times 10^6$ g/mol, where the conformation becomes independent of *M* and represents a micro gel structure (Schmidt, Nerger, & Burchard, 1979; Burchard, 1999). Such low values of around 0.3 have been observed before for oat β-glucan (Håkansson et al.), although micro gel structures are by definition not expected for molecularly dissolved β-glucan (linear chain) (Graham & Cameron, 1998). However, these type of structures were previously observed for high *M* molecules like the linear poly(vinyl)acetate (Schmidt, Nerger & Burchard, 1979) and have also been observed for hyperbranched polymers e. g. glycogen (Fernandez, Rojas & Nilsson, 2011). Furthermore, looking at both the apparent density and the r_{rms}/r_{hyd} values for oat (Fig. 1C), the results seem to be contradictive. At first, a growth of individual smaller aggregates or molecularly dissolved single molecules is expected to decrease the apparent density with an increasing size. However, for higher *M* ($> 10^5$ g/mol), the apparent density increases. Nevertheless, the low values for r_{rms}/r_{hyd} might indicate that most of the aggregates' mass is located in the center, and the structure becomes less and less dense when going towards the perimeter, where β-glucan chains have less conformational freedom and stretch out to accommodate other chains in the aggregate. Therefore, the results could suggest a higher level of aggregation, where already present aggregates of lower *M* form secondary aggregates. This was also suggested earlier (Håkansson et al., 2012). Furthermore, the possibility of spherical solvent-draining particles with a higher polymer density in the core of the aggregate and a lower density towards the perimeter, into the solvent protruding chains could be characterized as fringed micelles being involved in network formation (Grimm, Krüger & Burchard, 1995) or micro gel-like particles (Sitar, Aseyev & Kogej, 2014). However, care should be taken when interpreting apparent density values for an increasing *M* range with simultaneously changing conformational/shape data from r_{rms}/r_{hyd} since it might be influenced by elongation of the molecules' branches and backbone to some extent (Dervilly-Pinel, Thibault & Saulnier, 2001).

The apparent density of barley β-glucan (Fig. 1D) shows a similar behavior as oat, with initially decreasing values for lower *M* species. In contrast to oat, barley β-glucan doesn't show a defined inflection point, the values even out at a rather constant level. However, the results still indicate, that over the whole *M* distribution the sample components drastically change, which is also represented in the wide range of r_{rms}/r_{hyd} from ~0.3-1.5 over the *M* distribution.

Furthermore, it can be stated, that the majority of the β-glucan of both grains is present at lower *M* values as can be seen from the differential weight fractions (Fig. 1C for oat and 1D for barley, black solid line), and thus, the discussed macromolecular and aggregated structures are only present in low concentration. For barley β-glucan, the distinguished increase of the differential weight fraction at high $M > 2 \times 10^7$ g/mol should be seen as an artefact, due to a low concentration signal from dRI at high retention

times (Fig. 1A, blue line) and can therefore be neglected.

Kratky plots for oat and barley (Fig. 2A and B) β-glucan suggest the presence of hyperbranched structures. For both oat and barley, data points taken from a retention time of 20 min (Fig. 2A) gave no information about a possible conformation at $u < 1$ as all theoretical values overlap and no tendency of following one specific theoretical curve can be seen. For values of $u > 1$ (Fig. 2A), β-glucan from oat (red dots) seems to follow the polydisperse rod-like conformation whereas β-glucan from barley (blue dots) seems to follow the theoretical values of a hyperbranched structure. The results in Fig. 2A should be interpreted with care as the analytes might be too small at this retention time in relation to the wavelength of the MALS light source used (λ = 658 nm) (Hupfeld, 2009). For longer retention times (Fig. 2B), data points for oat (red dots) are overlapping several theories, but approaching values between monodispersed random coil behavior (c) and hyperbranched structures (d) for higher u values. The fractions eluting from the AF4 channel have a narrow size distribution but are, however, not monodisperse, and hence the monodispersed random coil behavior (c) is less probable. Barley (Fig. 2B, blue dots) as well as oat β-glucan (Fig. 2B, red dots) seems to follow the theoretical values for hyperbranched structures (d). Yet, it is well known that β-glucan is a linear polysaccharide without branches and therefore expected to behave as a chain-like molecule, being flexible due to the ß(1→3) linkages. Only aggregated structures of the linear molecule are likely to cause the hyperbranched conformational property observed. A proposal of how such aggregated β-glucan structures may look like has been previously suggested and discussed in detail by Håkansson et al. (2012), where the linear chains assemble to a dense core with chains protruding into the surrounding. Similar considerations have been proposed by Vårum, Smidsröd, & Brant (1992) suggesting cereal β-glucan to aggregate in micellar-like structures and by Grimm et al. (1995) as fringed micelle structures where a dense core is resulting from an alignment of ß-glucan chains. Sitar et al. (2014) investigated poly(methacrylic acid) chains with random coil structures, where the atactic species in the Kratky plots follow as well the theory of hyperbranched structures, referred to as Debye-Bueche scattering function. More detailed, the Debye-Bueche scattering function describes hyperbranched flexible chains and micro gels from chemically cross-linked flexible chains (Savin 2004, Burchard 2004). Hence, this literature is supporting our results showing β-glucan assembling and forming (hyperbranched-like structural) aggregates. To complement the results obtained by AF4, cryo-TEM was utilized (Fig. 3A for oat and Fig. 3B for barley β-glucan). Here the results indicate as well the aggregation of β-glucan as seen before. β-Glucan from oat (Fig. 3A) shows highly aggregated arrangements with a quite complex network formation as seen before for polymeric aggregates of linear amylose (Buléon, Véronès & Putaux, 2007). The aggregates of the linear β-glucan molecules appear in the micrographs like hyperbranched structures, supporting results obtained from Kratky plots. Long chain molecules are aggregating to form wide-spread networks, most likely inducing a behavior similar to high *M* branched molecules. The wide-spread network formation allows speculation about possible micro gel formation through aggregation (Burchard, 1999) as the previously obtained values for r_{rms}/r_{hyd} (Fig. 1C) suggest. It should be mentioned, that the size of the aggregates (up to approximately 250 nm in radius) shown in the micrographs (Fig. 3A) is larger than the maximum size obtained from the AF4 results (max. value ~140 nm in r_{rms}). This might be due to the fact, that it is not possible in the micrographs to distinguish individual aggregates and comparison between the two radii is further complicated by the fact that the r_{rms} will depend on how the mass is distributed in the aggregates. Furthermore, sample preparation by shock-freezing with liquid ethane as needed for cryo-TEM might lead to artifacts including molecules arranging themselves according to their size in areas of the grid with higher water layer thickness or mesh grid depth (Hupfeld, 2009), giving the appearance of slightly larger aggregates. The predominant presence of the aggregates close to the grid supports this. That would explain as well the large amount of aggregates visible in the micrographs, although the differential weight fraction for both extracts (Fig. 1C and D, black lines) showed the majority of the sample at lower sizes (oat: 5×10^5 g/ mol ≈ 80

nm; barley: 10^5 g/mol ≈ 70 nm) and low concentrations for high *M* species. Nevertheless, a possible explanation is also that lower amounts of high *M* species can be lost during AF4 analysis. As the recovery values for oat β-glucan from the AF4 channel are relatively low (78 %), some loss of the largest aggregates could occur. The same highly aggregated and complex network as observed for oat can be seen in the micrographs of barley β-glucan (Fig. 3B), and the same conclusions can be drawn when comparing the results to Kratky plots. However, in addition to the large and loosely arranged aggregated structures, dense and very well defined round aggregates in the size range of 50 to >170 nm in radius are present. These aggregates tend to form groups, and can hardly be found as single structures, what could be as well related to the film depth on the grid. To make the r_{rms} from AF4 and the visible r_{hyd} from cryo-TEM radii somewhat more comparable, r_{hyd} is multiplied by 0.77 (according to the relation that $r_{rms}/r_{hyd} = 0.77$ applies for a spherical object) and homogeneous values in the range of 25 – 80 nm are obtained with considerable material present as seen from the dRI-signal in Fig. 1B. To our knowledge the presence of such distinct an relatively well-defined aggregates has not been reported previously.

Comparing the oat and barley samples, which both give values for $r_{hyd}/r_{rms} < 0.5$, indicating a micro gel structure (Fig. 1C and D) for high *M* where aggregates are present, it seems surprising that we can observe a different aggregation pattern with cryo-TEM. Oat β-glucan aggregates consist of more loosely arranged swollen aggregates with higher amounts of water trapped in the aggregated structure, as expected for a micro gel. Barley β-glucan shows, in addition to the loosely arranged swollen aggregates, relatively dense spherical structures. However, the AF4 results (Fig. 1D) show that the large aggregates are of micro gel conformation. This suggests that the micro gel conformation could originate from a heterogeneous distribution of mass in the spherical aggregates. A possibility is that the aggregates have polymer chains protruding in to the surrounding solution from the surface, which are not visible in the cryo-TEM micrographs (Fig. 3B). The presence of such chains could cause the hydrodynamic size to increase considerably. A somewhat similar solution behavior, i.e. a dense core with protruding chains giving rise to a large r_{hyd} in relation to r_{rms}, has previously been observed for modified starch (Nilsson et al. 2006). The suggestion is, again, in line with the previously reported fringed-micelle structure of β-glucan aggregates (Grimm, Krüger & Burchard, 1995).

It seems evident that the origin of the β-glucan plays a role in their physico-chemical behavior and variance of properties, and this may have an influence on their beneficial health effects. As previously discussed in literature (Lazaridou et al. 2007), there is a considerable variety in *M* and the distribution of β-1,3 and β-1,4 linkages in the β-glucan structure originating from different cereal origin, what can influence, besides others, their solution behavior and extractability (Immerstrand et al. 2009). Therefore, it seems reasonable that the aggregation behavior varies between β-glucan from different origin.

SAXS measurements were performed with the aim to get a more detailed picture of the aggregation behavior and conformation. However, it was not possible to extract data regarding conformation from the obtained results. As mentioned by Jeffries et al. (2016) a reason could be the heterogeneity of the sample caused by aggregates and the high polydisperse character of our β-glucan that can severely influence and complicate data analysis. Furthermore, the very dense and sphere-shaped aggregates as seen in Fig. 2B could influence the measurability of our samples in regard to SAXS. Such highly dense structures may make it difficult to analyse more distinct parts of the aggregates as overlapping structures result in an averaged signal. However, this can be a hint towards the trueness of the earlier discussed aggregates for barley β-glucan that can, due to their highly dense structure, not be analysed using SAXS. Nevertheless, it was possible to obtain results in structure-specific terms by utilizing the asymptotic behavior of the scattered intensity I(q) (Burchard, 2004) and to obtain the persistence length l_p of the oat β-glucan samples. A l_p of 2.4 nm was obtained from SAXS data for the β-glucan from oat whereas no l_p for barley was obtained. This is most likely due to an enhanced scattering from large

and denser structures (see respective micrographs in Fig. 3B), that mask the individual polymer configuration for the barley samples. For an oat β-glucan molecule, usually (up to 90 %) 2-4 glucose molecules are β-1,4 linked, forming the stiffest parts of the molecule, and are separated from each other through β-1,3 linkages (Izydorczyk, Macri & MacGregor, 1998a, 1998b). A rough estimation, considering the length of one glucose ring to be 0.85 nm and a single bond length of C-C to be 0.15 nm, 2 glucose units connected via a C-C (β-1,4) linkage would result in a total length of 1.85 nm and 3 glucose units connected via two C-C (β-1,4) linkages into a total length of 2.86 nm. Hence, these results show an average block length of ~2.5 glucose molecules and indicate that the β-1,4 linked glucose blocks form a stiff part of the β-glucan molecule in oat, whereas the β-1,3 linkages form the flexible parts of the molecule and can, hence, influence the molecular properties. In addition, it should be mentioned that the obtained values have to be considered as average l_p of the whole sample and hence, of the whole size distribution as the analysis was performed as a batch measurement. However, the results for l_p for oat β-glucan agree well with results formerly reported in literature i.e. on average 2.5 glucose residues (Lazaridou & Biliaderis, 2007).

5. Conclusion

The results presented in this paper show a range of conformational properties of β-glucan from oat and barley in terms of their aggregation behavior over the size distribution. β-Glucan is present as highly polydisperse polymers for low *M* in aqueous solution as well as in highly aggregated structures for high *M*, whereas the differential mass distribution has its maximum in lower *M* ranges, indicating that aggregates only appear in low concentration. Furthermore, regarding high *M* species, β-glucan seems to be aggregated in a widely distributed network, forming micro gels. Single long chain molecules assemble to form hyperbranched-like structures, what was confirmed with conformation studies including Kratky plots and analysis of the r_{hyd}/r_{rms} ratio and cryo-TEM micrographs. In addition, barley β-glucan showed surprisingly dense and relatively well-defined, sphere-shaped aggregates in cryo-TEM, which need further investigation.

However, these results indicate that earlier suggested high *M* aggregates are present in aqueous solution and give further insight into the solution behaviour of β-glucan, which may help to further understand the complex solution behavior of the dietary fiber.

6. Associated content

No associated content is attached.

7. Acknowledgements

Funding from the Swedish research council (VR), Stockholm, Sweden is gratefully acknowledged. Gunnel Karlsson, National Center for High-Resolution Microscopy (nCHREM), Polymer & Materials Chemistry at Lund University, Lund, Sweden, is acknowledged for sample preparation and performance of the cryo-TEM. The authors thank Dr. Matilda Ulmius-Storm and Dr. Marie-Louise Ainalem (European Spallation Source ESS AB) for fruitful discussions and ideas.

8. References

Agbenorhevi, J. K., Kontogiorgos, V., Kirby, A. R., Morris, V. J. & Tosh, S. M. (2011). Rheological and microstructural investigation of oat beta-glucan isolates varying in molecular weight. *International Journal of Biological Macromolecules*, 49, 369-377.

Andersson, M., Wittgren, B. & Wahlund, K. G. (2003). Accuracy in multiangle light scattering measurements for molar mass and radius estimations. Model calculations and experiments. *Analytical Chemistry*, 75(16), 4279-4291.

Andersson, M., Wittgren, B., Schagerlof, H., Momcilovic, D. & Wahlund, K. G. (2004). Size and structure characterization of ethylhydroxyethyl cellulose by the combination of field-flow fractionation with other techniques. Investigation of ultralarge components. *Biomacromolecules*, 5(1), 97-105.

Berry, G. C. (1966). Thermodynamic and Conformational Properties of Polystyrene. I. Light-Scattering Studies on Dilute Solutions of Linear Polystyrenes. *Journal of Chemical Physics*, 44(12), 4550-4564.

Buléon, A., Véronèse, G. & Putaux, J.-L. (2007). Self-Association and Crystallization of Amylose. *Australian Journal of Chemistry*, 60(10), 706-718.

Burchard, W. (1983). Static and dynamic light scattering from branched polymers and bio-polymers. *Advances in Polymer Science*, 48, 1-124.

Burchard, W. (1999). *Advances in Polymer Science*, 143, 113–194.

Burchard, W. (2004). Light Scattering Techniques. In Ross-Murphy, A.S. (Ed.), Physical Techniques for the Study of Food Biopolymers. (1st ed.) (pp. 151-213). Dordrecht, The Netherlands: Springer Science+Business Media.

Burchard, W. (2004). Angular Dependence of Scattered Light from Hyperbranched Structures in a Good Solvent. A Fractal Approach. *Macromolecules*, 37(10), 3841–3849.

Caldwell, K. D., Nguyen, T. T., Myers, M. N., & Giddings, J. C. (1979). Observations on nomalous Retention in Steric Field-Flow Fractionation. *Separation Science and Technology*, 14(10), 935-946.

Coviello, T., *Kajiwara*, K., *Burchard*, W., *Dentini*, M. & *Crescenzi*, V. (1986). Solution properties of xanthan. 1. Dynamic and static light scattering from native and modified xanthans in dilute solutions. *Macromolecules*, 19(11), 2826-2831.

Cui, S. W. & Wang, Q. (2009). Cell wall polysaccharides in cereals: chemical structures and functional properties. *Structural Chemistry*, 20, 291-297.

Dervilly-Pinel, G., Thibault, J.-F. & Saulnier, L. (2001). Experimental evidence for a semi-flexible conformation for arabinoxylans. *Carbohydrate Research*, 330(3), 365-372.

Einstein, A. (1905). Über die von der molekularkinetischen Theorie der Wärme geforderte Bewegung von in ruhenden Flüssigkeiten suspendierten Teilchen. *Annalen der Physik*, 17, 549-560.

European Food Safety Authority. Article 13(1) of Regulation (EC) No 1924/2006. EFSA Journal 2009, 7.

European Food Safety Authority. Article 14 of Regulation (EC) No 1924/2006. EFSA Journal 2010, 8.

Fernandez, C., Rojas, C. C. & Nilsson, L. (2011). Size, structure and scaling relationships in glycogen from various sources investigated with asymmetrical flow field-flow fractionation and 1H NMR. *International Journal of Biological Macromolecules*, 49(4), 458-465.

Giddings, J. C. (1981). Field flow fractionation. A versatile method for the characterization of macromolecular and particulate materials. *Analytical Chemistry*, 53(11), 1170-1178.

Gómez, C., Navarro, A., Gamier, C., Horta, A. & Carbonell, J. V. (1997) Physical and structural properties of barley (1 → 3),(1 → 4)-β-d-glucan. Part II. Viscosity, chain stiffness and macromolecular dimensions. *Carbohydrate Polymers*, 34(3), 141–148.

Graham, N. B. & Cameron, A. (1998). Nanogels and Microgels: The New Polymeric Materials Playground. In Srinivasan K.S.V. (Ed.), Macromolecules: New Frontiers Vol. 2 (pp. 531-535). New Delhi, India: Allied Publishers Ltd.

Grimm, A., Krüger, E. & Burchard, W. (1995). Solution properties of β-D-(1,3)(1,4)-glucan isolated from beer. *Carbohydrate Polymers*, 27(3), 205-214.

Hupfeld, S. PhD thesis, Departmenrt of Pharmacy, Faculty of Medicine. University of Tromsø *Norway, 2009. http://munin.uit.no/handle/10037/2134, accessed 2016-11-17*.

Håkansson, A., Magnusson, E., Bergenståhl, B. & Nilsson, L. (2012). Hydrodynamic radius determination with asymmetrical flow field-flow fractionation using decaying cross-flows. Part I. A theoretical approach. *Journal of Chromatography A*, 1253, 120-126.

Håkansson, A., Ulmius, M. & Nilsson, L. (2012). Asymmetrical flow field-flow fractionation enables the characterization of molecular and supramolecular properties of cereal beta-glucan dispersions. *Carbohydrate Polymers*, 87, 518-523.

Immerstrand, T., Bergenstahl, B., Tragardh, C., Nyman, M., Cui, S., Oste, R. (2009) Extraction of β-Glucan from Oat Bran in Laboratory Scale. *Cereal Chemistry*, 86 (6), 601-608.

Izydorczyk M. S., Macri, L. J. & MacGregor, A. W.

(1998a). Structure and physicochemical properties of barley non-starch polysaccharides – I. Water-extractable β-glucans and arabinoxylans. *Carbohydrate Polymers*, 35, 249-258.

Izydorczyk, M. S., Macri, L. J. & MacGregor, A. W. (1998b). Structure and physicochemical properties of barley non-starch polysaccharides - II. Alkali-extractable β-glucans and arabinoxylans. *Carbohydrate Polymers*, 35, 259-269.

Jeffries, C. M., Graewert, M. A., Blanchet, C. E., Langley, D. B., Whitten, A. E. & Svergun, D. I. (2016). Preparing monodisperse macromolecular samples for successful biological small-angle X-ray and neutron-scattering experiments. *Nature Protocols*, 11, 2122–2153.

Kratky, O. & Porod, G. (1949). Diffuse small-angle scattering of X-rays in colloid systems. *Journal of Colloid Science*, 4, 35-70.

Lazaridou, A. & Biliaderis, C. G. (2007). Molecular aspects of cereal β-glucan functionality: Physical properties, technological applications and physiological effects. *Journal of Cereal Science*, 1, 101-118.

Li, W., Cui, S.W. & Wang, Q. (2006). Solution and Conformational Properties of Wheat ß-D-Glucans Studied by Light Scattering and Viscometry. *Biomacromolecules*, 7, 446-452.

Li, W., Cui, S.W., Wang, Q. & Yada, R.Y. (2010). Studies of aggregation behaviours of cereal β-glucans in dilute aqueous solutions by light scattering: Part I. Structure effects. *Food Hydrocolloids*, 25, 189-195.

Magnusson, E., Håkansson, A., Janiak, J., Bergenståhl, B. & Nilsson, L. (2012). Hydrodynamic radius determination with asymmetrical flow field-flow fractionation using decaying cross-flows. Part II. Experimental evaluation. *Journal of Chromatography A*, 1253, 127-133.

Mäkelä, N., Sontag-Strohm, T., Maina, N.H. (2015). The oxidative degradation of barley β-glucan in the presence of ascorbic acid or hydrogen peroxide. *Carbohydrate Polymers*, 123, 390-395.

Nilsson, L. (2013). Separation and characterization of food macromolecules using field-flow fractionation: A review. *Food Hydrocolloids*, 30, 1-11.

Nilsson, L, Leeman, M., Wahlund, K. G. & Bergenståhl, B. (2006). Mechanical degradation and changes in conformation of hydrophobically modified starch. *Biomacromolecules*, 7, 2671-2679.

Othman, R. A., Moghadasian, M. H. and Jones, P. J. (2011). Cholesterol-lowering effects of oat β-glucan. *Nutrition Reviews*, 69(6), 299-309.

Papageorgiou, M., Lakhdara, N., Lazaridou, A., Biliaderis, C. G., & Izydorczyk, M. S. (2005). Water extractable (1 leads to 3, 1 leads to 4)-beta-D-glucans from barley and oats: an intervarietal study on their structural features and rheological behaviour. *Journal of Cereal Science*.

Regand, A., Chowdhury, Z., Tosh, S. M., Wolever, T. M. S. & Wood, P. (2011). The molecular weight, solubility and viscosity of oat beta-glucan affect human glycemic response by modifying starch digestibility. *Food Chemistry*, 129(2), 297-304.

Roger, P. & Colonna, P. (1992). The influence of chain-length on the hydrodynamic behavior of amylose. *Carbohydrate Research*, 227, 73-83.

Savin, G. & Burchard, W. (2004). Uncommon Solution Behavior of Poly(*N*-vinylimidazole). Angular Dependence of Scattered Light from Aggregates in Ethanol. *Macromolecules*, 37, 3005–3017.

Schmidt, M., Nerger, D. & Burchard, W. (1979). Quasi-elastic light scattering from branched polymers: 1. Polyvinylacetate and polyvinylacetate—microgels prepared by emulsion polymerization. *Polymers*, 20(5), 582-588.

Sitar, S., Aseyev, V. & Kogej, K. (2014). Microgel-like aggregates of isotactic and atactic poly(methacrylic acid) chains in aqueous alkali chloride solutions as evidenced by light scattering. *Soft Matter*, 10, 7712-7722.

Skendi, A., Biliaderis, C. G., Lazaridou, A. & Izydorczyk, M. S. (2003). Structure and rheological properties of water soluble β-glucans from oat cultivars of *Avena sativa* and *Avena bysantina*. *Journal of Cereal Science*, 38, 15–31.

Ulmius, M., Önning, G. & Nilsson, L. (2012). Solution behavior of cereal β-glucan as studied with asymmetrical flow field-flow fractionation. *Food Hydrocolloids*, 26, 175-180.

U.S. Food and Drug Administration. Federal Register 1992, 62, 15343-15344.

U.S. Food and Drug Administration. Federal Register 2008, 73, 47828-47829.

Vårum, K. M., Smidsrød, O. & Brant, D. A. (1992) Light scattering reveals micelle-like aggregation in the (1-3)(1-4)-β-d-glucans from oat aleurone. *Food Hydrocolloids*, 5, 497–511.

Wahlund, K. G. & Giddings, J. C. (1987). Properties of an asymmetrical flow field-flow fractionation channel having one permeable wall. *Analytical Chemistry*, 59(9), 1332-1339.

Wang, Q. & Ellis, P. R. (2014). Oat β-glucan: physicochemical characteristics in relation to its blood-glucose and cholesterol-lowering properties. *British Journal of Nutrition*, 112, Suppl. 2, 4-13.

Wittgren, B., Borgström, J., Piculell, L. and Wahlund, K. G. (1998). *Conformational change and aggregation* of k-carrageenan *studied* by flow field–flow fractionation and multiangle light scattering. *Biopolymers*, 45, 85-96.

Wolever, T. M., Tosh, S. M., Gibbs, A. L., Brand-Miller, J., Duncan, A. M., Hart, V., Lamarche, B., Thomson, B. A., Duss, R. & Wood, P. J. (2010). Physicochemical properties of oat β-glucan influence its ability to reduce serum LDL cholesterol in humans: a randomized clinical trial. *American Journal of Clinical Nutrition*, 92(4), 723-732.

Wood, P. J. (2004). Relationships between solution properties of cereal β-glucans and physiological effects – a review. *Trends in Food Science & Technology*, 15, 313-320.

Wu, J., Zhang, Y., Wang, L., Xie, B., Wang, H. & Deng, S. (2006). Visualization of Single and Aggregated Hulless Oat (*Avena nuda* L.) (1→3),(1→4)-β-d-Glucan Molecules by Atomic Force Microscopy and Confocal Scanning Laser Microscopy. *Journal of Agricultural and Food Chemistry*, 54(3), 925-934.

Zielke, C., Kosik, O., Ainalem, M.-L., Lovegrove, A., Stradner, A. & Nilsson, L. (2017). Characterization of cereal β-glucan extracts from oat and barley and quantification of proteinaceous matter. *PLoS ONE* 12(2): e0172034. doi:10.1371/ journal.pone.0172034.

Tab. 1: Summary of characterization of the β-glucan extracts from oat and barley including purity, average *M*, average r_{rms} and mass recovery from the AF4 channel.

β-glucan source	**β-glucan content [%(w/w)]**	M_w **[g/mol]**[a]	$r_{rms,\ z}$ **[nm]**[b]	**mass recovery [%]**[c]
oat	65	5.6×10^6	96	72
barley	53	2.4×10^6	82	98

[a] Weight-average *M*, [b] z-average, [c] from the AF4 channel, recovery of total injected mass, measured mass (integrated dRI-signal representing the concentration over the fractogram) / injected mass

Tab. 2: Brief overview of different ratios of r_{rms}/r_{hyd} and their conformation.

r_{rms}/r_{hyd}	**conformation**	**reference**
>2	elongated, rod-like	Coviello, Kajiwara, Burchard, Dentini, & Crescenzi, 1986;* Wittgren, Borgström, Piculell & Wahlund, 1998*
1.5-2	random coil	Burchard, 1983+; Roger & Colonna, 1992*
1-1.5	branched molecule	Burchard, 1999+
0.775	homogenous, smooth sphere	
<0.7	micro gel*	Schmidt, Nerger, & Burchard, 1979*

+ theoretical values, * experimental results

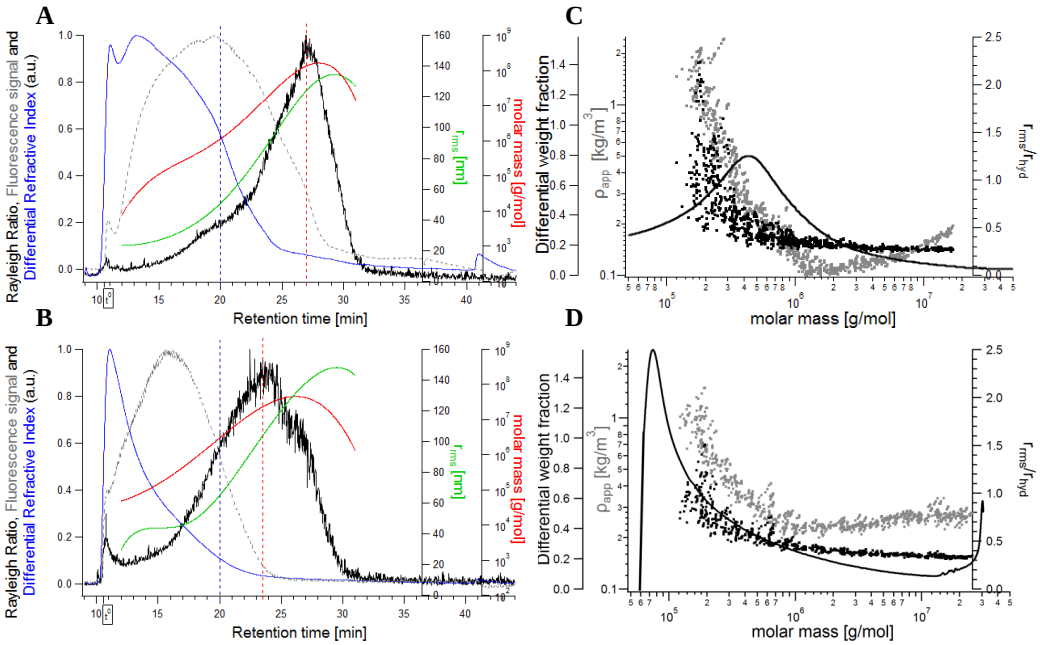

Fig. 1: **A** and **B**: AF4 fractograms, signals are: black line – Rayleigh ratio from MALS (a.u., 69.3 ° - 121.2 °), blue line – dRI signal, grey dashed line – fluorescence signal, red line – molar mass distribution [g/mol], green line – r_{rms} distribution [nm]. The blue dashed vertical line represents t_r = 20 min, whereas the red dashed horizontal line represents t_r = 27 min for **A** and t_r = 23.5 min for **B**. **C** and **D**: Differential weight fraction is represented as solid line, apparent density values in grey dots and the conformation ratio of r_{rms}/r_{hyd} is plotted in black dots. **A** and **C** present results for the β-glucan extract from oat; **B** and **D** from barley. (For interpretation of the references to color in this figure legend, the reader is referred to the web version of this article.)

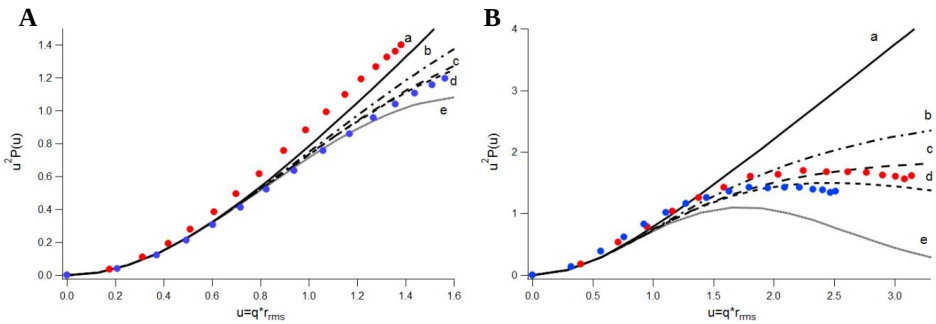

Fig. 2: Kratky plots for oat (red) and barley (blue); data points for Kratky plots are obtained from MALS data at (**A**) t_r = 20 min and (**B**) t_r = 27 min for oat and t_r = 23.5 min for barley as marked in Fig 1**A** and 1**C**, respectively, and a-e display the theory (Andersson, M. et al. 2004) with a = polydispersed rod, b = polydispersed random coil, c = monodispersed random coil, d = hyperbranched structure and e = polydispersed sphere. (For interpretation of the references to color in this figure legend, the reader is referred to the web version of this article.)

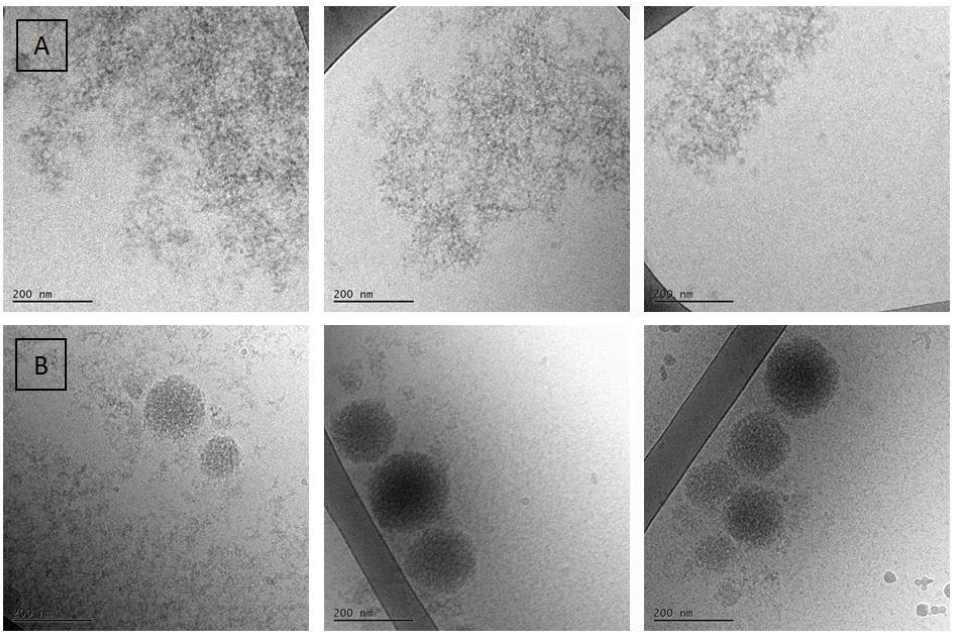

Fig. 3: cryo-TEM images of oat (**A**) and barley (**B**) β-glucan extracts.

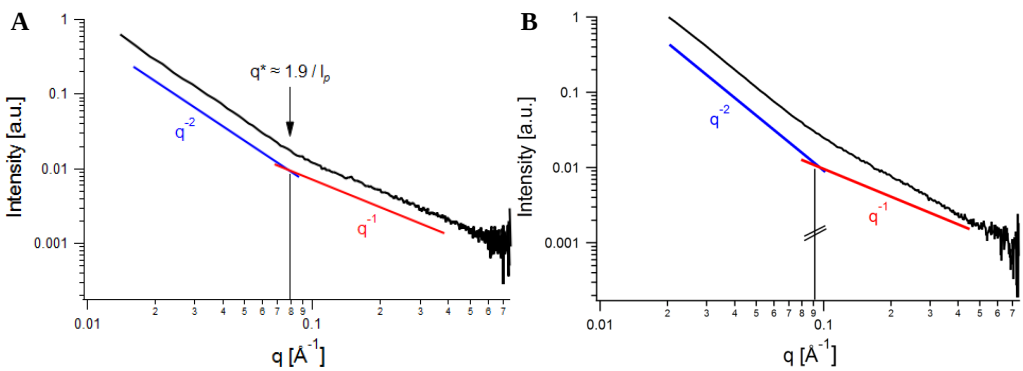

Fig. 4: SAXS data of oat (**A**) and barley (**B**) extracts. From the obtained SAXS data, *q** values were obtained at the transition point between two regimes by extrapolating. (For interpretation of the references to color in this figure legend, the reader is referred to the web version of this article.)

Paper III

Interaction between cereal β-glucan and proteins in solution and at interfaces

Zielke, C., Lu, Y., Poinsot, R. & Nilsson, L.

Submitted to Colloids and Surfaces B: Biointerfaces

Interaction between cereal β-glucan and proteins in solution and at interfaces

Claudia Zielke*, Yi Lu, Romane Poinsot, Lars Nilsson

Submitted to Colloids and Surfaces B: Biointerfaces – Under Review

*corresponding author: Claudia.Zielke@food.lth.se; Food Technology, Engineering and Nutrition, Faculty of Engineering LTH, Lund University, PO Box 124, S-221 00 Lund, Sweden

Abstract

Cereal β-glucan is well known for its beneficial health effects, such as lowering of blood cholesterol values and a reduced risk of coronary heart disease. These effects are often discussed in relation to the dissolution and aggregation behavior of the β-glucan during human digestion. Furthermore, potential proteinaceous material present is believed to have an important impact on the formation of viscous slurries during digestion and might influence the aggregation behavior of the β-glucan. Therefore, the interaction and aggregation behavior of a β-glucan isolate (OBC90) with two different proteins (gliadin and whey protein) was investigated in solution at different pH with regards to kinetics of aggregation and protein/β-glucan ratio and at interfaces. Aggregates were found at low pH and the aggregation and composition of aggregates seems to depend on the type of protein. Furthermore, phosphate was found at low concentrations in the β-glucan, most likely being the reason for the net negative charge at pH ≤4. Therefore, electrostatic interaction is suggested to play an important role for the aggregation between β-glucan and proteins.

Keywords: polysaccharide, asymmetric flow field-flow fractionation (AF4), multi-angle light scattering (MALS), differential refractive index (dRI), ellipsometry, gliadin, whey protein (WP), transmission, natural phosphate, electrostatic interaction

Abbreviations: AF4 asymmetric flow field-flow fractionation; dRI differential refractive index; DS degree of substitution; HPAEC-PAD high-performance anion-exchange chromatography equipped with pulse-amperometric detector; M molar mass; MALS multi-angle light scattering; OBC90 β-glucan extract with a purity of 90 %; P phosphate; WP whey protein

Introduction

Cereal β-glucan is an unbranched polysaccharide with β-D-glucopyranosyl residues linked via β(1→3) and β(1→4) linkages where blocks of trimers and tetramers of (1→4) linkages are separated through (1→3) linkages.[1] These irregular linkages influence the physiological properties of the molecule and make it, to some extent, water soluble. β-Glucan molecules have the ability to self-associate and form aggregates in solution, which may contribute to increased viscosity and the ability to form viscous slurries in the gut.[2] This fact can serve as a starting point for the investigation and understanding of the already established beneficial health effects of cereal β-glucan. [3-6]

When discussing health benefits of β-glucan, such as lowering of blood cholesterol values, reduced glycaemic and insulin responses [4], and hence, a reduced risk of coronary heart disease with increased daily intake, potential proteinaceous moieties are mentioned to have an important impact on physiological properties, on the formation of viscous slurries during digestion [2] and are said to influence the aggregation behavior of the β-glucan. Several findings have been reported suggesting a direct connection between proteins and β-glucan. Zhou at al. found that the addition of

proteases to β-glucan slurries has shown a decrease in viscosity, suggesting a direct connection between the amount of protein in the sample and the viscosity enhancing functionality of β-glucan [7]. The same result was obtained by Autio et al., where a trypsin treatment of oat β-glucan reduced the viscosity of the slurry [8]. Other results, utilizing asymmetric flow field-flow fractionation (AF4) in combination with several detectors for the analysis of molar mass (M) distributions of β-glucan in barley malts showed that a total protein digestion of β-glucan in solution decreased M of the β-glucan drastically, indicating a direct role of proteins in the formation of high M aggregates [9]. Forrest et al. investigated β-glucan and pentosans from barley in the endosperm cell wall of the grain utilizing molecular sieve chromatography and density-gradient ultracentrifugation, and suggested β-glucan to be firmly linked to one another by proteinaceous material forming high M aggregates of about 10^7 g/mol [10]. The aggregates were suspected to further associate in solution through ionic or hydrogen bonds forming even bigger and more complex structures [10]. Furthermore, the presence of amino acid residues in oat β-glucan was as well found and discussed by Vårum et al. [11]. Other studies suggested e. g. phosphate residues attached to oat β-glucan [12], and NMR evidence was found for C-6 bound phosphate ester groups [13], strengthening the assumption of proteins in the β-glucan samples, as reversible phosphorylation of the three hydroxyamino acids, serine, threonine and tyrosine, in proteins emerged as one of the most prominent types of modification [14]. Such a protein-linked phosphate group can form strong hydrogen bonds and ion bridges, both intra- and intermolecular, and might play a key role in forming stable aggregates by interacting with proteins thanks to electrostatic interactions. However, former results showed that β-glucan extracts from oat and barley flour, extracted in a gentle way and without the use of proteases to preserve its natural structure as it would be present in food, did not contain any protein [15]. Hence, in that study, proteins covalently bound to β-glucan were not found. Due to this broad range of diverse results, it is necessary to gain a better understanding of the β-glucan/protein interaction to attempt to draw uniform conclusions about the role of proteins within the solution and aggregation behavior of β-glucan.

A study by Magnusson and Nilsson [16] investigated the interaction between hydrophobically modified starch and egg yolk proteins in terms of their interaction and the stability of formed emulsions. Their results showed strong interaction between the compounds in solution at pH 4.0. Aggregates were furthermore investigated by transmission profiles, using a UV-Vis spectrophotometer. In the present study, the influence of proteins on the β-glucan aggregation behavior in solution was investigated, following a similar scheme. A β-glucan extract (OBC90, 90 % purity) from oat, formerly characterized by AF4 with multi-angle light scattering (MALS), differential refractive index (dRI) and fluorescence detectors as described previously [15], was mixed with different proteins, whey protein and gliadin, and analyzed in terms of aggregation and molecular size. Furthermore, the influence of protein concentration and different pH on the aggregation pattern was studied utilizing UV-Vis detection, total protein content analyzer after centrifugation and at interfaces utilizing ellipsometry.

Materials and Methods

Samples

The β-glucan sample used for the project is OBC90, a β-glucan extract provided by Swedish Oat Fiber, Väröbacka, Sweden, which is a 90% pure β-glucan isolate, where a technology has been applied to preserve a high level of molecular integrity compared to other wet purification techniques. No detectable proteins were found in the β-glucan sample. For the preparation of the AF4 carrier liquid, $NaNO_3$ (Merck, Darmstadt, Germany) and NaN_3 (BDH, Poole, UK) were used, whereas the Calcofluor for fluorescence labelling was fluorescent brightener 28 (Sigma Aldrich, Darmstadt, Germany) in tris(hydroxymethyl)-aminomethane (Merck). As proteins, whey protein (WP) purchased from Norrmejerier, Umeå, Sweden, and gliadin, purchased from Sigma Aldrich, were used. Lactic acid, acetic

acid and imidazole were purchased from Merck. pH values were adjusted with hydrochloric acid (HCl) or sodium hydroxide (NaOH) from Sigma Aldrich. All experiments were performed using pure water from a Milli-Q system (Millipore Corp., Billerica, Massachusetts, USA).

FFF analysis equipment and data processing

The AF4 instrument utilized was an Eclipse 3+ Separation System (Wyatt Technology Europe, Dernbach, Germany) connected on-line to a Dawn Heleos II MALS detector and an Optilab T-rEX differential refractive index (dRI) detector (both Wyatt), both operating at λ = 658 nm. An Agilent 1100 series isocratic pump with an in-line vacuum degasser delivered the carrier flow through the system; the sample was injected via an Agilent 1100 series autosampler (Agilent Technologies, Waldbronn, Germany). To ensure that the carrier liquid entering the system is particle and dust free, a filter-holder with a 100 nm pore-size polyvinylidene fluoride membrane (Millipore Corp.) was placed in between the pump and the AF4 channel inlet. The channel was a Wyatt long channel with a tip-to-tip length of 27.5 cm and a spacer creating a nominal channel thickness of 190 µm. The used ultra-filtration membrane forming the accumulation wall was made of hydrophilized polyethersulphone with a cut-off of 10 kDa (Microdyn-Nadir GmbH, Wiesbaden. Germany). The actual resulting channel thickness was experimentally determined to be 156 µm, using a calibration method with ferritin as described earlier [18]. For analysis, carrier liquid with 10 mM $NaNO_3$ and 0.02 % (w/v) NaN_3 in Milli-Q water was used. β-Glucan sample was prepared at a concentration of 4 mg/mL by dissolving the extracted β-glucan in the carrier liquid used for elution and boiling the suspension for 30 min until the β-glucan was dissolved. The sample was cooled down to 20 °C and filtered through a 22 mm syringe filter with a 0.45 µm pore size cellulose acetate membrane (VWR International) prior to injection onto the channel. Injection of the sample onto the channel was performed at a flow rate of 0.2 mL/min for 4 minutes. The sample volume injected was 40 µL to provide an injected mass of 160 µg. A focusing/relaxation step of 5 min was performed prior to elution with a focusing flow rate of 0.5 mL/min. A total time before elution of 10 min was obtained. The initial cross-flow rate during elution was 1 mL/min, the following exponential decay had a half-life of 4.5 min in order to avoid excessive retention and elution times. During the measurement, the detector flow rate was kept constant at 0.5 mL/ min. The void time (t^0) was calculated to 0.6 min

The use of a fluorescence detector in-line post-channel enabled the detection of the separation range where β-glucan is present in the sample. The detector used was a Jasco FP-1520 fluorescence detector (Jasco Inc., Easton, Maryland, USA) operating an Ushio Xenon Short Arc lamp (Ushio Inc., Tokyo, Japan). β-Glucan was labelled with Calcofluor utilizing the method described by Ulmius, Önning, & Nilsson [19], using a 25 mg/L Calcofluor solution in 0.1 M tris(hydroxymethyl)-aminomethane buffer (pH 8), measuring the emission at λ_{em}=445 nm (λ_{ex}=415 nm). r_{hyd} was calculated using FFF theory according to [18].

Dynamic light scattering

DLS measurements were performed to determine the average hydrodynamic size of the molecules. The sample was prepared by boiling in Milli-Q water at 1 mg/mL. The solution was cooled down to 20 °C and filtered as for the AF4 sample preparation. Subsequently, the sample was transferred to a disposable PS cuvette (VWR, Radnor, PA, USA) for DLS measurements in a Zetasizer (Malvern Instruments, Worcestershire, UK) equipped with a 532 nm laser. Measurements were performed in triplicates at 25 °C. The obtained data was collected by the Zetasizer Nano software (Malvern Instruments), whereas data analysis was performed by fitting the normalized experimentally measured time correlation function.

HPAEC-PAD analysis of monosaccharide sugar composition

HPAEC-PAD (high-performance anion-exchange chromatography equipped with pulse-amperometric detection) can analyse the monosaccharide composition of carbohydrates following acid hydrolysis. The analysis was performed according to Goubet et al. [17], with

50 µg of β-glucan extract incubating for 1 h at 121 °C in 400 µL of 2 M TFA. The hydrolysates were lyophilised, subsequently re-suspended in water and analysed utilizing a Dionex ICS3000 HPLC equipped with CarboPac PA 20 column (Thermo Fisher Scientific Inc., Waltham, Massachusetts).

Preparation of the β-glucan and protein mixtures

Mixtures with β-glucan:protein mass ratios equal to 5:1, 2:1, 1:1 and 1:2 were prepared, with only β-glucan (1:0) and only protein (0:1) in solution as references. The buffer used to dissolve the β-glucan and protein samples prior to mixing consisted of 10 mM lactic acid, 10 mM acetic acid, 10 mM imidazole and 10mM tris(hydroxymethyl)-aminomethan. pH values were adjusted to pH 3, 4, 5, 7 or 9 with HCl or NaOH. For pH 7 measurements, the buffer contained only 40 mM imidazole. In all experiments, different volumes of 0.5 M NaCl solution were added as follows to adjust the ionic strength to the same value, as differences in ionic strength might influence the aggregate formation: pH 3.0 – 0.09 mL, pH 4.0 – 3.04 mL, pH 5.0 – 7.39 mL, pH 7.0 – 6.45 mL. The values correspond to a total buffer volume of 0.5 L. β-Glucan was dissolved at a concentration of 2.5 g/L while boiling for 30 min with vigorous stirring and subsequently, the solution was given time to cool down to 20 °C. WP and gliadins were dissolved at 1 g/L with vigorous stirring at 20 °C until the solution was clear.

Transmission measurements

The interaction between β-glucan and protein was studied by measuring the transmission as a function of time for all mass ratios. The substances were directly mixed in the cuvettes (VWR semi-micro in polystyrene), whereas the respective protein solution was added first, and β-glucan in solution was added last. Note that the ratios are reported according to mass and not volume. No stirring or shaking was applied. The transmission was determined at 590 nm with a UV-Vis spectrophotometer (Beckman Cary 50) directly after mixing (0 minutes) and 3, 9, 27, 81 and 162 minutes after mixing according to Magnusson et al. [16] Three repetitions were performed to validate the results.

Ellipsometry

Silica surfaces were prepared from polished silicon wafers (p-type, boron-doped, resistivity of 1-20 Ωcm) purchased from Linköping University (Department of Chemistry, IFM, Linköping University, Linköping, Sweden) and SWI (Semiconductor Wafer, Inc., Taiwan). These wafers are ideal for ellipsometry experiments due to their extreme flatness and high reflectivity. The silica surfaces were produced by thermal oxidation (at approx. 900 °C) on silicon substrate, which is composed of silanol hydroxyl groups (Si-OH) with approximately five OH groups per nanometer resulting in surface properties easy to modify. The oxidized substrates were cut into small slides (~ 0.5 x 4.0 cm) and the surfaces were cleaned in a basic boiling mixture of 25 % NH_4OH : 30 % H_2O_2 : H_2O (v/v/v: 1/1/5) for 5 min. Subsequently, the slides were rinsed with water, followed by boiling in an acidic mixture of 32 % HCl : 30 % H_2O_2 : H_2O (v/v/v: 1/1/5) for 5 min. The substrates were then thoroughly rinsed with water and ethanol and stored in absolute ethanol (>99%) until further use.

Hydrophobization is achieved by gas-phase silanization after cleaning [20]. The substrates were rinsed with ethanol (>99%), dried with N_2 gas, and then plasma cleaned (Harrick Scientific Corp., model PDC-3XG) for 5 min to remove contamination from the surface. Afterwards, the surfaces were placed with their shiny side upwards in a desiccator with 1 mL dimethyloctylchlorosilane (DMOCS, 97%, Fluka). The desiccator was pumped for 20 minutes to create underpressure status and left overnight at room temperature. The silanized surfaces were immersed in THF (>99%, Honeywell, Germany) and sonicated for 20 min. The surfaces were collected in absolute ethanol and sonicated for another 20 min, before being stored in absolute ethanol until further use.

The ellipsometry set-up used in this study has been previously described in detail by Wahlgren and Arnebrant [21]. The instrument used was an Automated Null Ellipsometer (Type 43603-200E, Rudolph Research, Hackettstown, NJ, USA), which is capable to measure adsorption in situ under a wavelength of 401.5 nm with an incidence angle of 67.85°.

The surface was placed inside an 8 mL trapezoidal-shaped cuvette with a thin glass window made of glass coverslip. The sample cell was thermostated to 25 °C and agitated with a magnetic stirrer at 80 rpm.

Before measuring sample adsorption, the silica surface properties in the respective buffer solutions were determined. The complex refractive indices of the substrate and medium were determined by measuring the ellipsometric angles (ψ and Δ) in buffer (pH 4) with or without added NaCl and averaged over four different zones to minimize optical imperfections. The correction values have to be below ±0.5° so that further measurements can be performed. Silica surface properties were calculated in buffer solutions with different ionic strength, and proteins in the corresponding buffer solutions were added into the cuvette until the surface was saturated with protein. Protein, β-glucan and buffer solutions were prepared as described in 2.4. The surfaces were rinsed with buffer to remove the non-adsorbed protein in solution, before adding β-glucan in corresponding buffer into the cuvette. By monitoring the changes in amplitude and phase of the reflected light, the adsorbed mass was calculated with a three-layer model using 0.75 mL/g and 4.1 g/mL as values for partial specific volume and ratio of the M and molar refractivity, respectively. The adsorbed mass Γ (mg/m^2) can be calculated according to Eq. (1), where df represents film thickness, nf and nm are the refractive indices of the film and medium, respectively, A/M is the ratio of M and molar refractivity and vd refers to the partial specific volume.

$$\Gamma = \frac{3*df*f(nf)*(nf-nm)}{A/M-vd*(nm^2-1)/(nm^2+2)} \quad (1)$$

$$\text{with } f(nf) = \frac{nf-nm}{(nf^2+2)*(nm^2+2)} \quad (2)$$

Phosphate analysis

To quantify the phosphate content in the β-glucan sample, the method described by Murphy and Riley [22] was used, also referred to as Ascorbic Acid Standard Method (American Public Health Association [23]). The procedure is based on UV-Vis spectroscopy, where ammonium molybdate and antimony (as potassium antimonyl tartrate solution) react together in an acidic medium with orthophosphate, forming a heteropoly acid that is reduced to the intensely coloured molybdenum blue by ascorbic acid. The absorption of the complex formed is measured at its maximum at λ=882 nm. Former results [12] showed that the optimum antomonyl concentration was 0.4 mg/ 50 mL final volume. At this concentration, molybdenum blue attained its maximum intensity after 10 min.

For the reagent solution, 20 g of ammonium molybdate was dissolved in Milli-Q water and diluted to 500 mL, whereas 0.27 g of potassium antimonyl tartrate was dissolved in 100 mL Milli-Q water. Subsequently, 125 mL of 5 N sulphuric acid was mixed thoroughly with 37.5 mL of ammonium molybdate solution and 75 mL of 0.1 M ascorbic acid as well as 12.5 mL of potassium antimonyl tartrate to obtain the final reagent solution. All solutions were prepared fresh, due to a limited stability of <24 hours.

Two standard solutions of phosphate as free phosphate were prepared for the calibration curve, containing 50 mg P(as phosphate)/L and 2.5 mg P/L, by dissolving potassium dihydrogen phosphate in Milli-Q water. β-Glucan was diluted in water with a concentration of 2.5 g/L. Given that the cuvettes have a light path of 1 cm, phosphate concentration range for the calibration curves should be between 0.15 mg/L and 1.30 mg/L, as suggested by the American Public Health Association [23]. Therefore, 0.1; 0.2; 0.3; 0.5; 0.8; 1 and 1.3 mg/L were chosen as concentrations for the calibration curve (data not shown). Fitting coefficients of the linear curve passing through 0 were determined by utilizing a plotting program.

Solutions were diluted with Milli-Q water in 50 mL volumetric flasks. Approximately 30 to 40 mL of Milli-Q water was provided before adding the freshly-prepared reagent solution and adjusting to a total volume to 50 mL. The final concentration of β-glucan was 0.5 g/L. The solution was then well agitated and kept for not less than 10 min but not more than 30 min at room temperature before the optical density of the solution at 882 nm was determined. Three repetitions were performed.

After analysis and prior to further experiments, volumetric flasks used for the phosphate determination were filled with concentrated sulphuric acid to avoid adsorption of phosphate on the glass surface and prevent from phosphate contamination, stored overnight and rinsed and stored with Milli-Q water until the next measurement.

The Degree of Substitution (DS) was calculated by dividing the number of phosphate by the number of glucose unit (Eq. (3)). β-(1→3) and β-(1→4) linked D-glucosyl residues have a M of 162 g/mol whereas the M of phosphate is 95 g/mol, and hence:

$$DS = \frac{c(phosphate)/95}{c(\beta\text{-glucan})/162} \quad (3)$$

with *c(phosphate)* being the concentration of phosphate in the sample, and *c(β-glucan)* the concentration of β-glucan.

Results and discussion

Characterization of β-glucan (OBC90)

The β-glucan was analysed in terms of M and size distribution using AF4-MALS-dRI in combination with fluorescence detection for Calcofluor-labelled β-glucan. The AF4-MALS-dRI fractogram, fluorescence signal, M and root-mean-square radius (r_{rms}) distributions from the extract are displayed in Fig. 1A and plotted vs the retention time. The fractogram shows that the sample contains high M β-glucan (10^5 – $5x10^7$ g/mol) and large sizes (r_{rms} from 50 to 125 nm). The dRI signal (concentration) shows that the sample is broadly distributed over the whole elution range, whereas the fluorescence signal induces, that β-glucan is present at all elution times. The differential weight fraction displayed in Fig. 1B shows a maximum M around $8x10^5$ g/mol. By forming the ratio of r_{rms}/r_{hyd}, information about the conformation of the β-glucan can be obtained. Values below 0.7 represent a microgel structure [24]. As seen in Fig. 1B, values for r_{rms}/r_{hyd} range only between 0.1 - 0.5, introducing a microgel structure for this β-glucan sample. DLS measurements of the β-glucan (data not shown) resulted in a Z-average diameter of around 350 nm, and hence an average r_{hyd} of ~175 nm. As seen from Fig. 1A, the r_{rms} at the maximum of the MALS signal is 60 nm. Forming the ratio of r_{rms}/r_{hyd} with these values, a ratio of 0.34 is obtained suggesting once more the micro-gelled structure. However, the DLS result for an average r_{hyd} is likely to be somewhat overestimated as DLS is performed in batch mode without resolved sizes and due to β-glucan polydispersity (Fig. 1A).

The results from HPAEC-PAD analysis are the following in µg(monosaccharide)/mg(β-glucan): arabinose 2.22±0.06; galactose 0.68±0.07; glucose 820±12; xylose 6.64±0.05; whereas no fucose, mannose or glucuronic acid were detected. Hence, main impurities of the extracts were identified as degradation products from starch (glucose results including β-glucan and starch degradation), with minor amounts of arabinose and xylose. On a dry weight basis, 82.05% (w/w) of the hydrolyzed β-glucan sample is glucose. In order to compare these values with the β-glucan content (90 %), the values need to be recalculated to correct for the difference in M (glucose: 180 g/mol and glucose pyranosyl unit in a β-glucan chain: 162 g/mol). Therefore, a correction factor (162[g/mol]/180[g/mol]) is multiplied with the obtained glucose content in order to estimate how much glucose originates from β-glucan (and e.g. not from starch residues). The results prove the purity of β-glucan to be 91 %, and approximately 8% of the samples' glucose doesn't originate from β-glucan.

Presence of aggregates

Transmission profiles were recorded in the pH range 3-9 to investigate the interaction between β-glucan and proteins. For the mixture between WP and β-glucan at pH 3 (Fig. 2A), lower transmission values for protein/β-glucan ratios of 2:1, 1:1 and 1:2 display the formation of an insoluble complex, with the lowest transmission for a higher amount of β-glucan. Hence, the quantity of the aggregates seems to depend more on the β-glucan concentration than on the protein concentration. A slight statistically significant decrease, compared to the references (pure WP solution, pure β-glucan solution) of the transmission at a ratio of 5:1 can be recognized, indicating the presence of aggregates. Given that the transmission immediately decreases after

mixing (0 min, black line), aggregates seem to form rapidly. Fig. 3A shows the transmission values at pH 3 as a function of time. A decrease in transmission at t=0 min is followed by increasing transmission values from 9 to 162 min, especially for the ratio of WP:β-glucan of 1:2. This could be explained by the sedimentation that occurred in the spectrophotometer cuvettes due to aggregate formation, making the recorded transmission more intense over time as the aggregates settle in the cuvette.

Formation of aggregates between WP and β-glucan can also be observed at pH 4 (data not shown). Similar to pH 3 (Fig. 3A), the transmission value at pH 4 (Fig 3B) resolved by time reaches a minimum value for the WP:β-glucan ratio of 1:2, giving a hint that the amount of aggregates might depend on the protein:β-glucan ratio. Compared to pH 3 (Fig. 3A), the aggregation at pH 4 (Fig 3B) might be more important, since the transmission values for pH 4 are lower at every ratio investigated. As well as in pH 3, transmission increases from 9 to 162 min, reaching a value even higher than that at t=0. The fact that sedimentation of particles occurs really fast could indicate that the aggregated particles formed in pH 4 are bigger than the ones formed in pH 3. A slight decrease in transmission is observed at a ratio of 1:0, showing a somewhat low solubility of the WP at pH 4. WP solution is a mixture of different proteins (α-lactoglobulines, β-lactoglobulines, serum albumins, etc.) whose isoelectric points (pI) are in a pH range from 4.8 to 5.3. Consequently, at pH 4 WP are closer to their pI than at pH 3 and tend to be less soluble. No aggregates were found for WP:β-glucan at pH 5 and higher (data not shown).

The same analyses were performed for the mixture of gliadin and β-glucan. Aggregates were found at pH 3 only at a ratio of gliadin:β-glucan of 1:2 (Fig. 2B) whereas at pH 4 (Fig. 2C), transmission values at ratios of 5:1; 2:1; 1:1 and 1:2 were much lower than for the mixture with WP (Fig. 2A). Indeed, as Fig. 2C shows, relative transmission values of the mixtures after 162 min are all below 20 %. Furthermore, aggregates can be identified at pH 5 (Fig. 3C), whereas no aggregates were found for WP:β-glucan at pH 5 (data not shown). At this pH, no differences in transmission were detected between gliadin:β-glucan ratios of 5:1 and 2:1 but it was found that their transmission was lower than the ones of 1:1 and 1:2 (data not shown). It is noteworthy that transmission at pH values where aggregation was observed only marginally increases after 27 min so sedimentation of the aggregates between gliadin and β-glucan is not as important as for WP and β-glucan.

No aggregates were observed at pH> 5 for the mixture with gliadin and at pH> 4 for the mixture with WP and β-glucan (data not shown). Moreover, different transmission values for the same protein/β-glucan ratios were obtained. This displays that formation of aggregates not only depends on the pH of the solution but also on the type of proteins. The pI of gliadin is 6.4 and, as previously said, WP have a pI within the pH range of 4.8 to 5.3. Therefore, lower pI might be in direct correlation to the pH values where aggregates are formed. Furthermore, as reported by Korompokis et al. [25], β-glucan are slightly net negatively charged (ζ-potential = -0.19 ± 0.07 mV) at pH 3, whereas both proteins, being below their pI, are positively charged. Hence, the polysaccharide and protein probably attract each other to form an insoluble complex and the interaction may thereby be electrostatic. At pH ≥ 7, both β-glucan (ζ-potential = -1.53 ± 0.08 mV) and proteins are net negatively charged, what might explain the lack of aggregate formation as they repel each other.

Magnusson and Nilsson [16], as well as Neirynck et al. [26] observed a maximum for the interaction of hydrophobically modified starch and egg yolk proteins and between WP and pectin at a ratio of 2:1. In contrast, for the system investigated here, aggregation was detected at every ratio at pH 3 and pH 4 for the mixture between WP and β-glucan and at pH 4 and pH 5 for the mixture between gliadin and β-glucan. However, transmission decreases with increasing β-glucan concentration in the mixture, and for the mixture with WP, it seems that the concentration of β-glucan enhanced the amount of aggregates.

Influence of salt addition on aggregation

Fig. 4 shows transmission values as a function of time for the WP:β-glucan ratio of 1:2 and

the gliadin:β-glucan ratio of 1:1, with and without extra NaCl added at pH 4. These ratios were chosen, as there is a clear reduction in transmission indicating formation of aggregates directly after mixing, whereas a concentration of 340 mM NaCl was chosen to confirm if the interactions are electrostatic or not, as at this ionic strength, any electrostatic interaction should be efficiently screened out. For both WP and gliadin, the transmission of the mixtures with added NaCl is significantly higher compared to analysis without NaCl. It can be concluded, that at higher ionic strength, no aggregates are detected while they should be observed at this given ratio and pH.

The transmission value of WP:β-glucan (Fig. 4) is not, unlike the other mixture with gliadins (Fig. 4), close to 100 %. It might be explained by the fact that, as seen in Fig. 2A, pure WP are not well soluble in the buffer causing a starting turbidity of the sample. Identical measurements were performed at pH 3 for gliadin:β-glucan and WP:β-glucan ratios of 1:2 and also at pH 5 for the gliadin:β-glucan ratio of 2:1. Similar results were obtained: no aggregates could be detected when NaCl is added (results not shown).

To gain additional insight into the underlying mechanism of aggregate formation, interaction between β-glucan and the two proteins were investigated at interfaces using ellipsometry. Experiments were performed at pH 4 as at this pH aggregation occurred. A solid clean hydrophobic surface was prepared and protein solution was added until the surface was saturated. β-Glucan in solution was then added and the adsorbed mass difference was recorded as presented in Fig. 5. The adsorption plateau for WP was determined to approximately 1.9 mg/m^2 which corresponds to full surface coverage and is in the range for what has previously been reported in literature [21], whereas the adsorption plateau for gliadin is somewhat higher i.e. approximately 4.1 mg/m^2, which is as well in accordance to literature [27]. The higher plateau value suggests a thicker adsorbed layer and may indicate multilayer adsorption with a more loosely adsorbed outer region. After rinsing with the same buffer solution, β-glucan in pH4 buffer was added into the cuvette with the by protein saturated surface. An increase or decrease in adsorbed mass by β-glucan indicates attractive interaction between the adsorbed protein layer and the β-glucan, while constant adsorbed mass would indicate a very limited or no interaction. For the experiment where the surface is already covered by WP, addition of β-glucan increases the adsorbed mass (Fig. 5). Thus, attractive interaction occurs at the surface which is in agreement with the aggregate formation at pH 4 (Fig. 3B). For the corresponding experiment with gliadin, the introduction of β-glucan lowers the adsorbed mass. A possible explanation for this is that when the β-glucan is introduced it removes some of the outer more loosely adsorbed gliadin by forming soluble complexes. As discussed above, the adsorbed mass of gliadin is somewhat high suggesting a somewhat thicker adsorbed layer. For the buffer solutions with higher ionic strength (added NaCl), β-glucan did not increase the adsorbed mass, neither for gliadin (Fig. 5, top, blue) nor for whey proteins (Fig. 5, bottom, green), indicating that β-glucan was not adsorbing onto the protein layer. Hence, the higher ionic strength seems to screen any attractive interaction between the adsorbed protein layer and the β-glucan. The result is in good agreement with the results of the transmission experiments (Fig. 4) where aggregate formation was strongly suppressed at higher ionic strength. Thus, the results suggest that electrostatics play a major role in the interaction and aggregation of the macromolecules.

However, β-glucan molecules are considered uncharged, so can they be involved in electrostatic interactions? It has been shown in literature that phosphate groups linked to β-glucan may be present. Ghotra et al. [13] found C-6 carbon bound phosphomonoesters and an unknown form of phosphorous, possibly phospholipids or phosphoproteins in purified oat β-glucan, possibly causing the β-glucan molecule to seem net negatively charged. Vårum & Smidsød [11] as well as Korompokis et al. [25] suggested a slightly negative net charge in β-glucan aggregates. Therefore, the *Murphy and Riley method* [22] was used to investigate presence and concentration of phosphate in the β-glucan sample. From the obtained calibration curve (data not shown) the following relation was obtained (Eq. 4):

$$Absorbance = 0.6808 * c(phosphate) \quad (4)$$

An amount of 0.136±0.002 mg P (as phosphate)/L was found in the solution of β-glucan, resulting in 0.027% of phosphate (w/w, dry basis). Thus, the degree of substitution (DS) calculated utilizing Eq. 3 is equal to $4.6*10^{-4}$, representing the number (in moles) of phosphate per mole of β-(1→4)-linked D-glucosyl residues. Ghotra et al. [13] found, that the total phosphorous content in purified oat β-glucan was 0.201%. (w/w, DS=0.011), which is approximately 24 times higher than the phosphate content found in this study. Furthermore, Ghotra and al. [13] used lab-purified β-glucan under different extraction conditions, which could further explain differences with our results. Nevertheless, phosphate was found in low quantities in β-glucan. Phosphorous comes from inorganic phosphates and also from the possible presence of phospholipids or phosphoproteins. These phosphate residues could give rise to negative charges found in β-glucan and explain the suggested electrostatic interactions between proteins and polysaccharide. However, it seems somewhat surprising that such low amounts of phosphate substituents manage to induce aggregates able to lower the transmission values as much as observed. A possibility could be that the phosphate groups are unevenly distributed within the β-glucan molecule. The phosphate groups could be located in clusters e. g. heterogeneously in the polymer chain, which is known to occur in other polysaccharides such as amylopectin. [28] Furthermore, the phosphate substituents could be unevenly distributed over the M distribution, but from the results presented in this paper it is not possible to draw distinctive conclusions.

Again, results have been reported by Vårum et al. [11] as well as by Korompokis et al. [25], suggesting that β-glucan is a slightly net negatively charged molecule at pH 3. Gliadin and WP, both being below their pI at pH 4, are net positively charged. Hence, the polysaccharide and protein most likely attract each other to form aggregates through attractive electrostatic interaction. Furthermore, as described by Korompokis et al. [25], at pH ≥ 7 both β-glucan (ζ-potential = -1.53 ± 0.08 mV at pH 7 (10 mM $NaNO_3$, 3 mM NaN_3)) and proteins are net negatively charged, which would explain the lack of aggregate formation due to less attractive electrostatic interaction. It can be concluded, that aggregation of proteins and β-glucan seems to have strong contributions from electrostatic interaction. However, the role of charged groups in β-glucan during the aggregation process still needs further investigation and the possibility of other forces contributing to aggregation, such as apolar effects, can't be ruled out.

Composition of aggregates

Aggregates were analysed with the *Dumas Method* to measure the quantity of proteins [29]. Fig. 6 shows the percentage of protein in the observed aggregates, compared to the initial quantity in the proetin:β-glucan mixtures at pH 3 and pH 4. For WP:β-glucan, aggregates of different ratios at pH 3 (Fig. 6A) show protein contents between 12 and 22 %, with highest content at a ratio of 1:1. Compared to the aggregates at pH 4 (Fig. 6B), less proteins from the mixtures are present in the aggregates at pH 3. It could corroborate the fact that for each ratio the transmission value is lower at pH 4 than at pH 3 (Fig. 3A,B) so the amount of aggregates seem to be higher at pH 4. More closely, WP:β-glucan aggregates of different ratios at pH 4 (Fig. 6B) range in average percentages between 10-50 %. There is no significant difference between the ratios but the tendency that more β-glucan present in solution seems to form aggregates with higher protein content is visible. This observation also confirms the lowest transmission value obtained for the ratio 1:2 in Fig. 2A. For gliadin:β-glucan at pH 4 (data not shown), the percentage of the protein in aggregates, compared to its initial value, is only around 3% and hence, lower than the percentage for WP. Besides, there is no significant difference between the ratios (all below 3%), underlining the results from Fig. 3C, where transmission values of all ratios were somewhat similar.

It can be noted, that gliadin and WP show different behaviours in the aggregates. The percentage of WP found in the aggregates seems to depend on the quantity of β-glucan in the solution mixture (Fig. 6B). For gliadin, the percentage of protein in aggregates compared to the initial quantity in the mixtures, is low (<3 %, data not shown) and in a similar range for every gliadin:β-glucan ratio. Here, the initial amount of β-glucan doesn't seem to

influence the end-percentage of protein in the aggregates.

An explanation for that could be that negatively charged β-glucan at pH 3 and pH 4, and positively charged WP are attracted to each other and hence, the more β-glucan in solution, the more WP will be attracted by the polysaccharides. This could also explain the differences observed in transmission at pH 3 and pH 4 (Fig. 3A,B). However, it doesn't apply for gliadins. Only a low amount of initial gliadin seems to end up in aggregates at pH 4 although the transmission of the corresponding mixtures are very low (Fig. 3C), indicating that the formed complex might be composed mainly of β-glucan.

Conclusion

Two different types of aggregates have been obtained at different pH values by mixing proteins (WP or gliadin) and a β-glucan isolate (OBC90) at several mass ratios. The interaction between proteins and polysaccharides appears to have strong electrostatic contributions. At pH values, where interaction is observed, proteins are net positively charged and β-glucan is slightly negatively charged causing attraction between the molecules. The β-glucans' negative charges can originate from phosphate found at low concentrations in the β-glucan and could be the reason why the molecules attract each other to form aggregates at low pH. Moreover, the extent of aggregation between WP and β-glucan depends on the mixing ratios whereas there is no ratio dependency between gliadin and β-glucan. Thus, the aggregation process and composition of the aggregates depends on the type of protein. Indisputable, this study confirmed that β-glucan and proteins can aggregate under the suggestion of electrostatic contributions.

Acknowledgement

Funding from the Swedish research council (VR), Stockholm, Sweden is gratefully acknowledged. Dr. Ondrej Kosik, Rothamsted Research, Harpenden, UK, is acknowledged for the work on HPSEC-PAD. Furthermore, we are greatly thankful for Dr. Cristina Teixera's for her help with the protein analysis (Centrum för preventiv livsmedelsforskning/Food for Health Science Centre at Lund University, Lund, Sweden). SOLVE Research & Consultancy AB, Lund is gratefully acknowledged for allowing use to use their DLS instrument.

References

[1] A. Lazaridou and C. G. Biliaderis, J. Cereal Sci., 1 (2007) 101.

[2] T. M. Wolever, S. M. Tosh, A. L. Gibbs, J. Brand-Miller, A. M. Duncan, V. Hart, B. Lamarche, B. A. Thomson, R. Duss and P. J. Wood, Am. J. Clin. Nutr., 92 (2010) 723.

[3] European Food Safety Authority 1. EFSA Journal. 2009;7.

[4] European Food Safety Authority 2. EFSA Journal. 2010;8.

[5] U.S. Food and Drug Administration. Federal Register. 1992;62: 15343-15344.

[6] U.S. Food and Drug Administration. Federal Register. 2008;73: 47828-47829.

[7] M. Zhou, K. Robards, M. Glennie-Holmes and S. Helliwell, J. Sci. Food and Agr., 80 (2000) 1486.

[8] K. Autio, O. Myllymaki, T. Suortti, M. Saastamoinen and K. Poutanen, Food Hydrocolloid, 5 (1992) 513.

[9] C. Zielke, C. Teixeira, H. Ding, S. Cui, M. Nyman and L. Nilsson, Carbohyd. Polym., 157 (2017) 541.

[10] I. S. Forrest and T. Wainwright, J. I. Brewing, 83 (1977) 279.

[11] K. M. Vårum and O. Smidsrød, Carbohyd. Polym., 9 (1988) 103.

[12] L. Acker, W. Diemair and E. Samhammer, Zeitschrift für Lebensmittel-Untersuchung und Forschung, 100 (1955) 180.

[13] B. S. Ghotra, T. Vasanthan, M. Wettasingh and F. Temelli, Food Hydrocolloid., 21 (2007) 2056.

[14] T. Hunter, Philos. Trans. R. Soc. Lond. B. Biol. Sci., 367 (2012) 2513.

[15] C. Zielke, O. Kosik, M.-L. Ainalem, A. Lovegrove, A. Stradner and L. Nilsson, PLOS ONE, 12 (2017) e0172034.

[16] E. Magnusson and L. Nilsson, Food Hydrocolloid, 25 (2011) 764.

[17] F. Goubet, C. J. Barton, J. C. Mortimer, X. Yu, Z. Zhang, G. P. Miles, J. Richens, A. H. Liepman, K. Seffen and P. Dupree, Plant J., 60 (2009) 527.

[18] A. Håkansson, E. Magnusson, B. Bergenståhl and L. Nilsson, J. Chromatogr. A, 1253 (2012) 120.

[19] M. Ulmius, G. Önning and L. Nilsson, Food Hydrocolloid, 26 (2012) 175.

[20] D. P. Chang, M. Jankunec, J. Barauskas, F. Tiberg and T. Nylander, Appl. Mater. Interfaces, 4 (2012) 2643.

[21] M. Wahlgren and T. Arnebrant, J. Colloid Interface Sci., 148 (1992) 201.

[22] J. Murphy and J. P. Riley, Anal. Chim. Acta, 27 (1962) 31.

[23] American Public Health Association, American Water Works Association, Water Environment Federation (1999), Standard Methods for the Examination of Water and Wastewater

[24] M. Schmidt, D. Nerger and W. Burchard, Polymers, 20 (1979) 582.

[25] K. Korompokis, L. Nilsson and C. Zielke, Manuscript submitted to Food Hydrocolloids and attached to this manusctript

[26] N. Neirynck, P. Van der Meeren, M. Lukaszewicz-Lausecker, J. Cocquyt, D. Verbeken and K. Dewettinck, Colloids Surf. A: Physicochem. Eng. Aspects, 298 (2007) 99.

[27] L. Wannerberger, M. Wahlgren and A.-C. Eliasson, Cereal Chem., 73, (1996) 499.

[28] A. Blennow, A. M. Bay-Smidt, C. E. Olsen and B. L. Møller, Int. J. Biol. Macromolec., 27 (2000) 211.

[29] J.-P. Dumas, Ann. Chim. Phys., 2 (1831) 198.

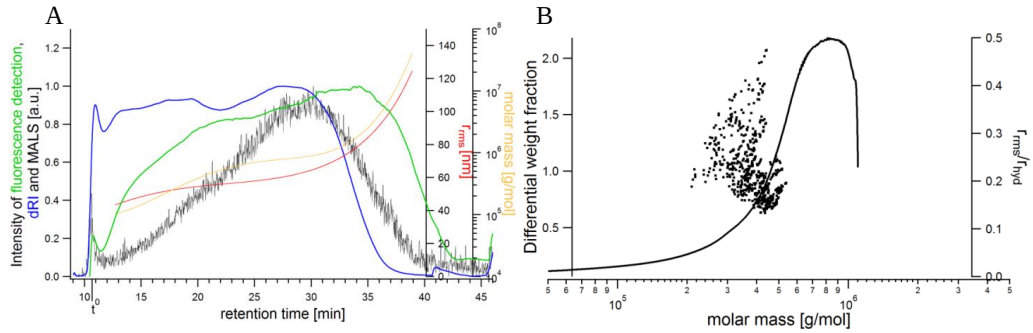

Fig. 1: **A** shows a fractogram of the β-glucan extract OBC90 plotted vs retention time [min]. The colors denote: green – fluorescence signal of in-line Calcoflour labelled β-glucan at λ_{ex} = 415 nm and λ_{em}= 445 nm [a.u.], blue – dRI signal [a.u.], black – Rayleigh ratio from MALS [a.u., 69.3° - 121.2°], yellow – M distribution [g/mol], red – r_{rms} distribution [nm]. **B** displays the differential weight fraction of ß-glucan is represented as solid line and the conformation ratio of r_{rms}/r_{hyd} is plotted in black dots, all vs. the molar mass [g/mol].

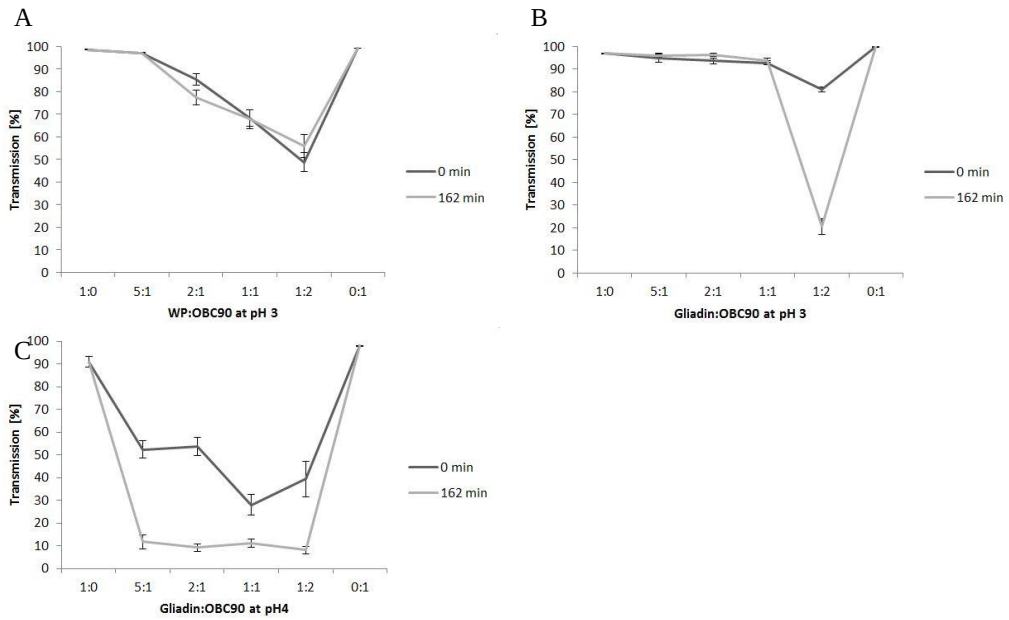

Fig. 2: Relative transmission, corrected for the transmission of the buffer, as a function of protein:OBC90 mass ratio at different pH. The error bars show the standard error of the mean. **A**: WP:OBC90 mass ratio at pH 3. **B**: Gliadin:OBC90 mass ratio at pH 3. **C**: Gliadin:OBC90 mass ratio at pH 4.

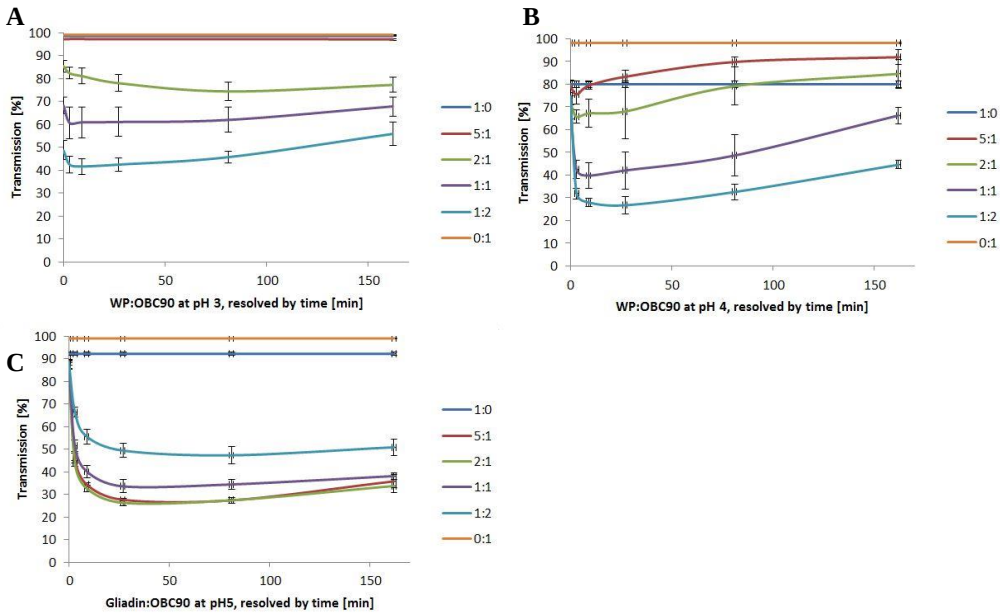

Fig 3: Transmission values as a function of time for different protein:OBC90 mass ratios at different pH. The error bars show the standard error of the mean. **A**: WP:OBC90 at pH3, **B**: WP:OBC90 at pH4, **C**: Gliadin:OBC90 at pH5.

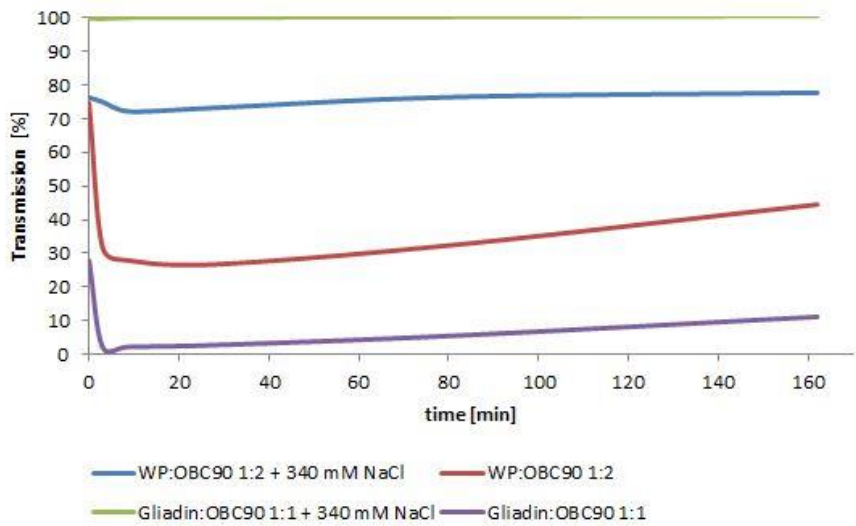

Fig 4: Transmission values as a function of time for one protein:OBC90 mass ratios, with and without NaCl added at pH 4.

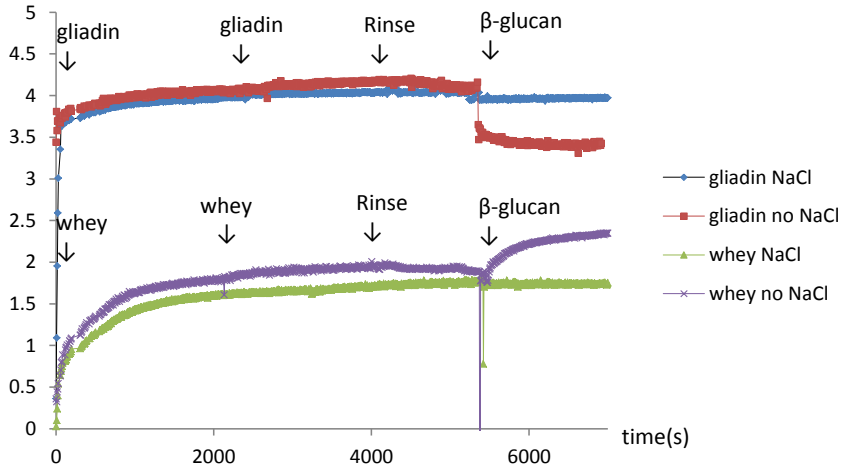

Fig. 5: Results of the Ellipsometry measurements. Adsorbed mass (mg/m^2) plotted versus time [sec].

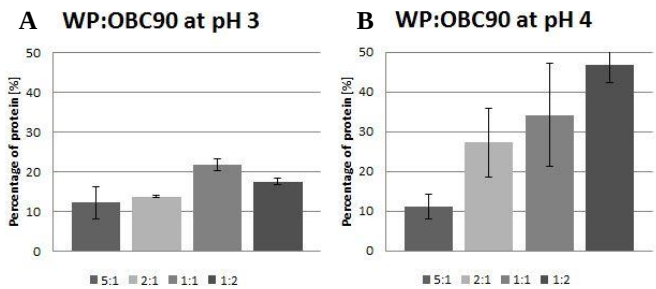

Fig 6: Percentage of protein in the aggregates, compared to initial quantity in the mixtures between WP and β-glucan in solution. The error bars show the standard error of the mean.

Paper IV

Characterization of the molar mass distribution of macromolecules in beer for different mashing processes using asymmetric flow field-flow fractionation (AF4) coupled with multiple detectors

Choi, J., Zielke, C., Nilsson, L. & Lee, S.

Analytical and Bioanalytical Chemistry (2017) 409, 4551-4558.

Anal Bioanal Chem (2017) 409:4551–4558
DOI 10.1007/s00216-017-0393-8

RESEARCH PAPER

Characterization of the molar mass distribution of macromolecules in beer for different mashing processes using asymmetric flow field-flow fractionation (AF4) coupled with multiple detectors

Jaeyeong Choi[1] · **Claudia Zielke**[2] · **Lars Nilsson**[2] · **Seungho Lee**[1]

Received: 17 February 2017 / Accepted: 3 May 2017 / Published online: 15 May 2017

Abstract The macromolecular composition of beer is largely determined by the brewing and the mashing process. It is known that the physico-chemical properties of proteinaceous and polysaccharide molecules are closely related to the mechanism of foam stability. Three types of "American pale ale" style beer were prepared using different mashing protocols. The foam stability of the beers was assessed using the Derek Rudin standard method. Asymmetric flow field-flow fractionation (AF4) in combination with ultraviolet (UV), multiangle light scattering (MALS) and differential refractive index (dRI) detectors was used to separate the macromolecules present in the beers and the molar mass (*M*) and molar mass distributions (*MD*) were determined. Macromolecular components were identified by enzymatic treatments with β-glucanase and proteinase K. The *MD* of β-glucan ranged from 10^6 to 10^8 g/mol. In addition, correlation between the beer's composition and foam stability was investigated (increased concentration of protein and β-glucan was associated with increased foam stability).

Keywords Beer · Macromolecules · Asymmetric flow field-flow fractionation (AF4) · Mashing · Enzymatic treatment · β-glucan · Protein aggregates

Electronic supplementary material The online version of this article (doi:10.1007/s00216-017-0393-8) contains supplementary material, which is available to authorized users.

✉ Jaeyeong Choi
feelcjy@gmail.com

✉ Lars Nilsson
lars.nilsson@food.lth.se

✉ Seungho Lee
slee@hannam.ac.kr

[1] Department of Chemistry, Hannam University, Daejeon 34054, Republic of Korea

[2] Department of Food Technology, Engineering and Nutrition, Lund University, P.O. Box 124, SE-221 00 Lund, Sweden

Introduction

Beer is the world's most popular and consumed drink after water and tea; it is also the oldest alcoholic beverage [1–3]. Beer is mainly composed of water, a starch source from malting barley or other cereals, and flavoring from hops. Beer is comprised of complex macromolecules, such as polysaccharides and proteins (polypeptides) [4].

Generally, the process of beer production can be divided into malting and brewing, whereas brewing can also be divided into several principal steps: mashing, boiling, fermenting, and maturation. Among them, mashing is an important step as it determines the total material that can be extracted from the malt and present starch is enzymatically converted into lower molar mass (*M*) sugars [4], resulting in the sweet wort. Malted barley contains various enzymes, such as α-amylase, β-amylase, β-glucanase, cystase, protease, and others [5, 6], which to various extents will digest malt macromolecules into smaller species. The wort composition is essential for beer quality, and a number of factors influence the mashing process and, thus, wort composition and properties. Important factors are water composition, grist composition, pH, mash thickness, dissolved oxygen, etc. Another key parameter when discussing the properties of the sweet wort (and eventually the finished beer) is the mash profile (i.e., temperatures and time); however, the mash profile can be changed relatively easy compared to other parameters [6].

The quality of beer will begin to decrease depending on the storage time and temperature after packaging. Therefore, it is essential to assess the stability of the beer. The presence of

some proteins results in beer that appears hazy, and polysaccharides with high *M* tend to increase the viscosity and turbidity of beer [6–9].

Foam stability of beer is often closely related to consumer satisfaction. Several beer constituents are associated with foam formation and stability: hops (iso-α-acids), proteins, and polysaccharides [10–12]. The enzymatic activity during mashing will affect proteins and polysaccharides and, thus, change beer properties like viscosity and foam stability. The characterization of beer macromolecules is typically based on methods described by the European Brewery Convention (EBC) [13], e.g., high-performance liquid chromatography (HPLC) and matrix-assisted laser desorption/ionization time of flight mass spectrometry (MALDI-TOF-MS) for the analysis of β-glucan and proteins but they only provide information for relatively low-*M* materials [14, 15]. β-glucan is commonly analyzed with fluorimetry as described by Munck et al. [13]. However, the type of beer or wort has to be regarded as dark samples can influence the absorbance and, hence, the β-glucan content may be underestimated. Using Calcofluor as labeling agent for β-glucan during fluorimetry might introduce additional errors, as the complex formation between Calcofluor and β-glucan molecules is not quantitative for β-glucan below 10^4 g/mol, resulting in a lower detector response [16].

Furthermore, most of the EBC-described methods do not provide information on the *M*, molar mass distribution (*MD*), and possible aggregation of β-glucan, resulting in high-*M* species above 10^6 g/mol. One study assessed the influence of the *MD* of beer components on the intensity of palate fullness, but this study focused more on low-*M* (<10^5) beer components [17]. Another drawback with these techniques mentioned by the EBC is that, due to sample preparation, a non-native state of the constituents might be analyzed. Tomasi et al. developed a simple and suitable method to determine and characterize β-glucan in beer wort, utilizing size exclusion chromatography (SEC), coupled to different detectors such as light scattering, viscometer, and differential refractive index (dRI) detector, to obtain information on, e.g., molecular weight averages, fraction description, hydrodynamic sizes, and intrinsic viscosity [18].

A recent study has shown the suitability of asymmetric flow field-flow fractionation (AF4) to analyze the macromolecules for beer foam and liquid [19]. Tügel et al. obtained wide *MD* and were able to analyze high *M* species, suggesting that there could also be highly aggregated macromolecules. AF4 is a gentle, flow-based separation technique with the ability of determining *M* and *MD* of macromolecules in a broad range (10^3–10^{17} g/mol) due to the thin ribbon-like open channel without packing material [20, 21]. The absence of a stationary phase, compared to chromatographic techniques like HPLC and SEC, enables a separation of the macromolecules under gentle and "close to native" conditions. In brief, the separation in AF4 is based on the hydrodynamic size and the individual diffusion coefficients of the analytes that are relaxed after injection onto the channel in a field perpendicular to the accumulation wall during a focusing step. Smaller molecules will be relaxed higher up in the channel, bigger molecules closer to the accumulation wall. Due to the parabolic flow profile during elution, the small analytes will elute earlier as large species. The retention time (t_r) is directly related to the hydrodynamic radius of the analyte, and with the help of an in-line multiangle light scattering detector (MALS) and concentration detector, e.g., dRI, *M* and *MD* can be obtained. AF4 connected to various detectors has already been proven a powerful technique for the characterization of various food macromolecules [22].

The aim of this study was to further evaluate the applicability of AF4 for the efficient separation and characterization of macromolecules in beer. Furthermore, the aim was to investigate the influence of mashing conditions on the macromolecular properties and the relationship between the macromolecular composition and foam stability.

In this study, we produced beer using three different mashing processes. Each beer underwent enzymatic treatments for semi-quantitative and qualitative analysis of the present macromolecules. AF4 coupled with online ultraviolet (UV) detector, MALS, and dRI detectors was employed for the separation and characterization of *M* and *MD* of macromolecules in the beers. In addition, the foam stability for the different beer types was assessed using the Derek Rudin standard method [12, 23] to confirm the correlation between macromolecules and foam stability.

Materials and methods

Materials

Acetic acid, sodium acetate trihydrate, sodium azide (NaN_3), β-glucanase, and proteinase K were purchased from Sigma-Aldrich (St. Louis, MO, USA). The β-glucanase and proteinase K activities are ≥1.0 units/mg and ≥30.0 units/mg, respectively. All chemicals were of analytical grade and were used without further purification. The carrier liquid for AF4 was prepared with water purified through a Milli-Q plus purification water system (Millipore Co. Ltd., Billeria, USA, resistance = 18.2 MΩ/cm). The carrier liquid was vacuum-filtered through a 0.1 μm cellulose nitrate membrane filter (Whatman GmbH, Dassel, Germany) before it was used.

The materials used to produce the beer were the following: the grains used were Pale Malt (2 Row barley) UK (5.9 EBC) from Weyermann Malting (Bamberg, Germany), Cara-Pils/Dextrine (3.9 EBC), and Crystal 100 (100.0 EBC) from Viking Malt (Halmstad, Sweden), using a ratio of 18:1:1; the hops varieties used were Cascade (6.90% α-acid) and

Amarillo Gold (8.80% α-acid) both grown in the USA and supplied by Humlegården (Sollentuna, Sweden); and the yeast used was Safale US-05 (Fermentis/Lesaffre, Marcq-en-Baroeul, France).

Production of the beer

Three types of beer (reference beer, protein rest beer, and β-glucan rest beer) were produced on a 20 L scale using 20 L Braumeister (Speidel, Ofterdingen, Germany). Reference beer was produced using a typical saccharification rest for American ale production. Protein rest beer and β-glucan rest beer were incubated at temperatures of 50 and 37 °C for 30 min before the saccharification rest, to maintain proteinases and β-amylases at their optimum activity, respectively. An overview of the mashing process conditions can be found in Table 1. After mashing, all beers were boiled at 100 °C for 75 min, and subsequently given time to cool down to room temperature. Then, 11.5 g yeast were added to each batch for fermentation during 1 week at 17 °C. Prior to bottling and a second fermentation step for another week in the cold room, sediments like non-soluble proteins, yeast residues, and insoluble polysaccharides were removed.

Preparation of the beer samples

All types of beer were transferred into 2-mL plastic tubes and sonicated using an FS60 sonicator (Fisher Scientific, Ottawa, Canada) for 30 min for degassing at room temperature and 130 W. The effect of sonication on beer macromolecules was investigated in a previous paper and no influence on the sample was noticed [19].

Enzymatic treatments of the beer samples

Enzymatic treatments of the beer samples were carried out with β-glucanase and proteinase K to confirm the composition of macromolecules in beer. Beer samples were prepared in 1 mL amounts filled into a centrifuge tube, and 10 μL of enzyme/mL was added to the beer. Reaction times were optimized to reach the optimal enzyme activities for the samples, resulting in 24 h at 60 °C for β-glucanase and 12 h at 37 °C for proteinase K, respectively. Effects of the temperature treatment on the macromolecules of the beer were investigated to make sure that the temperature changes during enzymatic treatment did not affect the macromolecules. No difference was observed in AF4 fractograms and *MD* without enzyme but with the same temperature treatments.

AF4 analysis of the beer

The AF4 system used in this work was an Eclipse 2 system (Wyatt Technology Europe, Dernbach, Germany), coupled online with a S 4245 UV detector (Schambeck SFD GmbH, Bad Honnef, Germany) operated at a wavelength of 280 nm, a DAWN EOS MALS (Wyatt Technology, Santa Barbara, CA, USA) operated at a wavelength of 690 nm, and a RI-101 dRI detector (Shodex, Tokyo, Japan). The carrier liquid was pumped into the AF4 channel using an Agilent 1100 HPLC pump (Agilent Technologies, Waldbronn, Germany) with an in-line vacuum degasser, and the flow rate was measured by an OptiFlow 1000 Liquid Flowmeter (Agilent Technologies, Palo Alto, CA, USA). The analysis channel was an Eclipse AF4 long channel (Wyatt Technology, Europe, Dernbach, Germany) assembled with a regenerated cellulose membrane having a molecular weight cut-off (MWCO) of 10 kDa (Millipore, Bedford, USA) and a 350-μm-thick Mylar spacer. The actual channel thickness (= 234.6 μm) was determined from t_r of bovine serum albumin (BSA, MW = 66 kDa, Sigma-Aldrich, St. Louis, MO, USA) using the FFFHydRad 2.0 software [24]. The channel geometry was trapezoidal with a tip-to-tip length of 26.5 cm and a width at the inlet and the outlet of 2.2 and 0.6 cm, respectively. A 50-μL beer sample was injected into the AF4 channel at an injection flow rate of 0.2 mL/min for 3 min, and the focusing time was 3 min at 4.0 mL/min. The channel flow was kept constant at 1.0 mL/

Table 1 The mashing process for the three types of beer and semi-quantitative amounts of protein and β-glucan obtained from the MALS response, as well as gravity, alcohol content, pH, and viscosity for three types of beer

Mash step	Reference beer		Protein rest beer		β-glucan rest beer		
1	–		50 °C/30 min		37 °C/30 min		
2	67 °C/60 min		67 °C/60 min		67 °C/60 min		
3	75 °C/5 min		75 °C/5 min		75 °C/5 min		
Beer type	Semi-quantitative amounts (%)		Specific gravity		Estimated alcohol content (wt%)[a]	pH	Viscosity (mPa s)
	β-glucan	Protein	Original	Final			
Reference beer	68	32	1.057	1.013	4.6	4.4	1.45
Protein rest beer	59	25	1.063	1.014	5.1	4.4	1.48
β-glucan rest beer	45	33	1.055	1.016	4.1	4.4	1.28

[a] Estimated from specific gravity values

min, while the cross flow was exponentially decreasing from 4.0 to 0.2 mL/min with a half-life of 5 min and then kept at a constant cross flow of 0.2 mL/min for 30 min. The carrier liquid used was 50 mM of acetate buffer at a pH of 4.4, approximating the pH of beer. All AF4 experiments were performed at room temperature. The *M* and *MD* were determined by online AF4-MALS using the Berry method [25, 26], and all data processing was performed using ASTRA software (Version 6.1.1, Wyatt Technology). The d*n*/d*c* values of 0.185 and 0.150 mL/g were used to characterize the proteins (population 1) and polysaccharides (populations 2 and 3), respectively [27–30].

Assessment of beer foam stability

The foam stability was determined using Derek Rudin standard method [12, 23]. The device for the measurement of foam stability is shown in Fig. S1 in the Electronic Supplementary Material (ESM). The foam collapse rate was determined as follows: degassed beer was added up to the 6 cm mark and foamed by injecting nitrogen (N_2) or carbon dioxide (CO_2) gas at a rate of about 100 mL/min and a constant temperature of 20 °C until the foam reached the 40 cm mark. The time needed for the foam liquid interface to migrate from the 5 cm mark to the 2 cm mark was measured and, hence, the collapse rate was determined. Each measurement was repeated five times. As the foam stability is directly associated to the cleanliness of the glass, a washing step with ethanol was done prior to the next analysis, and the glass was given time to dry at room temperature.

Results and discussion

Characterization of the beer using AF4-UV-MALS-dRI

With the help of AF4-UV-MALS-dRI, the *M* and *MD* of each fraction were determined. Figure 1 shows AF4-UV-MALS-dRI fractograms for the three types of beer with their *MD*. It can be seen from Fig. 1a that there are three major populations of macromolecules in each beer. Protein rest and *β*-glucan rest beers have similar elution behaviors and *M* ranges for each population. In all beers, population 1 elutes during t_r of 2–6 min and has a *M* range of 2.0–4.0 × 10^4 g/mol. However, the dRI and UV fractograms (Figs. 2b, c) show different responses and, hence, indicate different amounts of low-*M* substances for each beer, whereas the reference beer shows the lowest dRI response but highest for UV and protein rest beer the highest dRI response but lowest for UV. In the case of the protein rest beer, the high dRI response compared to the reference beer could be expected as higher *β*-glucanase activity is present due to the protein rest at 50 °C. This may result in an increased concentration of the low-*M* substances and, hence,

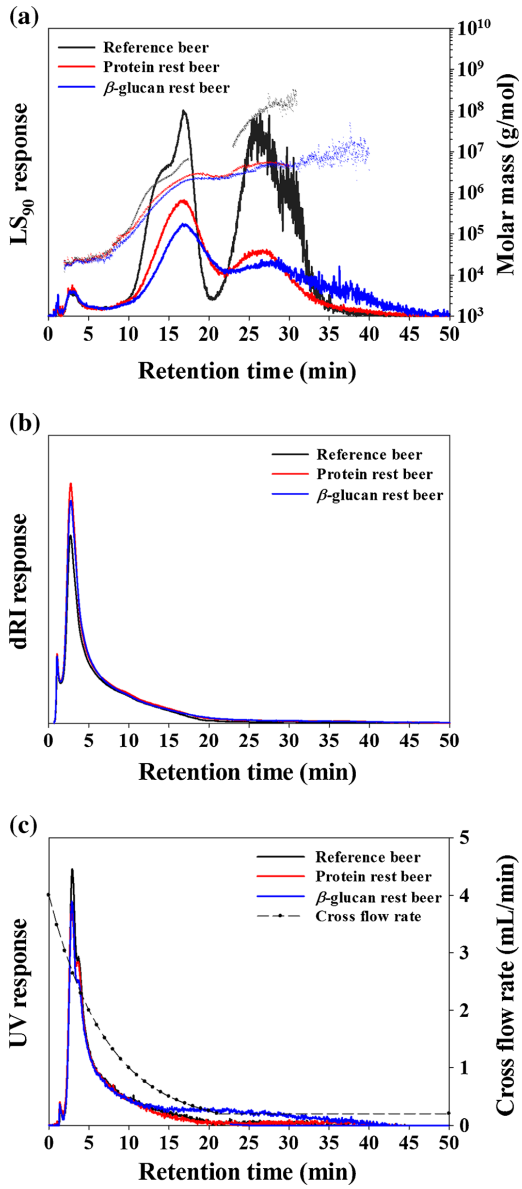

Fig. 1 AF4 fractograms for three types of beer. **a** LS_{90} response (*line*) and *M* (*symbol*). **b** dRI response. **c** UV response at 280 nm (*solid line*) with the condition of the cross flow rate (*broken line*)

the increase in dRI response. Population 2 was eluted with a t_r of 6–21 min, and all beers (reference, protein rest, and *β*-glucan rest) had a similar elution pattern but different *M* ranges of 5 × 10^4 to 7 × 10^6, 5 × 10^4 to 3 × 10^6, and 4 × 10^4 to 2 × 10^6 g/mol, respectively. Population 3 was eluted between 21 and

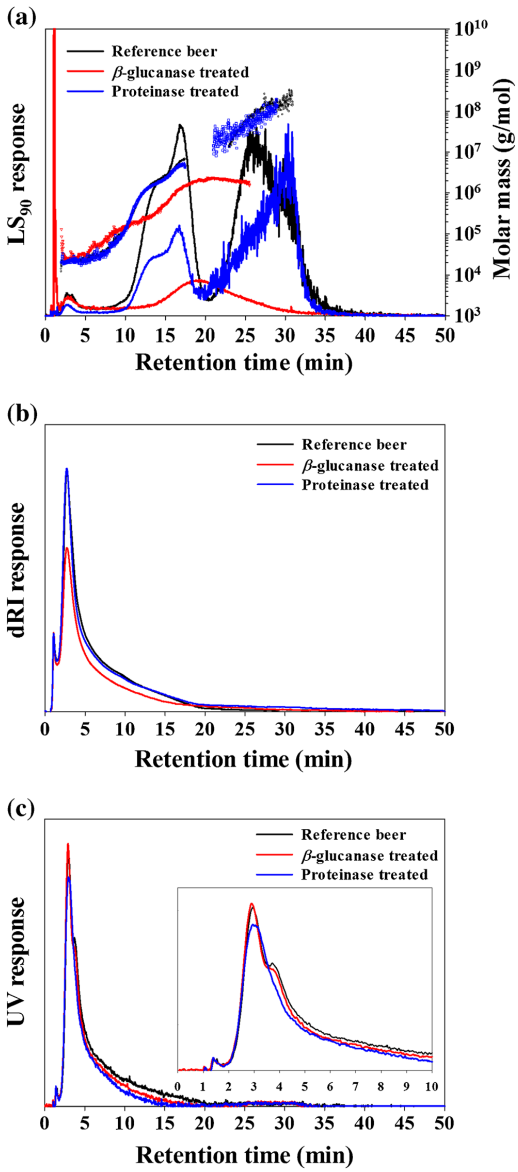

Fig. 2 AF4 fractograms of treated reference beer. **a** LS_{90} response (*line*) and *M* (*symbol*). **b** dRI response. **c** UV response at 280 nm. *β*-glucanase and proteinase treated in an incubator at 60 °C for 24 h and 37 °C for 12 h, respectively

50 min and each beer had a different signal pattern from MALS signal as well as different *M* ranges of 1×10^7 to 3×10^8, 2.5×10^6 to 5.5×10^6, and 2×10^6 to 1×10^7 g/mol, respectively. For all beers, the dRI is strongest for population 1, weaker for population 2, and very weak for population 3 indicating that these are present at lower concentrations (Figs. 2b, c). However, populations 2 and 3 are readily detectable with the MALS detector as the light scattering intensity is high for large analytes. The results show that the mashing conditions in the brewing process have a significant influence on the concentration and *M* range of beer components. The *M* range and the MALS response in the reference beer are higher than those of the protein rest and *β*-glucan rest beers which is likely to be a result of the higher enzymatic activity in the two latter. Accordingly, enzymatic treatments of the beers were used to investigate the chemical composition of the macromolecules.

Characterization of enzymatically treated beer

Reference beer was produced using the optimal (or general) mashing conditions for "American pale ale" style beer (see Table 1). Figure 2 shows the AF4 fractograms and *MD* of reference beer before and after enzymatic treatment with either *β*-glucanase or proteinase K. A significant change is observed in the MALS response (see Fig. 2a); moreover, the maximum *M* of populations 2 and 3 decreased after *β*-glucanase treatment, from 3×10^8 to 2.3×10^6 g/mol, but no significant change was observed after treatment with proteinase K (only the MALS intensity decreased), suggesting that the ultra-high *M* macromolecules (>10^7 g/mol) in populations 2 and 3 are considerably degraded by *β*-glucanase treatment (see symbol in Fig. 2a); thus, these analytes are to a large extent composed of *β*-glucan, and the *M* range of *β*-glucan was confirmed to be approximately 10^6 to 10^8 g/mol. The precise *M* range of proteins before and after enzymatic treatment was difficult to determine from AF4 results because there were only minor changes in the UV-absorbance, but not in t_r. Due to the differences, the signal could be identified as coming from proteinaceous matter, but the *M* range did not change.

Furthermore, proteins will affect the macromolecules' aggregation. Results demonstrated that proteinase K-treatment does not change the *M* range of populations 2 and 3 (Fig. 2a), but t_r of the peak maximum of population 3 increased with about 5 min, indicating a higher hydrodynamic size (r_{hyd}) of the species, which could indicate some aggregation of *β*-glucan in beer as no change in UV response is observed.

Figures 3 and 4 show the AF4 fractograms and *M* of protein rest and *β*-glucan rest beers before and after enzymatic treatments with *β*-glucanase and proteinase K. In these cases, the enzymatic treatment results differ from those of the reference beer. *M* of populations 1 and 3 increased after *β*-glucanase treatment and *M* of populations 2 and 3 increased after proteinase K treatment. Protein rest beer had a lower level of proteins than the reference beer and *β*-glucan rest beer (Table 1). Proteinase K treatments for protein rest and *β*-glucan rest beers showed different results regarding *MD*,

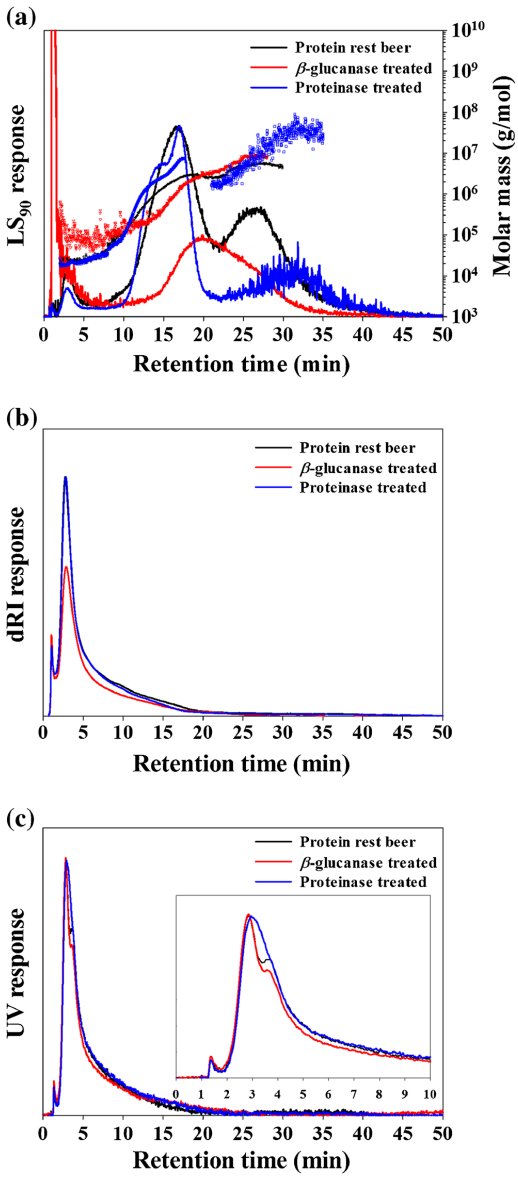

Fig. 3 AF4 fractograms of treated protein rest beer. **a** LS_{90} response (*line*) and *M* (*symbol*). **b** dRI response. **c** UV response at 280 nm. *β*-glucanase and proteinase K treated samples in an incubator at 60 °C for 24 h and 37 °C for 12 h, respectively

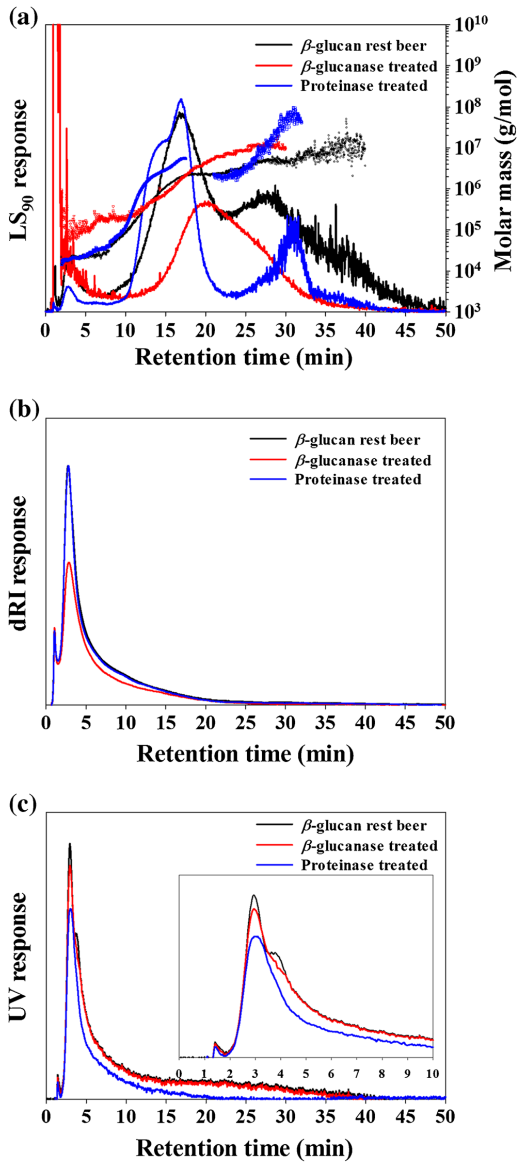

Fig. 4 AF4 fractograms of treated *β*-glucan rest beer. **a** LS_{90} response (*line*) and *M* (*symbol*). **b** dRI response. **c** UV response at 280 nm. *β*-glucanase and proteinase K treated samples in an incubator at 60 °C for 24 h and 37 °C for 12 h, respectively

compared to the untreated beers, i.e., the maximum *M* increased. The results show the presence of denser aggregates (i.e., higher *M* at the same t_r) which suggests that the protein plays an important role in determining the structure of the macromolecular aggregates. In addition, the void peak of the MALS detector increased after *β*-glucanase treatment for all beers, suggesting two possible explanations for this phenomenon: Firstly, aggregation of degraded *β*-glucan from *β*-glucanase treatment and secondly, aggregation of proteins might cause co-elution in steric/hyperlayer mode without

retention in the separation channel [31]. The relative amounts of macromolecules, such as protein and β-glucan, were determined from the area of MALS responses from 8 to 50 min (populations 2 and 3) for each beer. Table 1 shows the results for the relative amounts of protein and β-glucan in the macromolecules of each beer. As the results indicate, the reference beer has a higher amount (about 68%) of β-glucan than the other beers, and β-glucan rest and reference beers have more similar amounts (about 32%) of protein than protein rest beer. However, these values should be considered apparent as a direct comparison assumes that the apparent density and/or conformation are the same at same t_r in all three types of beer. AF4 separation occurs based on r_{hyd} and therefore, it might be possible that after an enzymatic treatment, species with similar r_{hyd} but with different M elute at the same t_r.

The concentrations of proteins and β-glucan are, in regard to literature, closely related to the foam stability of beer [7, 10–12]. Therefore, the foam stability of the beers was measured to investigate the correlation between stability and the amount of the respective macromolecules.

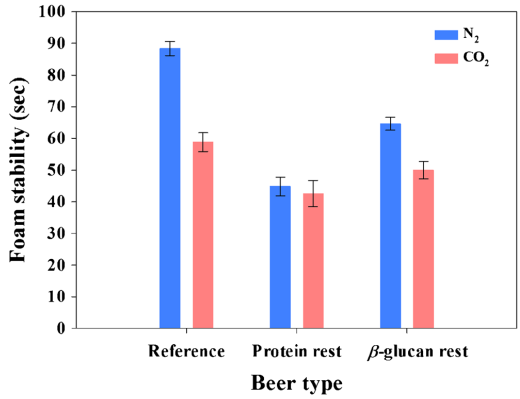

Fig. 5 The foam stability results for the three types of beer based on the Derek Rudin standard method. The analysis of each beer was repeated five times and the average values are shown including *error bars* (standard error of the mean with a 95% confidence interval). The injection flow rate of gas = 100 mL/min, temperature = 20 °C

Assessment of foam stability

It is known from literature that the foam stability is dependent on the concentrations of proteins and polysaccharides, e.g., β-glucan in the sample, and high-gravity beer has poorer foam stability [6, 12]. The specific gravities (SG), alcohol content, and viscosity values of the produced beers (reference, protein rest, and β-glucan rest beers) can be found in Table 1. The values for the original gravity show some variation which is probably originating from the different mashing profiles and the temperature effect on enzymatic activity. The variation should be considered small and the difference in alcohol content is not expected to play a large role for the aim of this paper. Figure 5 shows the assessment of foam stability for the three types of beer using different gases (N_2 and CO_2). The results show that the reference beer has the highest foam stability, followed by β-glucan rest beer and protein rest beer. Furthermore, it can be seen that the stability differed depending on the type of gas; for the reference and β-glucan rest beer, more stable foams were obtained when N_2 gas was used, whereas for protein rest beer, the result is not conclusive due to an insignificant difference. The lower foam stability for protein rest beer seems reasonable as the protein content is lower than in the other beers. However, higher foam stability is expected for N_2 gas, as it has a lower solubility in water than CO_2 gas and, thus, foam collapse originating from Ostwald ripening (disproportionation) is considerably slower [11, 12].

Furthermore, results imply that higher concentrations of protein and β-glucan were associated with higher foam stability (see Table 1 and Fig. 5) as the reference beer shows the highest foam stability. This is most probably due to good foam stabilizing properties of proteins. From the results (Fig. 5), it can be concluded that the effect of protein on the foam stability is higher compared to the effect of β-glucan. Nevertheless, higher β-glucan content increases the viscosity of beer. In turn, the increased viscosity slows down drainage of liquid from the lamellae in the foam and, thus, gives rise to higher stability. Comparing the results from protein rest to β-glucan rest beer, a higher content of protein (= β-glucan rest beer) seems to have a greater impact on foam stability than a higher content of β-glucan (= protein rest beer).

Conclusions

In this study, three types of beer were produced using different mashing processes, and the M range of macromolecules for reference, protein rest, and β-glucan rest beers were determined as 2.0×10^4–3×10^8, 2.0×10^4–5.5×10^6, and 2.0×10^4–1×10^7 g/mol, respectively. In addition, the M of β-glucan was confirmed to be in the range of about 10^6–10^8 g/mol. The relative amount and M range of macromolecules in each beer were determined using an AF4-UV-MALS-dRI setup before and after enzymatic treatment of the beers. For each beer (reference, protein rest, and β-glucan rest beers), the relative amount of protein (32, 24, and 33%) and β-glucan (68, 48, and 45%) was determined. Our results show that beer has a complex aggregated macromolecular composition consisting of proteins and polysaccharides. We were also able to make a direct connection between the AF4 results and the foam stability of the samples; with higher concentration of protein and β-glucan, the foam stability increased, whereas protein had a greater impact on foam stability than β-glucan. The results

presented in this paper should be helpful for analyzing beers on the macromolecular scale.

Acknowledgements The authors acknowledge the support provided by the National Research Foundation (NRF) of Korea (NRF-2013K2A3A1000086 and NRF-2016R1A2B4012105), support from Hannam University Research Fund, and support from the Swedish foundation for international cooperation for research and higher education (STINT).

Compliance with ethical standards

Conflict of interest There are no competing interests present and there are no patents, products in development or marketed products to declare. Furthermore, we agree with the policies on sharing data and materials, as in the guide for authors.

References

1. Arnold JP. Origin and history of beer and brewing: From prehistoric times to the beginning of brewing science and technology; A critical essay. Alumni Ass'n of the Wahl-Henius Institute of Fermentology; 1911.
2. Michel RH, McGovern PE, Badler VR. Chemical evidence for ancient beer. Nature. 1992;360(6399):24. doi:10.1038/360024b0.
3. Max N. The Barbarian's Beverage: A History of Beer in Ancient Europe. 1st ed. Taylor & Francis; 2005.
4. Bamforth C. Beer: tap into the art and science of brewing. 3rd ed. Oxford University press; 2009.
5. Esslinger HM. Handbook of brewing: processes, technology, markets. Wiley; 2009.
6. Priest FG, Stewart GG. Handbook of brewing. CRC Press; 2006.
7. Asano K, Shinagawa K, Hashimoto N. Characterization of haze-forming proteins of beer and their roles in chill haze formation. J Am Soc Brew Chem. 1982;40(4):147–54. doi:10.1094/ASBCJ-40-0147.
8. Siebert KJ, Carrasco A, Lynn PY. Formation of protein–polyphenol haze in beverages. J Agric Food Chem. 1996;44(8):1997–2005. doi:10.1021/jf950716r.
9. Steiner E, Becker T, Gastl M. Turbidity and haze formation in beer—insights and overview. J Inst Brew. 2010;116(4):360–8.
10. Bamforth CW, Kanauchi M. Interactions between polypeptides derived from barley and other beer components in model foam systems. J Sci Food Agric. 2003;83(10):1045–50. doi:10.1002/jsfa.1503.
11. Bamforth CW. The relative significance of physics and chemistry for beer foam excellence: theory and practice. J Inst Brew. 2004;110(4):259–66. doi:10.1002/j.2050-0416.2004.tb00620.x.
12. Bamforth CW. Foam: Practical Guides for Beer Quality. 1st ed. American Society of Brewing Chemists; 2012.
13. Munck L, Jorgensen K, Ruud-Hansen J, Hansen K. The EBC methods for determination of high molecular weight β-glucan in barley, malt, wort and beer. J Inst Brew. 1989;95(2):79–82. doi:10.1002/j.2050-0416.1989.tb04612.x.
14. Anderson I. The effect of β-glucan molecular weight on the sensitivity of dye binding assay procedures for β-glucan estimation. J Inst Brew. 1990;96(5):323–6. doi:10.1002/j.2050-0416.1990.tb01038.x.
15. Laštovičková M, Mazanec K, Benkovská D, Bobáľová J. Utilization of the linear mode of MALDI-TOF mass spectrometry in the study of glycation during the malting process. J Inst Brew. 2010;116(3):245–50. doi:10.1002/j.2050-0416.2010.tb00427.x.
16. Kim S, Inglett GE. Molecular weight and ionic strength dependence of fluorescence intensity of the Calcofluor/β-glucan complex in flow-injection analysis. J Food Compos Anal. 2006;19(5):466–72. doi:10.1016/j.jfca.2005.11.006.
17. Rübsam H, Gastl M, Becker T. Influence of the range of molecular weight distribution of beer components on the intensity of palate fullness. Eur Food Res Technol. 2013;236(1):65–75.
18. Tomasi I, Marconi O, Sileoni V, Perretti G. Validation of a high-performance size-exclusion chromatography method to determine and characterize β-glucans in beer wort using a triple-detector array. Food Chem. 2017;214:176–82. doi:10.1016/j.foodchem.2016.06.092.
19. Tügel I, Runyon JR, Gómez Galindo F, Nilsson L. Analysis of polysaccharide and proteinaceous macromolecules in beer using asymmetrical flow field-flow fractionation. J Inst Brew. 2015;121(1):44–8. doi:10.1002/jib.195.
20. Giddings JC. Field flow fractionation: a versatile method for the characterization of macromolecular and particulate materials. Anal Chem. 1981;53(11):1170A–8A.
21. Wahlund KG, Giddings JC. Properties of an asymmetrical flow field-flow fractionation channel having one permeable wall. Anal Chem. 1987;59(9):1332–9.
22. Nilsson L. Separation and characterization of food macromolecules using field-flow fractionation: a review. Food Hydrocoll. 2013;30(1):1–11. doi:10.1016/j.foodhyd.2012.04.007.
23. Rudin AD. Measurement of the foam stability of beers. J Inst Brew. 1957;63(6):506–9. doi:10.1002/j.2050-0416.1957.tb06291.x.
24. Håkansson A, Magnusson E, Bergenståhl B, Nilsson L. Hydrodynamic radius determination with asymmetrical flow field-flow fractionation using decaying cross-flows. Part I. A theoretical approach. J Chromatogr A. 2012;1253:120–6. doi:10.1016/j.chroma.2012.07.029.
25. Berry GC. Thermodynamic and conformational properties of polystyrene. I. Light-scattering studies on dilute solutions of linear polystyrenes. J Chem Phys. 1966;44(12):4550–64. doi:10.1063/1.1726673.
26. Andersson M, Wittgren B, Wahlund K-G. Accuracy in multiangle light scattering measurements for molar mass and radius estimations. Model Calculations and Experiments Anal Chem. 2003;75(16):4279–91. doi:10.1021/ac030128+.
27. Theisen A. Refractive increment data-book for polymer and biomolecular scientists: Nottingham University Press; 2000.
28. Steiner E, Gastl M, Becker T. Protein changes during malting and brewing with focus on haze and foam formation: a review. Eur Food Res Technol. 2011;232(2):191–204. doi:10.1007/s00217-010-1412-6.
29. Ulmius M, Önning G, Nilsson L. Solution behavior of barley β-glucan as studied with asymmetrical flow field-flow fractionation. Food Hydrocoll. 2012;26(1):175–80. doi:10.1016/j.foodhyd.2011.05.004.
30. Grimm A, Krüger E, Burchard W. Solution properties of β-D-(1, 3)(1, 4)-glucan isolated from beer. Carbohydr Polym. 1995;27(3):205–14. doi:10.1016/0144-8617(95)00056-D.
31. Myers MN, Giddings JC. Properties of the transition from normal to steric field-flow fractionation. Anal Chem. 1982;54(13):2284–9.

Paper V

Analysis of β-glucan molar mass from barley malt and brewer's spent grain with asymmetric flow field-flow fractionation (AF4) and their association to proteins

Zielke, C., Teixeira, C., Ding, H., Cui, S., Nyman, M. & Nilsson, L.

Carbohydrate Polymers (2017) 157, 541–549.

Carbohydrate Polymers 157 (2017) 541–549

Contents lists available at ScienceDirect

Carbohydrate Polymers

journal homepage: www.elsevier.com/locate/carbpol

Analysis of β-glucan molar mass from barley malt and brewer's spent grain with asymmetric flow field-flow fractionation (AF4) and their association to proteins

Claudia Zielke[a,*,1], Cristina Teixeira[b,1], Huihuang Ding[c], Steve Cui[c], Margareta Nyman[b], Lars Nilsson[a]

[a] Department of Food Technology, Engineering and Nutrition, Lund University, P.O. Box 124, 22100 Lund, Sweden
[b] Food for Health Science Centre, Kemicentrum, Lund University, P.O. Box 124, 22100 Lund, Sweden
[c] Guelph Food Research Centre, Agriculture and Agri-Food Canada, Guelph, Ontario N1G 5C9, Canada

ARTICLE INFO

Article history:
Received 29 August 2016
Received in revised form 6 October 2016
Accepted 15 October 2016
Available online 18 October 2016

Keywords:
Asymmetric flow field-flow fractionation (AF4)
Multiangle light scattering (MALS)
Calcofluor
Colonic health
Protein-carbohydrate complexes

ABSTRACT

β-Glucan benefits are related with its molar mass and it would be of interest to better understand how this parameter can be changed by processing and variety for design of food with specific health effects. For this purpose, extracts from barley malts and brewers' spent grain, processed at different conditions, were analysed regarding β-glucan content, molar mass, and protein content. Molar mass distribution was assessed using asymmetric flow field-flow fractionation (AF4) with multiangle light scattering (MALS), differential refractive index (dRI) and fluorescence (FL) detection. β-Glucan was detected in a wide molar mass range, <2000 to approximately 6.7×10^6 g/mol. Differences in molar masses were more noticeable between barley varieties and steeping malting conditions than by mashing of malt. Barley products processed to preserve β-glucan contained more β-glucan of high molar mass with potential to shift the fermentation site to the distal colon. Enzymatic degradation of proteins indicated presence of aggregates containing β-glucan and protein.

1. Introduction

β-Glucan, present in mainly barley and oats, have been associated with a number of health benefits. One mechanism behind these effects is related with their ability to increase butyric acid formation in the colon (Hamer et al., 2008). If barley is malted the butyric acid formation is increased considerably and so is the abundance of butyric acid bacteria (Bränning & Nyman, 2011; Zhong, Nyman, & Fak, 2015). This increase is suggested to be related with a changed molar mass and increased solubility of β-glucan (Nilsson & Nyman, 2005). However, since not all malts have the same ability to increase butyric acid formation (Zhong & Nyman, 2014), malting conditions and barley varieties used are of great importance. Solubility and molar mass can be changed by malting, e.g. by increasing temperature and pH to reduce β-glucanase activity (Haraldsson et al., 2004; Rimsten et al., 2002), or by shortening germination time to decrease β-glucan degradation (Hübner, O'Neil, Cashman, & Arendt, 2010). Information on probable changes of β-glucan molar mass distribution in relation to variety and processing conditions would increase the understanding of how these factors can be used to modulate functional properties of barley products.

Potential proteinaceous components associated with β-glucan are another aspect when discussing health benefits. Several publications imply the presence of proteinaceous matter (Acker, Diemair, & Samhammer, 1955; Ghotra, Vasanthan, Wettasinghe, & Temelli, 2007), and amino acid residues in β-glucan (Vårum & Smidsrød, 1988). These proteinaceous components may support formation of viscous slurries and affect the behaviour of β-glucan from a functional and nutritional viewpoint. Proteases added to oat β-glucan slurries have shown to decrease viscosity, suggesting a close connection between protein content and β-glucan properties (Autio, Myllymäki, Suortti, Saastamoinen, & Poutanen, 1992; Zhang, Doehlert, & Moore, 1997; Zhou, Robards, Glennie-Holmes, & Helliwell, 2000). Therefore, a better understanding of β-glucan properties in solution or dispersion is desirable, including the low

Abbreviations: AF4, asymmetric flow field-flow fractionation; a.u., arbitrary units; AX, arabinoxylan; BSG, brewer's spent grain; dRI, differential refractive index; dn/dc, refractive index increment; FL, fluorescence; HPSEC, high performance size exclusion chromatography; MALS, multiangle light scattering.

* Corresponding author.
E-mail address: Claudia.zielke@food.lth.se (C. Zielke).
[1] Equally responsible first authors.

http://dx.doi.org/10.1016/j.carbpol.2016.10.045
0144-8617/

molar mass range, and the presence and properties of proteinaceous components.

Cereal β-glucan is naturally polydisperse in size and molar mass, therefore it is required a separation method for accurate determination of molar mass over the whole size population. Size exclusion chromatography (SEC) is a commonly used separation method for polymers, which can be coupled with various detection methods. Molar mass is typically obtained either by calibration against standards or direct determination by multiangle light scattering (MALS). However, its upper limit of separation (exclusion limit) can limit the use for high molar mass species as well as aggregated species. Further drawbacks of separation with SEC are related to degradation of species of large size due to shear forces (Cave, Seabrook, Gidley, & Gilbert, 2009), causing an underestimation of the detected molar mass (Barth, Boyes, & Jackson, 1998), and the co-elution phenomena in the presence of branched analytes, for instance β-glucan aggregates (Håkansson, Ulmius, & Nilsson, 2012).

Another method for separation and characterization of relatively low molar mass polysaccharides is anionic exchange chromatography with pulsed amperometric detection (HPAEC-PAD). The resolution of HPAEC reaches a degree of polymerization (DP) up to 80, thus it can only be used for a rather narrow and low molar mass range (Hanashiro, Abe, & Hizukuri, 1996). Furthermore, the resulting chromatograms do not directly reflect the chain length distribution as PAD response changes with DP (lower detector response for higher DP), which can introduce experimental inaccuracies (Koizumi, Fukuda, & Hizukuri, 1991; Wong & Jane, 1997).

Asymmetric flow field-flow fractionation (AF4) is now well established for separation of molecules over a wide size range (approx. 2 nm to μm). AF4 is a gentle method as it utilises a flow-based separation without an additional stationary phase (Wahlund & Giddings, 1987), avoiding some of the drawbacks of SEC. The sample is injected onto a trapezoidal channel where separation occurs due to different diffusion coefficients of different sized molecules in the sample. The principles of AF4 separation can be found elsewhere (Wahlund & Nilsson, 2012). AF4 has previously been used for fractionation of cereal β-glucan but the focus has been mainly on the high molar mass (Ulmius, Adapa, Önning, & Nilsson, 2012; Ulmius, Önning, & Nilsson, 2012) and aggregates (Håkansson, Ulmius et al., 2012). In order to fractionate relatively small analytes in AF4, the membrane for accumulation wall requires a suitable molecular weight cut-off (MWCO) to avoid loss of analytes, and a relatively high volumetric cross-flow. A low MWCO and high cross-flow poses different challenges: due to the relatively limited membrane permeability, a higher pressure in the separation channel is required, which can cause leaks, membrane damage or cracking of the channel (Qureshi & Kok, 2010). Furthermore, the pressure drop over the membrane also increases which may give rise to difficulties in regulating the volumetric cross-flow.

As samples extracted from natural materials often contain mixtures of biomolecules it can be necessary to specifically identify β-glucan which can be achieved through specific labelling with Calcofluor, utilized in-line with SEC (Rimsten, Stenberg, Andersson, Andersson, & Åman, 2003) and AF4 (Ulmius, Adapa et al., 2012; Ulmius, Önning et al., 2012). Calcofluor forms a non-covalently linked complex with β-glucan of which the mechanism is not well understood. However, the formation of complexes between Calcofluor and β-glucan molecules below 10^4 g/mol is not quantitative as for those of high molar mass, resulting in a lower detector response (Kim & Inglett, 2006).

The aim of this study is to evaluate the possibility of separating and analysing barley β-glucan in a wide size range (including low molar mass analytes) with the aid of AF4, and based on these results to infer on the impact of processing and barley variety, which could be useful for design of food with specific health effects. For this purpose, extracts prepared from barley malts and brewers' spent grain were separated and characterized using AF4 in combination with the in-line detectors MALS and differential refractive index (dRI) for the determination of molar mass distributions. Furthermore, semi-quantitative detection of β-glucan (in-line labelled with Calcofluor) and protein was obtained from fluorescence (FL) and UV detectors.

2. Materials and methods

2.1. Materials

Two malts were produced at pilot scale by Viking Malt AB (Halmstad, Sweden) from different barley varieties, Tipple (TM) and Cinnamon (CM), at the same malting conditions (35 °C and 0.4% (v/v) lactic acid during steeping) to maintain β-glucan content (2.9 and 3.9 g/100 g, respectively). Pilsner malt and its by-product (further referred to as standard malt (SM) and standard brewers' spent grain (SBSG), respectively) derived from the same barley variety mixture composed of Tipple, Rosalina and Quench, were produced at pilot scale by Viking Malt AB: SM was prepared at typical malting conditions for pilsner malt (steeping 14.5 °C without lactic acid), and SBSG was a by-product of SM after mashing and drying at 48–55 °C for a total of 20 h, resulting in two products low in β-glucan content (both 0.5 g/100 g). K1500 and K3504 were prepared at two different malting conditions with barley variety Karmosé, at a laboratory scale at Lantmännen SW Seed AB (Svalöv, Sweden): 1500 and 3504 stand for temperature conditions (15 or 35 °C, respectively) and lactic acid concentrations (0.0 or 0.4% (v/v), respectively) in the steeping water, resulting in malts with different β-glucan content (3.6 and 4.7 g/100 g, respectively).

2.2. Chemicals

For AF4 analyses, NaN_3 (BDH, Poole, UK) and $NaNO_3$ (Merck, Darmstadt, Germany) were used in the carrier liquid. Fluorescence labelling was performed using Calcofluor fluorescent brightener 28 (Sigma Aldrich, Darmstadt, Germany) and tris(hydroxymethyl)-aminomethane (ICN Biomedicals Inc., Irvine, CA, USA).

For protein hydrolysis, protease (Pronase E – from *Streptomyces griseus*, type XIV), leucine aminopeptidase (from porcine kidney, type VI-S), and prolidase (from porcine kidney, lyophilised powder) were purchased from Sigma Aldrich (Darmstadt, Germany).

For all experiments, pure water from a Milli-Q system (Millipore Corp., Billerica, MA, USA) was used.

2.3. Sample extraction

Barley products were milled (A11 basic analytical mill, IKA, Staufen, Germany) until homogeneous powder was obtained. Flours were incubated in a boiling water-bath for 90 min, with 100 μL of a thermostable α-amylase (Termamyl, 300L Type DX, 300 KNU-T/g, Univar, Sweden) in 20 mL of 0.3 mg/mL $CaCl_2$ (Rimsten et al., 2003). Before freeze-drying, the samples were centrifuged (1500*g*, 15 min) and the supernatant was dialysed for 24 h against Milli-Q water (with water change after 2, 4 and 8 h), using a membrane with MWCO of 3.5–5 kDa (Spectra/Por Biotech CE, Spectrum Labs, Houston, TX, USA) that according to the provider would ensure removal of glucose units, some maltose but not molecules larger than maltose. The extraction yield was calculated as the weight of the freeze-dried sample after extraction divided by the weight of the flour before extraction.

2.4. Characterization of the extracts

β-Glucan content was determined with an enzymatic mixed-linkage β-glucan assay kit (K-BGLU, Megazyme International, Bray, Ireland). Arabinoxylan (AX) was quantified using a gas-chromatographic method for analysis of neutral sugars (Theander, Åman, Westerlund, Andersson, & Pettersson, 1995). Protein content was determined using an amino acid analyser after acid hydrolysis (Biochrom 30, Biochrom Limited, Cambridge, UK). Total starch was measured with an enzymatic assay using α-amylase and amyloglucosidase after solubilisation in KOH (Björck & Siljeström, 1992; Holm, Björck, Drews, & Asp, 1986).

2.5. Size exclusion chromatography

A Shimadzu HPLC System was used (LC-10ATVP Pump, SCL-10A System controller, and SIL-10ADVP Auto Sampler) with a UV detector (Viscotek 2600) and a refractive index detector. The column systems are two AquaGel PAA-M columns and a PolyAnalytik PAA-203 column (Polyanalytik Canada, London, Canada) combined in series. Detectors were calibrated by pullulans (JM Science Inc., New York, US), malto-oligosaccharides, and glucose (Sigma-Aldrich, Canada) with molar masses of 0.18 to ~708 g/mol. TriSEC software (Viscotek, USA) was used for extracting and analysing data. The molar mass distribution was calculated by conventional calibration method, of which the peak molar mass value (P) is determined through the retention volume of a refractive index and an UV detector by using the calibration curve (log molar mass vs. retention volume) from standards. The sample solutions were de-dusted by passing through a 0.45-um filter, and the injection volume was 100 μL. The eluent was 0.1 M $NaNO_3$ with 0.05% (w/w) NaN_3 at a flow rate of 0.6 mL/min, and the columns and detectors were maintained at 40 °C. Total volume and void volume of the columns were 34.9 mL and 14.2 mL, respectively. Data were analysed by OmniSEC 4.6.1 software (Ding et al., 2014).

2.6. AF4 analysis equipment and separation parameters

An AF4 system (Eclipse 3+, Wyatt Technology, Dernbach, Germany) was connected to a MALS, UV and dRI detectors. The UV-1000 spectrophotometer from Jasco (Jasco Corporation, Tokyo, Japan) operated at a wavelength of 280 nm, and Dawn Heleos II MALS detector and Optilab T-rEX dRI detector (both from Wyatt Technology) at a wavelength of 658 nm. An isocratic pump delivered the carrier flow to the system, whereas samples were injected via an autosampler (both Agilent 1100 series, Agilent Technologies, Waldbronn, Germany). The carrier liquid was composed of 10 mM $NaNO_3$ and 0.02% (w/v) NaN_3 in Milli-Q water and a 100 nm pore-size polyvinylidene fluoride membrane from Millipore Corp. was positioned between the pump and the Eclipse to ensure particle free carrier liquid. The AF4 channel was a long channel from Wyatt Technology (tip-to-tip length: 27.5 cm) with a 350 μm spacer (actual thickness determined to be 308 μm by calibration with ferritin (Håkansson, Magnusson, Bergenståhl, & Nilsson, 2012)). The ultra-filtration membrane forming the accumulation wall was a hydrophilised polyethersulphone (PES) with a MWCO of 5 kDa (Microdyn-Nadir GmbH, Wiesbaden, Germany).

Samples were prepared at 4 mg/mL of extract in AF4 carrier liquid under stirring in a water bath at 100 °C for 30 min, cooled to room temperature and filtered through a 0.2 μm pore size cellulose acetate membrane (VWR International, Radnor, PA, USA) prior to injection onto the channel. A sample volume of 160 μL was injected (resulting in an injected mass of 640 μg) at a flow rate of 0.2 mL/min for 4 min. The following focusing step was performed for 5 min at a flow rate of 1 mL/min before eluting the sample, which resulted in 10 min delay before the start of elution. The void time (t^0) was calculated to be 0.6 min (Håkansson, Magnusson et al., 2012). The applied cross-flow rate during elution had an initial value of 3 mL/min followed by an exponential decay with a half-life of 4.5 min according to Eq. (1),

$$Q_c(t) = Q_c(0) * e^{-\frac{ln2}{4.5}t} \quad (1)$$

where Q_c (t) is the cross-flow depending on time t and Q_c (0) the initial cross-flow rate. The detector flow rate was constant at 0.5 mL/min during all measurements. To ensure a clean channel prior to the next injection, the AF4 channel was flushed without any cross-flow for 16 min.

Total sample recoveries were obtained by determining the mass recovery of the analysed samples (filtered prior to injection and subsequent fractionation in the AF4 channel) using Astra Software versus an injection of the non-filtered sample onto the AF4-channel without focusing step and cross-flow. This ratio pictures sample losses during the whole analysis procedure.

2.7. Fluorescence detection of β-glucan

Extracts were labelled post-channel and in-line with Calcofluor prior to detection with MALS-FL as described previously (Ulmius, Önning et al., 2012), connected to a fluorescence detector (Jasco FP-1520) with excitation at λ_{ex} = 415 nm and emission at λ_{em} = 445 nm.

2.8. Total protein hydrolysis

Protein in the extracts was hydrolysed enzymatically based on the method described by Baxter, Phillips, Dowlati, and Johns (2004) to remove interference with the signals and to ensure that no co-elution with β-glucan occurred. Three proteolytic enzymes, protease (75 μL, 9.2 U/mL), leucine aminopeptidase (30 μL, 24 U/mL) and prolidase (15 μL, 180U/mL) were added to 15 mg of the extracts previously dissolved in 1.5 mL of sodium phosphate buffer (pH 7.5, 0.1 M). The mixture was separated in two aliquots and incubated for 20 h at 37 °C. Each enzyme was separately tested for β-glucanase activity using a kit for assay of *endo*-β-glucanases using beta-glucazyme tablets (T-BGZ, Megazyme International, Bray, Ireland), in which β-glucanase activity is directly related with the release of fragments of dyed Azurine-crosslinked barley β-glucan.

2.9. Data processing

Sample comparison was divided into three groups: (1) TM and CM i.e. malts from the two varieties processed with the same malting conditions, (2) SM and SBSG, where SBSG is a by-product of SM mashing, (3) K1500 and K3504, steeped at different conditions with the same barley variety.

Data obtained from UV, MALS, dRI and FL detectors after separation with AF4 channel were processed with Astra software (version 5.3.4.14, Wyatt Technology). Molar masses were determined as described by Berry (1966) and Andersson, Wittgren, and Wahlund (2003), using the data obtained from the scattering detectors 8–15 (scattering angles: 60.0°–132.2°) to make a 1st order fit. As d*n*/d*c* (refractive index increment) a value of 0.146 mL/g was used for the whole size distribution as defined in the literature for β-glucan in aqueous solutions (Li, Cui, Wang, & Yada, 2011). The second virial coefficient (A_2) was neglected.

3. Results and discussion

3.1. Composition of the extracts

All extracts contained high amounts of starch oligosaccharides (65–72 g/100 g), followed by protein (7–16 g/100 g), β-glucan

Table 1
Composition of barley products extracts (g/100 g, dry weight basis) and extraction yield (%, w/w).

Sample name	Extracts				
	Starch oligosaccharides[a]	β-Glucan[b]	AX[b]	Protein[a]	Extraction yield [%][a]
Tipple malt	72 ± 1	4.4	1	11 ± 1	38 ± 2
Cinnamon malt	72 ± 2	6.8	1	9 ± 1	54 ± 7
Standard malt	71 ± 1	0.7	2	7 ± 0.5	30 ± 2
Standard BSG	65 ± 1	1.4	3	16 ± 2	13 ± 1
Karmosé 1500	69 ± 2	4.4	2	10 ± 1	32 ± 2
Karmosé 3504	72 ± 2	6.5	2	10 ± 1	36 ± 1

[a] Values are mean ± SEM.
[b] SEM < 0.1.

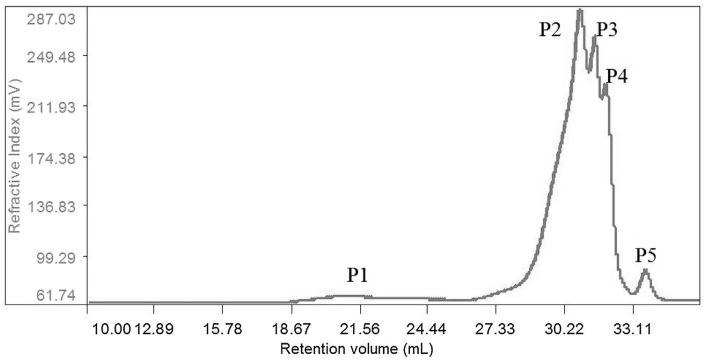

Fig. 1. HPSEC of Tipple malt with dRI detection. P1-2.1 × 10^6 g/mol, P2-6.0 × 10^3 g/mol, P3-0.5 × 10^3 g/mol, P4-0.4 × 10^3 g/mol.

(0.7–6.8 g/100 g) and AX (1–3 g/100 g) (Table 1). The yield of sample extraction was similar for K1500 and K3500 (32–36% (w/w)), indicating a minor effect of malt steeping conditions on the extractability of the compounds, including β-glucan. CM extractability was higher than TM (54 vs. 38% (w/w)), indicating a role of barley variety and its original characteristics, possibly due to different β-glucan content but also an effect from different structures and linkages with other components, such as protein and AX. Generally, high extractability corresponded to higher β-glucan content in the extract, except for SBSG, which had higher β-glucan content in the extract with a lower sample extractability compared to SM.

The high content of oligosaccharides is due to starch hydrolysis and can be explained by the action of α-amylase, i.e. hydrolysis of α-(1–4) but not of α-(1–6) bonds, resulting in the formation of oligosaccharides and dextrins larger than one glucose unit, which could not be completely removed through dialysis (Sundarram & Murthy, 2014).

With HPSEC analysis (Fig. 1, Tipple malt as representative example) it was possible to verify that a large part of the extracts molar mass was lower than malto-tetraose (666 g/mol), corresponding to the large amount of oligosaccharides remaining in the extracts after dialysis. These starch oligosaccharides do not interfere with AF4 analysis, since they would be flushed out through the membrane at the accumulation wall (MWCO 5 kDa) in the AF4 channel.

P2 (6.0 × 10^3 g/mol) in Fig. 1 most likely corresponds to low molar mass β-glucan, although it might be argued that P2 could be starch remnants or degraded β-glucan during sample extraction. However, α-amylase degrades starch to dextrins with DP < 10 (Lieberman, Marks, & Peet, 2013), thus it is unlikely that P2 is dextrins since its molar mass (6.0 × 10^3 g/mol) would correspond to DP ≈ 30. Furthermore, to not lose β-glucan of low molar mass, the step for inactivation of endogenous enzymes with 50% (v/v) ethanol described in the original extraction procedure was not performed (Rimsten et al., 2003). Therefore, some degradation of β-glucan might have occurred during extraction process, which could be about as high as 20% after 48 h of extraction (Rimsten et al., 2003). However, since the extraction time in the present study was much shorter (90 min) the degradation is probably negligible, and detected β-glucan of low molecular weight are likely to be characteristic of the samples, and not a product of degradation during sample extraction.

3.2. Characterization of extracts with AF4

AF4 fractograms of the extracts are shown in Fig. 2A–F. The FL signal after in-line Calcofluor-labelling illustrates where β-glucan is present in the fractograms. Average, minimum and maximum molar mass of β-glucan size distributions are summarised in Table 2. Fig. 3 shows TM, being representative of all samples, in-line Calcofluor-labelled compared to FL signal of non-labelled TM. Cumulative molar mass distributions of β-glucan are displayed in Fig. 4.

The total mass recovery was calculated as the percentage of determined masses (integration of dRI signal) between a filtered sample separated in the AF4 channel with cross-flow in relation to a non-filtered sample in elution mode (i.e. no relaxation step and cross-flow). The total mass recoveries from the AF4 channel are relatively low (30–41%) (Table 2). As all fractionated samples were filtered through a 22 mm syringe filter with a 0.2 μm pore size cellulose acetate membrane prior injection, sample concentration might decrease, but not necessarily β-glucan concentration. Previous results have shown that filtering samples prior injection onto the AF4 channel has no impact on β-glucan in a size

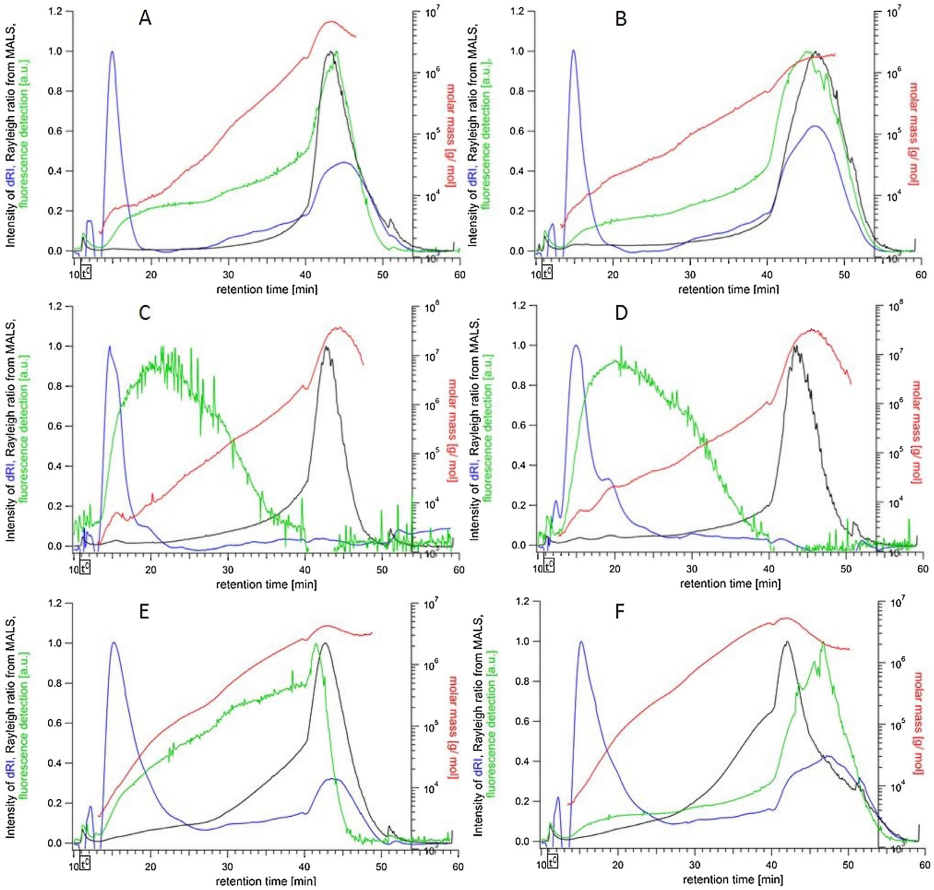

Fig. 2. AF4 fractogram of barley products extracts. (A) TM, (B) CM, (C) SM, (D) SBSG, (E) K1500, (F) K3504. Rayleigh ratio from MALS (black), dRI signal (blue), FL signal of in-line Calcofluor-labelled β-glucan (green) and molar mass (red). (For interpretation of the references to colour in this figure legend, the reader is referred to the web version of this article.)

Table 2
Summary of barley product extracts characterization with AF4, including total mass recovery from AF4 channel (%), and average molar mass (g/mol), minimum and maximum molar mass (g/mol) of β-glucan size distributions.

	Total Mass Recovery (%)[a]	Average molar mass (M_w)[b]	Min. – Max. molar mass[b]
Tipple malt	41	5.6×10^5	$2500 - 6.7 \times 10^6$
Cinnamon malt	34	3.3×10^5	$3000 - 1.9 \times 10^6$
Standard malt	34	5.1×10^4	$1700 - 2.0 \times 10^6$
Standard BSG	30	3.8×10^4	$2000 - 1.0 \times 10^6$
Karmosé 1500	35	3.4×10^5	$3500 - 4.3 \times 10^6$
Karmosé 3504	41	6.6×10^5	$4900 - 5.2 \times 10^6$

[a] Recovery of total injected mass after filtration and from AF4 channel.
[b] Weight average molar mass (M_w) calculated in the range of detected β-glucan from FL signal.

range below the pore size of the filters but improves signal-to-noise ratio (Zielke et al., submitted manuscript). Other reasons for low recoveries are loss of small molar mass species through membrane during separation in the channel, most likely from starch originating oligosaccharides, which are present in large amounts (Table 1 and Fig. 1).

FL signals (Fig. 2) show a wide range of β-glucan molar mass, from $<2 \times 10^3$ to $>10^6$ g/mol for all samples (Table 2).

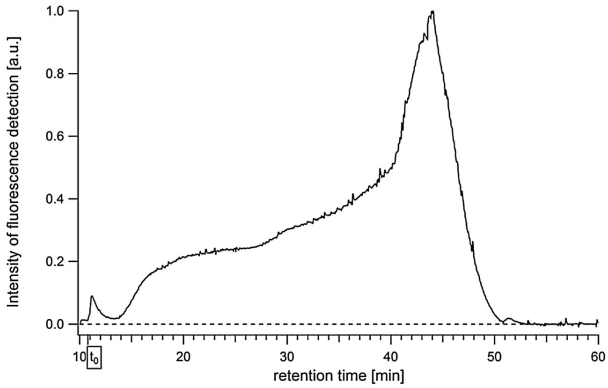

Fig. 3. AF4-FL fractogram of TM extract with in-line Calcofluor-labelling (solid line) β-glucan and of non-labelled TM extract (dashed line). FL signals at λ_{em} = 445 nm.

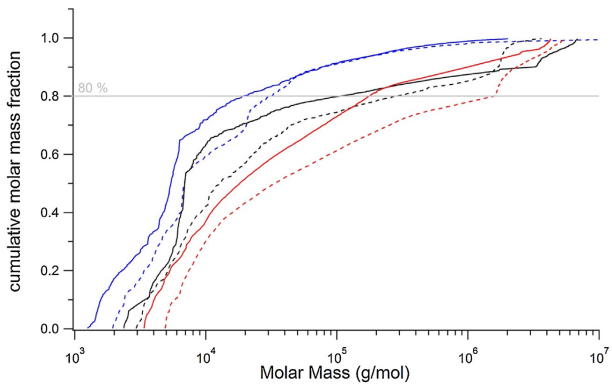

Fig. 4. Cumulative molar mass distributions of β-glucan in the extracts. TM (black solid), CM (black dashed), SM (blue solid), SBSG (blue dashed), K1500 (red solid), K3504 (red dashed). (For interpretation of the references to colour in this figure legend, the reader is referred to the web version of this article.)

Fig. 3 confirms that the FL signal originated from labelled β-glucan and that no intrinsic fluorescence influenced the results. A significant dRI signal at ~15 min suggests high concentration of low molar mass species which could be β-glucan, but also low degraded starch residues of high molar mass (P2, Fig. 1) or proteins that might co-elute. For retention times below 15 min there are still FL signals for all samples but of relatively low intensity (Fig. 2). This is probably influenced by a weaker complexation of Calcofluor with β-glucan below 10^4 g/mol (Jørgensen & Aastrup, 1988). Therefore, it is likely that β-glucan content in the low molar mass range is underestimated from the data obtained.

From the UV signal it was possible to estimate the amount of protein eluting in this retention range (10.6–20 min, examples in Fig. 5A and B) by integrating the UV signal and comparing it to the integrated dRI signal (Fig. 2). As the protein composition in the samples is not known, calculations were done using both a low (4 mL/(mg cm)) and a high (24 mL/(mg cm)) UV extinction coefficient (ε) for proteins as suggested by Fasman (1992). With the low ε, a maximum value of 6.0% for SBSG and 4.7% for SM of the total mass eluting in the retention time range of concern (10.6–20 min) would correspond to protein. All other samples had protein contents around or below 3% (TM: 2.8%; CM: 2.5%; K1500: 3.3%; K3504: 2.4%) in the same retention time range, which corresponded with the protein contents analysed between extracts (Table 1). Higher ε resulted in lower values of protein amount present compared to the total injected mass. This indicates that the impact of protein on dRI signal at short retention times (<20 min) is marginal.

Another concern when discussing the reliability of data is the use of the same value of dn/dc over the whole fractogram, which can cause errors since not only β-glucan are eluting. However, molar masses calculated from MALS and dRI are dependent on the dn/dc in a 1st order relationship, i.e. a 1% error in dn/dc will result in a 1% error in the determined molar mass (Podzimek, 2014). It is also clear from the above estimation of protein content that dn/dc-related errors caused by the presence of protein would be relatively small, thus, possible errors in the molar mass are relatively small.

Since the channel membrane MWCO was 5 kDa, analytes with lower molar mass would be expected to be undetectable. However, despite that MWCO is characterised by a molecular weight, the size of retained species is determined by a hydrodynamic size related to the dimensions of the pores of the membrane. Therefore, molecules with sufficiently large hydrodynamic size would still be

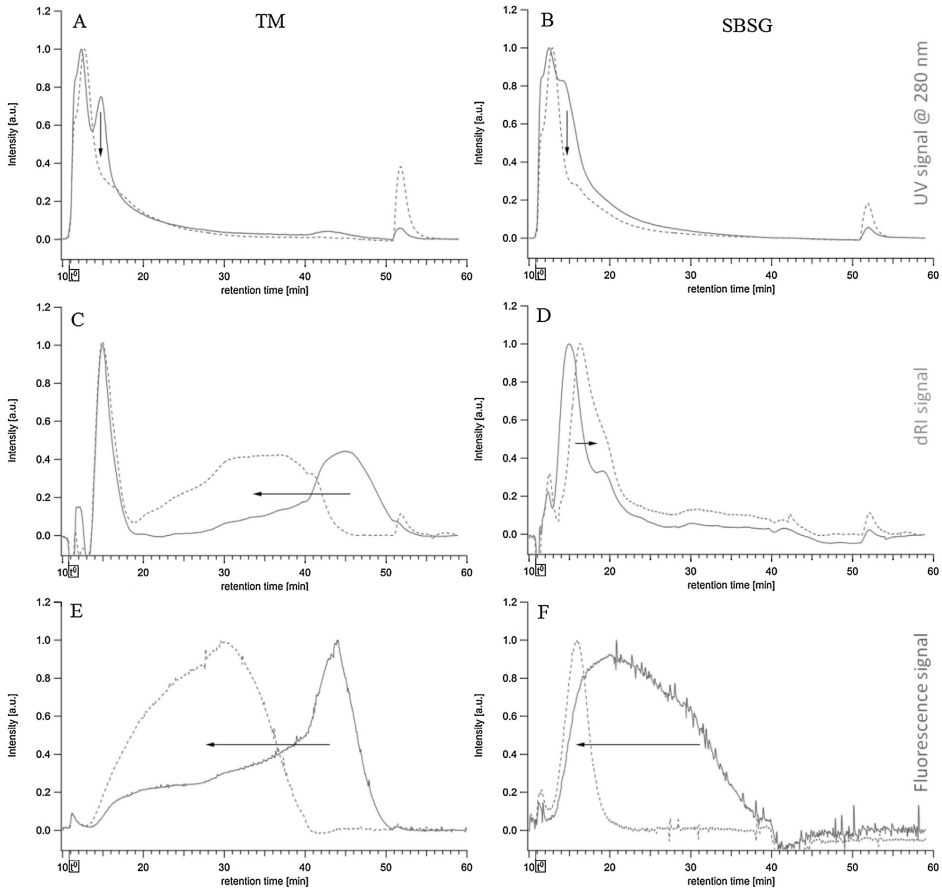

Fig. 5. AF4 fractograms of extracts from TM (left column) and SBSG (right column). Solid and dashed lines show results before and after enzymatic digestion respectively. UV signal (A and B), dRI signal (C and D), and FL signal of in-line Calcofluor-labelled extracts (E and F).

retained as they cannot penetrate through the porous membrane, making it difficult to determine the actual lower limit retention of the membrane.

The abrupt increase for all signals after 40 min (Fig. 2) was not sample-specific, but due to the cross-flow profile since at this retention time the exponentially decaying cross-flow changed to constant cross-flow at 0.1 mL/min. A release peak is also visible at 50.5 min when the cross-flow was turned off completely, and all material remaining in the channel was flushed out.

3.3. Effect of processing and variety on β-glucan barley products

Differences in β-glucan average molar mass range and average were more noticeable between different varieties (TM and CM) and steeping conditions (K1500 and K3504) than as an effect of mashing (SM and SBSG) (Fig. 2 and Table 2). β-Glucan minimum molar mass was lower in SM and SBSG (≤2000 g/mol) than the other samples (2500–4900 g/mol), and 80% of β-glucan was of lower molar mass range (2 and 3×10^4 g/mol) than the other samples (>1×10^5 g/mol) (Fig. 4). Low molar mass was expected, since one of the focuses when producing malts for beer such as SM is to degrade β-glucan to reduce wort viscosity that could otherwise cause problems during filtration in brewing processes (Izydorczyk, Biliaderis, & Lazaridou, 2006). SBSG average molar mass was lower than SM (3.8×10^4 vs 5.1×10^4 g/mol), most likely due to further β-glucan degradation during mashing.

β-Glucan average molar mass was higher in TM than in CM (5.6×10^5 vs 3.3×10^5 g/mol), and so was the maximum molar mass (6.7×10^6 g/mol vs 1.9×10^6 g/mol) (Fig. 2 and Table 2). However, 80% of β-glucan in TM was of molar mass lower that in CM (1×10^5 vs 3×10^5 g/mol), which indicates that CM has more β-glucan in the high molar mass range than TM (Fig. 4). This shows that despite the same malting conditions, barley variety can result in different β-glucan size profiles.

K1500 had lower β-glucan average molar mass than K3504 (3.4×10^5 vs 6.6×10^5 g/mol) (Table 2), and the detected β-glucan

was more prominent in the smaller size range for K1500 (80% below 2×10^5 g/mol) than for K3504 (80% below 2×10^6 g/mol) (Fig. 4). This indicates that β-glucan in K3504 was less degraded than in K1500, most probably due to high temperature and low pH (high lactic acid concentration) in the steeping water that inhibited β-glucanase activity, which was also shown in previous studies (Haraldsson et al., 2004).

Although soluble β-glucan are known to be highly fermented in the colon, the molar mass is of great importance for the place of fermentation. (Eswaran, Muir, & Chey, 2013). It may be speculated that β-glucan in TM, CM, K1500 and K3504 with a higher molar mass would be more slowly fermented and reach the distal colon to a greater extent than soluble β-glucan in SM and SBSG with a lower molar mass. In this respect, CM would be of special interest due to its higher content of high molar mass β-glucan. It has been shown that the place of fermentation can be shifted to the distal part of the colon by combining rapidly and slowly fermentable substrates (Henningsson, Björck, & Nyman, 2002). A mixture of β-glucan of low and high molar mass might thus be interesting since most colonic diseases occur in the distal part of colon.

3.4. Proteolytic enzyme treatment of extracts

UV-active analytes were detected at short retention times (Fig. 5A and B, solid lines), suggesting co-elution of proteins with low molar mass β-glucan. In an attempt to eliminate proteins, the extracts were enzymatically treated and re-analysed (Fig. 5: solid line (before) vs. dashed line (after enzymatic treatment)). The enzymes used for total protein digestion were tested for β-glucanase activity and no activity was recorded. TM was chosen as representative example for the results of all samples, except for SBSG that shows a different behaviour in dRI signal.

For both samples, the UV peak at 15 min retention time decreases after enzymatic treatment (Fig. 5A and B), indicating presence of proteins in this peak. However, the peak was not completely eliminated suggesting remaining proteins in the sample, which may be due to remnants of enzyme, insufficient treatment time or enzyme concentration.

For TM, dRI signal (concentration) shifted from long (~40–50 min) to shorter (~30–40 min) retention times after enzymatic digestion (Fig. 5C), suggesting a decrease of species with large hydrodynamic size to smaller hydrodynamic sizes. The FL signal (Fig. 5E) shows the same tendency, indicating that the population of β-glucan moved to shorter retention times after enzymatic treatment.

The interpretation of the dRI signal of SBSG (Fig. 5D) is not straightforward; dRI signal shift around 15 min to slightly higher retention times was visible suggesting the formation of species with a larger hydrodynamic radius. In contrast, the FL signal of SBSG (Fig. 5F) shifted to shorter retention times i.e. smaller hydrodynamic size, similar to TM.

Enzymatic treatment of extracts showed an impact on the concentration profile over the retention time and on the hydrodynamic size of β-glucan. Furthermore, the decrease in β-glucan hydrodynamic size after protein degradation suggests a close association between protein and β-glucan, such as linkages in barley cell-walls as previously suggested (Autio et al., 1992; Forrest & Wainwright, 1977; Wood, 2011; Zhang et al., 1997; Zhou et al., 2000). Furthermore, due to the presence of proteolytic enzymes in the gastro-intestinal tract, the presence of mixed aggregates could have implications for the size and molar mass of β-glucan reaching the colon, and therefore its fermentation site.

4. Conclusion

Different barley extracts were analysed in regard to their composition, β-glucan content and molar mass distributions. β-Glucan in a molar mass range from below 2000 g/mol to approximately 6.7×10^6 g/mol could be detected by AF4-FL-MALS-dRI. Steeping condition and variety had the highest impact on β-glucan molar mass distribution, compared with the product after mashing (SM vs. SBSG). Malts steeped at conditions intended to minimize β-glucan degradation (TM, CM and K3504), but also malt steeped at β-glucan degrading conditions (K1500) showed a wide distribution of β-glucan molar mass, especially those of high molar mass. Contrary, β-glucan of a lower and more narrowly distributed molar mass was found in the standard processed materials (SM and SBSG). The reduction of β-glucan molar mass after protein digestion suggests an association between these components, which due to proteases present in the gastrointestinal tract could influence β-glucan's molar mass and consequently its functionality in the colon.

Funding

This work was supported by TvärLivs [Formas no 222-2011-271 and Lantmännen Research Foundation]; and the Swedish research council (VR).

Acknowledgments

The authors thank Lantmännen SW Seed AB, Svalöv for allowing the use of the laboratory scale malting equipment, and Viking Malt AB for providing the barley products.

References

Acker, L., Diemair, W., & Samhammer, E. (1955). *The lichenin of oats. 1. Properties, preparation and composition of the muciparous polysaccharides*. Zeitschrift für Lebensmittel-Untersuchung und-Forschung.
Andersson, M., Wittgren, B., & Wahlund, K. G. (2003). Accuracy in multiangle light scattering measurements for molar mass and radius estimations. Model calculations and experiments. *Analytical Chemistry*, *75*(16), 4279–4291.
Autio, K., Myllymäki, O., Suortti, T., Saastamoinen, M., & Poutanen, K. (1992). Physical properties of (1 → 3), (1 → 4)-β-D-glucan preparates isolated from finnish oat varieties. *Food Hydrocolloids*, *5*(6), 513–522.
Barth, H. G., Boyes, B. E., & Jackson, C. (1998). Size exclusion chromatography and related separation techniques. *Analytical Chemistry*, *70*(12), 251–278.
Baxter, J. H., Phillips, R. R., Dowlati, L., & Johns, P. W. (2004). Glutamine in commercial liquid nutritional products. *Journal of Agricultural and Food Chemistry*, *52*(16), 4963–4968.
Berry, G. C. (1966). Thermodynamic and conformational properties of polystyrene. I. Light-scattering studies on dilute solutions of linear polystyrenes. *The Journal of Chemical Physics*, *44*(12), 4550–4564.
Björck, I. M. E., & Siljeström, M. A. (1992). In-vivo and in-vitro digestibility of starch in autoclaved pea and potato products. *Journal of the Science of Food and Agriculture*, *58*(4), 541–553.
Bränning, C. E., & Nyman, M. E. (2011). Malt in combination with lactobacillus rhamnosus increases concentrations of butyric acid in the distal colon and serum in rats compared with other barley products but decreases viable counts of cecal bifidobacteria. *The Journal of Nutrition*, *141*(1), 101–107.
Cave, R. A., Seabrook, S. A., Gidley, M. J., & Gilbert, R. G. (2009). Characterization of starch by size-exclusion chromatography: The limitations imposed by shear scission. *Biomacromolecules*, *10*(8), 2245–2253.
Ding, H. H., Cui, S. W., Goff, H. D., Wang, Q., Chen, J., & Han, N. F. (2014). Soluble polysaccharides from flaxseed kernel as a new source of dietary fibres: Extraction and physicochemical characterization. *Food Research International*, *56*, 166–173.
Eswaran, S., Muir, J., & Chey, W. D. (2013). Fiber and functional gastrointestinal disorders. *American Journal of Gastroenterology*, *108*(5), 718–727.
Fasman, D. G. (1992). *Practical handbook of biochemistry and molecular biology*. Boston: CRC Press.
Forrest, I. S., & Wainwright, T. (1977). The mode of binding of β-glucans and pentosans in barley endosperm cell walls. *Journal of the Institute of Brewing*, *83*(5), 279–286.
Ghotra, B. S., Vasanthan, T., Wettasinghe, M., & Temelli, F. (2007). 31P-nuclear magnetic resonance spectroscopic analysis of phosphorus in oat and barley β-glucans. *Food Hydrocolloids*, *21*(7), 1056–1061.

Håkansson, A., Magnusson, E., Bergenståhl, B., & Nilsson, L. (2012). Hydrodynamic radius determination with asymmetrical flow field-flow fractionation using decaying cross-flows. Part I. A theoretical approach. *Journal of Chromatography A*, *1253*, 120–126.

Håkansson, A., Ulmius, M., & Nilsson, L. (2012). Asymmetrical flow field-flow fractionation enables the characterization of molecular and supramolecular properties of cereal beta-glucan dispersions. *Carbohydrate Polymers*, *87*(1), 518–523.

Hübner, F., O'Neil, T., Cashman, K. D., & Arendt, E. K. (2010). The influence of germination conditions on beta-glucan, dietary fibre and phytate during the germination of oats and barley. *European Food Research and Technology*, *231*(1), 27–35.

Hamer, H. M., Jonkers, D., Venema, K., Vanhoutvin, S., Troost, F. J., & Brummer, R. J. (2008). Review article: The role of butyrate on colonic function. *Alimentary Pharmacology & Therapeutics*, *27*(2), 104–119.

Hanashiro, I., Abe, J.-I., & Hizukuri, S. (1996). A periodic distribution of the chain length of amylopectin as revealed by high-performance anion-exchange chromatography. *Carbohydrate Research*, *283*, 151–159.

Haraldsson, A. K., Rimsten, L., Alminger, M. L., Andersson, R., Andlid, T., Åman, P., et al. (2004). Phytate content is reduced and beta-glucanase activity suppressed in malted barley steeped with lactic acid at high temperature. *Journal of the Science of Food and Agriculture*, *84*(7), 653–662.

Henningsson, A., Björck, I., & Nyman, M. (2002). Combinations of indigestible carbohydrates affect short-chain fatty acid formation in the hindgut of rats. *Journal of Nutrition*, *132*(10), 3098–3104.

Holm, J., Björck, I., Drews, A., & Asp, N. G. (1986). A rapid method for the analysis of starch. *Starch—Stärke*, *38*(7), 224–226.

Izydorczyk, M. S., Biliaderis, C. G., & Lazaridou, A. (2006). Cereal beta-glucans. In *Functional food carbohydrates*. pp. 1–72. CRC Press.

Jørgensen, K. G., & Aastrup, S. (1988). Quantification of high molecular weight $(1\rightarrow3)(1\rightarrow4)$-β-D-glucan using calcofluor complex formation and flow injection analysis. II. Determination of total β-glucan content of barley and malt. *Carlsberg Research Communications*, *53*(5), 287–296.

Kim, S., & Inglett, G. E. (2006). Molecular weight and ionic strength dependence of fluorescence intensity of the calcofluor/β-glucan complex in flow-injection analysis. *Journal of Food Composition and Analysis*, *19*(5), 466–472.

Koizumi, K., Fukuda, M., & Hizukuri, S. (1991). Estimation of the distributions of chain length of amylopectins by high-performance liquid chromatography with pulsed amperometric detection. *Journal of Chromatography A*, *585*(2), 233–238.

Li, W., Cui, S. W., Wang, Q., & Yada, R. Y. (2011). Studies of aggregation behaviours of cereal β-glucans in dilute aqueous solutions by light scattering: Part I. Structure effects. *Food Hydrocolloids*, *25*(2), 189–195.

Lieberman, M., Marks, A. D., & Peet, A. (2013). *Marks' basic medical biochemistry: A clinical approach*. Philadelphia: Lippincott Williams & Wilkins.

Nilsson, U., & Nyman, M. (2005). Short-chain fatty acid formation in the hindgut of rats fed oligosaccharides varying in monomeric composition, degree of polymerisation and solubility. *British Journal of Nutrition*, *94*(5), 705–713.

Podzimek, S. (2014). Truths and myths about the determination of molar mass distribution of synthetic and natural polymers by size exclusion chromatography. *Journal of Applied Polymer Science*, *131*(7), n/a-n/a.

Rimsten, L., Haraldsson, A.-K., Andersson, R., Alminger, M., Sandberg, A.-S., & Åman, P. (2002). Effects of malting on β-glucanase and phytase activity in barley grain. *Journal of the Science of Food and Agriculture*, *82*(8), 904–912.

Rimsten, L., Stenberg, T., Andersson, R., Andersson, A., & Åman, P. (2003). Determination of β-glucan molecular weight using SEC with calcofluor detection in cereal extracts. *Cereal Chemistry Journal*, *80*(4), 485–490.

Sundarram, A., & Murthy, T. P. K. (2014). Alpha-amylase production and applications: A review. *Journal of Applied & Environmental Microbiology*, *2*(4), 166–175.

Theander, O., Åman, P., Westerlund, E., Andersson, R., & Pettersson, D. (1995). Total dietary fiber determined as neutral sugar residues, uronic acid residues, and Klason lignin (the Uppsala method): collaborative study. *Journal of AOAC International*, *78*(4), 1030–1044.

Ulmius, M., Adapa, S., Önning, G., & Nilsson, L. (2012). Gastrointestinal conditions influence the solution behaviour of cereal β-glucans in vitro. *Food Chemistry*, *130*(3), 536–540.

Ulmius, M., Önning, G., & Nilsson, L. (2012). Solution behavior of barley beta-glucan as studied with asymmetrical flow field-flow fractionation. *Food Hydrocolloids*, *26*(1), 175–180.

Vårum, K. M., & Smidsrød, O. (1988). Partial chemical and physical characterisation of $(1\rightarrow3)$, $(1\rightarrow4)$-β-d-glucans from oat (Avena sativa L.) aleurone. *Carbohydrate Polymers*, *9*(2), 103–117.

Wahlund, K. G., & Giddings, J. C. (1987). Properties of an asymmetrical flow field-flow fractionation channel having one permeable wall. *Analytical Chemistry*, *59*(9), 1332–1339.

Wahlund, K.-G., & Nilsson, L. (2012). Flow FFF—Basics and key applications. In R. S. K. Williams, & D. K. Caldwell (Eds.), *Field-Flow fractionation in biopolymer analysis* (pp. 1–21). Vienna: Springer Vienna.

Wong, K. S., & Jane, J. (1997). Quantitative analysis of debranched amylopectin by HPAEC-PAD with a postcolumn enzyme reactor. *Journal of Liquid Chromatography & Related Technologies*, *20*(2), 297–310.

Wood, P. J. (2011). Oat β-glucan: Properties and function. In *OATS: Chemistry and technology*. pp. 219–254. AACC International, Inc.

Qureshi, R. N., & Kok, W. T. (2010). Optimization of Asymmetrical Flow Field-flow Fractionation (AF4). *Lc Gc Europe*, *23*(1).

Zhang, D., Doehlert, D. C., & Moore, W. R. (1997). Factors affecting viscosity of slurries of oat groat flours. *Cereal Chemistry Journal*, *74*(6), 722–726.

Zhong, Y. D., & Nyman, M. (2014). Prebiotic and synbiotic effects on rats fed malted barley with selected bacteria strains. *Food & Nutrition Research*, *58*.

Zhong, Y. D., Nyman, M., & Fak, F. (2015). Modulation of gut microbiota in rats fed high-fat diets by processing whole-grain barley to barley malt. *Molecular Nutrition & Food Research*, *59*(10), 2066–2076.

Zhou, M., Robards, K., Glennie-Holmes, M., & Helliwell, S. (2000). Effects of enzyme treatment and processing on pasting and thermal properties of oats. *Journal of the Science of Food and Agriculture*, *80*(10), 1486–1494.

The effect of in vitro gastrointestinal conditions on the structure and conformation of oat β-glucan

Korompokis, K., Nilsson, L. & Zielke, C.

Food Hydrocolloids (2017) https://doi.org/10.1016/j.foodhyd.2017.11.007

Paper VI

The effect of *in vitro* gastrointestinal conditions on the structure and conformation of oat β-glucan

Konstantinos Korompokis, Lars Nilsson and Claudia Zielke*

Food Hydrocolloids (2017) https://doi.org/10.1016/j.foodhyd.2017.11.007

Food Colloids Group, Department of Food Technology, Engineering and Nutrition, Faculty of Engineering , Lund University P.O. Box 124, 22100 Lund, Sweden

*Corresponding author: C Zielke, Department of Food Technology, Engineering and Nutrition, Faculty of Engineering, Lund University P.O. Box 124, 22100 Lund, Sweden E-mail: claudia.zielke@food.lth.se

Abstract

A plethora of studies have shown that the physicochemical properties of oat β-glucan determine its health benefits. However, the impact of the passage through the gastrointestinal tract on the conformational and structural characteristics is not fully understood. The present study aims to elucidate the structure and conformation of gently extracted oat β-glucan before and after *in vitro* gastric and gastrointestinal digestion utilizing asymmetric flow field-flow fractionation (AF4) and NMR spectroscopy. The structural features and the bile acid-binding capacity of oat β-glucan were probed with NMR. Oat β-glucan without digestion presented primary aggregates with fringed micelle structure, and other high molar mass supramolecular secondary aggregates were detected. Under gastric conditions, the molar mass was reduced and an increase in apparent density, suggesting more compact and disrupted aggregates, was observed. In the intestinal phase, the conformation was restored as prior digestion. No effect of the digestive enzymes on the conformation of oat β-glucan was shown, except from a modest effect of pepsin under gastric conditions. In contrast, the bile acids induced alterations to the apparent density of the oat β-glucan aggregates indicating a molecular interaction which was further confirmed with NMR by observing numerous changes in the resonance of bile acids' carbons in presence of oat β-glucan. In conclusion, the examination of oat β-glucan under *in vitro* gastrointestinal conditions with AF4 and NMR sheds light on the aggregation behavior and interaction mechanisms and enables a rich gain of knowledge for its physiological effects.

Keywords: Oat β-glucan; *in vitro* digestion; Aggregation; Bile acids; Asymmetric Flow Field-Flow Fractionation; NMR

Abbreviations: AF4, asymmetric flow field-flow fractionation; a.u., arbitrary units; dRI, differential refractive index; FL, fluorescence detection; MALS, multi-angle light scattering; M, molar mass; NMR, nuclear magnetic resonance; r_{rms}, root-mean-square radius; r_h, hydrodynamic radius; SGF, simulated gastric fluids, SIF simulated intestinal fluids

1. Introduction

Oat (Avena sativa L.) is a rich source of soluble dietary fiber and bioactive compounds with pronounced health benefits. Mixed-linkage (1→3),(1→4)-β-D-glucans (referred to as β-glucan) are major structural components of the starchy endosperm cell walls. β-Glucan is a linear homopolysaccharide which consists of cellulose segments of consecutive glucose units linked with β-(1→4) glycosidic bonds and interrupted by single β-(1→3) links. During the last decades it has attracted interest

for its health-promoting properties, including cholesterol-lowering capacity and regulation of blood glucose levels, as well as antiproliferative, appetite-suppressing, immunomodulatory and antihypertensive effects (Daou & Zhang, 2012; Lazaridou & Biliaderis, 2007; Rebello, O'Neil, & Greenway, 2016; Thies, Masson, Boffetta, & Kris-Etherton, 2014; Wang & Ellis, 2014).

It has hitherto been shown that the physicochemical and structural properties govern the β-glucan's nutritional functionality (Wood, 2004) and several possible mechanisms have been suggested. One of the most discussed mechanisms is that β-glucan in solution can form gels and, therefore, is able to increase the viscosity of the digesta, resulting in a reduction of the macronutrient absorption rate (Wang et al., 2014). The formation of aggregates is critical for the formulation of gels and is highly dependent on the molar mass (M), the ratio of tri- and tetramers, hydrodynamic radius (r_h) and chain conformation (Agbenorhevi, Kontogiorgos, Kirby, Morris, & Tosh, 2011; Håkansson, Ulmius, & Nilsson, 2012; Li, Cui, Wang, & Yada, 2011). Another mechanism suggests that the association of β-glucan with bile salts during digestion mediates their fecal excretion and, therefore, stimulates their production anew by the liver using blood cholesterol (Andersson, Ellegard, & Andersson, 2002; Kim & White, 2010; Lia et al., 1995). Several in vitro studies have shown a possible interaction of β-glucan with bile salts (Kim et al., 2010; Kim & White, 2011; Zacherl, Eisner, & Engel, 2011) and NMR has been proven as a powerful tool for the detection of binding mechanisms on a molecular level (Gunness, Flanagan, & Gidley, 2010; Mikkelsen et al., 2014). However, the exploration of direct β-glucan-bile salt interactions under simulated gastrointestinal conditions and the impact on the conformation of β-glucan has not been reported.

It is evident that the understanding of the solution behavior of β-glucan in the digestive tract is vital in order to get fundamental knowledge of its action and, later, produce food products containing β-glucan with optimum functionality. In vitro models have been employed towards this direction with inconclusive results. Ulmius, Adapa, Önning, and Nilsson (2012) recorded disrupted aggregates of β-glucan under simulated gastric conditions (pH 1.2), probably due to acidic degradation. In the intestinal phase, the aggregates were re-arranged in a form of denser conformation and considerably larger size. The degradation of oat β-glucan in gastric conditions was also reflected as a reduction of viscosity (Dikeman, Murphy, & Fahey, 2006). In contrast, no degradation was detected at stomach-mimicking conditions (pH 1) by Johansson et al. (2006). However, the abovementioned pH values are close to or even lower than the gastric pH at fasting state and are not recommended for a static in vitro digestion model, where a higher average value is preferred taken into consideration the buffering effect of a normal meal (Minekus et al., 2014). The complexity and lack of uniform information for the supramolecular properties of β-glucan during gastrointestinal digestion imposes the conduct of studies combining state-of-the-art analytical techniques.

Asymmetric flow field-flow fractionation (AF4) is a powerful separation technique and, when connected with adequate detection systems, provides high quality information for the supramolecular properties of polydisperse polysaccharides. A wide size (approximately 2 nm to >1 μm) and M (>> 10^7 g/mol) range of particles can be efficiently separated by the chromatography-like AF4. The separation is not based on a chromatography column, but on a separation channel without stationary phase, considerably reducing shear forces and enabling gentle separation. The main principles of separation are described elsewhere (Wahlund, 2000; Wahlund & Giddings, 1987). The complementation of AF4 with multi-angle light scattering (MALS) and differential refractive index (dRI) detectors enables the acquisition of molecular features namely weight average M, root-mean-square radius (r_{rms}) and conformation of polysaccharides (Alftrén, Peñarrieta, Bergenståhl, & Nilsson, 2012; Dou, Zhou, Jang, & Lee, 2014; Nilsson, 2013).

The aim of the present study was to determine the structural and conformational features of oat β-glucan under simulated in vitro gastrointestinal conditions and elucidate the fundamental molecular and supramolecular mechanisms, which could play an important role for the understanding of its health benefits. AF4 was employed in order to obtain information about M and r_{rms} distributions, as well as conformational properties under

different gastrointestinal conditions, while NMR was for the investigation of structural characteristics and interaction with bile acids.

2. Materials and Methods

Materials

Oat β-glucan was extracted from Oatwell CreaNutrition Oat flour with β-glucan content of 28 % (w/w) (Swedish Oat Fibre AB, Väröbacka, Sweden). Acetone (technical grade) and ethanol (absolute grade) were purchased from VWR Chemicals, Fontenay sous Bois, France. Heat-stable α-amylase from Aspergillus oryzae (~30 U/mg) was purchased from Sigma Aldrich Co., St Louis, MO, USA. Pepsin from porcine gastric mucosa (3200 – 4500 U/mg protein), pancreatin from porcine pancreas (8 × USP specifications) and sodium deoxycholate were purchased from Sigma Aldrich Co., sodium cholate was obtained from AppliChem GmbH, Darmstadt, Germany, and potassium chloride, potassium phosphate monobasic, sodium bicarbonate, magnesium chloride hexahydrate, sodium chloride, ammonium carbonate, sodium hydroxide, hydrochloric acid alcium chloride for the simulated digestive fluids were purchased from Sigma Aldrich Co., VWR Chemicals and Merck KGaA, Darmstadt, Germany.

For the preparation of the AF4 carrier liquid, sodium nitrate (Merck KGaA) and sodium azide (BDH, Poole, UK) were used. Calcofluor fluorescent brightener 28 (Sigma Aldrich Co.) and tris(hydroxymethyl)-aminomethane (Merck KGaA) were used for the fluorescence labelling. Deuterium oxide (D_2O) for NMR spectroscopy was obtained from Sigma Aldrich Co. All experiments were performed using pure water from a Milli-Q system (Millipore Corp., Billerica, Massachusetts, USA).

β-Glucan extraction

The protocol for the extraction of β-glucan from oat flour and the characterization of the extracted matter is described in detail by Zielke, Kosik, et al. (2017). The content of β-glucan for the AF4 experiments was estimated to be 66 % (w/w) and for the NMR spectroscopy 87 % (w/w).

in vitro Digestion

An established static in vitro digestion method (INFOGEST) was employed for the simulated gastrointestinal conditions as described in the international consensus by Minekus, et al. (2014). The oral phase of digestion was omitted. A solution of the β-glucan extract in Milli-Q water was prepared in a concentration of 2 mg/mL. The β-glucan solution was mixed with simulated gastric fluids (SGF) and pepsin solution (2000 U/mL in final digestion mixture) to a ratio of 1:1 (v/v) and a final volume of 5 mL. The digestion mixture was incubated for 2 h at 37 °C and pH 3.0, under continuous stirring. The gastric chyme was mixed with the simulated intestinal fluids (SIF), containing porcine pancreatin (100 U/mL in the final digestion mixture based on trypsin activity) and bile acids (5 mM sodium cholate and sodium deoxycholate in final digestion mixture) in a ratio of 1:1 (v/v) and a final digestion volume of 10 mL. The intestinal phase lasted 2 h at 37 °C and pH 7.0 under continuous agitation. These bile acids are main components of bile and were chosen as model bile acids for this study (Ifeduba & Akoh, 2015). Some samples were prepared with only gastric digestion. Furthermore, samples with and without enzymes and/or bile acids were prepared in different combinations. Aliquots of all samples (1 – 2 mL) were immersed in liquid nitrogen in order to cease the digestion and were kept for less than a week in the freezer (-20 °C) prior to analysis. The concentration of β-glucan after gastric digestion and after the complete gastrointestinal digestion was 1 mg/mL and 0.5 mg/mL, respectively, and was kept constant in all experiments. For the NMR analysis, the final volume of gastric and gastrointestinal digestion was adjusted to 10 mL and 20 mL, respectively, in order to yield 10 mg of β-glucan in each case.

AF4 instrumentation and data analysis

An Eclipse 3+ Separation System (Wyatt Technology Europe, Dernbach, Germany) was used for the characterization of β-glucan under different gastrointestinal conditions. A Dawn Heleos II multi-angle light scattering (MALS) detector operating at a wavelength of 658 nm and an Optilab T-rEX differential refractive index (dRI) detector (both Wyatt Technology

Europe) operating at the same wavelength were connected with the main system. The carrier flow was delivered through an Agilent 1100 series isocratic pump with an online vacuum degasser and an Agilent 1100 series autosampler (both Agilent Technologies, Waldbronn, Germany) handled the sample injection onto the AF4 channel. To ensure the absence of particles in the system, a filter-holder with a 100 nm pore-size polyvinylidene fluoride membrane (Millipore Corp.) was placed between the pump and the channel inlet. The AF4 channel was a Wyatt long channel with a tip-to-tip length of 27.5 cm and a nominal thickness of 190 µm. The actual thickness was calculated to be 184 µm by calibration with ferritin following a procedure proposed by Håkansson, Magnusson, Bergenståhl, and Nilsson (2012). The ultra-filtration membrane forming the accumulation wall was made of hydrophilized polyethersulphone with a molecular weight cut-off of 10 kDa (Microdyn-Nadir GmbH, Wiesbaden. Germany). The carrier liquid used for the analysis of the samples was prepared as a mixture of 10 mM $NaNO_3$ and 0.02 % (w/v) NaN_3 dissolved in Milli-Q water (pH 7.0). The carrier liquid was changed for the samples under gastric conditions to 50 mM phosphoric acid adjusted to pH 3.0 with 1 M NaOH, in order to simulate the pH of the gastric phase. β-Glucan samples without digestion, gastric and gastrointestinal digestion as well as samples with or without enzymes and bile acids in different combinations were analyzed with AF4-MALS-dRI. The frozen sample tubes were immersed in boiling water for 30 min in order to deactivate the enzymes and enhance β-glucan dissolution. When cooled down to room temperature (25 °C), the samples were filtered through a 0.45 µm pore size cellulose acetate membrane (VWR International) prior to injection onto the channel. Every sample was coupled with a sample free of β-glucan, serving as blank.

Prior to injection, an elution and focusing step of 1 min each were implemented. The injection of the sample onto the channel took place at a flow rate of 0.2 mL/min for the following 4 min. The injected sample volume was 80 µL for all samples, resulting in an injected mass of 160 µg for undigested β-glucan, 80 µg for β-glucan digested under gastric conditions and 40 µg for β-glucan digested under gastrointestinal conditions. A focusing/relaxation step of 5 min was performed prior to elution with a focusing flow rate of 0.5 mL/min resulting in a time before elution of 11 min and a calculated void time (t^0) of 0.4 min (Håkansson, Magnusson, et al., 2012). An exponential decay of the cross-flow was chosen, in order to avoid excessive retention and long elution times, according to Equation 1:

$$Q_c(t) = Q_c(0)e^{\left(\frac{-ln2}{t_{1/2}}\right)t} \quad (1)$$

where $Q_c(t)$ is the cross-flow rate as a function of time t after elution starts, $Q_c(0)$ is the initial cross-flow at the beginning of elution, and $t_{1/2}$ is the half-life of the exponential decay which determines how rapid the function is decreasing. $Q_c(0)$ was set to 1 mL/min and $t_{1/2}$ to 4.5 min. After elution, the AF4 channel was flushed without any cross-flow for 5 min. During all measurements, the detector flow rate was set constant at 0.5 mL/min. In between measurements, a run with only carrier liquid was performed in order to ensure a clean channel without residues from previous samples.

Post-channel fluorometry, connected to the AF4 set-up, enables the specific identification of β-glucan through targeted labelling of β-glucan of the purified extracts over the whole size distribution (Ulmius et al., 2012; Zielke, Kosik, et al., 2017). A Jasco FP-1520 fluorescence (FL) detector (Jasco Inc., Easton, Maryland, USA) operating an Ushio Xenon Short Arc lamp (Ushio Inc., Tokyo, Japan) was used. For the Calcofluor labelling of the β-glucan, a slightly modified method adopted from Ulmius, et al. (2012) was employed, using a 25 mg/L Calcofluor solution in 0.1 M tris(hydroxymethyl)-aminomethane buffer and measuring the emission at λ_{em} = 445 nm (λ_{ex} = 415 nm). The β-glucan extracts were labelled online post-channel with the Calcofluor solution at a constant flow rate of 0.5 mL/min and analyzed with MALS and FL.

Astra software, version 6.0 (Wyatt Technology Europe) was used for the processing of the data deprived from the AF4 separation and detectors. M and r_{rms} were obtained using the Berry method (Andersson, Wittgren, & Wahlund, 2003; Berry, 1966) performing a 1st order fit with the data obtained from the

scattering angles 5 – 18 (34.8° - 163.3°) for the samples from without and with gastric digestion and 5 – 16 (34.8° - 142.5°) for the samples from gastrointestinal digestion. Lower and higher angles were excluded when they did not provide precise responses. The refractive index increment dn/dc for β-glucan was set to 0.146 mL/g (Li et al., 2011), while the second virial coefficient was considered negligible.

The r_h, the ratio r_{rms}/r_h and the apparent density (ρ_{app}) were calculated with a MATLAB-based software (FFFhydRad 2.2.) (Håkansson, Magnusson, et al., 2012) using equations 2 – 5. r_h can be estimated using the Stokes-Einstein equation (Einstein, 1905):

$$r_{h,i} = \frac{k_b T}{6\pi\eta D_i} \quad (2)$$

where k_b is the Boltzmann constant, T is the temperature, η is the dynamic viscosity of the solvent and D_i is the diffusion coefficient.

The diffusion coefficient (D_i) can be calculated as described by Håkansson, Ulmius, et al. (2012):

$$\frac{dz_i}{dt} = f(Q_c)D_i \quad (3)$$

where z_i is the position of sample component i along the channel, t is the time and Q_c is the cross-flow rate.

The apparent density (ρ_i) for component i over a size distribution, is obtained from M and r_{rms} data as follows (Nilsson, Leeman, Wahlund, & Bergenståhl, 2006):

$$\rho_i = \frac{M_i}{V(r_{rms})_i} \cdot z \quad (4)$$

where M_i is M of component i, $V(r_{rms})$ is the volume of a sphere with root-mean-square radius r_{rms} and z is given by Eq.5, where r is the geometrical radius of a sphere.

$$z = \frac{V_{sphere}(r_{rms})}{V_{sphere}(r)} = \frac{r_{rms}^3}{r^3}$$

$$= \frac{(\sqrt{3/5}\cdot r)^3}{r^3} = \left(\frac{3}{5}\right)^{3/2} \quad (5)$$

Persistence length determination

The rigidity (stiffness) of the β-glucan chains can be described by the persistence length (l_p) and is estimated as follows (Dervilly-Pinel, Thibault, & Saulnier, 2001). The first step is to calculate the characteristic ratio C_∞ by solving Eq.6:

$$C_\infty = \frac{6r_{rms}^2 M_0}{I_0^2 M} \quad (6)$$

where M_0 is the molar mass of a β-D-glycopyranosyl residue which is equal to 162 g/mol (Li, et al., 2011), I_0 is the average length of a β-D-glycopyranosyl residue and is equal to 0.52 nm according to Eq.7.

$$I_0 = P_3 I_3^2 + P_4 I_4^2 \quad (7)$$

where P_3 and P_4 are the mole fractions of β-(1→3) linkages and β-(1→4) linkages which are calculated by the integration of their relative intensities of anomeric signals at 4.76 and 4.55 ppm, respectively, in the ^{1}H NMR spectrum (section 3.3) and I_3 = 0.48 nm and I_4 = 0.54 nm are the corresponding residue lengths (Li et al., 2011), respectively.

Therefore, l_p can be calculated:

$$l_p = \frac{(C_\infty + 1)\cdot I_0}{2} \quad (8)$$

where C_∞ is the characteristic ratio obtained by Eq. 6 and I0 is the average length of a β-D-glycopyranosyl residue obtained by Eq. 7.

Kratky plots

Utilizing the light scattering data from all MALS angles, conformational information derived from the angular variation of the scattered light can be obtained by creating Kratky plots (Andersson, Wittgren, Schagerlöf, Momcilovic, & Wahlund, 2004; Kratky & Porod, 1949). The angular variation can be estimated using the relationship (Eq. 9):

$$\frac{R_\theta}{K_c} = MP(u) \quad (9)$$

where Rθ stands for the Rayleigh ratio, K is an optical constant, c is the concentration of the analyte and M is the molar mass. P(u) is the scattering particle function and u is the product of r_{rms} and scattering vector q. The scattering vector q can be calculated from Equation 10:

$$q = \left(\frac{4\pi n_0}{\lambda_0}\right) \sin\left(\frac{\theta}{2}\right) \quad (10)$$

where n^0 is the refractive index of the solvent (1.33 for water), λ^0 the wavelength of the incident light (658 nm) and θ is the angle between the incident and the scattered light.

The construction of Kratky plots requires the plotting of $P(u)u^2$ as a function of u. Theoretical values of u and $P(u)u^2$ corresponding to differently shaped and structured polymer structures are plotted (Burchard, 1983; Burchard, 2004; Kratky et al., 1949) and compared with the obtained data for β-glucan without digestion and subjected to gastric and gastrointestinal digestion. In each of the three cases, light scattering data, M and r_{rms} corresponding to different β-glucan populations were utilized, as described above.

ζ-potential measurements

The ζ-potential of β-glucan solutions before and after gastric digestion was determined using a Zetasizer Nano ZS (Malvern Instruments Ltd., UK) at 25 °C. β-Glucan extract was dissolved in Milli-Q water with a concentration of 2 mg/mL. A second sample was prepared under simulated gastric conditions without pepsin. Each sample was analyzed in triplicate. The ζ-potential values are expressed as mean values ± standard deviation.

NMR spectroscopy

^1H and ^{13}C spectra were obtained with a suitable procedure for characterization of polysaccharides, as described by Nilsson, Gorton, Bergquist, and Nilsson (1996) with slight modifications. For the analysis of the undigested sample, 10 mg β-glucan were dissolved in 2 mL D_2O, resulting in a final concentration of 5 mg/mL. The solution was boiled for 20 min with continuous stirring. The sample was freeze-dried, re-dissolved in 2 mL of D_2O, boiled for 20 min and freeze-dried again. The whole procedure was repeated one more time to facilitate the exchange of hydroxylic protons and, consequently, reduce interference from the residual solvent resonance. The dried, deuterated sample was dissolved in 2 mL of D_2O and heated for 30 min at 100 °C before measurements. Samples undergone only gastric digestion, gastrointestinal digestion and gastrointestinal digestion without bile acids were prepared in such volumes that the final amount of β-glucan for NMR analysis was 10 mg. After digestion, the samples were boiled for 10 min to deactivate the enzymes and were then dialyzed in a Spectra/Por®3 Dialysis Membrane with 3.5 kD cut-off (Spectrum Laboratories, Inc., USA) to remove the electrolytes and enhance NMR resolution capacity. Subsequently, the digesta were freeze-dried and β-glucan residues were treated with D_2O as described before. The NMR measurements were performed at 353 K with a spectrometer (ARX 500, Bruker Fällanden, Switzerland) operating at 500 MHz.

3. Results

3.1. AF4 analysis

The extracted oat β-glucan was subjected to *in vitro* digestion and the fractograms of Calcofluor labelled β-glucan, separated by AF4 and analyzed using FL detection, are represented in **Fig. 1**. *M* and r_{rms} distributions were obtained utilizing dRI and MALS data.
The elution profile of extracted β-glucan without digestion displays a wide size distribution (13 – 40 min), as identified with fluorescence. *M* and r_{rms} are recorded within the range of $1.5 \times 10^5 – 3.0 \times 10^8$ g/mol and 24 – 157 nm, respectively (**Fig. 1A** and **1B**, red line). In the gastric phase, *M* shifts to lower values of $6 \times 10^4 – 1.6 \times 10^7$ g/mol and r_{rms} to 16 – 94 nm (**Fig. 1A** and **1B**, blue line), presenting a notably narrower size distribution (13 – 27 min). After the whole gastrointestinal digestion, the final *M* and r_{rms} ranges are $5 \times 10^5 – 3.9 \times 10^7$ g/mol and 52 – 147 nm, respectively, with elution times between 13 – 32 min (**Fig. 1A** and **1B**, purple line). In the latter case, the obtained data for analytes eluting between 13 – 20 min (close to the void peak) are imprecise and the determination of *M*, r_{rms} and conformation properties is unreliable and therefore not shown. These imprecise data could be originating from steric/hyperlayer effects (Caldwell, Nguyen, Myers, & Giddings, 1979) which lead to an inversion of elution order, and very large analytes are co-eluted with smaller analytes eluting Brownian mode (Wahlund et al., 1987). However, the dRI and MALS signals are very

low for this M range and, hence, no additional and reliable information on the species/kind/origin of these molecules can be extracted (**Suppl. Fig. 1 and 2**).

The conformational properties of β-glucan without and after gastric and gastrointestinal digestion were obtained by plotting the apparent density, r_{rms}/r_h and l_p over the entire M distribution (**Fig. 2** and **3**). Dissolved β-glucan without digestion could be divided into three distinct populations, as depicted in **Fig. 2A**. Population I is characterized by decreasing apparent density and r_{rms}/r_h values (from 1.5 to 0.6) with increasing M. When the apparent density reaches its minimum values (≈ 0.7 kg/m^3) at $M \approx 10^6$ g/mol, it remains at a rather constant level, while r_{rms}/r_h (≈ 0.6) does not have any dependence on the increasing M (population II). In population III, the apparent density increases for increasing M (> 5.5×10^6 g/mol), while r_{rms}/r_h is decreasing from 0.6 to 0.3. l_p increases from 2.4 to 4 nm for population I, and then continuously decreases for population II and III to the lowest value of 0.37 nm (**Fig. 3**). Different populations were also detected when β-glucan was exposed to gastric conditions (**Fig. 2B**). In population I, the apparent density and r_{rms}/r_h exhibit a concomitant decrease with increasing M (from 1.2 to 0.6 for r_{rms}/r_h), followed by a change at the infliction point of $M \approx 5 \times 10^5$ g/mol, where apparent density increases to higher levels with increasing M, whereas r_{rms}/r_h displays constant levels (≈ 0.5) (population III). An increase of l_p from 3.2 to 4.4 nm is observed for population I followed by a constant decrease for population III to the lowest value of 0.8 nm (**Fig. 3**). A behavior as seen in population II without digestion could not be observed for β-glucan after gastric digestion, whereas β-glucan after gastrointestinal digestion does not show population I in the studied M range. The apparent density of population II in the intestinal phase sustains constant levels (approximately 0.6 – 0.8 kg/m^3) in parallel with a decreasing r_{rms}/r_h from 1 to 0.7 (**Fig. 2C**). With higher M, the apparent density displays a rather significant increase above $M \approx 3 \times 10^6$ g/mol and r_{rms}/r_h continues decreasing from 0.7 to 0.3 (population III) (**Fig. 2C**). The l_p values constantly decrease from 6 nm to the lowest value of 0.7 nm over the M for population II and III (**Fig. 3**).

For a more extensive determination of the conformational properties of β-glucan, Kratky plots (**Fig. 4)** were constructed using MALS data for all the populations shown in **Fig. 2**. For β-glucan without digestion (**Fig. 4A**), the obtained u values for populations I and II are too low to be interpreted. However, population III displays a hyperbranched structure. Similarly, only population III of β-glucan in the gastric phase has a behavior similar to hyperbranched structure (**Fig. 4B**). Finally, both populations II and III of β-glucan after gastrointestinal digestion follow the pattern of the hyperbranched structure (**Fig. 4C**).

The possible interaction of the digestive enzymes and bile acids with β-glucan was investigated by comparing the apparent density of β-glucan with and without their presence (**Fig. 5**). In the gastric phase, an increased apparent density is detected in presence of pepsin for the high M species of population III, which reveals a change to the conformation of β-glucan (**Fig. 5A**). Regarding the role of digestive enzymes (pepsin and pancreatin) after the gastrointestinal digestion (**Fig. 5B**), there is a slight increase of apparent density for population II in presence of the enzymes but there are no significant differences in population III. Interestingly, the presence of bile acids in the digesta seems to affect the apparent density (**Fig. 5B**) as well. In order to exclude a synergetic effect of digestive enzymes and bile acids on the apparent density, a comparative graph of β-glucan after gastrointestinal digestion with and without enzymes and with and without bile acids is presented in **Fig. 5B**. For population II, the two cases without enzymes present a slightly higher apparent density. On the other hand, regarding population III, the influence of bile acids on the apparent density is more profound, since the two cases without bile acids demonstrate lower density in a consistent way, excluding any synergistic effect with digestive enzymes.

3.2. ζ-potential

The ζ-potential determination could provide useful information regarding any possible electrical charge of β-glucan in solution. Firstly, the β-glucan extract was dissolved in Milli-Q water at a concentration of 2 mg/mL and the ζ-potential was recorded to be -1.53 ± 0.08 mV.

Under simulated gastric conditions, the ζ-potential was decreased to -0.19 ± 0.07 mV.

3.3. NMR spectroscopy

The structural features of oat β-glucan were investigated with NMR spectroscopy. The peak assignment of ^{1}H and ^{13}C NMR spectra was based on literature (Colleoni-Sirghie, Bruce Fulton, & White, 2003; Dais & Perlin, 1982) and no deviations from the reported chemical shifts were detected (Suppl. Fig. 3). The ratio of β-(1→3) and β-(1→4) glycosidic bonds was estimated to be 1:2.5, as calculated by the integration of their corresponding relative intensities of anomeric signals at 4.76 and 4.55 ppm in the ^{1}H NMR spectrum (**Fig. 6A**) (Mikkelsen et al., 2010). β-Glucan after gastric digestion presented an identical spectrum (**Fig. 6B**).

The possible binding of bile micelles to β-glucan was investigated by direct comparison of bile acids' chemical shifts in the ^{13}C NMR spectra with and without the presence of β-glucan during gastrointestinal digestion. The relative chemical shifts are shown in **Table 1**. The well-resolved ^{13}C NMR spectrum of sodium cholate and sodium deoxycholate (spectrum not shown) presented separate peaks for each carbon and the assignment was conducted according to Barnes and Geckle (1982). This sample was prepared in presence of the digestive enzymes in order to exclude any perturbing effect of proteins on the resonance of carbon atoms. The addition of β-glucan during the gastrointestinal digestion led to numerous small changes regarding the chemical shifts (both upfield and downfield) of several carbon atom signals of the bile acids (**Table 1**). On the other hand, the presence of bile acids did not induce any changes on the resonance chemical shifts of β-glucan (data not shown).

4. Discussion

The investigation of the solution behavior of oat β-glucan without digestion revealed populations with various conformational properties (**Fig. 2A**). Population I exhibits decreasing apparent density and r_{rms}/r_h with increasing *M*. The displayed fractal scaling is typical for branched polymers. Since cereal β-glucan is not branched (Lazaridou et al., 2007), the existence of any molecularly dissolved β-glucan can be excluded and these structures should be considered as aggregates, as suggested previously by Håkansson, Ulmius, et al. (2012). In addition, the r_{rms}/r_h range is between 0.6 – 1.5 indicating a variety of structures present which could both include hyperbranched structures (r_{rms}/r_h = 1.2) and homogenous sphere-like structures (r_{rms}/r_h = 0.775) (Nilsson, 2013). No further conclusions regarding structure/conformation can be obtained from the Kratky plot due to low *u* values, resulting from low r_{rms} values (25 – 65 nm) in relation to the wavelength of the MALS-detector (658 nm) (**Fig. 4A**). However, as the results clearly suggest branched structures, the presence of individual β-glucan aggregates (primary aggregates) with fringed micelle structure should be considered, as previously suggested by Håkansson, Ulmius, et al. (2012). According to this aggregation model, there is side-to-side alignment of β-glucan chains, giving rise to a compact core and flexible protruding chains at the outer perimeter (Grimm, Krüger, & Burchard, 1995; Håkansson, Ulmius, et al., 2012). This model can explain the decreasing apparent density with increasing *M* of population I, where the higher *M* chains would need more space for the assembly of the primary aggregates. The parallel increase in size of primary aggregates and rigidity (**Fig. 3**) is supported by findings of Li et al. (2011) who showed that aggregated β-glucan had higher l_p compared to non-aggregated, correlating the aggregation with the stiffness of the supramolecular complexes. It is therefore assumed that the used model is valid for the aggregates of population I, presumably because there are not considerable deviations from the required assumptions of the model. However, taking the potential limitations of the model used into account, the values should be considered apparent. The increase of the persistence length over increasing *M*, could be attributed to different length of cellulose segments of β-(1→4) linked glucose units over the *M* distribution.

Population II demonstrates constant apparent density and r_{rms}/r_h with increasing *M* and a r_{rms}/r_h range between 0.5 – 0.6 denoting a swollen micro-gel structure (Schmidt, Nerger, & Burchard, 1979) (**Fig. 2A**). The regularity in the scaling of apparent density vs *M* could reveal secondary supramolecular aggregated

structures of primary aggregates (Fernandez, Rojas, & Nilsson, 2011). Attached primary aggregates of the same density and size could result to constant apparent density and r_{rms}/r_h. l_p is decreasing with increasing M, suggesting that the formation of secondary aggregates is associated with lower chain stiffness (**Fig. 3)**. However, caution should be taken for the interpretation of these results, as the aggregates of this population are very large in size, and deviate from the conditions for the applicability of the used model which assumes a single flexible polymer chain conformation.

Regarding population III (**Fig. 2A**), the high apparent density and the r_{rms}/r_h values below 0.5 denotes high density secondary aggregates with different scaling behavior, composed of penetrating primary aggregates (population I) into secondary aggregates (population II). Although r_{rms}/r_h indicates swollen micro-gel structures, the Kratky plot attributes a hyperbranched structure for the high density secondary aggregates (**Fig. 4A**). Kratky plots provide accurate information about the structure of particles with higher r_{rms}, since the u values depend on the wavelength of the radiation utilized. The extensive aggregation is accompanied with decreased rigidity (**Fig. 3)**. It is noteworthy, though, that the values are getting extremely low (even lower than the length of a glucose residue). The model is most likely not valid in this regime due to the presence of highly aggregated structures .

In the gastric phase, the conformation of β-glucan was significantly affected. The AF4 analysis demonstrated that the elution time and hence, r_h was notably reduced, leading to denser aggregates (**Fig. 1**), as also reflected in the apparent density along the M range (**Fig. 2B**). Population I is considered primary aggregates, as described before, and aggregates of constant apparent density (population II) are absent (**Fig. 2B**). Population III under gastric conditions contains more compact (**Fig. 2C**) and less stiff (**Fig. 3**) high density secondary aggregates with reduced M and disrupted morphology compared to population III without digestion**.**

In agreement with our results, Ulmius et al. (2012) reported disrupted aggregates after *in vitro* gastric digestion (pH 1.2), possibly attributed to acidic degradation. The lack of emerging peaks in the ^{1}H NMR spectrum (**Fig. 6B**) at 4.65 ppm (Colleoni-Sirghie, et al., 2003) does not support an increase of reducing ends (i.e. molecular degradation) in the gastric phase. Minekus et al. (2014) suggested the use of an average pH of 3.0 for the *in vitro* gastric phase, taking into account the buffering effect of a meal on the pH of fasting state (pH 2.0). The present results are consistent with Johansson et al. (2006), who did not report any degradation of oat β-glucan over a 12 h incubation in pH 1.0 and 37 °C which suggests that acidic degradation did not occur in the study by Ulmius et al. (2012).

Although β-glucan is widely considered as a neutral polysaccharide (Agbenorhevi, et al., 2011), its negative charge has been reported (Liu, Li, Ma, Chen, & Zhao, 2013; Sibakov, Abecassis, Barron, & Poutanen, 2014; Vårum & Smidsrød, 1988) and attributed to esterified phosphate groups in C6 position (Ghotra, Vasanthan, Wettasinghe, & Temelli, 2007). Indeed, the ζ-potential of undigested β-glucan was -1.53 ± 0.08 mV and in concordance with results from Wu, Deng, Tian, Wang, and Xie (2008). Under gastric conditions the ζ-potential was -0.19 ± 0.07 mV, most likely due to protonation of the phosphate groups and higher ionic strength as the ζ-potential is strongly dependent on the latter. Thus, the low pH and higher ionic strength in the gastric phase could induce loss of electrostatic repulsion between β-glucan chains, enabling the closer association of the primary aggregates and favoring a higher tendency for aggregation reflected as denser secondary aggregates of population III (**Fig. 2D**). The presence of pepsin led to a slightly increased apparent density of population III (**Fig. 5A**). This could possibly denote an interaction between pepsin and secondary β-glucan aggregates, especially since the close association of cereal β-glucan with proteins has been described in literature (Forrest & Wainwright, 1977; Zielke, Teixeira, et al., 2017). Nevertheless, pH had the greatest impact on the conformation of β-glucan.

The complete gastrointestinal digestion induced further conformational alterations (**Fig. 2C**). Primary aggregates (population I) were not detected, but their absence cannot be certain as the imprecise data at short AF4 elution times make the study of this population impossible. Population II demonstrates constant apparent density with decreasing r_{rms}/r_h over the increasing M, indicating secondary aggregates with a range of conformations (**Fig. 2C**). On the contrary, the Kratky plots suggest hyperbranched

morphology (**Fig. 4C**). Population III shows an increasing apparent density and decreasing r_{rms}/r_h, depicting high density secondary aggregates (**Fig. 2C**). The apparent density and l_p range of β-glucan without digestion and β-glucan subjected to gastrointestinal digestion (**Fig. 2** and **3**) show an almost identical pattern for populations II and III, suggesting that the denser aggregates during the gastric phase are unfolded or dissociated to a state without major differences to the initial state. The results are in agreement with Cleary, Andersson, and Brennan (2007) who demonstrated that the *M* of barley β-glucan was not decreased after *in vitro* digestion. However, the authors did not investigate conformational changes during the digestion.

Consistently, the presence of bile acids promoted changes in the apparent density distributions (**Fig. 5B**). However, rather small differences were shown, taking into account the small size of bile micelles (~ 2 – 5 nm) (Cheng, Oh, Wang, Raghavan, & Tung, 2014; Gunness, Flanagan, Mata, Gilbert, & Gidley, 2016) which contributes to minimal, yet detectable, changes to the molar mass/size of the β-glucan-bile acids complexes. The capacity of β-glucan to 'bind' bile acids has been confirmed in several *in vitro* studies (Kim et al., 2010; Kim et al., 2011; Kim & White, 2012) and it has been suggested that molecular interaction causing retention are more important than viscosity effects (Zacherl et al., 2011). In addition, the comparison of ^{13}C NMR spectra of bile acids in presence and absence of β-glucan after digestion revealed numerous changes in chemical shifts in various sites over the entire bile acid molecules (**Table 1**). These chemical shift changes suggest a direct, dynamic molecular association between β-glucan and bile acids, which alters the conformation of bile acids within the bile micelles and reduces their mobility (Gunness et al., 2010; Gunness et al., 2016). Furthermore, the lower intensity (spectrum not shown) of bile acid resonance suggests entrapment of bile acids in the local environment of β-glucan aggregates. However, caution should be taken for the interpretation of the NMR results, as changes in the resonance of bile acids in presence of β-glucan could derive from increased local concentration of bile acids which could be a result of confinement (Mikkelsen et al., 2014). This could especially apply since no changes of chemical shifts were observed in the β-glucan resonance. However, the vast abundance of non-interacting glucose units compared to the bile acids molecules could explain this lack of changes of chemicals shifts. Undoubtedly, though, AF4 was proven powerful for detecting conformational changes, proposing it as an interesting method for probing subtle interactions of polysaccharides with other molecules.

The digestive enzymes in the intestinal phase had a negligible impact on the apparent density of β-glucan aggregates (**Fig. 5B**). This implies that the possible effect of pepsin on the conformation of high density secondary aggregates (**Fig. 5A**) is specific to the gastric phase. It can be assumed that the low pH influences the association of β-glucan and pepsin and the subsequent normalization of pH at the intestinal phase disrupts these complexes. Overall, the lack of interactions between enzymes and β-glucan structures at the intestinal phase argues against any effect on the digestive enzymes.

To the best of our knowledge, this is the first time that AF4 and NMR synergistically ascribe the impact of the *in vitro* gastrointestinal environment on the structure and conformation of oat β-glucan as well as interaction with bile acids. β-Glucan presented various aggregation patterns which were notably affected in the *in vitro* gastric phase. The intestinal digestion resulted in a confirmation which appears similar to the initial and solely bile acids were shown to be associated with the β-glucan aggregates. The present holistic approach for the study of β-glucan under *in vitro* gastrointestinal conditions, with the powerful tools of AF4-MALS and NMR, provides insight into the solution/dispersion properties of oat β-glucan, its interaction with bile acids and potential mechanisms for health benefits.

5. Acknowledgements

Funding from the Swedish research council (VR), Stockholm, Sweden is gratefully acknowledged. The authors would like to thank Dr. Karl-Erik Bergquist, Center for Synthesis and Analysis, Lund University for his valuable help with NMR spectroscopy. Dr. Alejandra Castro, SOLVE Research and Consultancy AB is, also, acknowledged for support with ζ-potential measurements. The authors have no conflicts of interest to declare.

6. References

Agbenorhevi, J. K., Kontogiorgos, V., Kirby, A. R., Morris, V. J., & Tosh, S. M. (2011). Rheological and microstructural investigation of oat β-glucan isolates varying in molecular weight. *International Journal of Biological Macromolecules, 49*(3), 369-377.

Alftrén, J., Peñarrieta, J. M., Bergenståhl, B., & Nilsson, L. (2012). Comparison of molecular and emulsifying properties of gum arabic and mesquite gum using asymmetrical flow field-flow fractionation. *Food Hydrocolloids, 26*(1), 54-62.

Andersson, M., Ellegard, L., & Andersson, H. (2002). Oat bran stimulates bile acid synthesis within 8 h as measured by 7alpha-hydroxy-4-cholesten-3-one. *American Journal of Clinical Nutrition, 76*(5), 1111-1116.

Andersson, M., Wittgren, B., Schagerlöf, H., Momcilovic, D., & Wahlund, K. G. (2004). Size and structure characterization of ethylhydroxyethyl cellulose by the combination of field-flow fractionation with other techniques. Investigation of ultra-large components. *Biomacromolecules, 5*(1), 97-105.

Andersson, M., Wittgren, B., & Wahlund, K.-G. (2003). Accuracy in Multiangle Light Scattering Measurements for Molar Mass and Radius Estimations. Model Calculations and Experiments. *Analytical Chemistry, 75*(16), 4279-4291.

Barnes, S., & Geckle, J. M. (1982). High resolution nuclear magnetic resonance spectroscopy of bile salts: individual proton assignments for sodium cholate in aqueous solution at 400 MHz. *Journal Lipid Research, 23*(1), 161-170.

Berry, G. C. (1966). Thermodynamic and Conformational Properties of Polystyrene. I. Light-Scattering Studies on Dilute Solutions of Linear Polystyrenes. *The Journal of Chemical Physics, 44*(12), 4550-4564.

Burchard, W. (1983). Static and dynamic light scattering from branched polymers and biopolymers. In *Light Scattering from Polymers* (pp. 1-124). Berlin, Heidelberg: Springer Berlin Heidelberg.

Burchard, W. (2004). Light Scattering Techniques. In A. S. Ross-Murphy (Ed.), *Physical Techniques for the Study of Food Biopolymers* (pp. 151-213). Dordrecht, The Netherlands: Springer Science+Business Media.

Caldwell, K. D., Nguyen, T. T., Myers, M. N., & Giddings, J. C. (1979). Observations on Anomalous Retention in Steric Field-Flow Fractionation. *Separation Science and Technology, 14*(10), 935-946.

Cheng, C. Y., Oh, H., Wang, T. Y., Raghavan, S. R., & Tung, S. H. (2014). Mixtures of lecithin and bile salt can form highly viscous wormlike micellar solutions in water. *Langmuir, 30*(34), 10221-10230.

Cleary, L. J., Andersson, R., & Brennan, C. S. (2007). The behaviour and susceptibility to degradation of high and low molecular weight barley β-glucan in wheat bread during baking and in vitro digestion. *Food Chemistry, 102*(3), 889-897.

Colleoni-Sirghie, M., Bruce Fulton, D., & White, P. J. (2003). Structural features of water soluble (1,3)(1,4)-β-D-glucans from high-β-glucan and traditional oat lines. *Carbohydrate Polymers, 54*(2), 237-249.

Dais, P., & Perlin, A. S. (1982). High-field, 13C-N.M.R. spectroscopy of β-d-glucans, amylopectin, and glycogen. *Carbohydrate Research, 100*(1), 103-116.

Daou, C., & Zhang, H. (2012). Oat Beta-Glucan: Its Role in Health Promotion and Prevention of Diseases. *Comprehensive Reviews in Food Science and Food Safety, 11*(4), 355-365.

Dervilly-Pinel, G., Thibault, J.-F., & Saulnier, L. (2001). Experimental evidence for a semi-flexible conformation for arabinoxylans. *Carbohydrate Research, 330*(3), 365-372.

Dikeman, C. L., Murphy, M. R., & Fahey, G. C., Jr. (2006). Dietary fibers affect viscosity of solutions and simulated human gastric and small intestinal digesta. *Journal of Nutrition, 136*(4), 913-919.

Dou, H., Zhou, B., Jang, H. D., & Lee, S. (2014). Study on antidiabetic activity of wheat and barley starch using asymmetrical flow field-flow fractionation coupled with multiangle light scattering. *Journal of Chromatography A, 1340*, 115-120.

Einstein, A. (1905). Über die von der molekularkinetischen Theorie der Wärme geforderte Bewegung von in ruhenden Flüssigkeiten suspendierten Teilchen. *Annalen der Physik, 322*(8), 549-560.

Fernandez, C., Rojas, C. C., & Nilsson, L. (2011). Size, structure and scaling relationships in glycogen from various sources investigated with asymmetrical flow field-flow fractionation and 1H NMR. *International Journal of Biological Macromolecules, 49*(4), 458-465.

Forrest, I. S., & Wainwright, T. (1977). The mode of binding β-glucans and pentosans in barley endo-

sperm cell walls. *Journal of the Institute of Brewing, 83*(5), 279-286.

Ghotra, B. S., Vasanthan, T., Wettasinghe, M., & Temelli, F. (2007). 31P-nuclear magnetic resonance spectroscopic analysis of phosphorus in oat and barley β-glucans. *Food Hydrocolloids, 21*(7), 1056-1061.

Grimm, A., Krüger, E., & Burchard, W. (1995). Solution properties of β-D-(1, 3)(1, 4)-glucan isolated from beer. *Carbohydrate Polymers, 27*(3), 205-214.

Gunness, P., Flanagan, B. M., & Gidley, M. J. (2010). Molecular interactions between cereal soluble dietary fibre polymers and a model bile salt deduced from 13C NMR titration. *Journal of Cereal Science, 52*(3), 444-449.

Gunness, P., Flanagan, B. M., Mata, J. P., Gilbert, E. P., & Gidley, M. J. (2016). Molecular interactions of a model bile salt and porcine bile with (1,3:1,4)-beta-glucans and arabinoxylans probed by (13)C NMR and SAXS. *Food Chemistry, 197*(Pt A), 676-685.

Håkansson, A., Magnusson, E., Bergenståhl, B., & Nilsson, L. (2012). Hydrodynamic radius determination with asymmetrical flow field-flow fractionation using decaying cross-flows. Part I. A theoretical approach. *Journal of Chromatography A, 1253*, 120-126.

Håkansson, A., Ulmius, M., & Nilsson, L. (2012). Asymmetrical flow field-flow fractionation enables the characterization of molecular and supramolecular properties of cereal β-glucan dispersions. *Carbohydrate Polymers, 87*(1), 518-523.

Ifeduba, E. A., & Akoh, C. C. (2015). Microencapsulation of stearidonic acid soybean oil in complex coacervates modified for enhanced stability. *Food Hydrocolloids, 51*, 136-145.

Johansson, L., Virkki, L., Anttila, H., Esselström, H., Tuomainen, P., & Sontag-Strohm, T. (2006). Hydrolysis of β-glucan. *Food Chemistry, 97*(1), 71-79.

Kim, H. J., & White, P. J. (2010). In Vitro Bile-Acid Binding and Fermentation of High, Medium, and Low Molecular Weight β-Glucan. *Journal of Agricultural and Food Chemistry, 58*(1), 628-634.

Kim, H. J., & White, P. J. (2011). Optimizing the molecular weight of oat beta-glucan for in vitro bile acid binding and fermentation. *Journal of Agricultural and Food Chemistry, 59*(18), 10322-10328.

Kim, H. J., & White, P. J. (2012). Interactional effects of beta-glucan, starch, and protein in heated oat slurries on viscosity and in vitro bile acid binding. *Journal of Agricultural and Food Chemistry, 60*(24), 6217-6222.

Kratky, O., & Porod, G. (1949). Diffuse small-angle scattering of X-rays in colloid systems. *Journal of Colloid Science, 4*(1), 35-70.

Lazaridou, A., & Biliaderis, C. G. (2007). Molecular aspects of cereal β-glucan functionality: Physical properties, technological applications and physiological effects. *Journal of Cereal Science, 46*(2), 101-118.

Li, W., Cui, S. W., Wang, Q., & Yada, R. Y. (2011). Studies of aggregation behaviours of cereal β-glucans in dilute aqueous solutions by light scattering: Part I. Structure effects. *Food Hydrocolloids, 25*(2), 189-195.

Lia, A., Hallmans, G., Sandberg, A. S., Sundberg, B., Aman, P., & Andersson, H. (1995). Oat beta-glucan increases bile acid excretion and a fiber-rich barley fraction increases cholesterol excretion in ileostomy subjects. *American Journal of Clinical Nutrition, 62*(6), 1245-1251.

Mikkelsen, M. S., Cornali, S. B., Jensen, M. G., Nilsson, M., Beeren, S. R., & Meier, S. (2014). Probing interactions between beta-glucan and bile salts at atomic detail by (1)H-(1)(3)C NMR assays. *Journal of Agricultural and Food Chemistry, 62*(47), 11472-11478.

Mikkelsen, M. S., Jespersen, B. M., Møller, B. L., Lærke, H. N., Larsen, F. H., & Engelsen, S. B. (2010). Comparative spectroscopic and rheological studies on crude and purified soluble barley and oat β-glucan preparations. *Food Research International, 43*(10), 2417-2424.

Minekus, M., Alminger, M., Alvito, P., Ballance, S., Bohn, T., Bourlieu, C., Carriere, F., Boutrou, R., Corredig, M., Dupont, D., Dufour, C., Egger, L., Golding, M., Karakaya, S., Kirkhus, B., Le Feunteun, S., Lesmes, U., Macierzanka, A., Mackie, A., Marze, S., McClements, D. J., Menard, O., Recio, I., Santos, C. N., Singh, R. P., Vegarud, G. E., Wickham, M. S. J., Weitschies, W., & Brodkorb, A. (2014). A standardised static in vitro digestion method suitable for food - an international consensus. *Food & Function, 5*(6), 1113-1124.

Nilsson, G. S., Gorton, L., Bergquist, K.-E., & Nilsson, U. (1996). Determination of the Degree of Branching in Normal and Amylopectin Type Potato Starch with 1H-NMR Spectroscopy Improved resolution and two-dimensional spectroscopy. *Starch - Stärke, 48*(10), 352-357.

Nilsson, L. (2013). Separation and characterization of food macromolecules using field-flow fractionation: A review. *Food Hydrocolloids, 30*(1), 1-11.

Nilsson, L., Leeman, M., Wahlund, K. G., & Bergenståhl, B. (2006). Mechanical degradation and changes in conformation of hydrophobically modified starch. *Biomacromolecules, 7*(9), 2671-2679.

Rebello, C. J., O'Neil, C. E., & Greenway, F. L. (2016). Dietary fiber and satiety: the effects of oats on satiety. *Nutrition Reviews, 74*(2), 131-147.

Schmidt, M., Nerger, D., & Burchard, W. (1979). Quasi-elastic light scattering from branched polymers: 1. Polyvinylacetate and polyvinylacetate—microgels prepared by emulsion polymerization. *Polymer, 20*(5), 582-588.

Thies, F., Masson, L. F., Boffetta, P., & Kris-Etherton, P. (2014). Oats and CVD risk markers: a systematic literature review. *British Journal of Nutrition, 112 Suppl 2*, S19-30.

Ulmius, M., Adapa, S., Önning, G., & Nilsson, L. (2012). Gastrointestinal conditions influence the solution behaviour of cereal β-glucans in vitro. *Food Chemistry, 130*(3), 536-540.

Wahlund, K. G. (2000). Asymmetrical flow field-flow fractionation. In M. E. Schimpf, Caldwell, K., Giddings, J.C. (Ed.), *Field-flow fractionation handbook* (pp. 279-294). New York John Wiley & Sons Inc.

Wahlund, K. G., & Giddings, J. C. (1987). Properties of an asymmetrical flow field-flow fractionation channel having one permeable wall. *Analytical Chemistry, 59*(9), 1332-1339.

Wang, Q., & Ellis, P. R. (2014). Oat beta-glucan: physico-chemical characteristics in relation to its blood-glucose and cholesterol-lowering properties. *British Journal of Nutrition, 112 Suppl 2*, S4-s13.

Wood, P. J. (2004). Relationships between solution properties of cereal β-glucans and physiological effects — a review. *Trends in Food Science & Technology, 15*(6), 313-320.

Wu, J., Deng, X., Tian, B., Wang, L., & Xie, B. (2008). Interactions between Oat beta-Glucan and calcofluor characterized by spectroscopic method. *Journal of Agricultural and Food Chemistry, 56*(3), 1131-1137.

Zacherl, C., Eisner, P., & Engel, K.-H. (2011). In vitro model to correlate viscosity and bile acid-binding capacity of digested water-soluble and insoluble dietary fibres. *Food Chemistry, 126*(2), 423-428.

Zielke, C., Kosik, O., Ainalem, M.-L., Lovegrove, A., Stradner, A., & Nilsson, L. (2017). Characterization of cereal β-glucan extracts from oat and barley and quantification of proteinaceous matter. *PLOS ONE, 12*(2), e0172034.

Zielke, C., Teixeira, C., Ding, H., Cui, S., Nyman, M., & Nilsson, L. (2017). Analysis of β-glucan molar mass from barley malt and brewer's spent grain with asymmetric flow field-flow fractionation (AF4) and their association to proteins. *Carbohydrate Polymers, 157*, 541-549.

Table 1. ^{13}C chemical shifts of bile acids resonance alone and with the presence of oat β-glucan after gastrointestinal digestion and relative chemical shifts.

Carbon atom	Chemical shifts (ppm)		Relative chemical shifts†
	Bile acids (alone)	Bile acids (With β-glucan)	
C1	29.90	29.90	0.00
C2	32.73	32.48	-0.25
C3	69.17	68.70.	-0.47
C4	39.13	39.12	-0.01
C5	41.50	41.49	-0.01
C6	34.00	33.85	-0.15
C7	72.10	N.A. *	-
C8	39.56	39.56	0.00
C9	26.95	26.95	0.00
C10	34.27	34.27	0.00
C11	28.04	28.05	+0.01
C12	73.69	73.67	-0.02
C13	46.58	46.61	+0.03
C14	42.08	42.08	0.00
C15	23.14	23.14	0.00
C16	27.39	27.38	-0.01
C17	47.46	47.42	-0.04
C18	12.29	12.28	-0.01
C19	17.32	17.29	-0.03
C20	35.55	35.48	-0.07
C21	22.20	22.20	0.00
C22	35.13	N.A.	-
C23	35.09	35.08	-0.01
C24	N.A.	N.A.	-

† - Upfield shift, + Downfield shift

* not assigned

Legends for figures

Figure 1. Fractograms from AF4 analysis of oat β-glucan without digestion (red), gastric digestion (blue) and gastrointestinal digestion (purple). Normalized FL-signal (thin lines, A and B) displayed on the left axes and *M* (thick line, A) and r_{rms} (thick line, B) distributions on the right axes. Symbol t^0 refers to the void time (0.4 min). (For interpretation of the references to color in this figure legend, the reader is referred to the web version of this article.)

Figure 2. Apparent density (left axis) and r_{rms}/r_h (right axis) of oat β-glucan on a function of *M*. (A) Without digestion, (B) Gastric digestion, (C) Gastrointestinal digestion and (D) Comparative illustration of apparent densities of A, B and C. Colors assigned as mentioned in each graph. (For interpretation of the references to color in this figure legend, the reader is referred to the web version of this article.)

Figure 3. Persistence length (l_p) of oat β-glucan on a function of *M* without digestion and after gastric and gastrointestinal digestion. Colors assigned as mentioned in the graph. (For interpretation of the references to color in this figure legend, the reader is referred to the web version of this article.)

Figure 4. Kratky plots of oat β-glucan displaying the conformation of various populations. (A) Without digestion, (B) Gastric digestion and (C) Gastrointestinal digestion. Colors assigned as mentioned in each graph. (For interpretation of the references to color in this figure, the reader is referred to the web version of this article.)

Figure 5. Apparent density of oat β-glucan under gastric and gastrointestinal conditions plotted on a function of *M*. (A) Gastric digestion with and without pepsin, (B) Gastrointestinal digestion with enzymes and bile acids, without enzymes, without bile acids and without enzymes and bile acids. Colors assigned as mentioned in each graph. (For interpretation of the references to color in this figure legend, the reader is referred to the web version of this article.)

Figure 6. Partial ^{1}H NMR spectrum of oat β-glucan. (A) Without digestion and (B) Gastric digestion.

Figure 1

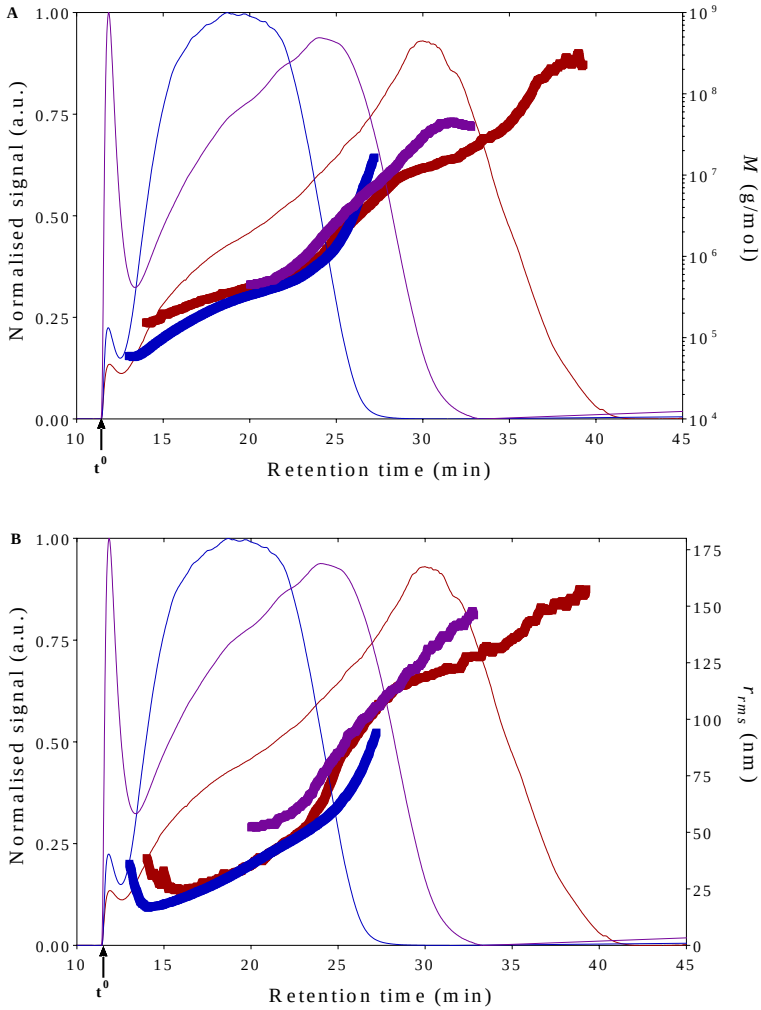

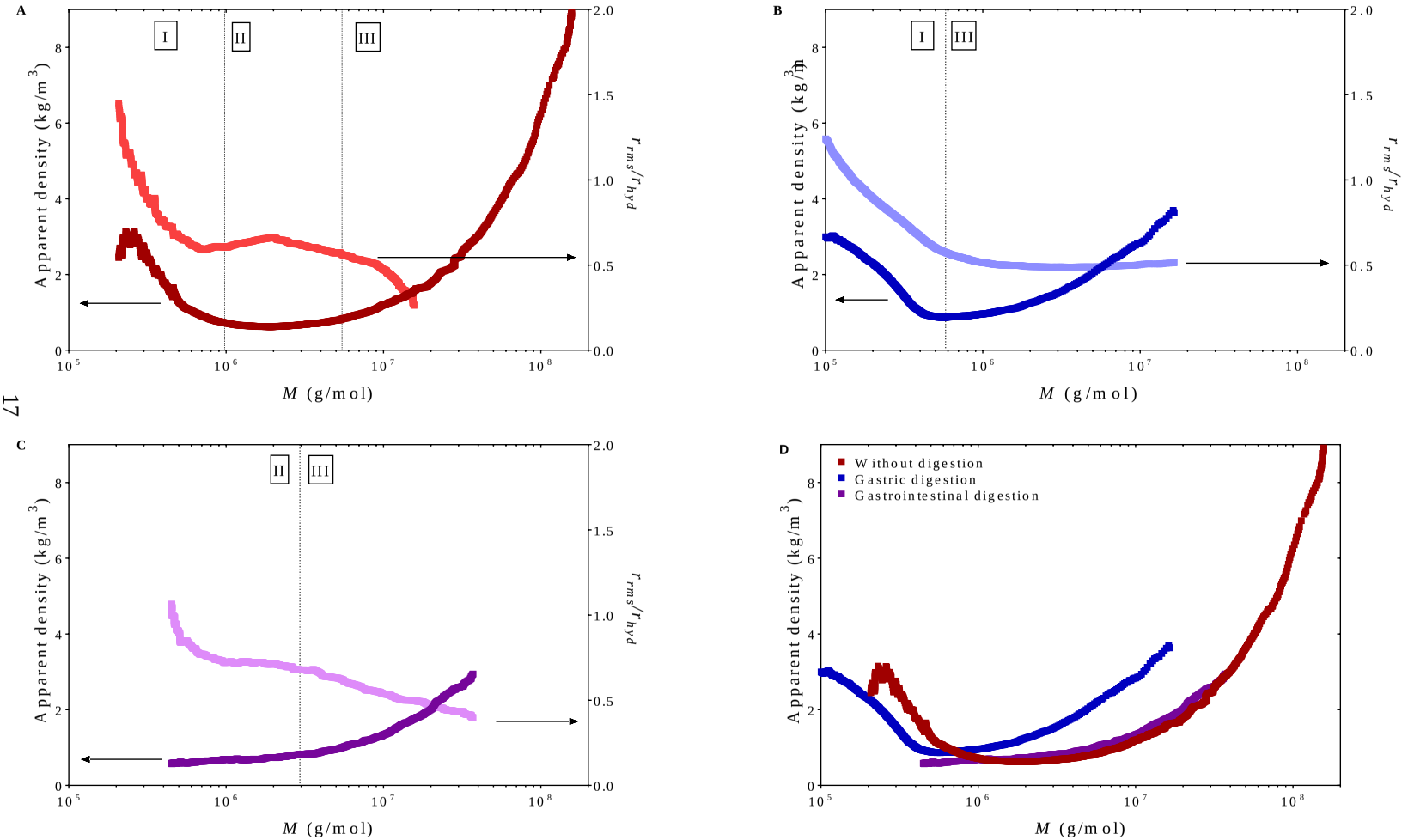
A
B
C
D
I
II
III
Apparent density (kg/m3)
M (g/mol)
rrms/rhyd
Without digestion
Gastric digestion
Gastrointestinal digestion

Figure 2

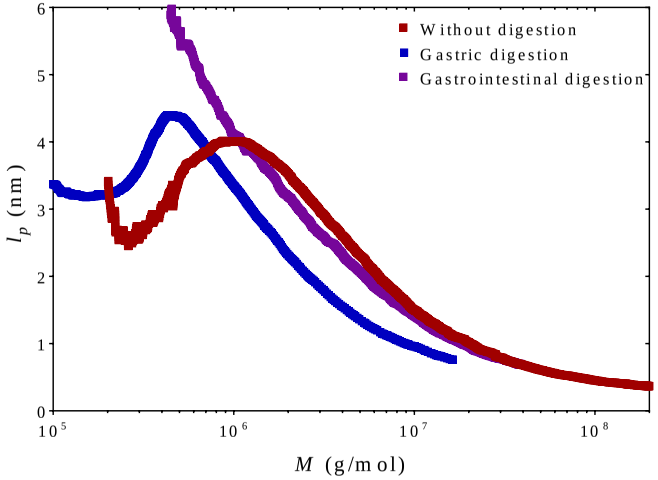
Without digestion
Gastric digestion
Gastrointestinal digestion
l_p (nm)
M (g/mol)
0
1
2
3
4
5
6
10^5
10^6
10^7
10^8

Figure 3

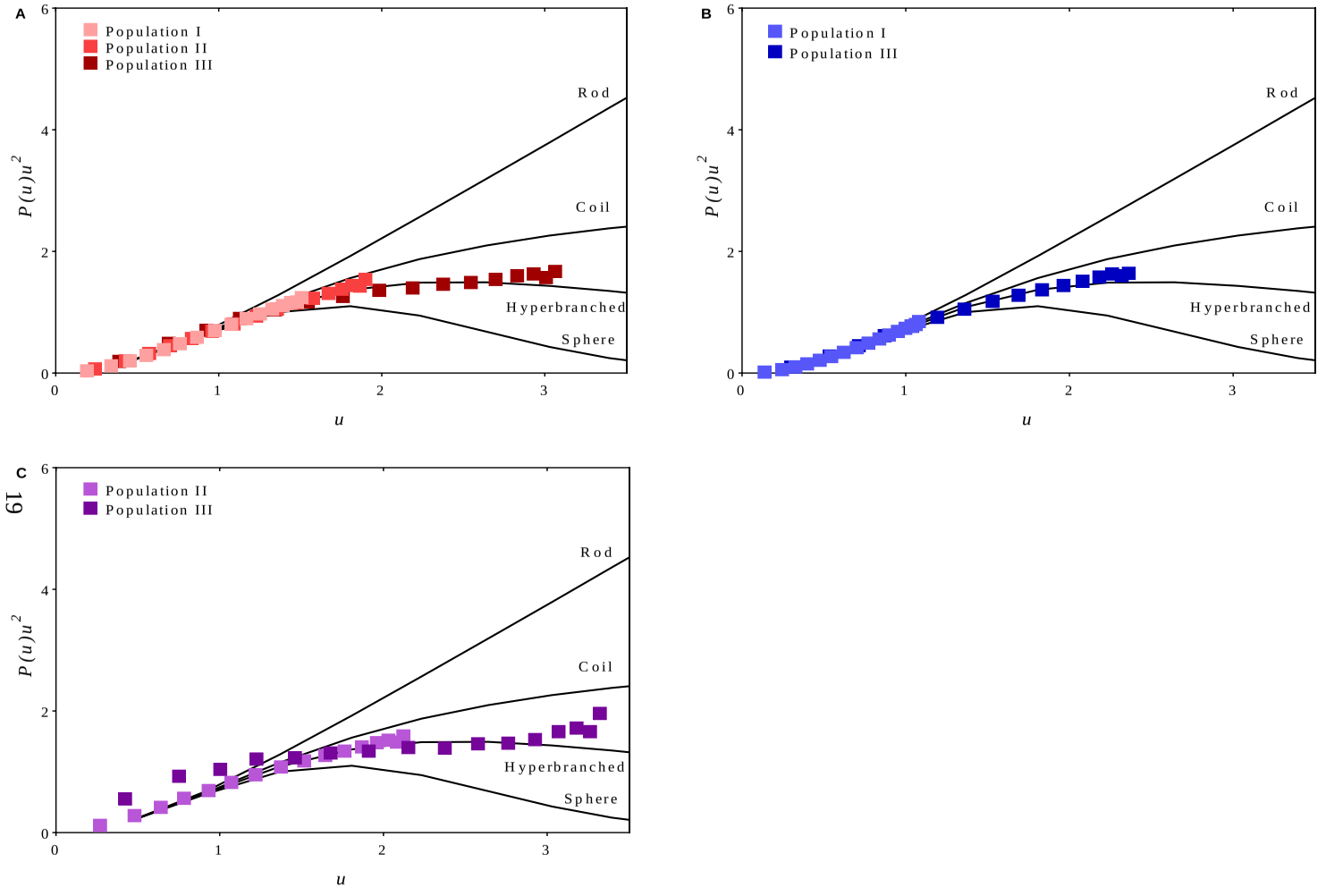
A
Population I
Population II
Population III
Rod
Coil
Hyperbranched
Sphere
$P(u)u^2$
u
B
Population I
Population III
Rod
Coil
Hyperbranched
Sphere
$P(u)u^2$
u
C
Population II
Population III
Rod
Coil
Hyperbranched
Sphere
$P(u)u^2$
u

Figure 4

Figure 5

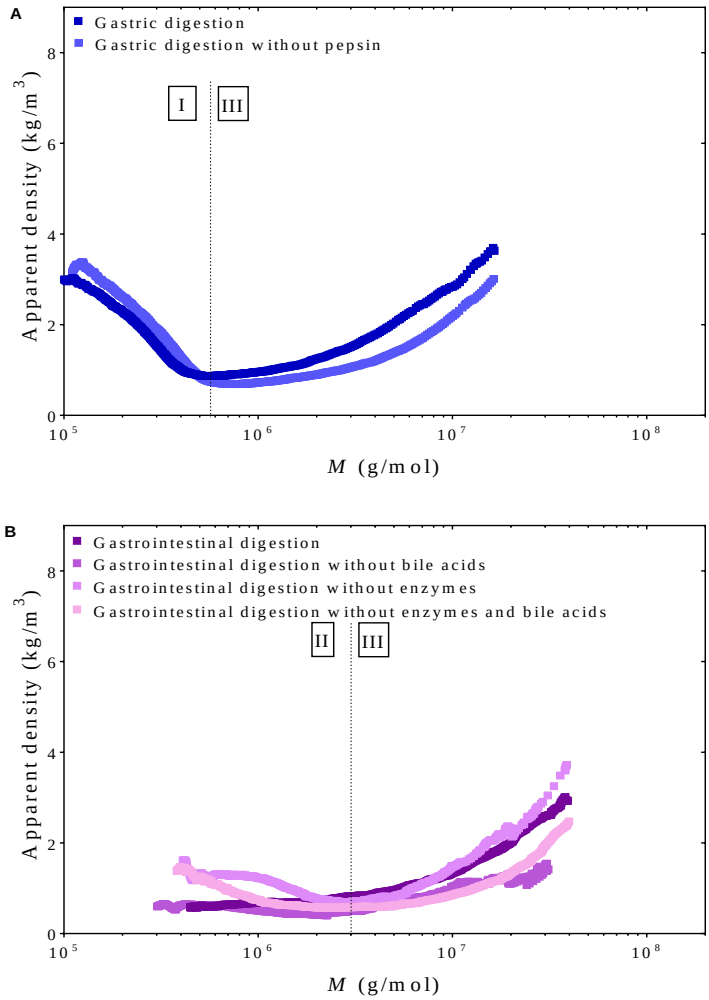
A
Gastric digestion
Gastric digestion without pepsin
I
III
Apparent density (kg/m3)
M (g/mol)
B
Gastrointestinal digestion
Gastrointestinal digestion without bile acids
Gastrointestinal digestion without enzymes
Gastrointestinal digestion without enzymes and bile acids
II
III
Apparent density (kg/m3)
M (g/mol)

Figure 6

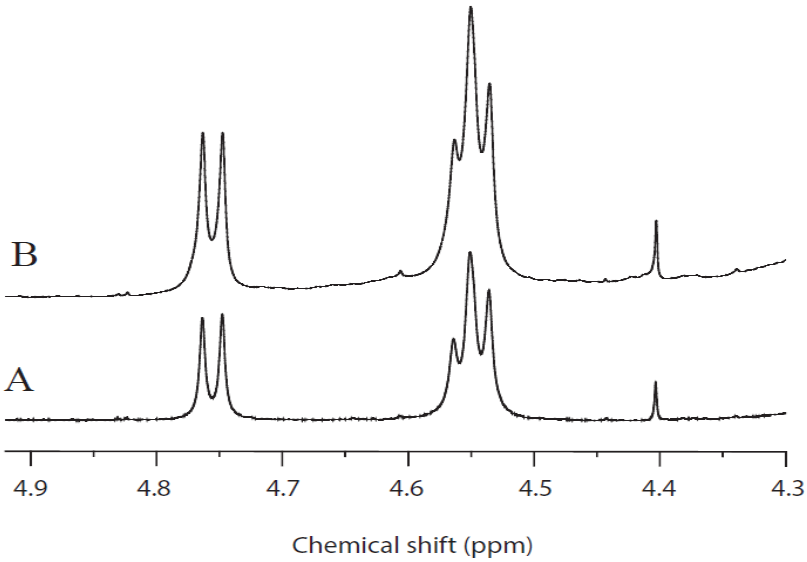

Co-elution effects can influence molar mass determination of large macromolecules with asymmetric flow field-flow fractionation coupled to multiangle light scattering

Perez-Rea, D., Zielke, C. & Nilsson, L.

Journal of Chromatography A (2017) 1506, 138-141.

Paper VII

Journal of Chromatography A, 1506 (2017) 138–141

Contents lists available at ScienceDirect

Journal of Chromatography A

journal homepage: www.elsevier.com/locate/chroma

Short communication

Co-elution effects can influence molar mass determination of large macromolecules with asymmetric flow field-flow fractionation coupled to multiangle light scattering

Daysi Perez-Rea[a,b], Claudia Zielke[b], Lars Nilsson[b,*]

[a] Center for Food and Natural Products, San Simon University, Cochabamba, Bolivia
[b] Food Colloids Group, Department of Food Technology, Engineering and Nutrition, Lund University, P.O. Box 124, S-22100 Lund, Sweden

ARTICLE INFO

Article history:
Received 14 March 2017
Received in revised form 5 May 2017
Accepted 12 May 2017
Available online 12 May 2017

Keywords:
Asymmetric flow field-flow fractionation (AF4)
Size distribution
Macromolecules
Root-mean-square radius (r_{rms})
Amylopectin
Multiangle light scattering (MALS)

ABSTRACT

Starch and hence, amylopectin is an important biomacromolecule in both the human diet as well as in technical applications. Therefore, accurate and reliable analytical methods for its characterization are needed. A suitable method for analyzing macromolecules with ultra-high molar mass, branched structure and high polydispersity is asymmetric flow field-flow fractionation (AF4) in combination with multiangle light scattering (MALS) detection. In this paper we illustrate how co-elution of low quantities of very large analytes in AF4 may cause disturbances in the MALS data which, in turn, causes an overestimation of the size. Furthermore, it is shown how pre-injection filtering of the sample can improve the results.

1. Introduction

Separation and characterization of ultra-high molar mass ($M > 10^7$ g/mol) macromolecules is often a challenging task. An example of a common and demanding macromolecule is amylopectin, which is the larger and more branched polymer found in starch. As starch is the most important source of energy in human diet and widely used in several industries e. g. food or pharmaceutical industry [1] it is crucial to identify routes to its characterization. Amylopectin is a highly branched biopolymer consisting of a large number of $\alpha(1 \rightarrow 4)$ linked glucose units with $\alpha(1 \rightarrow 6)$ linked branch points and typically contains large amounts of material with ultra-high molar mass. Being a biopolymer, amylopectin is also inherently polydisperse which contributes to the challenge of its characterization. Size exclusion chromatography (SEC) has widely been used for the analysis of size distributions of starch. Nevertheless, its use is limited by the columns relatively low exclusion limit compared to the size of amylopectin [2,3] and shear degradation of large amylopectin molecules, which has been shown to be unavoidable [4].

Another fractionation method found more suitable to achieve good size separation of starch and especially amylopectin is asymmetric flow field-flow fractionation (AF4) [5–9]. AF4 is, by now, relatively well known for overcoming some of the limitations of SEC i.e. much higher upper limit for size-based separation as well as avoiding shear degradation. Molar mass (M) and size distributions for biopolymers are typically obtained through coupling of AF4 to multiangle light scattering (MALS) and differential refractive index (dRI) detectors enabling a direct determination of M and size (root-mean-square radius, r_{rms}) in eluting fractions.

AF4 can operate in two different separation modes: the Brownian (or "normal") mode or the steric/hyperlayer mode. In the Brownian mode separation is based on the diffusion coefficient (i.e. hydrodynamic size) of analytes with smaller analytes eluting earlier than larger [10]. In the steric/hyperlayer mode, a combination of steric effects and hydrodynamic lift forces govern the separation resulting in larger analytes eluting before smaller [11]. The transition between the two modes of separation is somewhat dependent on separation conditions such as the crossflow velocity applied [12]. In practice, this also means that both modes of separation may occur in parallel and, thus, give rise to co-elution of relatively small as well as relatively large analytes. In turn, this may distort size determination from MALS as eluting fractions may contain analytes of vastly different sizes.

* Corresponding author.
E-mail address: lars.nilsson@food.lth.se (L. Nilsson).

http://dx.doi.org/10.1016/j.chroma.2017.05.029
0021-9673/

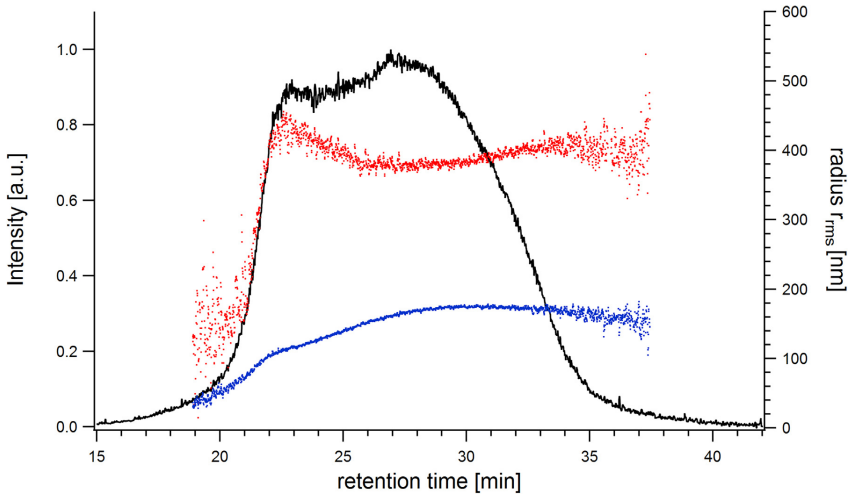

Fig 1. Fractogram for amylopectin displaying Rayleigh ratio from MALS (black), r_{rms} obtained from scattering angles 4–9 (red), r_{rms} obtained from scattering angle 9–14 (blue). (For interpretation of the references to colour in this figure legend, the reader is referred to the web version of this article.)

The reported results will illustrate phenomena and errors in AF4-MALS analysis of amylopectin which originate from co-elution effects and will be useful to consider in the analysis of ultra-large, polydisperse macromolecules.

2. Materials and methods

The amylopectin (waxy maize starch) was obtained from Lyckeby, Kristianstad, Sweden. Solutions were prepared by initial dissolution in DMSO (VWR BDH Prolabo, Stockholm, Sweden) and then diluted with the AF4 carrier liquid consisting of 10 mM NaNO3 (AppliChem, Darmstadt, Germany) and 0.02% NaN3 (BDH, Poole, UK) prepared with milliQ water (Millipore Corp., Bedford, MA, USA) as described previously [5]. Starch concentration in the prepared samples was determined spectrophotometrically after enzymatic degradation using the Megazyme Total Starch Kit (Megazyme International, Wicklow, Ireland) as described previously [5].

The AF4 instrument was an Eclipse 3+ Separation System (Wyatt Technology, Dernbach, Germany). The system was connected to a Dawn Heleos II multiangle light scattering (MALS) detector and an Optilab T-rEX differential refractive index (dRI) detector (both Wyatt Technology), both operating at a wavelength of 658 nm. An Agilent 1100 series isocratic pump with an in-line vacuum degasser and Agilent 1100 autosampler (both Agilent Technologies, Waldbronn, Germany) delivered carrier liquid and handled sample injection onto the AF4 channel. To ensure that particle free carrier liquid entered the system, a filter-holder with a 100 nm pore-size polyvinylidene fluoride membrane (Millipore Corp.) was placed between the pump and the channel inlet. The channel was a Wyatt short trapezoidal channel with a tip-to-tip length of 17.4 cm (inlet breadth 2.17 cm and outlet breadth 0.37 cm), assembled with a 350 μm spacer. The ultra-filtration membrane used to form the accumulation wall in the AF4 channel was regenerated cellulose with a 10 kDa cut-off, purchased from Microdyn-Nadir GmbH, Wiesbaden, Germany, and the actual channel thickness was calibrated to 309 μm [13], according to Håkansson et al. [14] The sample was injected onto the channel with an injection flow of 0.2 mL/min with a total time for injection/relaxation of 6 min. The crossflow during the injection and focus/relaxation was 0.5 mL/min. The detector flow was constant during the whole run at 1 mL/min. The initial cross-flow during elution was set to 0.5 mL/min with an exponentially decaying half-life of 4 min, reaching a constant crossflow of 0.08 mL/min at 20 min (the time before elution was 10.5 min). The void time (t^0) was 0.4 min.

The data obtained from MALS and dRI detectors after the AF4 separation was processed using the Astra software (v. 5.3.4.14, Wyatt Technology). M and r_{rms} distributions were calculated using the Berry method [15,16] and the refractive index increment (dn/dc) for amylopectin was 0.146 mL/g [17], while the second virial coefficient A_2 was considered negligible.

3. Results

Fig. 1 shows an AF4 fractogram of amylopectin as Rayleigh ratio from MALS plotted vs. retention time (t_r) as well as r_{rms} distributions as determined from two different MALS scattering angle intervals (angles 4–9, corresponding to 25.9°–69.3° and 9–14, corresponding to 69.3°–121.2°). Fig. 2 shows the Berry plot obtained from the MALS data at t_r = 23 min in Fig. 1 and the corresponding 1st order fit. It is obvious that considerable curvature is present in the Berry plot which results in a poor fit.

In order to investigate this further, the amylopectin sample was filtered pre-injection through a 0.45 μm regenerated cellulose syringe filter. The starch content before filtration was determined to 0.28 mg/mL, and after filtration to 0.27 mg/mL i. e. a sample loss of approx. 4% due to filtration. The sample was again analyzed and the resulting fractogram is shown in Fig. 3. The results show an increased selectivity on r_{rms} compared to the unfiltered sample and a lower r_{rms} over the peak. Fig. 4 displays a good 1st order fit of the Berry plot of MALS-data from t_r = 23 min in Fig. 3.

4. Discussion

It is clear from the Berry plot in Fig. 2 (obtained from the MALS data at t_r = 23 min in Fig. 1), that substantial curvature can

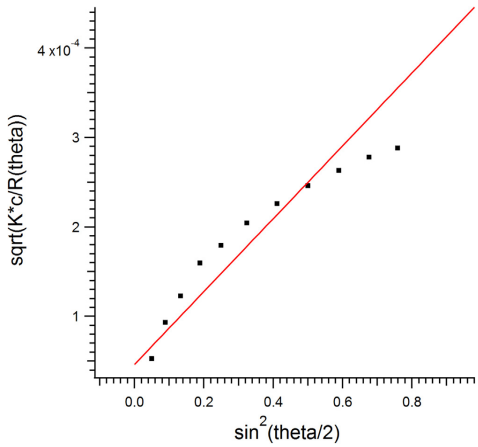

Fig. 2. Berry plot and corresponding 1st order fit of MALS-data from t_r = 23 min in.

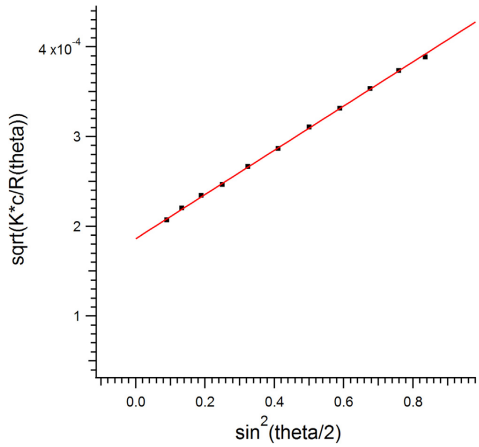

Fig. 4. Berry plot and corresponding 1st order fit of MALS-data from t_r = 23 min in.

be observed which results in a poor fit. Different scattering angle intervals can be chosen to obtain a higher quality fit and the resulting r_{rms} are shown in Fig. 1. For the higher scattering angles (9–14) lower values for r_{rms} are obtained, and vice versa for the lower scattering angles (4–9). The results for the lower scattering angle range also indicate very poor selectivity on r_{rms} and in the earlier part of the peak even reverse order elution appears to occur. The reverse order elution is a characteristic of the so-called steric/hyperlayer elution which is well known for large analytes [11]. Thus, it seems that in this range co-elution in steric/hyperlayer and Brownian mode elution occur simultaneously. In the presented results the transition between the two modes of separation would occur around an analyte diameter of approximately 1 μm [12]. It should be stressed that co-elution could, at least partially, be influenced by carefully selecting the flow conditions in the separation which is beyond the scope of the current investigation.

The results from the higher scattering angle range show a higher (but relatively low) selectivity on r_{rms}. Together, the results suggest that the curvature observed in Fig. 2 is caused by co-elution of large analytes that interferes strongly with the MALS detection. As the large analytes will dominate the light scattering at lower angles, the determined r_{rms} is therefore larger when utilizing the low scattering angle range. The opposite is true for the high scattering angle

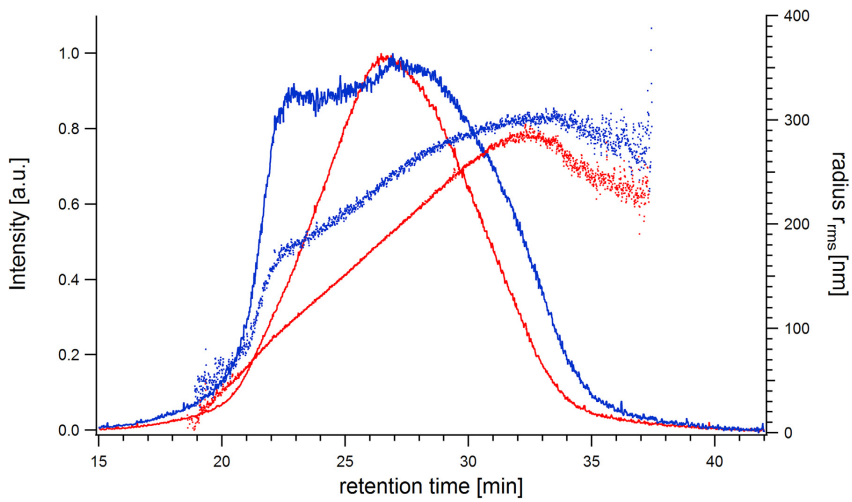

Fig. 3. Fractogram for the filtered (0.45 μm) amylopectin sample (red) overlayed with the unfiltered sample (blue, from Fig. 1) as Rayleigh ratio from MALS and r_{rms} vs. t_r. The r_{rms} was in both cases obtained from a 1st order fit of scattering angles 5–15. (For interpretation of the references to colour in this figure legend, the reader is referred to the web version of this article.)

range where less influence of the large co-eluting analytes on the scattered light occurs.

To investigate the validity of the result the ratio between r_{rms} and r_h can be determined. As the sample is amylopectin, the expected r_{rms}/r_h should correspond to that of a hyperbranched polymer structure (i.e. theoretically approx. 1.2 [18]). Experimental values for amylopectin have been reported in the range 1.0–1.3 [19]. The r_h was determined from AF4 theory at $t_r = 27$ min and the obtained r_{rms}/r_h is 1.0 when utilizing the higher scattering angle interval for r_{rms} determination which is in good agreement with the expected values. When utilizing the lower range of scattering angles for r_{rms} determination, r_{rms}/r_h is approximately 2.4 which appears nonsensical for amylopectin as it would correspond to a rod-like structure of aspect ratio > 25 [20]. For polymers, similar values of r_{rms}/r_h have been reported for relatively stiff elongated molecules such as cellulose derivatives [21] and xanthan gum [22]. Thus, it is clear, in this case, that the lower scattering angle range results in an overestimation of r_{rms} related to co-elution of large species.

The results after filtering of the amylopectin sample show, as mentioned before, an increased selectivity on the obtained r_{rms} compared to the unfiltered sample. The filtering caused a sample loss of only 4% (w/v). Furthermore, lower r_{rms} values over the peak are obtained. Calculating the r_{rms}/r_h (at $t_r = 27$ min) now for the filtered sample, a value of 1.2 is attained, which is in good agreement with the expected range discussed above. The Berry plot at $t_r = 23$ min is shown in Fig. 4 and displays a high quality linear fit over the scattering angle range used. Thus, we conclude that the presence of only a low amount of large analytes (most likely non-dissolved fragments from amylopectin dissolution) is sufficient to cause a significant disturbance in the determination of r_{rms}.

5. Conclusion

In this study, we were able to point out challenges when analyzing macromolecules with ultra-large molar mass and complex structures, such as amylopectin, with AF4-MALS detection. Co-elution of large analytes, present only at very low amounts, may cause considerable disturbances in the light scattering data and, hence, in the determination of r_{rms}. Thus, great care must be taken in evalutating AF4-MALS as well as in sample preparation and method development to avoid experimental artifacts.

Acknowledgements

Funding from the Swedish International Development Agency (SIDA/SAREC) and the Swedish Research Council (VR) is gratefully acknowledged.

References

[1] A.-C. Eliasson, M. Gudmundsson, Starch: physicochemical and functional aspects, in: A.-C. Eliasson (Ed.), Carbohydrate in Food, 2nd edn., Taylor & Francis Group, Boca Ratón-Florida, 2006, pp. 391–470.
[2] W. Kim, C.H. Eum, S. Lim, J. Han, S. You, S. Lee, Separation of amylose and amylopectin in corn starch using dual-programmed flow field-flow fractionation, Bull. Kor. Chem. Soc. 28 (2007) 2489–2520.
[3] F.A. Messaud, R.D. Sanderson, J.R. Runyon, T. Otte, H. Pasch, S.K.R. Williams, An overview on field-flow fractionation techniques and their applications in the separation and characterization of polymers, Prog. Polym. Sci. 34 (2009) 351–368.
[4] R.A. Cave, S.A. Seabrook, M.J. Gidley, R.G. Gilbert, Characterization of starch by size-exclusion chromatography: the limitations imposed by shear scission, Biomacromolecules 10 (8) (2009) 2245–2253.
[5] D. Perez-Rea, B. Bergenståhl, L. Nilsson, Development and evaluation of methods for starch dissolution using asymmetrical flow field-flow fractionation. Part I: dissolution of amylopectin, Anal. Bioanal. Chem. 407 (2015) 4315–4326.
[6] A. Rolland-Sabaté, P. Colonna, M.G. Mendez-Montealvo, V. Planchot, Branching features of amylopectins and glycogen determined by asymmetrical flow field flow fractionation coupled with multiangle laser light scattering, Biomacromolecules 8 (2007) 2520–2532.
[7] M. van Bruijnsvoort, K.-G. Wahlund, G. Nilsson, W.T. Kok, Retention behaviour of amylopectins in asymmetrical flow field-flow fractionation studied by multi-angle light scattering detection, J. Chromatogr. A 925 (2001) 171–182.
[8] K.G. Wahlund, M. Leeman, S. Santacruz, Size separations of starch of different botanical origin studied by asymmqetrical-flow field-flow fractionation and multiangle light scattering, Anal. Bioanal. Chem. 399 (2011) 1455–1465, http://dx.doi.org/10.1007/s00216-010-4438-5.
[9] S. You, S.G. Stevenson, M.S. Izydorczyk, K.R. Preston, Separation and characterization of barley starch polymers by a flow field-flow fractionation technique in combination with multiangle light scattering and differential refractive index detection, Cereal Chem. 79 (2002) 624–630.
[10] K.G. Wahlund, J.C. Giddings, Properties of an asymmetric flow field-Flow fractionation channel having one permeable wall, Anal. Chem. 59 (1987) 1332–1339, http://dx.doi.org/10.1021/ac00136a016.
[11] K.D. Caldwell, Steric field-flow fractionation and the steric transition, in: M. Schimpf, K.D. Caldwell, J.C. Giddings (Eds.), Field-Flow Fractionation Handbook, Wiley-Interscience, New York, 2000, pp. 79–94.
[12] M.N. Myers, J.C. Giddings, Properties of the transition from normal to steric field-flow fractionation, Anal. Chem. 54 (1982) 2284–2289, http://dx.doi.org/10.1021/ac00250a032.
[13] C.A. Gonzalez-Bermudez, A. Castro, D. Perez-Rea, C. Frontela-Saseta, C. Martinez-Gracia, L. Nilsson, Physicochemical properties of different thickeners used in infant foods and their relationship with mineral availability, Food Res. Int. 72 (2015) 62–70.
[14] A. Håkansson, E. Magnusson, B. Bergenståhl, L. Nilsson, Hydrodynamic radius determination with asymmetrical flow field-flow fractionation using decaying cross-flows. Part I. A theoretical approach, J. Chromatogr. A. 1253 (2012) 120–126, http://dx.doi.org/10.1016/j.chroma.2012.07.029.
[15] G.C. Berry, Thermodynamic and conformational properties of polystyrene. I. Light-scattering studies on dilute solutions of linear polystyrenes, J. Chem. Phys. 44 (1966) 4550–4564.
[16] M. Andersson, B. Wittgren, K.-G. Wahlund, Accuracy in multiangle light scattering measurements for molar mass and radius estimations. Model calculations and experiments, Anal. Chem. 75 (2003) 4279–4291.
[17] A. Theisen, C. Johann, M.P. Deacon, S.E. Harding, Refractive Increment Data-Book for Polymer and Biomolecular Scientists, Nottingham University Press, Nottingham, UK, 2000, ISBN 1-897676-29-8.
[18] W. Burchard, Branched polymers II, in: J. Roovers (Ed.), Advances in Polymer Science, vol. 143, Springer International Publishing AG, Berlin-Heidelberg, 1999, pp. 113–194.
[19] P. Roger, L.A. Bello-Perez, P. Colonna, Contribution of amylose and amylopectin to the light scattering behaviour of starches in aqueous solution, Polymer 40 (1999) 6897–6909.
[20] S. Hansen, Translational friction coefficients for cylinders of arbitrary axial ratios estimated by Monte Carlo simulation, Chem. Phys. 121 (2004) 9111–9115, http://dx.doi.org/10.1063/1.1803533.
[21] S. Nilsson, L.-O. Sundelöf, B. Porsch, On the characterization principles of some technically important water soluble non-ionic cellulose derivatives, Carbohyd. Polym. 28 (1995) 265–275.
[22] T. Coviello, K. Kajiwara, W. Burchard, M. Dentini, V. Crescenzi, Solution properties of xanthan. 1. Dynamic and static light scattering from native and modified xanthans in dilute solutions, Macromolecules 19 (1986) 2826–2831, http://dx.doi.org/10.1021/ma00165a027.

Co-Elution Phenomena in Polymer Mixtures Studied By Asymmetric Flow Field-Flow Fractionation (AF4)

Zielke, C., Fuentes, C., Piculell, L. & Nilsson, L.

Submitted to Journal of Chromatography A

Paper VIII

Co-Elution Phenomena in Polymer Mixtures Studied By Asymmetric Flow Field-Flow Fractionation (AF4)

Claudia Zielke[*a], Catalina Fuentes[a,b], Lennart Piculell[c], Lars Nilsson[a]

Submitted to Journal of Chromatograhy A

[a] Food Technology, Engineering and Nutrition, Faculty of Engineering LTH, Lund University, PO Box 124, S-221 00 Lund, Sweden
[b] School of Chemistry, Faculty of Pure and Natural Sciences, San Andrés University, PO Box 303, La Paz, Bolivia
[c] Physical Chemistry, Lund University, PO Box 124, S-221 00 Lund, Sweden

[*]corresponding author, claudia.zielke@food.lth.se

Abstract

Most polymers generally have complex characteristics. Analysis and understanding of these characteristics is crucial as they, for instance, influence functionality. Separation and analysis of samples of polymers, biopolymers in particular, is challenging since polymers typically display broad distributions in size and molar mass (M) and/or their tendency to form aggregates. Only few analytical techniques are suitable for the task. AF4-MALS-dRI is highly suited for the task, but the analysis can nevertheless be challenging for complex samples and heterogeneous mixtures of polymers that exhibit wide size distributions or aggregation. For such systems, systematic and thorough method development is a requirement. An often observed phenomenon in AF4 of samples with a high polydispersity is a downturn in M vs. elution time, especially common at high retention. This result is often dismissed as an artifact attributed to various errors in detection and data processing. In this work, we utilize AF4-MALS-dRI to separate and analyze binary mixtures of the well-known polysaccharides pullulan and glycogen, or pullulan and poly(ethylene oxide), respectively, in solution. The results show that an observed downturn - or even an upturn - in M can be a correct result, caused by inherent properties of the analyzed polymers.

Keywords: hydrodynamic radius (r_h), molar mass (M) distribution, multi-angle light scattering (MALS), asymmetric flow field-flow fractionation (AF4), glycogen, pullulan, poly(ethylene) oxide

Abbreviations: AF4 - asymmetric flow field-flow fractionation; dRI - differential refractive index; M - molar mass; MALS - multi-angle light scattering, PEO - poly(ethylene) oxide, r_h - hydrodynamic radius; r_{rms} - root-mean-square radius; R_θ - Rayleigh ratio; t^0 - void time

1. Introduction

Polysaccharides are often complex in that they feature more or less wide distributions in primary structure, molar mass (M), size and/or solution behavior. Notably, many of these characteristics profoundly influence the functionality of the substances. Separation and analysis of polymers can be very challenging and few analytical techniques are suitable for the task. The challenges are typically related to the broad distributions in terms of size and M but often also to the presence of highly branched structures and/or a tendency to form

supramolecular aggregates in solution. To obtain conformational and structural data over the entire size distribution of a polymer sample is therefore of fundamental importance for the understanding of their behavior. However, the separation and analysis of complex polymer samples can be very challenging, and few analytical techniques are suitable for the task.

The most commonly used analytical separation technique for polymers is size exclusion chromatography (SEC).[1] Here, M is typically obtained either by direct determination with a multi-angle light scattering (MALS) detector or by calibration against standards. However, drawbacks with this method are its exclusion limit (upper limit of separation), which can limit the use for high M species, as well as degradation of large size species due to shear forces in the column [2], resulting in an underestimation of M [3]. Furthermore, co-elution phenomena in the presence of branched analytes may occur, as has previously been shown for polymer standards [4].

AF4 is a unique and highly versatile method that has been shown to be especially applicable to analytical separation of polymers and aggregated structures [5]. It is a chromatography-like technique based on a laminar flow of a carrier liquid along a thin separation channel, in combination with a crosswise flow, which is driving sample components to the accumulation wall at the bottom of the channel. The accumulation wall consists of a semipermeable ultra-filtration membrane through which the crossflow permeates. The induced crossflow field interacts with any macromolecule or particle in the channel and size separation occurs due to the fact that the elution time is inversely proportional to the diffusion coefficients of the sample components and, thus, the hydrodynamic diameter. In general, sizes from approximately 2 nm up to >1 µm in diameter can be separated. For more detailed descriptions of the technique of AF4 the interested reader is referred to other literature [6-10]. The potential of AF4 for the characterization of polymers was demonstrated at an early stage for polysaccharides, showing fast separations with high resolution [9]. In order to obtain accurate and reliable information about sample properties, as for instance size and M, adequate detection such as multi-angle light scattering (MALS) and differential refractive index (dRI) detectors are utilized. The advantages and possibilities for analysis of polymers with AF4-MALS-dRI have been shown by several authors [11-14], also in combination with fluorescence detection for characterization of polysaccharides [15-17]. Still, M and size determination can be challenging when, for instance, analyzing samples containing ultra-large ($M>10^7$ g/mol) branched species [18] and/or heterogeneous mixtures of biopolymers exhibiting wide size distributions. For such analytes, thorough and systematic method development is an absolute requirement.

An often observed phenomenon in AF4 is a downturn in the M vs. elution time (especially at high retention) as shown in several publications [17,19-22]. This feature is often regarded as an artifact caused by various errors in data originating from detectors and subsequent data processing, and hence not considered further. However, since the separation in the channel is depending on differences in analyte hydrodynamic radii (r_h), a downturn could also be a true result, if the sample contains distinct populations of molecules that differ in their respective relations between r_h and M. This could arise, e.g., if the populations differ in conformation and the scaling between M and size. With this work, we will show that a downturn in the M signal may indeed result from a correct analysis of a mixed polymer sample, caused by such differences in the inherent properties of the individual polymers.

In order to study the above mentioned phenomena, we use the common and well known (in terms of size, structure and conformation) polymers glycogen, pullulan, and poly(ethylene) oxide PEO, which are here separated and analyzed individually and as binary mixtures. Both glycogen and pullulan are polysaccharides consisting of glucose residues. However, glycogen forms hyper-branched structures with branches connected by α(1→6) glycosidic to linear chains linked via α(1→4) glycosidic bonds. In contrast, pullulan is a linear polymer where consecutive maltotriose units (3 glucose residues linked via α(1→4) glycosidic bonds) are connected to each other by α(1→6) glycosidic bonds. PEO is also a linear polymer, with ethylene oxide as the repeating unit ($H-(O-CH2-CH2)_n-OH$). The specific polymer samples chosen in this study have overlapping M distributions, but the three different polymer types display large

differences in their size (r_h) at a given M. Several publications have already shown the possibility of separating these polymers utilizing AF4 and suitable detectors [11,23-25] and pullulan is often used as a reference standard [26].

2. Experimental section

Materials and sample preparation for AF4

Glycogen from bovine liver type IX was purchased from Sigma Aldrich, Darmstadt, Germany. Pullulan with a wide size distribution (10^5 g/mol - 10^7 g/mol) was obtained from Guangzhou Medcan Pharmatech LTD., Guangdong, China. Poly(ethylene) oxide PEO with a narrow molecular weight distribution (M_w=106 000 g/mol, M_n=101 000 g/mol given by the manufacturer) was purchased from PSS Polymer Standards Service GmbH, Mainz, Germany. The samples used for the analysis were prepared as 1 mg/mL solutions where the powder was dissolved in AF4 carrier liquid (10 mM $NaNO_3$ (Merck, Darmstadt, Germany) and 0.02 % (w/v) NaN_3 (BDH, Poole, UK) dissolved in pure water from a Milli-Q system (Millipore Corp., Billerica, Massachusetts, USA)) under vigorous stirring (resulting in a pH of 7)). The injected amount per sample/mixture was 50 µl, corresponding to a polymer mass of 50 µg. The mixed samples were prepared at a volume ratio of 1:1.

FFF analysis and data processing

For all experiments described in this publication, the asymmetric flow field-flow fractionation (AF4) instrument used was an Eclipse 3+ Separation System (Wyatt Technology Europe, Dernbach, Germany). The system was connected to an Optilab T-rEX differential refractive index (dRI) detector and a Dawn Heleos II multi-angle light scattering (MALS) detector (both Wyatt Technology), both operating at a wavelength of 658 nm. An Agilent 1100 series isocratic pump with an in-line vacuum degasser delivered the carrier flow through the system and an Agilent 1100 series autosampler (both Agilent Technologies, Waldbronn, Germany) handled the sample injection onto the AF4 channel. A filter-holder with a 100 nm pore-size polyvinylidene fluoride membrane (Millipore Corp., uncharged) was placed between the pump and the channel inlet to ensure that only particle free carrier liquid entered the system. The separation channel used was a Wyatt long channel with a tip-to-tip length of 27.5 cm and the ultra-filtration membrane to form the accumulation wall was regenerated cellulose with a nominal 10 kDa cut-off (Microdyn-Nadir GmbH, Wiesbaden, Germany) and a 350 µm spacer. The actual thickness of the channel was 275 µm (calibration with ferritin [27]). Flow conditions were as follows: injection flow of 0.2 mL/min for 2 min (in focus mode) + 2 min of focusing without injection, channelflow Q_{out} =1 mL/min, initial crossflow Q_c =1.5 mL/min with a linear decrease rate of 0.117 mL/min^2 for 12 min was applied, minimum Q_c =0.1 mL/min, the void time (t^0) was calculated to be 0.6 min whereas the time before elution was 6 min. Processing of the data obtained from MALS and dRI detectors after the AF4 separation was done using Astra software in version 5.3.4.14 (Wyatt Technology Europe). M and r_{rms} were calculated using the Berry method [28,29] performing a 1st order fit with the data obtained from the chosen scattering angles 8-17 (60.0 ° - 152.5°). For simplification, the refractive index increment dn/dc for the polysaccharides used was set to an average value of 0.14 mL/g (pullulan – 0.14-0.16 mL/g, PEO – 0.13 mL/g, glycogen – 0.146 mL/g) [30], while the second virial coefficient A_2 was considered negligible.

3. Results and Discussion

AF4-MALS-dRI results from the analysis of pullulan and glycogen individually and in mixture can be seen in Fig. 1. Fig. 1A displays the intensity of the MALS signal (left axis) of pullulan (blue), glycogen (red) and a mixture of both (black) plotted vs. the retention time (t_r) as well as their M distributions (dotted curves, right axis). Glycogen shows a peak maximum in MALS signal at t_r=12.5 min, and with a M range from approximately 3x10^5 g/mol to 10^7 g/mol. Pullulan elutes in a broad peak with a maximum at t_r= 18 min and a M range from approximately 10^5 g/mol to 10^7

g/mol. The two polysaccharide samples have an overlapping M range but glycogen elutes at shorter t_r which is an expected consequence of its more compact branched structure. Furthermore, striking differences in the plots of M versus t_r between the individual polymer samples and the mixture are visible. At any given t_r, the more compact glycogen has a higher M than the linear pullulan. For the mixture, the determined M at any t_r is an intensity-weighted average of the contributions from the two different polymers. Hence, in the early t_r region, where comparable amounts of glycogen and pullulan elute together, the M distribution for the mixture falls in between those of the individual polysaccharides. Above approximately 17 min, however, pullulan should be the totally dominating component in the mixture, according to the MALS fractograms for the individual polymers. Consequently, a downturn in M (black dashed) of the mixture eventually occurs at ~14 min, followed by an upturn at ~16 min. Notably, however, in the high t_r region where only pullulan should be eluting, the M curve for the mixture is displaced to lower t_r compared to the curve for pullulan alone. This result is consistent with the MALS results, which also show that the broad peak at high t_r elutes earlier in the mixture (black curve) than the peak of the single pullulan (blue).

As an indication that size separation is indeed achieved, Fig. 1B displays the r_{rms} (dotted curves) vs. t_r of glycogen (red), pullulan (blue) and a mixture of both (black). Also shown are the dRI fractograms (solid lines). Strictly, the separation mechanism in AF4 is based on analyte diffusion coefficient (not r_{rms}) which is realted to r_h through the Stokes-Einstein equation. Nevertheless, the individual samples as well as the mixture all show a smooth and monotonic increase in size (r_{rms}) over the entire fractogram with no downturn, indicating that size separation does occur. In addition, only minor deviations are visible when comparing the r_{rms} distributions for pullulan, glycogen and their mixture, unlike the findings for M (Fig. 1A). We note, however, that a slight shift of the distribution in the fractogram towards lower t_r is visible also for the r_{rms} data (as for the M data, Fig. 1A) in the high-t_r region, where pullulan should dominate.

To test another polymer mixture, pullulan was mixed with PEO, an as well linear polymer that has a lower M than pullulan at any given radius at the utilized solution conditions. Fig. 2 displays the MALS signals of pullulan (blue), PEO (green) and a mixture of both (black, solid lines, left y-axis) plotted vs. t_r as well as their M distributions (dotted lines, right y-axis). The chosen PEO sample has a much narrower M distribution than pullulan, centered around 10^5 g/mol, resulting in a much narrower peak than for pullulan. Note that the M curve for PEO alone shows lower values than that for pullulan at a given t_r, in contrast to the results for glycogen (Fig. 1A). Nevertheless, similarly as for the glycogen/pullulan mixture, the MALS signals as well as the M distributions of PEO and pullulan overlap (Fig. 2A). As for the glycogen/pullulan mixture (Fig. 1A), the M curve for the PEO/pullulan mixture runs in between the curves for the individual polymers in the short t_r region where PEO and pullulan co-elute. However, when the contribution from PEO starts to vanish (around t_r=15 min) a clear upturn of the M curve can be observed for the mixture. At higher t_r, where essentially only pullulan elutes, the fractogram for the mixture runs above that for pullulan alone. r_{rms} data for the PEO/pullulan mixture shows as well a smooth and monotonic increase in size, indicating that separation according to size occurred (Fig. 2B).

From the results in Figures 1 and 2, it is clear that a significant downturn, or an upturn, in M vs. t_r or loss of M selectivity should occur in mixtures of polymers with distinctly different size distributions, if the polymers also individually have distinctly different relationships between r_h and M. In the region where the polymers co-elute, the recorded M is an average between the results for the individual polymers, but a "kink" in the curve (downturn or upturn) eventually occurs at high t_r, when the peak from the polymer with the largest size starts to dominate. We should here recall that variations in the relationship between r_h and M can occur even within a sample of, nominally, a single type of polymer. This could, for instance, originate from differences in polymer primary structure over the size distribution (branched vs. linear polymer chains). Furthermore, partial aggregation of polymer molecules in solution

can create larger aggregates/particles that differ in density and scaling properties from the individual molecules from which they are formed. Such particles could elute later than the individual polymers and could cause a leveling off, or even a downturn, in the plot of M versus t_r). Fig. 1A already shows a downturn for glycogen M at high t_r. In the case of glycogen, a fraction of supramolecular glycogen species, referred to as glycogen α-particles, which can consist of several β-particles (primary glycogen molecules) [31] could be responsible for such a downturn.

A consistent observation from the results in Figs. 1 and 2 is that shifts in t_r of MALS and dRI peak maxima arise for the polymer mixtures, compared to the results for the individual polymers. Comparing MALS data in Fig. 1A and Fig. 2A, and dRI data in Fig. 1B and Fig. 2B, it can be seen that the peak maxima move in the mixtures. The latter effect might arise when mixed polymer sample interact intermolecular what influences the elution behaviour. These interactions should be particularly important during the focusing/relaxation step in the analysis as this generates a sample zone of higher concentration than the original sample. Hence, it is of interest to make an attempt to estimate the concentration of the polymer sample during the focusing/relaxation step.

By injecting a dye (bromophenol blue) onto the channel, we could visualize and estimate the focusing band width to 22 mm and the focusing band depth to 2 mm. The third dimension of the effective sample volume is the average distance l of the concentrated sample from the wall, which is determined by the polymer diffusion coefficient D and the crossflow velocity U_d. An estimate of l is given by Eq. 1 [32], which is valid only under the assumption that the transverse flow velocity at any time in the channel is much smaller than the average longitudinal flow velocity, resulting in a parabolic flow profile along the channel. Furthermore, it is assumed that the pressure drop along the channel is much lower than the pressure drop across the accumulation wall (ensuring a homogeneous permeation of the carrier through the membrane) and that l « channel height.[32]

$$l = \frac{D}{U_d} \qquad \text{(Eq. 1)}$$

For a dilute polymer solution, the polymer diffusion coefficient is given by the Stokes-Einstein equation (Eq. 2) [33].

$$D = \frac{k_B T}{6\pi\eta r_h} \qquad \text{(Eq. 2)}$$

where k_B is the Boltzmann constant, T is the absolute temperature, and η is the viscosity of the solvent. Utilizing AF4 theory [27], we estimate r_h to 20 nm at t_r =15 min, where the downturn in the M distribution signal occurs for the glycogen/pullulan mixture, resulting in $D = 1.1 \times 10^{-11}$ m^2s^{-1}. Inserting the latter value and a crossflow velocity of 6.8×10^{-6} m s^{-1} in equation 1, we obtain l = 1.6 µm. Multiplying l with the focusing band width (22 mm) and the focusing band depth (2 mm) we obtain a sample volume V_l below l as $V_l = 7 \cdot 10^{-11}$ m^3. Eq 3 describes the AF4 concentration profile [34], under the assumption that Eq 1 is valid,

$$c(y) = c_0 exp^{\frac{-y\,U_d}{D}} \qquad \text{(Eq. 3)}$$

where c(y) is the concentration at distance y from the accumulation wall and c_0 is thecentration of analyte at the accumulation wall. From Eq. 3 we can estimate the fraction of the sample that is contained below l in the focusing/relaxation step. The result is that 63 % of the sample is contained at distances ≤ l =1.6 µm from the accumulation wall. Since the injected amount was 20 µg, we finally obtain an average sample concentration c present in V_l as 179 g/L, that is, 18 % (w/w) for the conditions applied in the experiments (Figs. 1 and 2). This simple estimation clearly shows that a very high polymer concentration should be generated during the focusing step. In fact, at such high concentrations the assumptions underlying our calculation should not hold. Specifically, the Stokes-Einstein equation (Eq. 2) is only applicable in dilute sample regimes below the overlap concentration c*, which for the substances used in this study should be between 0.1-1 % (w/w). [35] Above c* the diffusion can be much slower, and it also varies strongly with concentration. Thus, D in Eq. 3 should vary with y. However, to gain values for c present in V_l lower than 1 % (w/w), a sample amount of below 1 µg had to be injected, which resulted in an insufficient signal from the utilized detectors (results not shown).

Hence, the firm conclusion from our calculation is that the concentration of our polymer samples should be quite high during the focusing/relaxation step, and well into the semi-dilute region (c » c*), although the true concentration profile is unknown. At such high concentrations, the polymer molecules interpenetrate and interact extensively. A well-known resulting phenomenon in semi-dilute mixtures of polymers of different composition and conformation is a demixing into two liquid phases, each one enriched in one of the polymer species [36-38]. This is because interactions between similar chains are typically preferred in a mixed polymer solution. However, from this study it seems mandatory to focus future work on the investigation of how the concentration profile looks in detail to be able to draw firm conclusions on its influence on interactions in polymer mixtures.

4. Conclusions

To our knowledge, the present study represents the first attempt to interpret the downturn phenomenon often observed in an AF4 analysis of complex polymer solutions. If the dissolved polymers differ widely regarding both their size range and their individual size - M relationship, "kinks" can arise in the M vs t_r plots at high t_r, when the eluted fractions no longer contain the mixed polymer but only the polymer exhibiting the largest r_h. Differences in the relationship between size and M can be due to either differences in structure (e.g. linear vs. branched, as for pullulan and glycogen) or differences in conformation and scaling of mass vs. r_h (as for pullulan and PEO). However, variations in the relation between r_h and M can occur even within a sample of, nominally, a single type of polymer, owing to, for instance, partial aggregation. The results in this work, thus demonstrate, that the often observed downturn phenomenon of M at high t_r could indeed be a correct experimental result, reflecting real properties of a heterogeneous polymer solution.

We believe that this work is important for researchers in the field of separation science and will help to better interpret existing and future characterization results regarding complex polymers and their mixtures. However, to establish the exact mechanism that gives rise to the observed shifts in t_r, more detailed investigations and further studies are required, especially in order to investigate the behavior of polymer mixtures during the focusing/relaxation step.

5. Acknowledgements

Funding from the Swedish Research Council (VR) is gratefully acknowledged.

6. References

1. Harding, S. E. Carbohydr. Res. 2005, 340, 811–826.
2. Cave, R. A.; Seabrook, S. A.; Gidley, M. J.; Gilbert, R. G. Biomacromolecules 2009, 10(8), 2245–2253.
3. Barth, H. G.; Boyes, B. E.; Jackson, C. Anal. Chem. 1998, 70(12), 251–278.
4. Otte, T.; Pasch, H.; Macko, T.; Brüll, R.; Stadler, F.J.; Kaschta, J.; Becker, F.; Buback M. J. Chromatogr. A. 2011, 1218(27), 4257-4267.
5. Nilsson, L. Food Hydrocolloid. 2013, 30, 1-11.
6. Litzén, A.; Wahlund, K. G. Anal. Chem. 1991, 63, 1001-1007.
7. Litzén, A. Anal. Chem. 1993, 65, 461-470.
8. Wahlund, K. G.; Giddings, J. C. Anal. Chem. 1987, 59, 1332-1339.
9. Wahlund, K. G.; Litzén, A. J. Chromatogr. 1989, 461, 73-87.
10. Wahlund, K. G.; Nilsson, L. In Field-flow fractionation in biopolymer analysis. Williams, S. K. R.; Caldwell, K. Eds.; Springer Verlag: Wien, 2012; pp. 1-21.
11. Adolphi, U.; Kulicke, W. M. Polymer 1997, 38, 1513-1519.
12. Roessner, D.; Kulicke,W.M. J. Chromatogr. A. 1994, 687(2), 249-258.
13. Wittgren, B.; Wahlund, K. G. J. Chromatogr. A. 1997, 760, 205-218.
14. Wittgren, B.; Wahlund, K. G. J. Chromatogr. A. 1997, 791, 135-149.

15. Alftrén, J.; Peñarrieta, J. M.; Bergenståhl, B.; Nilsson, L. Food Hydrocolloids 2012, 26 (1), 54-62.
16. Ulmius, M.; Adapa, S.; Önning, G.; Nilsson, L. Food Chem. 2012, 130(3), 536–540.
17. Zielke, C; Teixeira, C; Ding, H; Cui, S; Nyman, M; Nilsson, L. Carbohyd. Polym.2017, 157, 541–549.
18. Perez-Rea, D.; Bergenståhl, B.; Nilsson, L. Anal. Bioanal. Chem. 2015, 407, 4315-4326.
19. Otte, T.; Pasch, H.; Macko, T.; Brüll, R.; Stadler, F.J.; Kaschta, J.; Becker, F.; Buback, M. J. Chromatogr. A. 2011, 1218, 4257-4267.
20. Pitkänen, L.; Striegel, A. M. Analyst 2014, 139,5843-5851.
21. Zielke, C.; Kosik, O.; Ainalem, M.-L.; Lovegrove, A.; Stradner, A.; Nilsson, L. PLoS ONE 2017, 12(2): e0172034. doi:10.1371/journal.pone.0172034
22. Fuentes, C.; Zielke, C.; Prakash, M.; Kumar, P.; Penarrieta, J.M.; Eliasson, A.-C.; Nilsson, L. Food Chem. 2016, 213, 768-774.
23. Fernandez, C.; Rojas, C. C.; Nilsson, L. Int. J. Biol. Macromol. 2011, 49, 458-465.
24. Andres-Brull, M.; Al-Assaf, S.; Phillips, G. O.; Jackson, K. Anal. Methods 2013, 5, 4047.
25. Pasch, H.; Makan, A. C.; Chirowodza, H.; Ngaza, N.; Hiller, W. Anal. Bioanal. Chem. 2014, 406(6), 1585–1596.
26. Leeman, M.; Wahlund, K. G.; Wittgren, B. J. Chromatogr. A. 2006, 1134, 236-245.
27. Håkansson, A.; Magnusson, E.; Bergenståhl, B.; Nilsson, L. J. Chromatogr. A. 2012, 1253, 120-126.
28. Berry, G. C. J. Chem. Phys. 1966, 44 (12), 4550-4564.
29. Andersson, M.; Wittgren, B.; Wahlund, K. G. Anal. Chem. 2003, 75 (16), 4279-4291.
30. Theisen, A.; Johann, C.; Deacon, M.P.; Harding, S.E. Refractive Increment Data-Book for Polymer and Biomolecular Scientists, Nottingham University Press: Nottingham, UK, 2000. ISBN: 1-897676-29-8
31. Manners, D. J. Carbohydr. Polym. 1991, 16, 37-82.
32. Litzén, A. Anal. Chem. 1993, 65, 461-470
33. Einstein, A. Ann. Phys. 1905, 17, 549-560.
34. Wahlund, K. G.; Giddings, J. C. Anal. Chem. 1987, 59, 1332-1339.
35. Ying, Q.; Chu. B. Macromolecules 1987, 20, 362-366.
36. Gibbs, J. W. In The Scientific Papers Vol 1 Thermodynamics; Longmans, Green and Co: London, New York and Bombay, 1906, p 476.
37. Atkins, P. W. In Physical Chemistry (8th Ed.); Atkins, P. W.; de Paula, J. Eds.; Oxford University Press: Oxford New York, 2006, pp. 200-240.
38. Walsh, D. J.; Graessley, W. W.; Datta, S.; Lohse, D. J.; Fetters, L. J. Macromolecules 1992, 25, 5236-5240.

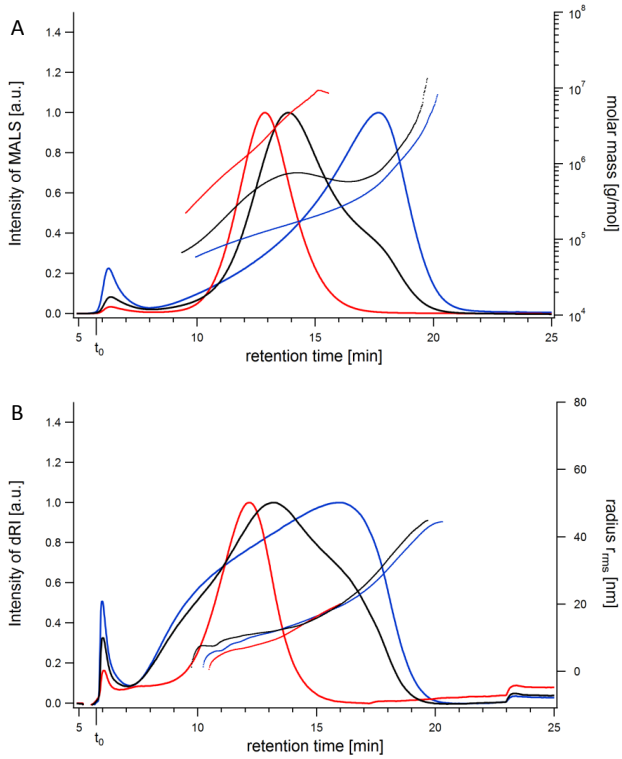

Fig. 1: Fractograms of pullulan (blue), glycogen (red) and a mixture of both (1:1, black). A displays Rayleigh ratio from MALS (solid lines, left y-axis, a.u.) and M distribution (right y-axis, g/mol). B displays dRI signal (solid lines, left y-axis, a.u.) and root-mean square radius (r_{rms}) distribution (right y-axis, nm). The void time (t^0) was calculated to be 0.6 min.

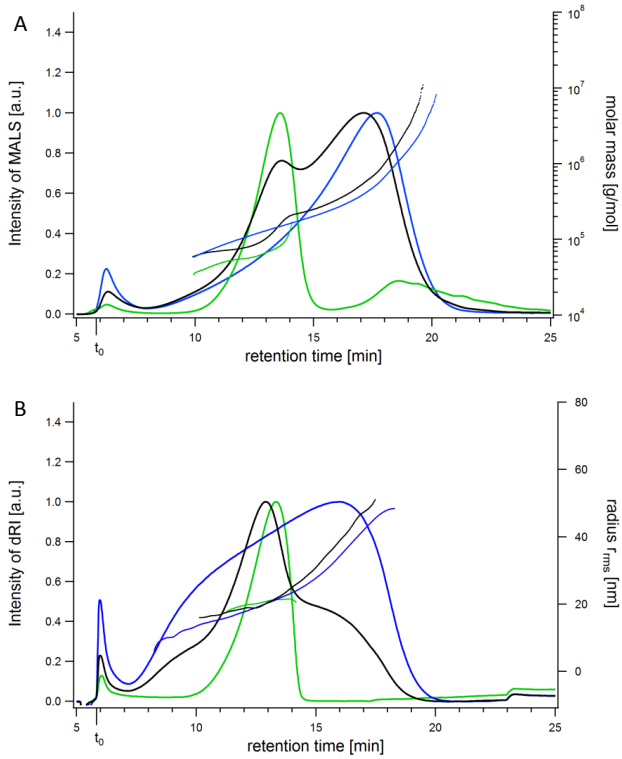

Fig. 2: Fractograms of pullulan (blue), PEO (green) and a mixture of both (1:1, black). A displays Rayleigh ratio from MALS (solid lines, left y-axis, a.u.) and M distribution (right y-axis, g/mol). B displays dRI signal (solid lines, left y-axis, a.u.) and root-mean square radius (r_{rms}) distribution (right y-axis, nm). The void time (t^0) was calculated to be 0.6 min.